UiT THE ARCTIC UNIVERSITY OF NORWAY

FACULTY OF SCIENCES, DEPARTMENT OF GEOLOGY

Structural development and metallogenesis of Paleoproterozoic volcano-sedimentary rocks of the Rombak Tectonic Window

—

Tine Larsen Angvik

A dissertation for the degree of Philosophiae Doctor – August 2014

Table of content

Hat og kjærlighet er to sider av samme mynt.

Trikset er bare å snu mynten - Harry Hole

Preface

The study and writing of this PhD thesis was carried out during the period of 2009-2014. The project is a collaboration between University of Tromsø and the Geological Survey of Norway (NGU). The project was funded by NGU which also provided an office and great colleagues. I started the PhD with a wide perspective of geology, all the way from structural to ore geology. I collected a handful of supervisors named Steffen Bergh, Iain Henderson, Jan Sverre Sandstad and Krister Sundblad to help me to understand the big questions.

Throughout the PhD period I spent time at the University of Tromsø for several courses and supervisor workshops. I also completed one course at the Norwegian University of Science and Technology (NTNU) and one at the University of Oulu in Finland. Ten months were spent at the University of Western Australia, where I analysed zircons for U/Pb dates and joined an additional Australian gold project which benefitted my PhD project.

The PhD study is mainly based on field mapping, structural measurements and sampling. Four summers were spent in the Rombaken Tectonic Window with all conditions of weather from snow to hot summer days. Most localities were remote which involved lots of walking, camping and carrying in high latitude (north) mountain areas.

The included papers are written by myself under guidance of my supervisors, Are Korneliussen and Leon Bagas. The papers are placed in a natural order with themes of: I) A structural study, II) Geochemical, geochronological and tectonic study, III) Spatial relationship between mineral deposits and structures in the field area, and IV) a regional perspective.

After much sweat and many tears, fights, kindness, laughs and cries, I have finally got to the point where there is only light and no tunnels. I can look back at great and hard working years with many new experiences and great acquaintances on the way.

List of publications

I. Angvik, T. L.*, Bergh, S.G. and Henderson, I.H.C.; (manuscript). Svecofennian oblique transpression and strain partitioning in a Paleoproterozoic mid-crustal granite-greenstone setting: An example from the Rombak Tectonic Window, North Norway.

II. Angvik, T. L.*, Bagas, L. and Korneliussen, A.; (manuscript). Geochemical evidence for arc-related setting of Paleoproterozoic (1790 Ga) volcano-sedimentary and plutonic rocks of the Rombak Tectonic Window.

III. Angvik, T. L.*, Sandstad, J. S. and Sundblad, K.; (manuscript). The timing of sulphide deposits and their spatial relation to the Rombaken-Skjomen Shear Zone, northern Norway.

IV. Angvik, T. L.*, Henderson, I.H.C. and Bergh, S. G.; (manuscript). Svecofennian shear zone networks of the Rombak Tectonic Window, North Norway: Structural architecture and regional correlation with the Fennoscandian shield.

Conference proceedings:

Larsen, T., Sundblad, K., Henderson, I.H.C., Bergh, S. G., Bagas, L., Sandstad, J. S., Andersen, T. and Simonsen, S, 2013. Recognition of Svecofennian sulphide bearing crust in the Rombak region, northern Norway. Abstract Norwegian Winter Meeting, Geological Society of Norway.

Korneliussen, A., Larsen, T. and Bagas, L., 2013. On the Paleoproterozoic Andeans-type volcano-sedimentary setting of the Rombak basement window in northern Norway, and the relevance for gold deposits. Abstract Norwegian Winter Meeting, Geological Society of Norway.

Larsen, T., Bergh, S.G. & Henderson, I.H.C., 2012. A model of tectonic transpression and strain partitioning for Paleoproterozoic ductile shear zones in the Rombak tectonic window, northern Norway. 34th International Geological Congress (IGC), Brisbane, Australia, 5-10 August 2012.

Larsen, T., Sundblad, K. & Sandstad, J.S., 2012. Geochemical evidence for genesis of the Au occurrences along the Svecokarelian Rombaken-Skjomen shear zone, northern Norway. 34th International Geological Congress (IGC), Brisbane, Australia, 5-10 August 2012.

Larsen, T., Henderson, I.H.C., Sandstad, J. S,. Bergh, S. G., 2011. Svecofennian deformation and associated shear zone related sulphide mineralisation in the Rombak Tectonic Window, North Norway. Abstract Norwegian Winter Meeting, Geological Society of Norway.

Larsen, T., Bergh, S. G., Henderson, I.H.C., Korneliussen, A., Sandstad, J. S. & Kullerud, K., 2010. Svecofennian structural development and metallogenesis of Paleoproterozoic volcano-sedimentary rocks of the Rombak Tectonic window. Abstract 29th Nordic Geological Winter Meeting, Geological Society of Norway.

Popularisation

NRK Newton, 2014. Gull i mobiler. National television, NRK Newton, 02.02.2014. http://tv.nrk.no/serie/newton/dmpv74000414/02-02-2014

Larsen, T., 2013. Smart og full av gull - Er du en av de som sitter med kommodeskuffen full av brukte mobiltelefoner? Da er du kanskje rikere enn du trodde. Din og min smart telefon er nemlig spekket med edle metaller. NGU official webpage, 17. september, 2013.

* The authors name has changed from Tine Larsen to Tine Larsen Angvik during the process of writing the PhD.

Acknowledgements

I would first of all like to thank my supervisors Iain Henderson and Steffen Bergh for their support, scientific discussions for structural geology and patience with my writing skills to develop. I would also like to thank my supervisors in mineral deposit geology; Jan Sverre Sandstad and Krister Sundblad.

Large thanks to NGU for giving me the opportunity of work and for financing of this Ph.D study. NGU have further encouraged me to visit the University of Western Australia and to work, collaborate and build my own scientific network. In Australia I got in touch with Dr. Leon Bagas who included me within the University and gave me valuable help and support with the SHRIMP II zircon U/Pb dating.

Thanks to the department of Mineral Resources at NGU which have been very supportive and understanding through the whole PhD. process. Thanks to Are Korneliussen for providing me with his geochemistry data. Thanks to Peter Ihlen for reading through my manuscript with excellent constructive comments. Thanks to Krister Sundblad for constructive discussions in field and for correcting a manuscript. Thanks to my field assistants and to "Bob" who kindly stepped in over night when one assistant had to leave. Thanks to Bjørn Wissing at the NGU lab for always being positive and available when I was in need of help. Thanks to Trond Slagstad for scientific advice. Thanks to Ben Snook for correcting my English in the introduction chapter. Thanks to Agnes Raaness for music advice. Thanks to all my friends for personal advice.

Last, I would like to thank my family for all their support and a special thanks is for my boyfriend Rikard who has done a million small things to support me in my everyday life.

1. Introduction

The relationship between mineral deposits and structural evolution are known to be closely related (e.g. Robb, 2005). This necessitates the need to understand the large scale tectonics which will lead to knowledge of the local tectonics, structural development and chronology in order to understand the location and distribution of mineralisation.

1.1 Precambrian tectonic models

The Precambrian is the first time period of the Earth's crust and marks the start of plate tectonics. There are still open questions of when, how and why plate tectonics developed (e.g. Cawood et al., 2006; Kranandonk, 2010). The young hot Earth is believed to be different to the modern Earth in terms of the proportions of mantle heat, little or no oxygen, calcareous based life and a different atmosphere (Gerya, 2014 and references therein). There is also ongoing debate as to whether the onset of tectonism was derived from modern horizontal subduction driven tectonism or vertical movements with crustal diapirism, vigorous mantle convection or plume derived magmatism (e.g. de Wit, 1998; Hamilton, 1998).

There are mainly two large tectonic features that dominates the evolution of Precambrian tectonism. These are the break-up of one or several large supercontinents and the onset of active margins and orogenies. The continental breakup led to basin development, ocean floor spreading and sedimentation and the orogenies were a result of processes involving subduction, ocean arcs, back arc basins, volcanism and magma plumes.

1.1.1 Late Archean breakup of the supercontinent

The late Archean was dominated by the breakup of the supercontinent(s) (Bleeker, 2003). The break-up of the continent(s) were responsible for the formation of a number of Archean greenstone belts around the world (e.g. Condie, 1981; Kranedonk et al., 2009). The rocks in these basins are closely associated with iron oxide mineralisation (BIF) most likely because the iron content in the oceans was high. Oxygen from micro organisms reacted with the iron, and iron was precipitated and deposited on the ocean floor together with marine sediments (e.g. Barley et al., 2005; Groves & Bierlein, 2007; Cloud, 2008). The Archean basins and BIF deposits were commonly accreted onto a continent and intruded by granites.

1.1.2 Archean and Proterozoic orogenies

Accretionary and collisional orogenies are the two main orogenic types during the Precambrian. Accretionary orogens contributes largely to continental growth and form by the subduction of oceanic crust on an active continental margin that also incorporates material from all crustal fragments (Cawood et al., 2014). The average accretionary orogen lifespan is approximately 70–700 My in the Archean and 50–100 My in pre-1 Ga Proterozoic orogens. The Torngat Orogen in Canada (Girard, 1993), and the Svecofennian Orogen in Fennoscandia (Beunk & Page, 2001) are examples of Precambrian accretionary belts. During super-continental assembly, many post-Archean accretionary orogens tend to terminate by continent-continent collision (Condie, 2007). It has been demonstrated that accretionary orogens are globally important to mineral deposits (Groves & Bierlein, 2007).

Collisional orogenies started to develop during the late Proterozoic and essentially consist of two continents colliding (e.g. Hamilton, 1998). The collision is believed to be the end member of an ocean closure, the last stage of the Wilson cycle. Collisional orogenies are narrower than accretionary orogens and do not contribute to crustal growth (e.g. Windley, 1992; Vaughan et al., 2005). Ultra high pressure metamorphic continental rocks are an important characteristic from a modern type collisional orogen (e.g. Liou et al., 2004) and have at the earliest been found in Neoproterozoic rocks (e.g. Jahn et al., 2001; John et al., 2004). The Canadian Trans-Hudson orogen is an example of an accretionary belt that developed from a continent-continent collision (Lewrya et al., 1994).

1.2 Transpressional tectonic models

The term transpression is used to explain oblique convergent plate margins (e.g. Harland, 1971). The composite nature of transpressional orogens has been modelled and tested mathematically (e.g. Sanderson & Marchini 1984; Tikoff & Fossen 1993). Notably, the concept of strain partitioning of the two end-member styles, (i.e. pure-shear and simple-shear components of the deformation in transpressive settings), is used in order to describe homogenous deformation.

The main structures which develop in such regimes are either separate steep strike- and oblique-slip faults occurring in an anastomosing pattern with both pure shear and simple shear components (e.g. Carreras et al. 2010) or contractional (thrust-related) structures (e.g. Tavernelli et al. 2004). Models have been developed which explain strain partitioning of the steep strike-, oblique-slip and contractional components, including simple shear models (Harland, 1971; Sanderson & Marchini, 1984), monoclinic models (Jones et al., 2004 and references therein), complex triclinic transpression and inclined extrusion models (Davis & Titus, 2011 and references therein). These processes may operate independently or in combination, thus accounting for the usually very complex styles of deformation in transpressive settings. The different transpressive styles and their resulting geometries are outlined below.

1.2.1 Simple shear models

Simple shear is a noncoaxial plain strain, such as when a square is changed into a parallelogram. All sides remain parallel, but the sides have changed length and direction. The top and bottom of the square retain the same size, height and retain the same orientation (Davis & Reynolds, 1996).

1.2.2 Monoclinic models

A monoclinic symmetry model can be explained as a distorted "cube" where two of the angles are not normal to each other, producing either strike- and dip-parallel lineations depending on the amount of accumulated deformation and the angle of convergence across the shear zone (Fossen & Tikoff, 1993; Ghosh, 2001; Dewey, 2002). However, the monoclinic model cannot be used to explain oblique-plunging lineations (Sullivan & Law, 2007; Davis & Titus, 2011).

1.2.3 Coupled boundary model

In a coupled boundary model cleavage/foliation formed during folding and/or lateral shearing will dip away from the center of the shear zone and be vertical in the central, high-strain portion of the shear zone (Dutton, 1997). The margins of the shear zone, on the other hand, will experience the most pronounced pure shear component and the maximum plunge of the lineation (Robin & Cruden, 1994; Dutton, 1997)

1.2.4 Triclinic transpression model

The transpressive triclinic model combines the end-member pure shear and simple shear components, and in such a model all stretching lineations will be oblique to the strike of the shear zones (e.g. Hudleston et al. 1988; Sullivan & Law 2007; Davis et al. 2011).

1.3 Relevant Precambrian tectonic frameworks in the Fennoscandian shield

1.3.1 Archean terrains

The Fennoscandian shield forms the north western part of the East European Craton. The Archean rocks are located in the north eastern part of the shield, in northern Norway, Sweden, Finland and the north western part of Russia. The Archean terrains are intercalated with intrusions and elongated basins from the Proterozoic. In Norway, a large proportion of the Archean rocks are covered with Caledonian thrust nappes and hidden under glacial cover in Sweden (Melquist et al., 1999).

The Archean rocks are dominated by Mesoarchean and Neoarchean rocks. The oldest rocks are found in Finland and Russia (2.8-3.0 Ga). The younger rocks commonly consist of migmatitic tonalite, trondhjemite and granodiorite complexes (predominantly 2.7-2.8 Ga), and volcano-sedimentary greenstone belts from an arc-like environment (c. 2.8 Ga) (Hölttä et al., 2008; Lahtinen et al., 2011). The end of Archean is tectonically dominated by accretion and collision of the Kola province and the Karelian Craton (Hölttä et al., 2008).

1.3.2 Paleoproterozoic rifting

The onset of the Paleoproterozoic was marked by deep weathering, erosion (c. 2.4 Ga) and glaciations of the Archean continent(s) which was followed by a large tectonic rifting event at 2.4-2.1 Ga. The rift event has associated intrusions of mafic dykes and deposition of fluvial, shallow- and deep- marine sediments (Laajoki, 2005: Vulollo & Huhma, 2005; Melezhik, 2006) and is the reason why the Paleoproterozoic rocks are intercalated within the Archean rocks. Rift-related magmatic rocks in central Lapland and Kola suggest that the rifting continued locally until 1.98 Ga (Hanski et al., 2005; Peltonen, 2005).

1.3.3 Paleoproterozoic orogenies

The Lapland-Kola orogen (1.94-1.86 Ga) and the Svecofennian orogen (1.92-1.79 Ga) are the main tectonic events of the Paleoproterozoic (Daly et al., 2006; Lahtinen et al., 2008). The Lapland-Kola orogen consist of large volumes of felsic granulites and a lesser amount of juvenile island arc rocks. The orogen is believed to be a continent-continent collision and is relatively small compared to the Svecofennian Orogen (Daly et al., 2006). The crustal growth of the

Svecofennian is large and is believed to be an accretional compilation of several stages of orogens and tectonic fragments (e.g. Nironen, 1997; Korja et al., 2006; Lahtinen et al., 2008). The fragments consist of island arc and subduction-related and basinal metasedimentary rocks (e.g. Korneliussen & Sawyer, 1989; Sawyer & Korneliussen, 1989; Väisänen & Mänttaäri, 2002). The rocks were accreted on to the continent along an array of major NW to N striking crustal scale shear zones which progressively developed across the Archean and the Paleoproterozoic continent(s) (e.g. Larsen et al., 2013; Angvik, 2014 manuscript included) . These shear zones have been found to be interesting for orogenic gold prospecting (e.g. Bark & Weihed, 2007; Eilu et al., 2014). The orogeny has two metamorphic peaks at 1.88-1.87 and 1.83-1.80 Ga which are separated by an unconformity with lateritic paleo soils (Lahtinen & Nironen, 2010). Late- to post-collisional granites (c. 1.8 Ga) are found across the whole of Fennoscandia from Russia to Norway and are closely related to deformation-related mineralisation from the orogeny (e.g. Eklund et al., 1998).

1.3.4 Caledonian Orogeny

The Caledonian Orogeny was a modern style continent-continent collision between the Laurentia and Baltica continents during the Ordovician and Silurian. It is characterised by Phanerozoic rocks from the Iapetus Ocean forming a shallow dipping nappe wedge. The far-travelled nappes are remnants from the ocean and fragments from the subducting Baltic plate. The Caledonian nappes were emplaced from the west, over and onto the older Baltic continent and geographically make up a large part of the outcropping surface rocks throughout Norway (e.g. Bryhni & Sturt, 1985). The Paleoproterozoic and Archean rocks in Norway are therefore only possible to study as tectonic windows in Norway, but are in contrary well exposed because of recent glacial erosion. The Caledonian nappes have, to various degrees, reworked the underlying Paleoproterozoic basement. The increased complexity of structures and associated mineralisation associated with Caledonian re-working should always be considered (e.g. Larsen et al., 2010; Torgersen et al., 2013).

1.4 Relationships of ore deposits and the Precambrian tectonic models in the Fennoscandian shield

The Precambrian ore deposits in Fennoscandia are closely related to the tectonic growth of the Fennoscandian shield and genetic models of the deposits are intimately associated with the tectonic evolution (e.g. Weihed et al., 2005). The Precambrian ore deposits are accumulated mainly in the Proterozoic crust, but several important deposits are also found in the Archean crust. This may be due to under exploration and the lack of accessibility to areas or outcrop (e.g. Weihed et al., 2005).

2. Study area and objectives of the study

2.1 Study area

The study area is, the Rombak tectonic Window (RTW) is located east of the town of Narvik in Northern Norway and is a partly remote and alpine mountain area close to and across the border into Sweden. The rocks are a Paleoproterozoic basement culmination as an tectonic inlier surrounded by Caledonian thrust nappes. The newly glaciated area provides rocks with good exposure and outcrops.

2.2 Objectives of the study

Structural controls of mineral deposits have received considerable attention in the world and are an important aspect for mineral exploration. Fluids and melts are carriers of valuable elements that are trapped, cooled and deposited along structures (e.g. Robb, 2005). The knowledge of structural control of the RTW has been poorly known (Korneliussen et al., 1986), but mineral prospecting for gold and sulphides has been active for more than a hundred years in the area (e.g. Blomlie, 2011).

The main objective of this study is to evaluate the structural, tectonic and sulphide deposit styles within the RTW and develop a genetic model to spatially understand the locations of the gold and sulphides in relation to the structures.

To accomplish this, we combined sampling, structural and bedrock mapping from the field with geophysical data in the light of previous work. The unusually well exposed rocks in the RTW provides peculiar information on structures and mineralisation. The knowledge from the RTW will contribute to understanding similar, but more poorly exposed areas, for example in Sweden, Finland or Australia. The results and conclusions of this study may also lead to potential finds of valuable gold or sulphide deposits in the RTW and other areas.

The main objective was approached through four different aspects:

1. **Structural study of the Rombaken Tectonic Window**

   The first part of the study combined helicopter born EM and Radiometric data with bedrock and structural field mapping. The study focuses mainly on the structural development of the area. The integration of the data resulted in a structural model involving four different stages of deformation have which developed during the Svecofennian orogeny.

2. **Geochronology and tectonic study**

   The second part of the study focuses on the geochronology and tectonic development of the sedimentary and magmatic rocks in the RTW. Zircons from mutually crosscutting syn-tectonic granites was used to establish the timing of deformation and was integrated with existing geochemical data. This part of the study resulted in absolute constraints on the tectonic model developed above, underpinning the complex structural evolution.

3. **Genetic and structurally spatial relationships for mineral deposits**

   A large part of the study focuses on the interplay between the structural development and the gold and sulphide deposits in the area. Field studies, geochemical sampling and the established structural model were used to understand the timing of, and relationship of the mineralisation to the deformation. A metallo-genetic model and spatial relationships where established in relation to the structural evolution.

4. **Regional perspective**

The last part of the study combines the newly-developed model of the Rombak Tectonic Window within a regional tectonic perspective. The tectono-metallogenetic model for the RTW is used to understand the development of the Paleoproterozoic evolution in the western part of the Fennoscandian shield and integrates previous studies from Finland, Sweden and Norway. This resulted in a new regional tectonic model for the Paleoproterozoic of the Fennoscandian shield combining structural, tectonic and genetic models of mineralisation.

3. Methods

3.1 Field mapping and structural analysis

Four summers and a total of 19 weeks of fieldwork were undertaken within the RTW. Detailed fieldwork was concentrated at the Haugfjellet, Norddalen and Gautelis localities, but visits have also been to Sildvika, Rombaksbotten, the West Troms gneiss complex and the Mauken Tectonic Window. All localities have excellent exposure and outcrops with freshly glaciated rocks.The main focus has been bedrock and structural mapping, describing old prospects and showings and picking samples for thin-section, geochemistry and age relations. Bedrock mapping was especially emphasised in Norddalen and Gautelis because of the lack of details and connection to structures.

Extensive structural field analyses was done at all the localities with a Brunton compass measuring orientations of the observed structures, using the right hand rule technique with strike and dip. The kinematics was determined after kinematic indicators such as sigma clasts, extensional crenulation cleavage, C-S structures, tension gashes, displacements, asymmetric boudinage and folds in both x and y plane. The structural data were categorised into different localities and structural domains. The orientations where plotted as poles to planes, lineations, great circles and contours in stereo plots. Polar stereo nets were used, with the lower hemisphere Schmidt net projection using a prototype plot program developed at University of Tromsø. All the structural data was put together with the new bedrock map for interpretation on the local scale and then and further for interpretation on a regional scale which resulted in a structural evolution model for RTW.

Single orientated and non-orientated samples, and systematic collection of samples across sections, were taken from areas of special interests. The samples were further brought to the lab for preparation for geochemistry, microscopy or geochronology.

Mapping of the mineral deposits was carried out by visits to several older showings and one dismantled mine. They were described visually, structurally and sampled for geochemistry and thin sections. Samples were also taken at other localities where the concentration of sulphides was high. Additionally, a handheld XRF was used at selected localities.

3.2 Geophysics

Helicopter-borne magnetic, EM and Radiometric measurements were carried out over most of the RTW in August-September 2011 (Rodinov et al., 2012). The data were processed by the geophysics team at NGU. Because the instruments were partly destroyed during the flight, the EM data contains a signal with a higher proportion of noise. This made the geological interpretation of the EM data more challenging.

3.3 Drill core logging

Drill core BH-1-1995 from Haugfjellet was logged at the Løkken drill core facility. The core was logged on a scale 1:20. The core was described with emphasis on sedimentation, deformation and sulphide mineralisation. A handheld XRF (Thermo Niton XL3t) was used to analyse the core every 20cm for light and heavy elements (Mining mode).

The cores from Gautelis were poorly marked and did not correspond to the rocks observed in field. Detailed analyses of these cores was therefore not carried out.

3.4 Whole rock analysis

Whole rock analysis of samples from the RTW are a compilation of pre-existing samples and new samples collected during the course of this study. The new samples were used for investigating the sulphide mineral content and the relation to the structures (manuscript (IV)), the older samples were taken from the NGU database and Korneliussen et al. (1986) from metasedimentary, metavolcanite and intrusive rock samples. These were plotted into geochemical diagrams in order to establish their tectonic setting at the time of deposition and together with the age relationships, develop a detailed progressive tectonic model for the RTW through the Archean and Paleoproterozoic time. The samples have been collected over years and sent to different labs for analysis.

The new samples were prepared by crushing and milling at the Geological Survey of Norway (NGU). The samples were sent to ALS in Sweden for whole rock and trace elements analysis. The major oxides concentrations were determined by wavelength-dispersive XRF on fused disks (after Norrish & Hutton, 1969). Trace elements Y, Zr, Nb, Rb, Ba, Sr Pb, V, Cu, Zn, and Ni were determined by wavelength-dispersive XRF on a pressed pellet (after Norrish & Chappell, 1997).

Sc, Co, Cr, Cs, Hf, Ta, Th, U, La, Ce, Nd, Sm, Eu, Tb, Yb and Lu, were analysed by instrumental neutron activation analysis (NAA). The samples were plot in a spider diagram with selected metals, and normalised to the average composition of unmineralised and undeformed metagreywacke sampled at different localities at Haugfjellet and to the host rock in the undeformed and unmineralised area nearby the sample in order to determine metal anomalies locally and more regional compared to the developed structural model.

3.5 Optical microscopy and Scanning Electron Microscope (SEM)

Polished and unpolished thin sections where prepared by the lab at NGU. The samples were examined in transmitted and reflected light at the NGU. The microscope used was a Zeiss Axioplan 2 Imaging, Hal 100. The SEM type Leo 1450VP was used for analysing selected areas in the thin section for composition and mineral recognition. The analysis was semi-quantitative and was carried out using Oxford instrument EDS with $10mm^2$ and accelerating voltage 15kV.

3.6 SHRIMP U-Pb zircon dating

The samples were picked from the granites based on their syntectonic relationship with the structures. Observations of mutual crosscutting relationships between the D_3-D_4 structures and the granites where documented and by dating the zircons of the granites, the framework for the structural development would also have an approximate age determination.

Samples for zircon dating were crushed, milled and separated at NGU lab. Zircon crystals were handpicked from the heavy mineral separate with the aid of a binocular microscope. In general, up to 150–200 representative crystals are selected for igneous rocks, and all grains are picked for sedimentary rocks containing detrital zircons. Crystals are mounted in 25 mm diameter Epofix epoxy disks, and the mount surface polished to expose the grain interiors.

Each mount typically contains minerals from three different samples, which are aligned in rows, together with several crystals or crystal fragments of reference materials (BR266 and OGC1 were used as U–Pb calibration standards for zircon).

Mount-making and backscattered electron and cathodoluminescence (CL) imaging were completed at the Center for Microscopy, Characterisation and Analysis at the University of

Western Australia. Gold coating and SHRIMP analysis were carried out at the John de Laeter Center for Isotope Research at Curtin University in Western Australia.

Zircon grains were analysed using the SHRIMP-II facility housed within the John de Laeter Centre for Mass Spectrometry at Curtin University of Technology. Procedures for SHRIMP U–Pb isotopic analysis followed those described by Compston et al. (1984), and Stern (2009). Targeted grains were sputtered using an O2– primary beam with a 30 µm–diameter spot, and six cycles of sequential measurements of peaks in the secondary ion beam at mass stations 196 (90Zr2O+), 204 (204Pb+), 204.1 (background), 206 (206Pb+), 207 (207Pb+), 208 (208Pb+), 238 (238U+), 248 (232ThO+) and 254 (238UO+) were made using an electron multiplier in pulse counting mode.

The effect of Pb/U fractionation in measurements of the unknowns was corrected by reference to interspersed analyses of the laboratory U–Pb standard zircon BR266 (U = 909 ppm, 207Pb/206Pb age = 559; Stern, 2001) and OGC1 (207Pb/206Pb age = 3465 Ma; Stern et al., 2009).

The measured 204Pb was used for common Pb correction. The data was compiled using the ISOPLOT 3.0 and Squid 1.0 programs (Ludwig, 2003; Ludwig, 2009). Individual analyses are reported with 2 σ uncertainties; weighted averages of age are also reported at the confidence of 2 σ .

3.7 Pb/Pb isotope studies

Pb/Pb isotope studies are useful for understanding the tectonic history of the Pb minerals. By understanding the half-lives of the parent generating Pb isotopes you can get information of differentiation events and time constrains.

7 galena samples were picked from Sildvika, Haugfjellet and Cunojavri and sent further to the University of Oslo for analysis. 2-3 grains of galena washed 10 sec in 4N HNO3, then in MQ water. Two drops of 4N HNO3 were added. After 30 sec 50 µl were pipette out and thinned with 2% HNO3 to analysable concentration. For secondary dissolution, the same record was followed, but the 50 µl that were pipette out was damped before dilution.

The analyses were done on Nu Plasma MC-ICPMS. First 30 sec of background measurements with ESA deflector before mass of 208 and 201 was measured. The background signal was deducted and corrected for Hg by 204Hg/202Hg = 0.2299. Thallium is added the samples and standard for correction for mass fractionation, an adjusted 205/203 = 2.38895 was used.

4. Summary of the papers and their synthesis

4.1. Paper I

Angvik, T. L., Bergh, S.G. and Henderson, I.H.C.; (manuscript). Svecofennian oblique transpression and strain partitioning in a Paleoproterozoic mid-crustal granite- greenstone setting: An example from the Rombak Tectonic Window, North Norway.

The RTW is situated within the Paleozoic Caledonian thrust nappes in Northern Norway. The Rombak-Skjomen shear zone (RSSZ) is a major crustal scale Paleoproterozoic ductile structure that cuts through Paleoproterozoic metasedimentary and felsic igneous rocks of the RTW. This excellently exposed tectonic window is an important link to the understanding of both the basement rock outliers in western Norway and the juvenile Paleoproterozoic rocks of the Fennoscandian shield to the east in Finland and Sweden.

The main deformation in the Rombak window is of Svecofennian age (1.92-1.75 Ga) and located within several N-S trending metasedimentary belts which are the locus for ductile folds, thrusts and anastomosing shear zones. The RSSZ has a complex structural evolution and geometry strain partitioning with four phases of deformation; early pure shear folding event (D_1), pure shear dominated fold-thrust belt event (D_2), two phases of combined simple shear and pure shear oblique systems with a conjugate set of N-S trending sinistral reverse oblique-slip shear zones (D_3), and a NE-SW dextral reverse oblique-slip shear zone event (D_4) where the fold-thrust belt is nearly fully overprinted. Syn-Tectonic granites have a complex inter-relationship with this deformation sequence. The crosscutting relationship between the granite and the structures shows that the granite cuts the fold-thrust belt and parts of the oblique-slip deformation and can also be locally cut by the D_4 event consistent with syn- to late orogenic plutonism.

We present a strain partitioning model for the RSSZ where high and low strain domains interacting, in an overall oblique transpressional setting.Strain partitioning developed progressively from a monoclinic transpressional symmetry with pure shear and the development of an initial fold-thrust belt to a triclinic transpressional symmetry with combined simple shear and pure shear resulting in oblique-slip shear zones. In this scenario the anastomosing arrays of steep mylonitic shear zones (D_3) may have formed from a strain pattern of triclinic deformation superimposed on the earlier monoclinic fold-thrust belt deformation (D_1-D_2), leaving isolated domains of the monoclinic deformation intact. The D_1-D_4 progressive structural events led to a complex outcrop pattern with remnant blocks of fold-thrust belt segmented and attenuated by two later phases of steep reverse oblique-slip ductile shear zone fabrics which shows a regional conjugate pattern with the direction of main principal shortening in a WNW-ESE direction.

Regional EM and radiometric data support the tectonic model and demonstrate that graphitic shales and potentially mineralised bodies in the fold-thrust belt have been dextrally displaced up to 6 km along the strike of the D_4 shear zones, demonstrating the structural control on both the mineralisation processes and the subsequent post-mineralisation modification The understanding of the structural evolution of the RSSZ in the Rombak Tectonic Window is important in order to understand the Svecofennian orogeny in the Norwegian portion of the Fennoscandian shield and to possibly be able to link the structures to the east and also to understand how progressive transpressive margins may develop in general.

4.2. Paper II

Angvik, T. L., Bagas, L. and Korneliussen, A.; (manuscript). Geochemical evidence for arc-related setting of Paleoproterozoic (1790 Ga) volcano-sedimentary and plutonic rocks of the Rombak Tectonic Window

This paper presents geochemical and geochronological data that underpins the structural model presented in Paper I. The RTW is an inlier exposed through Caledonian nappes and represents the western-extension of the Proterozoic Fennoscandian Shield containing similar aged granites, which are exposed in Sweden and Finland to the east. Detailed field analysis in Paper I demonstrates that the granites are syn- to post-tectonic with respect to large N-S trending oblique-slip structures within the inlier, and therefore our age determinations bracket both the

timing of the deformation. The geochemistry shows a complex geology with strongly deformed meta-sedimentary belts consisting of turbeditic sequences (greywacke and shale), graphitic shale, quartzite, conglomerate, and marble. These rocks are interbedded with volcanic successions of mafic/intermediate to felsic volcanites.
The same geochemical characteristic outline of the metasedimentary and metavolcanic rocks. The ca. 2000 – 1867 Ma metamorphosed greywacke and shale plot within an active continental margin or island arc setting in discrimination diagrams. The ca. 1900 Ma mafic and ultramafic rocks in the RTW plot predominantly in the continental to oceanic arc fields. We suggest that the metasedimentary rocks in the RTW were deposited in an island arc to active continental margin setting, from a provenance dominated by mafic to intermediate and felsic volcanic rocks derived from the mantle.
The ca. 1788 Ma felsic intrusive rocks can be classified as I-type, partially fractionated A-type granites (Fig. J). These rocks plot in the late-orogenic to anorogenic fields associated with a volcanic-arc to within plate setting (Fig. L), which is similar for the ca. 1900 Ma metasedimentary and volcanic units. The granite was intruding and melting those units during the accretion and Svecofennian orogeny and formed in late- to post-collisional settings.

Sensitive high-resolution ion-microprobe U–Pb dating of zircons from monzogranites from the RTW in north-central Norway yielded and age of 1786 ± 8 – 1790 ± 8 Ma, which are within error of each other.

We suggest that the rocks have developed in one progressive tectonic event. From an island arc affinity with mafic intrusions, intermediate volcanites developing and with the tonalite basement as a source. Through progression of the island arc, it is changing into a continental arc with felsic volcanites and granite plutonism which are all accreted on to the Baltic continent, a total progression in a period of a ~70 million years.

4.3. Paper III

Angvik, T. L. and Sandstad, J. S; (manuscript). The timing of sulphide deposits and their spatial relation to the Rombaken-Skjomen Shear Zone, northern Norway.

The Rombaken Tectonic Window (RTW) is a Paleoproterozoic inlier within the Caledonian nappes of northern Norway. The bedrock consists of Svecofennian granites intruded into metasedimentary and metavolcanic rocks, which appear as N-S trending parallel belts widening and thickening along strike. Sulphide mineralisations in the RTW, including As-Au, Cu and Pb-Zn, have long been explored for gold in the area and the need for a better understanding of the geological evolution of the area has increased. Recent tectonic and structural models have verified a large scale Svecofennian Rombaken-Skjomen shear zone (RSSZ), which can be traced across the whole window and into Sweden. The model consists of four deformation events that includes two N-S striking, east verging fold-thrust (D_1-D_2) and two oblique-slip events with steep ductile N-S striking (D_3) and NE-SW (D_4) striking shear zones. Several known sulphide mineralisations are found along, within and near this regional shear zone. In the present study we have studied several of these for their genesis, timing and spatial relationship to the RSSZ. We found at least four stages of mineralisation including; 1) D_0 syngenetic bedding parallel Zn-Pb SEDEX deposits, 2) D_3-D_4 syntectonic metasomatic As-Au-Fe deposit and 3) D_3-D_4 orogenic gold, both along the regional shear zone, including remobilisation of the SEDEX mineralisations and as 4) D_3-D_4 Cu-Au in late Svecofennian quartz veins. The formation of most of the sulphide mineralisations in RTW is very complex with several stages of remobilisation and deformation, that are spatially and temporally linked to the development of RSSZ

4.4 Paper IV

Angvik, T. L., Henderson, I.H.C. and Bergh, S. G.; (manuscript). Svecofennian shear zone networks of the Rombak Tectonic Window, North Norway: Structural architecture and regional correlation with the Fennoscandian shield.

The northern part of the Fennoscandian shield is made of several domains of varying ages from Archean to Paleoproterozoic age. These domains comprise areas within the Kola province in Russia and the Northern part of Norway, Sweden and Finland. The evolution of these rocks is extremely complex and is dominated by several continental break-ups, the development of several micro continents, island arc development and the closing of the Kola ocean with subsequent subduction, accretion and orogeny. Globally, Archean and Paleoproterozoic crust is commonly juvenile and the Fennoscandian shield is regarded as having a high mineral potential.

The Fennoscandian shield in Norway occurs as inliers and outliers under the Caledonian thrust nappes and has not been included in previous regional studies. Because of new knowledge (Paper I) of the structural relationship to the sulphide mineralisation (Paper III) in the Rombak Tectonic Window (RTW) and the similarities of the rocks elsewhere, it is demonstrated in this paper that the Norwegian part of the Fennoscandian shield is directly related to the rocks found in particular Sweden and Finland. The rocks show evidence of the same break-up activity in the Archean to one or several rifted micro continents filled with Paleoproterozoic basin sediments and the development of island arcs and back arc basins creating volcanoclastic rocks. The Archean and Paleoproterozoic boundary (The Luleå-Jokkmokk zone) can be traced in an arcuate geometry, bending northwards towards the RTW and into the Senja Shear Belt. In addition, the Bothnian basin and the Arvidsjaur sediments can also be traced with a similar geometry towards the RTW. During subduction, accretion and orogeny almost identical ductile structures developed across the Northern Fennoscandia during the Svecofennian Orogeny. Striking similarities are also seen in the nature of the structural evolution with the initial development of fold-thrust structures which were subsequently overprinted by strike- or oblique-slip shear zones. These shear zones follow an overall NW-SE regional trend, but are in Norway deflected into a more N-S trend. This paper documents that along the Archean-Paleoproterozoic boundary in Norway and Sweden there are several occurrences of steep NE-SW striking ductile shear zones which crosscut all earlier structures. A major finding of this paper is that these structures are interpreted to have developed during the final stage of the orogeny forming a secondary orocline which deflects the orogen from a NW to a N-trend. The complete orogenic system has made a major and complex impact on the juvenile crust and is responsible for the creation and remobilisation of numerous deposits in the whole of the Fennoscandian crust. By improving the understanding these major structures and their relationship to mineralisation we may be able to point out areas of high mineral potential in the future.

5.0 Synthesis

5.1 Formation and tectonic evolution of the RTW

The rocks of the RTW show a complex geology interpreted to have developed in one progressive tectonic event from those with an island arc affinity, with mafic intrusions and intermediate volcanites, forming a transition into a continental arc affinity with felsic volcanites and granite plutonism. This complex sequence was then accreted eastwards on to the Baltic continent.

The lithologies consist of a deformed metasedimentary belt with turbiditic sequences (greywacke and shale), graphitic shale, quartzite, conglomerate, and marble. The metasedimentary rocks are interbedded with volcanic successions of mafic/intermediate to felsic volcanites. These belts occur as rafts within a coarse grained weakly deformed granite.

The geochemical characteristics of the metasedimentary and metavolcanic rocks are similar. The ca. 2000 – 1867 Ma metamorphosed greywacke and shale display an active continental margin or island arc setting. The ca. 1900 Ma mafic and ultramafic rocks of the RTW demonstrate continental to oceanic arc affinity. The metasedimentary rocks in the RTW were deposited in an island arc to active continental margin setting, developing from a provenance dominated by mafic to intermediate and felsic volcanic rocks derived from the mantle.

The ca. 1788 Ma felsic intrusive rocks can be classified as I-type, partially fractionated A-type granites and are interpreted as late-orogenic to anorogenic associated with a volcanic-arc to within plate setting, similar to the ca. 1900 Ma metasedimentary and volcanic units. The granite was intruding and assimilating the metasedimentary units and formed in late- to post-collisional settings. Field observations, which show that the RTW granites are syntectonic and intimately associated with the complex deformation sequence, in combination with sensitive high-resolution ion-microprobe U–Pb dating of zircons from monzo-granites yielded ages of 1786 ± 8 to 1790 ± 8 Ma, which are also interpreted to be the age of deformation and accretion associated with the Svecofennian orogeny.

5.2 Structural evolution of RTW

A complex, multi-stage crustal-scale ductile shear zone array has been documented to intersect the RTW. These structures are all of Svecofennian age and developed during four stages of deformation. We present a strain partitioning model of interacting high-low strain domains for the RSSZ, in an overall oblique transpressional setting.The strain partitioning may have developed from a monoclinic transpressional symmetry (pure shear or oblique-slip shear) to a triclinic transpressional symmetry during progressive deformation through time.

D_1 and D_2 represents the initiation of the Svecofennian deformation in the RTW. The D_1 structures consist of an early pure shear folding with isoclinal, S-striking and east verging folds. These are refolded by a pure shear fold-thrust belt event (D_2), dominated by S-striking upright, east verging and open folds. Throughout the progression of the accretion the structures have developed into combined simple shear and pure shear oblique systems with a conjugate set of N-S trending, steep and ductile oblique-slip shear zones (D_3) with a dominantly sinistral shear sense that follow the strike direction of the D_2 fold limbs and segment, fold and steepen parts of the earlier-formed structures. The D_4 event is represent by steep, ductile, NE-SW dextral oblique-slip shear zones that obliquely cut and attenuate both the D_1-D_2 fold-thrust event and the subsequent D_3 oblique ductile shear zones.

In our strain partitioning model, the four progressive structural events lead to a complex outcrop pattern of remnant fold-thrust belt blocks which have been segmented and attenuated by two later phases of steep oblique-slip ductile shear zone fabrics. These show a regional conjugate pattern with the direction of main principal shortening in a WNW-ESE direction. This complex, multi-stage ductile transpression is collectively termed the Rombak-Skjomen Shear Zone (RSSZ).

5.3 Spatial relationship of sulphide deposits to RSSZ

Several of the known sulphide mineralisations found along the RSSZ have been studied for their genesis, timing and spatial relationship to the shear zone. At least four different styles of mineralisation are found. These are: 1) syn-genetic bedding parallel Zn-Pb SEDEX deposits, 2) D_3-D_4 syntectonic metasomatic As-Au deposit and 3) orogenic gold both along the D_3-D_4 regional shear zone including remobilised SEDEX and 4) Cu-Au in late D_3-D_4 Svecofennian quartz veins. The SEDEX deposits are the oldest deposits found along the beds with primary structures. These deposits are interpreted to be of syn-genetic origin prior to the complex Svecofennian deformation sequence outlined above. They are found within the greywacke with

Andean type margin affinity, and may represent the stage before accretion. The SEDEX deposits have however been intersected by the D_3 shear zones and the mineralisation along RSSZ does therefore show complex mineral assemblages. The metasomatic As-Au deposits are found in areas with a relationship with a combination of shear zones, shear zone related dolerite intrusions crosscutting metagreywacke and marble. This deposit type is interpreted to have developed as a result of a combination of fluids transported along the D_3-D_4 shear zones, the heat sourced from the dolerite and the change of pH from the intersection with the marble. Orogenic gold is found with As and remobilised Pb-Zn along the D_3-D_4 shear zones and as a late stage brittle-ductile Cu-Au rich quartz veins which are interpreted to be related to fluids carried along the large shear zone.

It is found that most of the formation of sulphide mineralisation in the RTW is very complex with several stages of remobilisation and deformation that are closely related to the development of dominantly the D_3- D_4 shear zone in space and time. The presented model show how these mineralisations are related to the RSSZ in a regional tectonic setting through time (fig. 1)

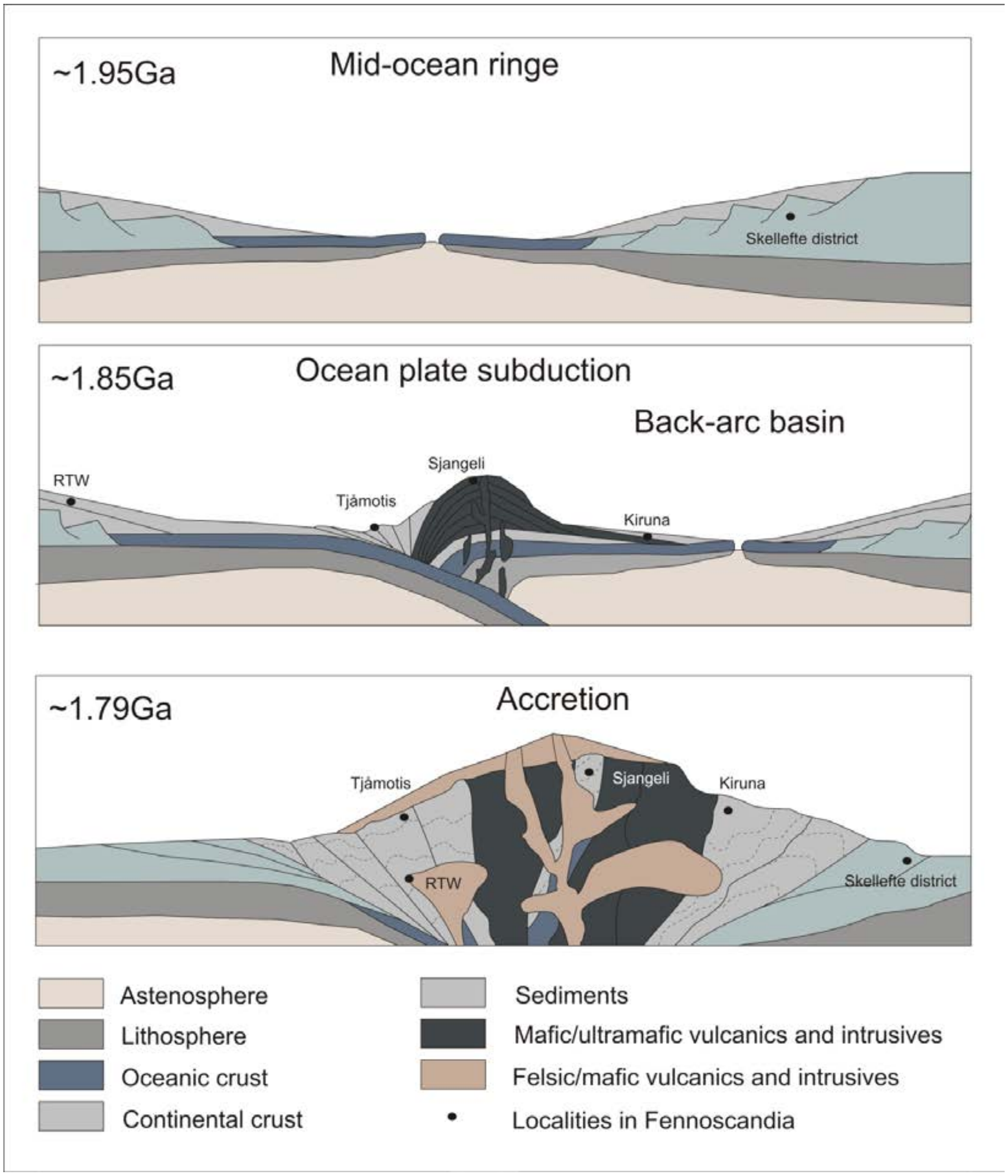

Fig. 1. Tectonic model of the Svecofennian orogeny with timing and spatial relationship to the sulphide and gold deposits in the RTW and nearby in Sweden. The model demonstrates the different stages of a progressive development from basin on an active margin to the accretion and orogeny.

5.4. RTW as a part of the Svecofennian orogeny in Fennoscandia

The evolution of the lithologies of the Fennoscandian shield with respect to regional scale tectonic environment is extremely complex and is dominated by several continental break-ups, development of several micro continents, island arcs and the closing of the Kola ocean with related subduction, accretion and orogeny. The RTW is part of the Fennoscandian shield and remarkable and extensive similarities are observed in the nature and evolution of the Svecofennian structures are observed across the shield. This large orogenic system has had a major and complex impact on the juvenile crust and is responsible for the creation and remobilisation of several deposits across the whole of the Fennoscandian Shield. In consequence, the Norwegian part of the Fennoscandian shield is directly related to the rocks found in particular areas of Sweden and Finland and therefore a regional model is proposed for the Svecofennian shield developing progressively into an orocline geometry.

The Archean rocks in the northern Fennoscandian Shield show evidence of similar break-up activity, fragmenting Archean into several micro-continents. Sedimentary basins filled with Paleoproterozoic sediments and associated island arcs and back arc basins were formed, creating volcanoclastic rocks. The Archean and Paleoproterozoic boundary (The Luleå-Jokkmokk zone) has a NW-SE trend in Sweden but is deflected northwards towards the RTW and into the Senja Shear Belt. A similar deflection is observed in the Bothnian basin and in the Arvidsjaur sediments, which thin out and disappear towards the RTW.

A remarkably similar structural evolution occurred over the whole of northern Fennoscandia, involving the initial development of fold-thrust belt structures followed by cross-cutting oblique-slip shear zones during subduction, accretion and orogeny. These shear zones follow an overall NW-SE trend in Sweden and Finland, but are in Norway deflected into a more N-S trend. Along the Archean-Paleoproterozoic boundary in Norway and Sweden there are several occurrences of steep NE-SW striking oblique-slip shear zones, crosscutting all earlier structures. These structures were developed during the final stage of the orogeny, creating a secondary orocline, deflecting the shear zone array to the north (Fig. 2).

This regional-scale model contributes to a better understanding of the structures that developed during the accretion and evolution of the Svecofennian orogeny. In addition, this model provides a basis for a better understanding of metallogenic processes associated with both syn-tectonic mineralisation and the complex geometries produced of mineralised bodies that are modified by them.

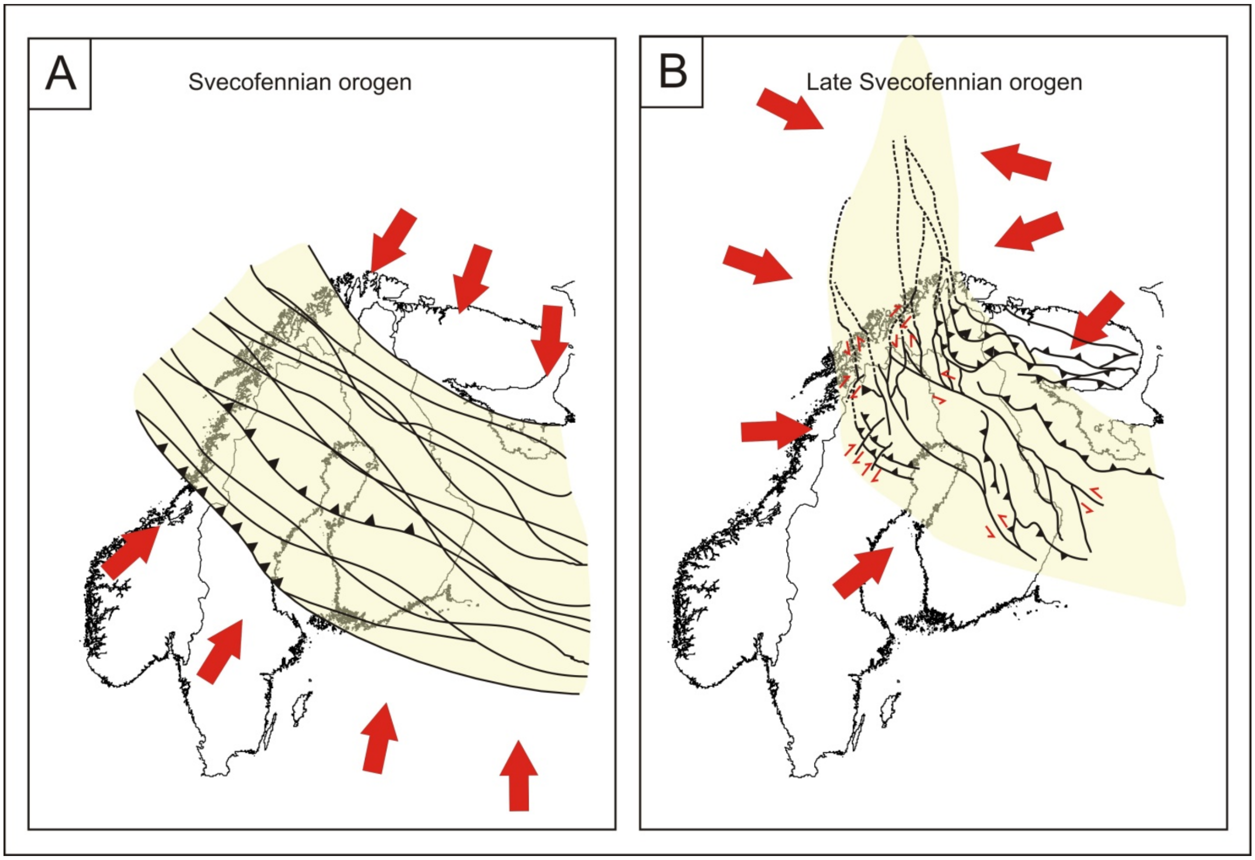

Fig. 2. A tectonic model over the Fennoscandian shield where the early stages of the orogen were dominated by N-S contraction and the late stage of orogeny was dominated by a shift of movement to NE-SW collision which caused the western part to med northwards and developed a secondary orocline model.

6.0 Future work

6.1. Further structural studies

This study was confined to the eastern part of the RTW exclusively in Norway and shows that there is a regional crustal-scale Paleoproterozoic ductile shear zone array (RSSZ)cutting through the full length of the tectonic window. Regional scale magnetic data shows the RSSZ but also several anomaly parallel to it. Similar shear zones show evidence of continuation into Sweden and through areas of high mineral potential. These areas in Sweden have been studied regarding the mineral deposits and their age relationships (e.g. Adamek, 1975; Romer & Boundy, 1988; Romer, 1989).However, no modern structural analysis has been carried out in these areas in Sweden This suggests that the RSSZ continues further into Sweden. continued structural analysis on the Swedish part of the RTW is important to underpin the findings of the current research and to continue to develop an improved regional-scale structural model of the Fennoscandian shield. In addition, an integration of structural observations from the Swedish part of the RTW would lead to a refinement of the regional structural model but also provide the opportunity to discover, as yet, unknown mineral deposits, both in the Swedish part of the RTW and elsewhere.

6.2 Metallogenic studies

Fluid inclusion studies use trapped fluids in a mineral to find the pressure and temperature at the time of mineralisation (e.g. Roedder, 1985). Applying such a study on the gold and sulphide mineralisation in the RTW would help to more fully understand the genetic relationships of the mineralisation.

This study demonstrate that while some mineral deposits within the RTW are syn-genetic, others are clearly remobilised. Fluid inclusion studies would hopefully allow the delineation of syn-genetic mineralisation from remobilised mineralisation allowing the determination of different conditions and genetic relationships of the mineralisation type and style to temperature and pressure.

6.3. 3D structural and metallogenic model

3D modeling is a powerful tool to view and understand the nature and interaction of structures, lithology boundaries and the geometrical extent of mineral deposits.

The RTW is an area with incised topography, an abundance of complexly interacting structures, numerous drill cores and a range of different styles of mineral deposits. Areas with such a wealth of information can be used to create detailed and accurate 3D models. The topography within the RTW provides natural cross sections with information on lithologies and structures, while drill cores give depth information. The geometrical nature of mineral deposits and their relationship to the complex structural evolution can be sampled and plotted.

Such a 3D model would be both a very valuable educational and exploration tool for the RTW, providing easily understandable and accessible data for scientists, prospectors or students. Such a model could additionally be used for calculating more detailed mineral deposit information, particularly deposit size, grade and detailed geometry.

7.0 References

Adamek, P. M. (1975). Geology and Mineralogy of the Kopparåsen Uraninite-sulphide Mineralisation: Norrbotten County, Sweden. Avhandlingar och uppsatser - Sveriges Geologiska Undersökning ; serie C 712.

Bark, G. and Weihed, P. (2007). Orogenic gold in the Lycksele - Storuman ore province, northern Sweden; the Paleoproterozoic Fäboliden deposits. Ore Geology Reviews 32: 431-451.

Barley, M. E., Bekker, A. and Krapez, B. (2005). Late Archean to Early Paleoproterozoic global tectonics, environmental change and the rise of atmospheric oxygen. Earth and Planetary Science Letters 238: 156– 171.

Beunk, F. F. and Page, L. M. (2001). Structural evolution of accretional continental margin of the Paleoproterozoic Svercofennian orogen in southern Sweden. Tectonophysics 339: 67-92.

Bleeker, W. (2003). The late Archean record: puzzle in ca. 35 pieces. Lithos 71: 99–134.

Blomlie, T. (2011). Skatter i fjell - På tur i bergverkshistorien til Ballangen, Evenes, Narvik og Tysfjord. Museum Nord.

Bryhni, I. and Sturt, B. A. (1985). Caledonides of southwestern Norway. In: The Caledonide Orogen—Scandinavia and Related Areas, (eds) D. G. Gee and B. A. Sturt. Wiley and Sons: 89–107.

Carreras, J., Czeck, D. M., Druguet, E. and Hudleston, P. J. (2010). Structure and development of an anastomosing network of ductile shear zones. Journal of Structural Geology 32(5): 656-666.

Cawood, P. A., Kröner, A. and Pisarevsky, S. (2006). Precambrian plate tectonics: Criteria and evidence. GSA Today 16(7).

Cloud, P. (2008). Paleoecological Significance of the Banded Iron-Formation. Economic Geology 68: 1135-1143

Compston, W., Williams, I. S. and Meyer, C. (1984). U–Pb geochronology of zircons from lunar breccia 73217 using a sensitive high mass-resolution ion microprobe. Journal of Geophysical Research 89: 252–534.

Condie, K. C. (1981). Archean greenstone belts. Elsevier Scientific Publishing Company, Amsterdam. Development in Precambrian Geology 3.

Condie, K. C. (2007). Accretionary orogens in space and time. GSA Memoirs 2007 200: 145-158

Daly, J. S., Balagansky, V. V., Timmerman, M. J. and Whitehouse, M. J. (2006). The Lapland-Kola orogen: Paleoproterozoic collision and accretion of the northern Fennoscandian lithosphere. Geological Society, London, Memoirs 2006 32: 579-598.

Davis, G. H. and Reynolds, S. J. (1996). Structural Geology og rocks and regions. John Wiley & sons, inc second edition.

Davis, J. R. and Titus, S. J. (2011). Homogeneous steady deformation: A review of computational techniques. Journal of Structural Geology 33(3): 1046–1062.

de Wit, M. J. (1998). On Archean granites, greenstones, cratons and tectonics: does the evidence demand a verdict? Precambrian Research 91: 181–226.

Dewey, J. F. (2002). Transtension in arcs and orogens. Int. Geol. Rev 44: 402-438.

Dutton, B. J. (1997). Finite strains in transpression zones with no boundary slip. Journal of Structural Geology 19: 1189–1200.

Eilu, P., Sorjonen-Ward, P., Nurmi, P. and Niiranen, T. (2014). A Review of Gold Mineralisation Styles in Finland. Economic Geology 98(7): 1329-1353.

Eklund, O., Konopelko, D., Rutanen, H., Fröjdö, S. and Shebanov, A. D. (1998). 1.8 Ga Svecofennian post-collisional shoshonitic magmatism in the Fennoscandian shield. Lithos 45: 87–108.

Fossen, H. and Tikoff, B. (1993). The deformation matrix for simultaneous simple shearing, pure shearing, and volume change, and its application to transpression/transtension tectonics. Journal of Structural Geology 15: 413-422.

Gerya, T. (2014). Precambrian geodynamics: Concepts and models. Gondwana Research 25: 442–463.

Ghosh, S. K. (2001). Types of transpressional and transtensional deformation. In: Koyi, H.A. & Mancktelow, N.S. (eds) Tectonic Modeling: A Volume in Honor of Hans Ramberg. Geological Society of America Memoir 193: 1–20.

Girard, R. (1993). Orogen-scale strain partitioning and an analogy to shearbands in the Torngat Orogen, northeastern Canadian Shield. Tectonophysics 224: 363–370.

Groves, D. I. and Bierlein, F. P. (2007). Geodynamic settings of mineral deposit systems. Journal of the Geological Society, London 164: 19–30.

Hamilton, W. B. (1998). Archean magmatism and deformation were not products of plate tectonics. Precambrian Research 91: 143–179.

Hanski, E., Huhma, H. and Perttunen, V. (2005). SIMS U-Pb, sm-Nd isotope and geochemical study of arkosite-amfibolite suite, Peräpohja Schist Belt: evidence for ca. 1.98 Ga A-type felsic magmatism in northern Finland. Geological surveu of Finland Bulletin 77: 5-29.

Harland, W. B. (1971). Tectonic transpression in Caledonian Spitsbergen. Geological Magazine 108: 27-41.

Hudleston, P. J., Schultz-Ela, D. and Southwick, D. L. (1988). Transpression in an Archean greenstone belt, northern Minnesota. Canadian Journal of Earth Sciences 25: 1060-1068.

Hölttä, P., Balagansky, V., Garde, A. A., Mertanen, S., Peltonen, P., Slabunov, A., Sorjonen-Ward, P. and Whitehouse, M. (2008). Archean of Greenland and Fennoscandia. . Episodes 31: 13–19.

Jahn, B., Caby, R. and Monie, P. (2001). The oldest UHP eclogites of the world: age of UHP metamorphism, nature of protoliths, and tectonic implications. Chemical Geology 178: 143–158.

John, T., Scherer, E. E., Haase, K. and Schenk, V. (2004). Trace element fractionation during fluid-induced eclogitization in a subducting slab: trace element and Lu–Hf–Sm–Nd isotope systematics. Earth and Planetary Science Letters 227: 441–456.

Jones, R. R., Holdsworth, R. E., Clegg, P., McCaffrey, K. and Tavarnelli, E. (2004). Inclined transpression. Journal of Structural Geology 26: 1531–1548.

Korja, A., Lahtinen, R. and Nironen, M. (2006). The Svecofennian orogen: a collage of microcontinents and island arcs. Geological Society, London, Memoirs 2006 32: 561-578.

Korneliussen, A. and Sawyer, E. W. (1989). The geochemistry of Lower Proterozoic mafic to felsic igneous rocks, Rombak Window, North Norway. NGU Bulletin 415: 7-21.

Korneliussen, A., Tollefsrud, J. I., Flood, B. and Sawyer, E. (1986). Precambrian volcano-sedimentary sequences and related ore deposits, with special reference to the Gautelisfjell carbonate-hosted gold deposit, Rombaken basement window, Northern Norway. NGU report 86(193): 44.

Kranendonk, M. J. V. (2010). Two types of Archean continental crust: Plume and plate tectonics on early Earth American Journal of Science 210: 1187-1209.

Kranendonk, M. J. V., Kröner, A., Hegner, E. and Connelly, J. (2009). Age, lithology and structural evolution of the c. 3.53 Ga Theespruit Formation in the Tjakastad area, southwestern Barberton Greenstone Belt, South Africa, with implications for Archean tectonics. Chemical Geology 261: 115–139.

Laajoki, K. (2005). Karelian supracrustal rocks. In: Lehtinen, M., Nurmi, P. A. and Rämö, O. T. (eds) Precambrian Geology of Finland - Key to the Evolution of the Fennoscandian Shield. Developments in Precambrian Geology, Elsevier, Amsterdam 14: 279-342.

Lahtinen, R., Garde, A. A. and Melezhik, V. A. (2008). Paleoproterozoic evolution of Fennoscandia and Greenland. Episodes 31(1).

Lahtinen, R., Hölttä, P., Kontinen, A., Niiranen, T., Nironen, M., Saalmann, K. and Sorjonen-Ward, P. (2011). Tectonic and metallogenic evolution of the Fennoscandian shield: key questions with emphasis on Finland. Geological Survey of Finland, Special Paper 49: 23–33.

Lahtinen, R. and Nironen, M. (2010). Paleoproterozoic taterittic paleosol-ultra-mature/mature quartzite-meta-arkose successions in southern Fennoscandia-intra-orogenic stage during the Svecofennian orogeny. Precambrian Research 183: 770-790.

Larsen, T., Bergh, S. G., Henderson, I., Korneliussen, A. and Kullerud, K. (2010). Svecofennian structural development and metallogenesis of Paleoproterozoic volcano-sedimentary rocks of Rombak Tectonic widow. NGF abstract proceedings of the Geological Society of Norway 1, 2010, 29th Nordic Geological winter meeting, Oslo.

Larsen, T., Sundblad, K., Henderson, I., Bergh, S. G., Bagas, L., Sandstad, J. S., Andersen, T. and Simonsen, S. (2013). Recognition of Svecofennian sulphide bearing crust in the Rombak region, northern Norway. NGF abstract proceedings of the Geological Society of Norway 1, 2013, 32nd Nordic Geological winter meeting, Oslo.

Lewrya, J. F., Z. Hajnalb, A. Greenc, S.B. Lucasd, D. Whited, M.R. Staufferb, K.E. Ashtone, W. Weberf and Clowesg, R. (1994). Structure of a Paleoproterozoic continent-continent collision zone: a LITHOPROBE seismic reflection profile across the Trans-Hudson Orogen, Canada. Tectonophysics 232(1-4): 143–160.

Liou, J. G., Tsujimori, T., Zhang, R. Y., Katayama, I. and Maruyama, S., 2004. . 46, . (2004). Global UHP metamorphism and continental subduction/collision: the Himalayan model. International Geology Review 46: 1–27.

Ludwig, K. R. (2003). Isoplot/Ex version 3: A Geochronological Toolkit for Microsoft Excel, User’s Manual. Berkeley Geochronology Center Special Publications 4: 70.

Ludwig, K. R. (2009). SQUID 2: A User’s Manual. Berkeley Geochronology Center Special Publication 5: 110.

Melezhik, V. A. (2006). Multiple causes of Earth's earliest global glaciation. Terra Nova 18: 130-137.

Mellqvist, C., Öhlander, B., Skiöld, T. and Wikström, A. (1999). The Archean–Proterozoic Paleoboundary in the Luleå area, northern Sweden: field and isotope geochemical evidence for a sharp terrane boundary. Precambrian Research 96(3-4): 225–243.

Nironen, M. (1997). The Svecofennian Orogen: a tectonic model. Precambrian Research 86: 21-44.

Norrish, K. and Chappell, B. W. (1997). X-ray fluorescence spectrometry. In: Zussman, J. (Ed.), Physical Methods in Determinative Mineralogy, 2nd Edition. Academic Press, London: 201–272.

Norrish, K. and Hutton, J. T. (1969). An accurate X-ray spectrographic method for the analysis of a wide range of geological samples. Geochim Cosmochim Acta 33: 431–453.

Peltonen, P. (2005). Ophiolites. In: Lehtinen, M., Nurmi, P. A. and Rämö, O. T. (eds) Precambrian Geology of Finland - Key to the Evolution of the Fennoscandian Shield. Developments in Precambrian Geology, Elsevier, Amsterdam 14: 237-278.

Robb, L. J. (2005). Introduction to Ore-Forming Processes. Blackwell Publishing.

Robin, P.-Y. F. and Cruden, A. R. (1994). Strain and vorticity patterns in ideally ductile transpressional zones. Journal of Structural Geology 16: 447-466.

Rodionov, A., Ofstad, F. and Koziel, J. (2012). Helicopter-borne magnetic, electromagnetic and radiometric geophysical survey in Rombaken area, Narvik, Nordland. NGU report 2012.022.

Roedder, E. (1958). Technique for the extraction and partial chemical analysis of fluid-filled inclusions from minerals. Econ. Geol. Mag. 53: 235–269.

Romer, R. L. (1989). Interpretation of the lead isotopic composition from sulfide mineralisations in the Proterozoic Sjangeli area, northern Sweden. NGU Bulletin 415: 57-69.

Romer, R. L. and Boundy, T. M. (1988). Interpretation of lead isotope data from the uraniferous Cu-Fe-sulphide mineralisations in the Proterozoic greenstone belt at Kopparåsen, northern Sweden. Mineral Deposita 23: 256-261.

Sanderson, D. J. and Marchini, R. D. (1984). Transpression. Journal of Structural Geology 6: 449-458.

Sanderson, D. J. and Marchini, W. R. D. (1984). Transpression. Journal of Structural Geology 6(5): 449-458.

Sawyer, E. W. and Korneliussen, A. (1989). The geochemistry of Lower Siliciclastic turbidites from the Rombak Window: implications for paleogeography and tectonic settings. NGU Bulletin 415: 23-38.

Stern, R. A. (2009). Measurement of SIMS instrumental mass fractionation of Pb isotopes during zircon dating. Geostandards and Geoanalytical Research 33(2): 145-168.

Sullivan, W. A. and Law, R. D. (2007). Deformation path partitioning within transpressional White Mountain shearzone, California and Nevada. Journal of Structural Geology 29: 583-598.

Tavarnelli, E., Holdsworth, R. E., Clegg, P., Jones, R. R. and McCaffrey, K. J. W. (2004). The anatomy and evolution of a transpressional imbricate zone Southern Uplands, Scotland. Journal of Structural Geology 26: 1341-1360.

Tikoff, B. and Fossen, H. (1993). Simultaneous pure and simple shear; the unifying deformation matrix. Tectonophysics 217: 267-283.

Torgersen, E., Viola, G., Sandstad, J. S. and Stein, H. (2013). Structural constraints on the formation of Cu-rich mesothermal vein deposits in the Repparfjord Tectonic Window, northern Norway. SGA biennial conference 2013 - Uppsala. Oral presentation, session 3.8.

Vaughan, A. P. M., Leat, P. T. and Pankhurst, R. J. (2005). From: Vaughan, A. P. M., Leat, P. T. and Pankhurst R. J. (eds.), 2005. Terrane processes at the Margins of Gondwana. Geological Society, London, Special Publications 246: 1-21.

Vulollo, J. and Huhma, H. (2005). Paleoproterozoic mafic dikes in NE Finland. In: In: Lehtinen, M., Nurmi, P. A. and Rämö, O. T. (eds) Precambrian Geology of Finland - Key to the Evolution of the Fennoscandian Shield. Developments in Precambrian Geology, Elsevier, Amsterdam 14: 195-236.

Väisänen, M. and Mänttaäri, I. (2002). 1.90-1.88 Ga arc and back-arc basin in the Orijavri area, SW Finland. Geological survey of Finland, Bulletin 74: 185-214.

Weihed, P., Arndt, N., Billström, K., Duchesne, J.-C., Eilu, P., Martinsson, O., Papunen, H. and Lahtinen, R. (2005). 8: Precambrian geodynamics and ore formation: The Fennoscandian Shield. Ore Geology Reviews 27: 273-322.

Windley, B. F. (1992). Proterozoic collisional and accretionary orogens. In: Condie, K.C. (Ed.), Proterozoic Crustal Evolution. Elsevier, Amsterdam: 419–446.

Paper I

Tine L. Angvik, Steffen G. Bergh and Iain C. Henderson

Svecofennian oblique transpression and strain partitioning in a Paleoproterozoic mid-crustal granite-greenstone setting: An example from the Rombak Tectonic Window, North Norway

(manuscript)

Svecofennian oblique transpression and strain partitioning in a Paleoproterozoic mid-crustal granite-greenstone setting: An example from the Rombak Tectonic Window, North Norway

Angvik, T.L.[1, 2], Bergh, S.G.[2] & Henderson, I.H.C. [1]

(1) Geological Survey of Norway, Leiv Eirikssonsvei 39, 7040 Trondheim

(2) Dept. of Geology, University of Tromsø, 9037 Tromsø

Abstract

The Rombak-Skjomen shear zone (RSSZ) is a major crustal scale Paleoproterozoic ductile structure that cuts through Paleoproterozoic metasedimentary and felsic igneous rocks of the Rombak Tectonic Window, situated within the Paleozoic Caledonian thrust nappes, Northern Norway. This window is an important link to understand and tie the basement rock outliers to the west in Norway and the juvenile Paleoproterozoic rocks of the Fennoscandian shield to the east in Finland and Sweden.

The main deformation in the Rombak window is of Svecofennian age (1.92-1.75 Ga) and located within several N-S running metasedimentary belts consisting of ductile folds, thrusts and anastomosing shear zones. The RSSZ has a complex structural evolution and geometry also involving syn-deformational injection of granitoids and strain partitioning with four phases of deformation; Early pure shear folding event (D_1), pure shear dominated fold-thrust belt event (D_2), two phases of combined simple shear and pure shear oblique systems with a conjugate set of N-S trending sinistral reverse oblique-slip shear zones (D_3), and a NE-SW dextral reverse oblique-slip shear zone event (D_4) where the fold-thrust belt is nearly fully overprinted. The crosscutting relationship between the granite and the structures shows that the granite cuts the fold-thrust belt and parts of the oblique-slip deformation and can also be locally cut by the D_4 event consistent with syn- to late orogenic plutonism.

We present a strain partitioning model of interacting high-low strain domains for the RSSZ, in an overall oblique transpressional setting.The strain partitioning have developed progressively from a monoclinic transpressional symmetry with pure shear and fold-thrust belt to a triclinic transpressional symmetry with combined simple shear and pure shear resulting in oblique-slip shear zones. In this scenario the anastomosing arrays of steep mylonitic shear zones (D_3) may have formed from a strain pattern of triclinic deformation superimposed on the earlier monoclinic fold-thrust belt deformation (D_1-D_2), leaving isolated domains of the monoclinic deformation intact. These four progressive structural events lead to a complex outcrop pattern of remnant fold-thrust belt blocks segmented and attenuated by two later phases of steep reverse oblique-slip ductile shear zone fabrics which shows a regional conjugate pattern with the direction of main principal shortening in a WNW-ESE direction.

Regional EM and radiometric data support the tectonic model and demonstrate that graphitic shales and potentially mineralized bodies in the fold-thrust belt have been dextrally displaced up to 6 km. The understanding of the structural evolution of the RSSZ in the Rombak Tectonic Window is important in order to understand the Svecofennian orogeny in the Norwegian portion of the Fennoscandian shield and to possibly be able to link the structures to the east and also to understand how progressive transpressive margins may develop in general.

Keywords: Transpression, Paleoproterozoic, ductile structures, oblique-slip shear zone, fold-and-thrust belt.

1.0 Introduction

Crustal-scale ductile shear zones are common structures that develop during an orogenic event, and such shear zones may reflect potential terrane boundaries (c.f. Park 2005) between assembled older crustal blocks or intracrustal shear zones. Such boundaries can help to restore the craton outline and the cratonic margin characteristics and to unravel cycles of tectono-magmatic events (cf. Bleeker 2003). It is improbable that two converging crustal plates move in a uniform direction, but more likely oblique to each other forming a transpressional system. This may include both perpendicular and sideway motions of plates relative to the main shortening direction. The resulting complex strain patterns during Precambrian tectonism forming as a result of simple shear, pure shear, dilation, transpression or transtension are still a rather poorly defined issue (cf. Garde et al. 2002).

Transpression was first used by Harland (1971) to explain oblique convergent plate margins and has been used to explain many orogenic belts such as the Gondwanian Orogen (Curtis, 1998) the Torngat Orogen (Girard, 1993), and the Svecofennian Orogen (Beunk & Page, 2001). The composite nature of transpressional orogens has been modelled and tested mathematically (e.g. Sanderson & Marchini 1984; Tikoff & Fossen 1993). Notably, the concept of strain partitioning of the two end-member styles, i.e. pure-shear and simple-shear components of the deformation in transpressive settings, is widely used in order to describe homogenous deformation. However, a number of issues still remain vague, for example the nature of interaction, the mechanisms of initiation and evolution of folds, thrusts and oblique-slip faults in space and time, and the controlling factors such as bed rock anisotropy, pre-existing structures, rheology-lithology, regional versus local stress fields, strain intensity and the angle of convergence (e.g. Tavarnelli et al. 2004 and references therein).

The main structures developing in such regimes are either separate strike/oblique-slip faults occurring in an anastomosing pattern with both pure shear and simple shear components (e.g. Carreras et al. 2010) or contractional (thrust-related) structures and domains (e.g. Tavernelli et al. 2004). Many attempts have also been made to develop models to explain strain partitioning of the strike-slip and contractional components, including simple shear models (Harland, 1971; Sanderson & Marchini 1984), monoclinic models (Jones et al. 2004 and references therein), complex triclinic transpression and inclined extrusion models (Davis et al. 2011 and references therein). These processes may operate independent or in combination, thus accounting for the usually very complex styles of deformation in transpressive settings.

The Rombak Tectonic Window (RTW) within the Caledonides of North Norway (Figs. 1 and 2) is an outstanding well exposed example of a Paleoproterozoic, orogenic mid-crustal granite-greenstone province that experienced a complex evolution and structural history, assumed to be of Svecofennian age (1.92-1.75 Ga; Lahtinen et al. 2005). This window is dominated by Paleoproterozoic metavolcanic and metasedimentary rocks (<2.3 Ga), defining NNW-SSE trending narrow fold-thrust belts and a major ductile shear zone, the Rombak-Skjomen shear zone (RSSZ) (Larsen et al., 2010). These belts and shear zones are intruded by mafic to intermediate 1.9-1.7 Ga granitic batholiths (Korneliussen et al. 1986; Romer 1987, Korneliussen & Sawyer 1989; Bargel et al. 1995).

Previous studies in the area have focused on the bedrock petrology and geochemistry (Korneliussen et al. 1986; Korneliussen & Sawyer 1989. The deformation style is described as N-S striking, steep foliation in the metasedimentary rocks and locally within the adjacent granites. Also NE-SW striking, steep mylonitic shear zones with dominantly dextral shear sense (Priesemann, 1984a; Priesemann, 1984b; Skonseng, 1985 Korneliussen et al., 1986; Naruk 1987), and interpreted to be with relation to the high mineral potential in the area (Coller, 2004).

This paper describes and outlines the geometry, kinematics and relative timing of the RSSZ and discuss its interaction with fold- and thrust structures of the easternmost N-S striking metasedimentary belt and adjacent granites (Fig. 2) in the Rombaken Tectonic window. We present a model of the belt as a transpressive segment in the Svecofennian orogenic belt with strain partitioning structures involving both fold-thrust belt structures and oblique-slip zones (cf. Larsen 2010).

2.0 Regional geology and setting of the Rombak Tectonic Window

The Precambrian Fennoscandian shield (Fig. 1) makes up large parts of Norway, Sweden, Finland and Russia and is composed of Archean to Neoproterozoic crustal rocks. The shield has a long evolution and growth history reflected by a complex array of ductile shear zones, representing different orogens arranged as narrow linear belts (e.g. Hölttä et al. 2008; Lahtinen et al. 2008; Korja et al. 2006). The oldest Archean craton dominates the northeastern part; the Paleoproterozoic Svecofennian domain including the Bothnian basin and Svecokarelian orogen is present in the middle, and Transcandinavian igneous belt and Sveconorwegian orogeny makes up the southwest (Fig. 1) (Gaál & Gorbatschev 1987; Gorbatschev & Bogdanova 1993; Hölttä et al. 2008; Lahtinen et al. 2008). The Fennoscandian shield is bounded in the west by the Caledonian nappes (Bergström & Gee 1985), which itself also includes a number of tectonic outliers west of the Caledonides (e.g. Lofoten, Vesterålen and western Troms) and inliers, or tectonic windows farther east.

The largest of the tectonic windows in the north-Norwegian Caledonides is the RTW (Fig. 2), which accordingly offers an important data source between the autochthonous NW

Fennoscandian Shield and basement provinces west of the Caledonides (i.e. in Lofoten and western Troms; Bergh et al. 2010, 2012) and the eastern basement region (e.g. Braathen & Davidsen 2000). The RTW is dominated by a Paleoproterozoic greenstone-granite suite (Foslie, 1916; Korneliussen et al, 1986; Myers & Krøner 1994) including six narrow N-S and NNW-SSE trending metasedimentary belts. These belts consist of felsic metavolcanic rocks in the southwestern belt and metasedimentary rocks consisting of basal meta-conglomerates, -quartzites, -sandstones, -schists, -greywacke and -tuff in adjacent belts. They are surrounded/ intruded by granitic and syenitic batholiths (c. 1.9-1.7 Ga) and mafic dyke swarms are intruding or surrounding the metasedimentary belts (Fig. 2; Korneliussen et al. 1986). The metasedimentary rocks have been the locus for ductile deformation into zones of NNW-SSE trending major fold-thrust belt systems and subsidiary oblique-slip shear zones. A major regional ductile shear zone, the Rombak-Skjomen shear zone (Larsen et al. 2010), traverses the entire window from north to south (Fig. 2). The structural analysis and understanding of the structural evolution of this shear zone is the main aim for the present work.

The tectonic evolution and metamorphic history of the RTW is poorly investigated (cf. Larsen 2010), despite a general knowledge of the age, petrology and geochemistry of the area (e.g Priesemann, 1984a; Priesemann, 1984b; Skonseng 1985; Korneliussen et al. 1986; Romer & Boundy 1988; Romer 1989; Naruk 1987; Coller, 2004). The metamorphic grade in the metasedimentary units is variable, ranging from upper greenschist facies to locally amphibolite facies conditions during the Svecokarelian (also termed Svecofennian) event (c. 1.82 Ga) (Sawyer 1986; Korneliussen & Sawyer 1986) and during intrusion of granitoid plutons (1.78 Ga). These early episodes were followed by low-grade greenschist-facies retrogression and ductile folding and shearing (mylonitisation), which is also thought to be of Svecofennian age (1.8-1.6 Ga). The metamorphic rocks in the RTW have signs of retrogradation and metamorphosed at temperatures at 575-600ºC. The pressure is moderate to high, at 6kb in the south, decreasing northwards due to a change from deeper to higher structural levels (Apted & Liou, 1983; Flood 1984; Korneliussen & Sawyer, 1986; Sawyer, 1986).

Previous structural studies within the RTW focused on the kinematics of inferred late-post Caledonian structures subjected to extensional reworking along the margin of the window and that metasedimentary rocks in the area is correlated to the lowermost Caledonian Dividalen Group (Cashman 1989; Rykkelid & Andresen 1992). Caledonian reworking in the RTW is discussed (see Birkeland 1976; Romer 1987; Korneliussen & Sawyer 1986; Romer & Boundy 1988; Tull1977; Motuza1998). The objective herein is to document that deformation features within the RSSZ are part of a multiphase transpressional orogen that is Paleoproterozoic in age. This is further backed by recent U-Pb zircon age dating of a granite intrusion intruding along and across the shear zone yielding an age of 1789 ± 6 Ma (Larsen et al., 2013), which verifies that the deformation of the area, as well as the presumed basal Caledonian (Paleozoic) metaconglomerates are truly Svecofennian in age.

3.0 Structure and architecture of the RTW

The dominant major structural feature of the RTW is the Rombaken-Skjomen Shear Zone (RSSZ; Fig. 2). The RSSZ shows a complex geometry, varying in across strike width from 7 km to 20 m (Fig. 2). Our field data, combined with EM gravity and magnetic maps of the RTW (Fig. 3), show an anastomosing deformation pattern with steep ductile, mylonitic shear zones and tight to isoclinal folds segmenting lenses of less intensely deformed blocks, in which primary bedding is often preserved, with macro-scale upright folds and gently dipping reverse faults (fold-thrust belt).

The RSSZ shows a complex evolutionary sequence including four Paleoproterozoic deformation events (D_1-D_4); D_1 is an early fold event occurring as refolded folds in D_2 structures. During D_2 deformation a low angle, top-to-east fold and thrust belt developed. D_3 structures are steeply dipping N-S trending ductile oblique-slip shear zones and related steeply-plunging folds that segment the D_2 fold and thrust belt. D_4 structures are steeply dipping NE striking oblique-slip ductile shear zones that diagonally crosscut and displace the D_3 structures.

In our detailed structural analysis, we subdivide the area (Fig. 2) into three geographically distinct localities, from north to south, Jernvann-Haugfjellet, Norddalen and Gaultelisvatten. Each area displays characteristically different structural and tectonic styles reflecting different aspects of the kinematics and strain partitioning evolution.

3.1 D_1 and D_2 Fold-thrust belt structures

D_1 and D_2 folds are preserved in lower strain domains within the RSSZ. In these domains bedding structures are well preserved in meta-sedimentary rocks. Bedding is either flat-lying or forms open, upright, east verging folds which are often cut and displaced by gently west-dipping ductile shear zones (thrusts) consisting of partly-mylonitized schists, which often form duplex structures The thrusts are especially focused in graphitic schists. A weak metamorphic, steeply-dipping, N-S trending axial planar cleavage is commonly developed in the folded strata (e.g. Norddalen and Gautelis localities).

F_1 and F_2 folds are spatially and temporally associated with the low-angle shear zones. Observations of tight to isoclinal F_1 folds are sparse, observed at one locality in the western part of a ca. 3 km wide fold-thrust belt at Norddalen (Fig. 4).F_1 fold wavelengths range from micro scale to several meters, locally overturned towards the east (Figs. 4 and 5) and are locally refolded by upright, asymmetric F_2 folds. The F_1 folds have most commonly sub-horizontal to shallow dipping axial surfaces with moderate to gently-plunging fold axes to the NNW, N and/or SSE (Fig. 4)

The dominant map-scale folds of the RTW are D_2 upright, east-verging and asymmetric with related ductile thrusts. The F_2 folds and thrusts are most prominent in Norddalen, forming a belt up to three kilometers wide. F_2 folds are generally coaxial with F_1. They are upright to asymmetric and east-verging with moderate to gently west-dipping axial surfaces (S_2), sub-parallel to S_1 thrusts. Some F_2 folds are highly sheared along their limbs, within imbricate thrust stacks(Fig. 4). F_2 folds are open to tight with a steep to overturned forelimb and a shallow to steeply-dipping back limb. Fold wavelengths range from mappable scales to micro-scale (Figs. 3, 4 and 5). Cleavage is parallel to the thrust surfaces and is shallow dipping to sub-horizontal (Fig. 5). In Norddalen mappable N-S striking shallow west-dipping ductile S_2-thrusts commonly follow graphite schist horizons . Stretching lineations on the thrust surfaces plunge moderately N and NE with an oblique-slip component (Fig. 4). A similar fold-thrust belt is observed at Gautelis, but consists of either stacked and folded greywacke or conglomerate/breccia on top of thrust-detached marble (Fig 6 and 7). F_2 folds verges to ESE and plunge to NNW (Fig. 6D; subarea A) with associated hanging wall parallel thrusts with a NNW-SSE strike, or WSW plunging fold axis with NE-SW striking thrusts (Fig. 6D; subarea B). Symmetric detachment folds are observed in the basal Gautelis conglomerate in NE to E or SW to W plunging fold axes, similar to F_2 folds in subarea B (Figs. 6D and 7; subarea C). The detachment horizon for the thrusts is assumed to be localized within the thin carbonate bed that is only locally found below and between the green conglomerate beds. F_2 fold development in the Haugfjellet domain is more evolved and therefore the thrusts are not mappable.

3.2 D_3 and D_4 Oblique-slip structures

Regionally, the RSSZ displays two orientations of steep N-S (D_3) and NE-SW (D_4) anastomosing pattern of shear zones (Fig. 3). The dominant N-S trend follows the regional geometry of the metasedimentary belts. The NE-SW trending shear zones, appear to truncate or fold the metasedimentary belts diagonally (Fig. 3). EM gravity and magnetic data from Norddalen shows a regional scale bending of the N-S trending belt and a c. 5km dextrally displacement of the graphitic schist in direction of the NE-SW trending D_4 shear zone (Fig. 3). The D_3 and D_4 shear zones are steep, ductile and reverse oblique-slip shear zones. They are characterised by a sub-vertical mylonite fabric and shallowly-plunging stretching lineations (Figs. 6, 8, 9 and10), localized steeply-plunging drag folds in the metasedimentary rocks (Figs. 5 and 9) and off-set lithologies in cross-section and map view (Fig. 9G).

Internally, the D_3 and D_4 shear zones display a large variation in strain, with high-strain ultra-mylonites alternating with lower strain areas of proto- and ortho-mylonites (Sibson, 1977), where bedding and other primary features are locally preserved in low strain lenses in a complex anastomosing network (Fig.10). The shear zone thickness varies from millimeter to kilometer scale and influence the thickness of the metasedimentary belt. The metasedimentary belt is generally narrower where there is a higher frequency of shear zones and a higher strain gradient. There is a large variation in strain gradient and shear zone frequency (Fig. 11) from both the outcrop scale down to the microscopic level (Fig. 8 and 10). The shear zones commonly follow lithological heterogeneities, particularly in zones of competency contrast along the metasedimentary - granite contacts (Fig. 10) and along more incompetent internal metasedimentary horizons. For example, shear zones are more frequently localised along marble and graphitic schist horizons (Fig. 6). Carbonate beds are also often attenuated and disappear along specific oblique-slip shear zones.

D_3 structures

The D_3 shear zones dominate the geometry of the northern part of the RSSZ from the Norddalen in the south to Haugfjellet area in the north but are pervasive within the whole length of the inlier. Their orientation strikes N-S (set I) to NNW-SSE (set II) and have a dominant reverse sinistral oblique-slip component (Fig. 8). However, in the Haugfjellet area these D_3 shear zones are characterised by an equal amount of both sinistral and dextral reverse steep oblique-slip shear zones. D_3 shear zones in the Norddalen area are parallel to the N-S striking D_2 folds and thrusts. They are mainly observed to be sinistral reverse oblique-slip shear sense indicators in field (Fig. 9E). The dominant D_3 stretching lineation for all localities plunges moderately to steeply to the NNE (Figs. 4, 6 and 8).

These localized steep D_3 shear zones consistently overprint F_2 fold limbs and segments the macro scale fold-thrust structures along the F_2 fold limbs (fig 4 and 8). The fold-thrust belt is highly segmented into steeply-dipping duplex-like geometries by the oblique-slip structures (Fig. 4). Originally shallowly-plunging F_2 fold axes were rotated into steeper orientations (Figs. 4, 8 and 9). The D_3 shear zones are more spatially associated with tighter and steeper plunging fold structures than in the D_1 and D_2 domains.The fold styles vary from asymmetric to isoclinal within the mylonite zones, often forming drag-folds with hinge thickening and limb thinning. In lower strain domains they are open to tight similar folds with a slight limb thinning (Fig. 9A, B and C).

D_4 structures

The D_4 shear zones are localized diagonal to the D_3 shear zone at several localities along the eastern side of the RTW (Fig. 2). These geographically constrained shear zones are best developed in the southerly part of the inlier and can be traced from Gautelis area and NE into the Sjangeli area in Sweden (Figs. 3 and 8). The D_4 structures strike NE-SW and sigma-clasts, duplexes and extensional crenulation cleavages (NSC) suggest a predominantly reverse dextral shear sense (Fig. 9F). In the Gautelis area the D_4 ductile shear zones are characterised by the most intense mylonitic fabrics and the largest D_4 structure in the whole of the RSSZ, the Gautelis

Mylonite Zone (GMZ). This ductile D_4 shear zone is approximately 800m wide and at least 5 km long and parallel to the main direction and part of the large D_4 structure that can be traced into Sweden. The GMZ displays a complex tectonic interfingering of different lithological lenses (Fig: 6 and 11; GMZ). and the presence of internally complex high and low-strain domains (Fig. 10 and 11).

3.3 Crosscutting relationships with syntectonic granites

The deformation sequence is polyphase in the deformed metasedimentary rocks, as we observe consistent cross-cutting relationships between the structural styles. The D_1fold are refolded and thrusted by D_2 structures. The D_3 structures are following, but thin and slightly cut the D_2 fold structures and the D_4 structures cuts and drag fold the D_3 structures.

We also observe crosscutting relationships between the ductile structures and both granitic and mafic intrusions found within the metasedimentary units of the RTW. Both sets of intrusions have a strong spatially association with the RSSZ. Specifically, the intrusive bodies occupy different sites spatially associated with the ductile shear zones; they are localised adjacent to a mylonite zone, they are cut by a mylonite zone, or they are found as randomly spaced undeformed bodies.

The granites are generally coarse grained and cut the stratigraphic beds and folds in all the structural domains. In the Haugfjellet area the granite cuts the steeply plunging D_3-D_4 folds, while on the other hand, it is locally transected by D_3-D_4 shear zones by either cutting dykes diagonally across or cutting into large bodies (Fig. 8). Similarly, in the Norddalen area the granitic intrusions cut the D_2 folded and thrusted metasedimentary rocks, but are also deformed by D_3-D_4 folding and shearing into the granite bodies (Fig. 6). Moreover the same type of shear zone parallel granite dikes within the shear zone in the Gautelis domain is completely mylonitized by D_3 and D_4 shear zones, but are also cut by the major granite body(Fig. 10). This suggests that the granite intrusions are syntectonic to the D_3 and D_4 structures.

The mafic intrusions are found along the whole RSSZ, but are most abundant in the Gautelis area. These mafic intrusions are always parallel to the D_3 and especially the D_4 shear zones, They are either used as deformation paths which are strongly mylonitized of D_4 shear zones or are undeformed and sometimes with shear zones cutting along the boundary sides of the intrusions (Fig 7D).These observation also suggest a syntectonic setting to the D_3 and D_4 structures. Which are confirmed when both the granite and mafic intrusion are present together, the granites and mafic dykes show mutual cross-cutting relationships (Fig. 6).

4.0 Discussion

The structural architecture of the RTW resulting from Paleoproterozoic deformation allow insight into aspects that may have controlled the formation and distribution of the different fold-thrust and reverse oblique-slip strain domains. In order to establish an overall kinematic evolutionary/tectonic model for the RTW and the encompassing RSSZ, we will address specifically, the structural chronology and relative timing of deformation, the mechanical factors controlling the types of deformation, and the kinematics and strain partitioning of the deformation. Similar approaches have been successfully used in many other partitioned tectonic settings of various ages; e.g. the active San Andreas Fault (e.g. Babcock 1974; Sylvester & Smith 1976, 1987; Burgmann 1991; Fossen et al.,1994), Cenozoic transform tectonism in the North Atlantic/Svalbard (e.g. Harland 1979; Braathen & Bergh 1995; Braathen et al. 1999; Leever et al., 2011), and Proterozoic-Archean transpressive tectonism in northern Fennoscandia (cf. Bergh et al. 2010) and Laurentia/Greenland (Garde et al. 2002).

4.1 Structural chronology and relative timing of the deformation

Excellent exposure, aerial photographs and new high-resolution geophysical data allow the relative timing of folds, thrusts, foliations, oblique-slip ductile shear zones and intrusive rocks to be determined (Fig. 3). Detailed structural mapping and interpreted cross-sections (Figs. 4 and 6) provided a framework for defining at least four main structural groups, including contractional fold-thrust structures and steep ductile, dominantly oblique-slip ductile shear zones. We observe a progressive deformation sequence that encompasses; (1) N-S trending isoclinal upright folds (D_1), (2) N-S trending, upright and east-verging, asymmetric folds and low-angle thrusts associated with a fold-thrust belt (D_2), (3) N-S and NW-SE trending steep ductile oblique-slip shear zones (D_3) and (4) NE-SW trending, steep mylonitic, dextral oblique-slip shear zones (D_4). These groups of structures and their chronology are largely responsible for the complex structural architecture of the RTW (Fig. 3), as discussed below.

Upright isoclinal Fl folds are preserved only within the Norddalen fold-thrust belt domain and are rarely observed. They have NNW-SSE trending fold axes and steep, subvertical axial surfaces, and these early folds have been mostly coaxially re-folded by upright, east-verging D_2 folds and associated low-angle D_2 thrusts (Fig.4). Relative fold geometries suggest D_1 and D_2 folds formed in an overlapping contractional strain regime characterised by, e.g. successive and/or progressive ENE-WSW shortening. Isolated remnants of D_1-D_2 folds and thrusts are preserved within the GMZ, with folds trending NE-SW and with moderately-plunging axes, slightly oblique to D_1 fold axes in the Norddalen domain, and suggestive of NW-SE oblique contraction during their formation (cf. Priesemann 1984b). Alternatively, we interpret this deviation as the result of a ca. 45° clockwise block rotation of the fold-thrust belt structures during subsequent oblique-slip shearing in the GMZ. In the Haugfjellet area, in contrast to Norddalen, primary bedding is scarcely observed in low strain domains between the steep ductile shear zone. Present, bedding is strongly attenuated and D_1-D_2 fold axes rotated into steep plunges. This kind of discontinuous rotation of fold-thrust structures by oblique-slip shearing both across-strike and along-strike resulted in complex structural segmentation and attenuation of the RTW belt.

The oblique-slip ductile shear zones (D_3-D_4) in the RTW consistently post-date the fold-thrust belt related structures. The Norddalen locality displays a clear age relationship between D_2, D_3 and D_4 (fig 4) in that D_3 is consistently parallel to the trend of the fold-thrust belt structures (D_2) by following weak layers and lithological boundaries. D_4 obliquely cross-cuts both bedding, D_2 fold-thrust structures and D_3 shear zones. This locality also demonstrates that the oblique-slip shear zones likely evolved in a time-progression after initial E-W contractional fold-thrust belt generation (Fig. 4), in the form of variably, NW-SE directed sinistral shear zones (D_3) and dextral NE-SW shear zones (D_4) in a dominantly transpressional tectonic setting. The overall N-S trends of the fold and shear zone arrays, their mainly sinistral shear-sense and dextral, mutually cross-cutting shear zones, and the oblique stretching-lineations (Figs 4, 6 and 8) suggest formation during NE-SW directed transpression.

The absolute age of the structures within the RTW has been previously considered as Paleoproterozoic by Korneliussen et al. (1986), Korneliussen & Sawyer (1986) and Bargel et al. (1995), while a Caledonian age was inferred by Birkeland et al. (1976), Naruk (1987), Cashman (1990) and Rykkelid & Andresen (1995). Argumentation for a Caledonian age of the deformation relies on the metasedimentary units in the RTW being interpreted as Neoprotorozoic in age, corresponding to the Dividal Group. In such a context Birkeland (1976) concluded that the D_2 folds in the area were Caledonian in age, as these folds affected the assumed Neoproterozoic Dividalen Group.

The present work demonstrates that the folding pre-dated the deposition of the Neoproterozoic Dividal group, and thus is Proterozoic in age (cf. Larsen 2010). For example, the metasedimentary rocks thought to be Neoprotorozoic in age are strongly deformed and make up distinct attenuated segments of the RSSZ, and furthermore, the steeply dipping ductile shear zones associated with D_3 and D_4 events are discordantly cut by the flat-lying Caledonian thrust sheet structures (Andresen, 1988). New radiometric age determinations (Larsen et al., 2013) of syn- to post-tectonic granite intrusions discussed above, which are spatially and temporally related to the shear zone development, suggesting a Paleoproterozoic age, thus precluding a Caledonian age for the deformation.

4.2 Mechanical control

There are mechanical controls on oblique convergent plate settings, which include lithospheric boundary conditions, lithological heterogeneity, rheology, heterogeneities in the strain field (pure- and simple-shear), relative angle of principal stress in oblique transpression, and the presence of intrusive melts (e.g. Fossen & Tikoff, 1993; Jones & Tanner 1994; Tikoff & Fossen 1993; Teyssier et al. 1995; Brown & Solar, 1998; Barraud et al. 2001; Tavarnelli et al. 2004: Whitney et al. 2007; Schrank et al, 2008). Our data suggests that the overall controlling element of the deformation in the RTW is the RSSZ and the nature of its evolution. This regional scale ductile shear zone is localized in contrastingly different rock types and borders different deformation domains from pure shear dominated in the contractional fold-thrust belt in the Norddalen locality, to combined pure and simple shear domains in the Haugfjellet and Gautelis localities, and with several sets of oblique-slip shear zones. This suggests that the mechanical control excerted by the RSSZ have been influenced by spatial subdivision of low and high strain domains and distinct differences in rheology resulting in distributed and localised deformation zones. Notably, high-strain localised deformation occurs along heterogeneities within the bedrock: (i) along weak sedimentary horizons, (ii) along geometrical shapes defined by pre-existing structures, (iii) parallel with mafic intrusive rocks, and (iv) along the boundaries of granite intrusions. For example, in the contractional Norddalen domain, the main D_2 thrust zones are located within stacked black schist, grey schist and marble horizons, suggesting the formation of fold-thrust structures are largely lithologically controlled (Fig. 4). Similarly, remnants of fold and thrust structures in the Gautelis oblique-slip domain are preserved as detachment folds and thrusts in carbonate and graphite schists. Therefore, we conclude that the internal sedimentary rheology, i.e. pre-existing anisotropy (cf. Evans et al. 2003; Montési & Hirth 2003; Tavarnelli et al. 2004; Schrank et al. 2008; Larsen et al., 2010), played a major mechanical control in partitioning of the deformation, at least on the earliest, contractional stages of the deformation in the RTW.

Weak sedimentary rocks and pre-existing structures may also control the formation of later ductile structures, in this case the D_3 and D_4 oblique-slip structures in the RSSZ. In the RTW the stratigraphic units in the Norddalen domain and the carbonate horizon at Gautelis, in which a major mylonitic shear zone developed (GMZ), provided the locus for oblique-slip reactivation. For example, the major SET III (D_4) shear zone at Gautelis is localised along the highly competent interface between the metasedimentary units and the tonalitic basement complex to the east (Fig. 6). These oblique-slip shear zones are mostly steeply-dipping and developed preferentially parallel to steeply-oriented fabrics, e.g. bedding and cleavages of D_1-D_2 folds and steep thrusts (D_2) in the fold-thrust domains. In Norddalen, the sinistral oblique-slip folds adjacent to D_4 shear zones have the same trend as the upright D_1-D_2 folds. At Haugfjellet, steep oblique-slip shear zones are mostly confined to the steep limbs of steeply-plunging folds (Fig. 8). Several of the shallow dipping D_2 thrusts were steepened and reactivated as D_3 and D_4 oblique-slip shear zones.

These observations suggest that the contrasting deformation styles in segments/domains across as well as along-strike in the RTW were influenced by lithological heterogeneities. Similar conclusions have been reached by e.g. Jones & Tanner (1994), Tavernelli et al. (2004) and Bergh et al. (2010) from the study of interacting contractional and oblique-slip features in various transpressive settings. Jones & Tanner (1994) described how partitioning of transpressive strain occurs when stress is applied oblique to pre-existing weakness zones. Tavernelli et al. (2004) showed how the deformation evolution and geometry is highly depending on the anisotropy of the rocks. Bergh et al. (2010) demonstrated progressive Paleoproterozoic deformation in the West Troms Basement Complex, north Norway, that involved early formed ductile thrusts and upright macrofolds whose steep limbs and corresponding steepened early-stage thrusts were reactivated by orogen-parallel, steep oblique-slip shear zones and subvertical folds.

In a constantly evolving strain field, in the middle crust level and at medium grade metamorphic conditions as in the RTW, the fine-grained metamorphic rocks deform easier than their coarse-grained counterparts, and the deformation will thereby be localized in the fine grained rocks and modified by deformation processes such as ductile flow, recrystallization and recovery (e.g. Evans et al. 2003; Montési & Hirth 2003). Examples include fine-grained mafic dykes in the Gautelis domain and graphitic black schist in the Norddalen domain. Similarly, high-strain mylonitic shear zones in the Gautelis domain localised along steep boundaries of rheologically different schist and granitic intrusive rocks (fig. 11) and mafic dykes and the surrounding host rock (Fig. 7). Such relationships have been observed across the entire RTW, suggesting regional-scale control of mechanical anisotropies. At Gautelis, mafic dykes have a NW-SE trend (Fig. 7), and they likely acted as both incompetent deformation channels and competent lenses. Dykes intruded along NE-SW shear zones were also ductily deformed (Fig. 4), supporting synchronous intrusion and deformation. However, some granitic bodies which are intruded after the initial phase of D_2 folding are subsequently cut by steep ductile shear zones (D_3 and D_4). It is also notable, that the mafic dykes in general intruded in two or more generations as they mutually cross-cut the granites (cf. Korneliussen et al. 1986). Therefore, we can clearly document the syn-tectonic nature of both the granitic and mafic intrusions, and thus enable to infer their controlling effect on the deformation features. Syn-tectonic intrusion (melt) paths are known from many studies (e.g. Barraud et al. 2001; Brown & Solar 1998; Pavlis 1995), and they may control the channelized melt flow pattern and thus localize the intrusion on the deformation fabrics. For example Brown & Solar (1998) showed that granite melts found in dilatant shear fractures are driven by both buoyancy forces and tectonically induced melt pressure. In accordance with their findings, we have demonstrated that granite and mafic dykes associated with RSSZ consistently intruded parallel to the D_3 and D_4 steep ductile shear zones, the shear zones and the melts forming a complex interplay. If these shear zones controlled the melt pathway, the intrusions likely modified the competency contrast with the surrounding metasedimentary rocks to influence the nucleation sites of the shear zones.

4.3 Kinematic models with emphasis on strain partitioning

The concept of strain partitioning is widely used to explain simultaneous interaction of pure shear contraction and strike-slip (simple shear) deformation in a transpressive setting both in the ductile and brittle regimes (cf. Harland & Wright, 1979; Sanderson & Marchini 1984; Tavarnelli et al. 2004). The nature of interaction is however, generally hard to evaluate, since e.g. the regional and local strain-stress fields, strain intensity and the angle of obliquity can be highly variable in such settings (Sanderson & Marchini 1984). In a simple shear setting, the structures formed as a result of instantaneous strain will have an angle of obliquity ca. 45^{o} to the main shear zone and the resulting strain will be fully distributed (e.g. Harland 1971; Sanderson & Marchini 1984; Zoback et al. 1987). During progressive oblique convergence the direction of the maximum instantaneous shortening direction becomes increasingly perpendicular to the shear zone boundary and the degree of strike-slip partitioning increases (Sanderson & Marchini 1984). The overall result may be full partitioning of the contractional and strike-slip components and the formation of domains with localized ductile shear zones and corresponding off-fault contractional domains. Alternating complexities of deformation partitioning may arise if the nature of strain varies between monoclinic and triclinic transpression (Fossen & Tikoff, 1994; Jones et al. 2004; Tavernelli et al. 2004) and inclined extrusion (Jones et al. 2004).

In the RTW there is evidence for interacting pure shear and simple shear structures in segments or domains along the RSSZ, thus inferring strain partitioning. The fold-thrust belt in the Haugfjellet and Norddalen domains and the dominant GMZ in the Gautelis oblique-slip domain are all well-constrained examples of such segments. On the other hand, the documented relative timing between the contractional and oblique-slip structures is partly in conflict with a full partitioning model (Sanderson & Marchini 1984). Accordingly, in the RTW, the deformation domains may have developed independently, in a time-progressive manner, either as fold-thrust belt or oblique-slip features.

A fold-thrust character of the deformation was likely favoured in the early stages of deformation, at least in the Norddalen domain, and this may have been due to a high angle of obliquity of the regional strain axes relative to the metasedimentary units/basins and their boundaries to the surrounding rocks. In the Haugfjellet domain, there is an equal amount of contractional structures relative to oblique-slip shear zones, and both sinistral and dextral shear-senses occur in the oblique slip shear zones. Most of the stretching-lineations in the fold-thrust structures are perpendicular to the structural trends, while they are mostly oblique to slightly oblique on the steep ductile shear zones (Fig 8). This may imply that the finite strain of the Haugfjellet domain was more pure-shear dominated, at least in the initial stages, and that the strain axes were rotated during progressing deformation and orogenic accretion/wedge build-up and switched into a weakly partitioned system characterised by sinistral and dextral oblique-slip shearing (i.e. a conjugate system) rather than a fold-thrust belt. Similar interpretations were made by e.g. Tikoff & Greene (1997), Curtis (1998) and Holdsworth et al. (2002). The Haugfjellet domain also differs somewhat with respect to strain orientation from the interpreted regional strain (Fig. 8), and this may be explained by local strain partitioning largely unrelated to the regional strain axes (cf. Jones & Tanner 1993). The Gautelis domain, on the other hand, is composed mainly of the RSSZ including the GMZ, and thus may be considered a oblique-slip (simple shear dominated) segment of the RTW.

The sinistral dominated oblique-slip shear zone recorded in the Norddalen domain and the oblique-dextral shear zones in the Norddalen and Gautelis domains show a clear dextral off-set and bending of structures and corresponding lateral displacement (Fig. 4). However, these shear zones display moderate-plunging stretching-lineations supportive of a deformation regime with a combination of pure shear and simple shear (e.g. Sullivan & Law 2007; Davis et al. 2011), rather than a distributed simple shear displacement mechanism (e.g. Ramsay & Graham 1970; Harland 1971; Sanderson & Marchini 1984). The sinistral ductile shear zones in these domains show a dominating stretching-lineation plunging to the NW, whereas the dextral shear zone has stretching-lineations plunging towards the NE. This supports a model with a changing regional strain field (axes) from NW-SE to NE-SW during progression of the deformation, generating two localized transpressional ductile shear zones.

Transpressional models involving monoclinic symmetries were first developed by Sanderson & Marchini (1984) and followed by several authors (e.g Fossen & Tikoff 1993; Simpson & De Paor 1993) and compared with field examples (e.g. Ring 1998; Baird & Hudleston 2007; Vitale & Mazzoli 2009). A monoclinic symmetry model can be explained by a distorted "cube" where two of the angles are not normal to each other, producing either strike- and dip-parallel lineations depending on the amount of accumulated deformation and the angle of convergence across the shear zone (Fossen & Tikoff 1993; Ghosh 2001; Dewey 2002). The Norddalen domain may be an example of a monoclinic deformation symmetry, since the stretching-lineations on both the steep shear zones and the low-angle thrusts are dip-slip (i.e. pure shear dominated). The Gautelis domain also displays remnant blocks of pure shear dominated fold-thrust belt structures within the more oblique-slip dominated domain.

The monoclinic model, however, cannot be used to explain oblique-plunging lineations (Sullivan & Law 2007; Davis & Titus 2011). Oblique-plunging lineations may either form in coupled boundary models (Robin & Cruden 1994; Dutton 1997) or during triclinic transpression (Jones & Holdsworth 1998; Lin et al. 1998; Jones et al. 2004). In case of a coupled boundary model cleavage/foliation formed during folding and/or lateral shearing will dip away from the center of the shear zone and be vertical in the central, high-strain portion of the shear zone (Dutton 1997). The margins of the shear zone, on the other hand, will experience the most pronounced pure shear component and the maximum plunge of the lineation (Robin & Cruden 1994; Dutton 1997). The transpressive triclinic model combines the end-member pure shear and simple shear components, and in such a model all stretching lineations will be oblique to the strike of the shear zones (e.g. Hudleston et al. 1988; Sullivan & Law 2007; Davis et al. 2011).

In the RTW, the overall internal character of the RSSZ would suggest synchronous pure-shear and simple-shear deformation although elements of the earlier-formed fold-thrust structures may have been locally preserved (see earlier discussion). The fact that both sinistral and dextral oblique-slip shear zones occur there, and that the stretching-lineations for the sinistral and dextral shear zones both display major oblique trends (Figs. 4, 6 and 8), the most likely interpretation would be that of a triclinic transpressional model (cf. Holdsworth et al. 2002; Tavarnelli et al. 2004). In cases where a monoclinic symmetry of structures exist, this may be explained by a high ratio of pure shear relative to simple shear, and progressive transition into triclinic geometries through time if the ratio of simple versus pure shear increases (Kuiper et al. 2011).

The intensity of strain in the RSSZ may be used as well, to infer lateral segmentation and strain partitioning in the RTW, since strain intensity commonly increases towards the center of the shear zone (Ramsay & Graham 1970; Robin & Cruden 1994). The strain pattern of the RTW is characterised by an anastomosing high-strain dominated shear zone pattern enveloping less deformed or low-strain fold-thrust belt domains and/or segments with highly variable width and extension along strike of the metasedimentary belt (Figs. 2, 4, 6 and 8). Notably, the width of the metasedimentary belts appear to correspond to the strain intensity, i.e. wide segments up to 10 km in the Haugfjellet and Norddalen fold thrust domains, while narrow (< 100 m) domains such as in the southern part of Haugfjellet define high-strain oblique-slip domains. These variations are also clearly inferred from the magnetic and gravity data of the RTW (Fig. 3).

4.4 Tectonic model

With regard to the discussion of relative timing of the deformation in the RTW, the mechanical factors controlling the deformation, and the kinematics and strain partitioning of the deformation, in particular along the RSSZ, we propose a kinematic and evolutionary model as follows (Fig. 12):

(1) D_1-D_2 event: An early deformation event involved E-W contraction and formation of N-S trending tight to isoclinal D_1-folds locally within the metasedimentary belts. Coaxial refolding and generation of major N-S trending upright D_2-folds likely formed in a progression of events, producing a fold-and thrust belt, as observed in the Norddalen domain, and associated axial-planar detachment folds, cleavages and low-angle thrusts. As the orogenic contraction proceeded, and likely also due to a shift to greater obliquity in the regional shortening direction relative to the fold- thrust belt, the initial gently west-dipping strata and low-angle D_2-thrusts were rotated into a steeper orientation. In conjunction with steep D_2 fold limbs these zones of weakness became the controlling factor for subsequent partitioning of the oblique strain.

(2) D_3 event: The overall oblique-convergent strain then was split into NW-SE directed transpressional domains with sinistral oblique-slip-slip shear zones (D_3) sub-parallel to the fold-thrust belt, effectively segmenting and attenuating the fold-thrust belt.

(3) D_4 event: During the latest ductile event, some of the reverse oblique-slip-slip shear zones of the RTW were subjected to NE-SW dextral transpressional shearing (D_4), and the strain was distributed diagonal relative to the metasedimentary units, causing further segmentation of the fold-thrust belt. At this stage, the RSSZ most likely formed as a through-going crustal feature within the overall and dominantly oblique strain-field. Strain partitioning proceeded and the fold-thrust belt structures and the sinistral ductile shear zones were modified by dextral shear zones (D_4) and were rotated or bent into steeply-plunging folds. We interpret the formation of these D_4 shear zones as forming an extensional crenulation cleavage type geometry, further attenuating the already segmented fold-thrust belt and steep D_3 shear zones.

The resulting complex geometry of the RTW and RSSZ included many different structural geometries and kinematic domains with isolated, steep shear zone bounding remnants of fold-thrust belt structures surrounded by an anastomosing network of ductile shear zone arrays (Fig. 3).

(4) Intrusions: Synchronous with the formation of the oblique-slip D_3-D_4 shear zones along the RSSZ, the metasedimentary belt was intruded by fine-grained mafic dyke swarms and granitic injections that may have played a critical role during the progressive evolution and further strain partitioning of the RTW. The oblique-slip shear zones may have been confined to areas undergoing very high end-member strain where the RSSZ split into subsets and detached or splayed into less competent rocks (black schists, marbles) or steep pre-existing fabrics (fold limbs), producing a variety of oblique mylonitic shear zone fabrics. This could have occurred along the boundaries of more competent granites, intrusives and mafic dykes. For example do mafic dykes intruded parallel to the shear zone and acted as nucleation sites for further shearing.

5.0 Conclusions

- A crustal scale steeply-dipping ductile shear zone with associated fold- thrust domains has been identified and systematically documented in Paleoproterozoic igneous and meta-supracrustal rocks of the Rombak Tectonic Window northern Norway.

- The Rombaken-Skjomen shear zone (RSSZ) shows temporal and spatial strain partitioning with four phases of deformation including: 1) D_1: early pure shear fold event 2) D_2: a pure shear dominated fold-thrust belt event, 3) D_3: two phases of combined simple shear and pure shear oblique systems with a conjugate set of N-S trending reverse oblique-slip shear zones, and 4) D_4: NE-SW dextral reverse oblique-slip shear zone event where the fold-thrust belt is nearly fully overprinted. These four progressive structural events likely originated in an overall oblique transpressive regime, leading to a complex outcrop pattern of remnant fold-thrust belt blocks surrounded and segmented by two later phases of steep oblique-slip ductile shear zone fabrics effectively attenuating the RSSZ along strike.

- Deformation in the RTW appears to have a strong mechanical control, both internally within the metasedimentary successions and between the metasedimentary rock and the surrounding granites and gneisses. Syn-tectonic granites intruded at various stages within the complex deformation sequence and played an important role in the mechanical control and resulting geometry of the RSSZ.

- The granitic bodies are interpreted to be syn-tectonic, and therefore, may display both cross-cutting and/or synchronous intruding relationships with respect to the early fold-thrust belt structures (D_1-D_2) and subsequent later strike slip structures (D_3-D_4).

- The RSSZ developed in successive stages during the same progressive deformation event in which we suggest that all stages of 1) detachment folding, 2) fold-thrusting, 3) reverse sinistral strike-slip shearing and 4) reverse dextral oblique-slip shearing have developed during strain partitioning.

- The strain partitioning may have developed from a monoclinic transpressional symmetry (pure shear or strike-slip shear) to a triclinic transpressional symmetry during progressive deformation through time, with oblique stretching lineations and combined fold-thrust belt and oblique-slip shear zones (sinistral and dextral). In this scenario the anastomosing arrays of steep mylonitic shear zones may have formed from a strain pattern of triclinic deformation superimposed on the earlier monoclinic fold-thrust belt deformation, leaving domains of the monoclinic deformation.

6.0 References

Andresen, A., 1988, Caledonian terrains of northern Norway and their characteristics: Trabajos de Geologia, Univ. de Oviedo, v. 17, p. 103-117.

Apted, M.J., and Liou, J.G., 1983, Phase relations among greenschist, epidote-amphibolite, and amphibolite in a basaltic system: American Journal of Science, v. 283-A, p. 328-354.

Babcock, E.A., 1974, Geology of the northeast margin of the Salton trough, Salton Sea, California: Geological Society of America Bulletin, v. 85, p. 321-332.

Baird, G.B., and Hudleston, P.J., 2007, Modeling the influence of tectonic extrusion and volume loss on the geometry, displacement, vorticity, and strain compatibility of ductile shear zones: Journal of Structural Geology, v. 29, p. 1665-1678.

Bargel, T.H., Bergstrøm, B., Boyd, R., and Karlsen, T.A., 1995, Geologisk kart, Narvik kommune M 1:100.000: Norges geologiske undersøkelse.

Barraud, J., Gardien, V., Allemand, P., and Grandjean, P., 2001, Analog Modelling of Melt Segregation and Migration During Deformation: Phys. Chem. Earth, v. 26, p. 317-323.

Bergh, S.G., K. Kullerud, K., Armitage, P.E.B., Zwaan, K.B., F. Corfu, F., Ravna, E.J.K., and Myhre, P.I., 2010, Neoarchean to Svecofennian tectono-magmatic evolution of the West Troms Basement Complex, North Norway: Norwegian Journal of Geology, v. 90, p. 21-48.

Bergh, S.G., Corfu, F., Myhre, P.I., Kullerud, K., Armitage, P.E.B., Zwaan, C.B., Ravna, E.J.K., Holdsworth, R.H., and A. Chattopadhya, 2012, Was the Precambrian basement of western Troms and Lofoten-Vesterålen in northern Norway linked to the Lewisian of Scotland? A comparison of crustal components, tectonic evolution and amalgamation history: Tectonics, In Tech, v. 11, p. 283-330.

Bergström, J., and Gee, D.G., 1985, The Cambrian in Scandinavia. In: D.G. Gee and B. A. Sturt (eds.) The Caledonian Orogen. Scandinavia related areas: John Wiley & sons, inc, Chichester, v. 247-271.

Beunk, F.F., and Page, L.M., 2001, Structural evolution of accretional continental margin of the Paleoproterozoic Svecofennian orogen in southern Sweden: Tectonophysics, v. 339, p. 67-92.

Birkeland, T., 1976, Skjomen, berggrunnsgeologisk kart 1:100 000: Norges Geologiske Undersøkelse.

Bleeker, W., 2003, The late Archean record: puzzle in ca. 35 pieces: Lithos, v. 71, p. 99–134.

Braathen, A., and Bergh, S.G., 1995, Kinematics of Tertiary deformation in the basement-involved fold–thrust complex, western Nordenskiöld-Land, Svalbard—tectonic implications based on fault–slip data-analysis: Tectonophysics, v. 249, p. 1–29.

Braathen, A., Bergh, S.G., and Maher, H.D.J., 1999, Application of a critical wedge taper model to the Tertiary transpressional fold–thrust belt on Spitsbergen: Geological Society of America Bulletin, v. 111, p. 1468–1485.

Braathen, A. and Davidsen B. (2000). "Structure and stratigraphy of the Paleoproterozoic Karasjokk Greenstone Belt, north Norway - regional implications." Norsk Geologisk Tidsskrift 80: 33-55.

Brown, M., and Solar, G.S., 1998, Shear-zone systems and melts: feedback relations and self-organization in orogenic belts: Journal of Structural Geology, v. 20, p. 211-227.

Burgmann, R., 1991, Transpression along the southern San Andreas fault, Durmid Hill, California: Tectonics, v. 10, p. 1152-1163.

Cagnard, F., Gapais, D. and Barbey, P. (2007). Collision tectonics involving juvenile crust: the example of the southern Finnish Svecofennides. Precambrian Research 154: 125–141.

Carreras, J., Czeck, D.M., Druguet, E., and Hudleston, P.J., 2010, Structure and development of an anastomosing network of ductile shear zones: Journal of Structural Geology, v. 32, p. 656-666.

Cashman, P.H., 1989, Geometry and kinematics of extensional deformation along the northern edge of the Rombak Window, Nordland, north Norway: NGU Bulletin, v. 415, p. 71-86.

Coller, D., 2004, Varden Ridge Target Generation Report: Golden Chalice Resources Inc report, v. GT 04-18D-01.

Curtis, M.L., 1998, Development of kinematic partitioning within a pure-shear dominated dextral transpression zone: the southern Ellesworth Mountains, Antarctica. In: Hodlsworth, et al. (eds.), 1998: Continental Transpressional and Transtensional Tectonics. Geological Society of London, Special publication, v. 135, p. 289- 306.

Davis, J.R., and Titus, S.J., 2011, Homogeneous steady deformation: A review of computational techniques: Journal of Structural Geology, v. 33, p. 1046–1062.
deformation matrix: Tectonophysics, v. 217, p. 267-283.

Dewey, J.F., 2002, Transtension in arcs and orogens: Int. Geol. Rev, v. 44, p. 402-438.

Dutton, B.J., 1997, Finite strains in transpression zones with no boundary slip: Journal of Structural Geology, v. 19, p. 1189–1200.

Evans, M.A., Lewchuk, M.T., and Elmore, R.D., 2003, Strain partitioning of deformation mechanisms in limestones: examining the relationship of strain and anisotropy of magnetic susceptibility (AMS): Journal of Structural Geology, v. 25, p. 1525–1549.

Flood, B., 1984, The Rombak project area, North Norway. Summary of work done 1983 and work program proposal for 1984: Arco Norway Inc, Hard Mineral section, v. 84-670-19.

Foslie, S., 1916, Avskrift av statsgeolog Steinar Foslies dagboksopptegnelse angående Sjangeli 1916: NGU Ba-rapport, v. 3336, p. 19 s.

Fossen, H., and Tikoff, B., 1993, The deformation matrix for simultaneous simple shearing, pure shearing, and volume change, and its application to transpression/transtension tectonics: Journal of Structural Geology, v. 15, p. 413-422.

Fossen, H., Tikoff, B., and Teyssier, C., 1994, Strain modeling of transpressional and transtensional deformation: Norsk Geologisk Tidsskrift, v. 74, p. 134-145.

Gaál, G., and Gorbatschev, R., 1987, An outline of the Precambrian Evolution of the Baltic Shield: Precambrian Research, v. 35, p. 15-52.

Garde, A.A., Chadwick, B., Grocott, J., Hamilton, M.A., McCafferey, K.J.W., and Swager, C.P., 2002, Mid-crustal partitioning and attachment during oblique convergence in an arc system, Paleoproterozoic Ketilidian orogen, southern Greenland: Journal of the Geological Society. London, v. 159, p. 247-261.

Ghosh, S.K., 2001, Types of transpressional and transtensional deformation. In: Koyi, H.A. & Mancktelow, N.S. (eds) Tectonic Modeling: A Volume in Honor of Hans Ramberg: Geological Society of America Memoir, v. 193, p. 1–20.

Girard, R., 1993, Orogen-scale strain partitioning and an analogy to shearbands

Gorbatschev, R., and Bogdanova, S., 1993, Frontiers in the Baltic: Precambrian Research, v. 64, p. 3-21.

Harland, W.B., 1971, Tectonic transpression in Caledonian Spitsbergen: Geological Magazine, v. 108, p. 27-41.

Harland, W.B., and Wright, N.J.R., 1979, Alternative hypothesis for the pre-Carboniferous evolution of Svalbard: Norsk Polarinstitutt Skrifter, v. 167, p. 89-117

Holdsworth, R.E., Tavarnelli, E., Clegg, P., Pinheiro, R.V.L., Jones, R.R., and McCaffrey, K.J.W., 2002, Domainal deformation patterns and strain partitioning during transpression: an example from Southern Uplands terrane, Scotland: Journal of the Geological Society. London, v. 159, p. 401-415.

Hölttä, P., Balagansky, V., Garde, A.A., Mertanen, S., Peltonen, P., Slabunov, A., Sorjonen-Ward, P., and Whitehouse, M., 2008, Archean of Greenland and Fennoscandia. Episodes, v. 31, p. 13–19.

Hudleston, P.J., Schultz-Ela, D., and Southwick, D.L., 1988, Transpression in an Archean greenstone belt, northern Minnesota: Canadian Journal of Earth Sciences, v. 25, p. 1060-1068.

in the Torngat Orogen, northeastern Canadian Shield: Tectonophysics, v. 224, p. 363–370.

Jones, R.R., and Holdsworth, R.E., 1998, Oblique simple shear in transpression zones. In: Continental Transpressional and Transtensional Tectonics. Holdsworth, R.E Strachan, R.A & Dewey, J.F. (eds). London: Spec. Publ. Geol. Soc., v. 135, p. 35-40.

Jones, R.R., and Tanner, P.W.G., 1994, Strain partitioning in transpression zones: Journal of Structural Geology, v. 17, p. 793.

Jones, R.R., Holdsworth, R.E., Clegg, P., McCaffrey, K., and Tavarnelli, E., 2004, Inclined transpression: Journal of Structural Geology, v. 26, p. 1531–1548.

Korja, A., Lahtinen, R., and Nironen, M., 2006, The Svecofennian orogen: a collage of microcontinents and island arcs: The Geological Society, London, Memoirs, v. 32, p. 561-578

Korneliussen, A., and Sawyer, E., 1986, Berggrunns- og malmgeologi med særlig vekt på muligheter for gull, sydlige deler av Rombakvinduet, Nordland: NGU Ba-rapport, v. 86.167.

Korneliussen, A., and Sawyer, E.W., 1989, The geochemistry of Lower Proterozoic mafic to felsic igneous rocks, Rombak Window, North Norway: NGU Bulletin, v. 415, p. 7-21.

Korneliussen, A., Tollefsrud, J.I., Flood, B., and Sawyer, E., 1986, Precambrian volcano-sedimentary sequences and related ore deposits, with special reference to the Gautelisfjell carbonate-hosted gold deposit, Rombaken basement window, Northern Norway: NGU report, v. 86, p. 44.

Korsman, K., Koistinen, T., Kohonen, J., Wennerström, M., Ekdahl, E., Honkamo, M., Idman, H. and Pekkala, Y. (1997). Bedrockmap of Finland 1:1000000:. Geol. Survey Finland, Espoo.

Kuiper, Y.D., Lin, S., and Jiang, D., 2011, Deformation partitioning in transpressional shear zones with an along-strike stretch component: An example from the Superior Boundary Zone, Manitoba, Canada: Journal of Structural Geology, v. 33, p. 192-202.

Lahtinen, R., Garde, A.A., and Melezhik, V.A., 2008, Paleoproterozoic evolution of Fennoscandia and Greenland: Episodes, v. 31.

Larsen, T., Bergh, S.G., Henderson, I., Korneliussen, A., and Kullerud, K., 2010, Svecofennian structural development and metallogenesis of Paleoproterozoic volcano-sedimentary rocks of Rombak Tectonic widow: NGF abstract proceedings of the Geological Society of Norway, v. 1, 2010, 29th Nordic Geological winter meeting, Oslo.

Larsen, T., Sundblad, K., Henderson, I., Bergh, S.G., Bagas, L., Sandstad, J.S., Andersen, T., and Simonsen, S., 2013, Recognition of Svecofennian sulphide bearing crust in the Rombak region, northern Norway: NGF abstract proceedings of the Geological Society of Norway, v. 1, 2013, 32nd Nordic Geological winter meeting, Oslo.

Lin, S., Jiang, D., and Williams, P.F., 1998, Transpression (or transtension) zones of triclinic symmetry: Natural example and theoretical modelling: in Holdsworth, R.E., et al., (eds)., Continental transpressional and transtensional tectonics: Geological Society of London Special Publication, v. 135, p. 41–57.

Montési, L.G.J., and Hirth, G., 2003, Grain size evolution and the rheology of ductile shear zones: from laboratory experiments to postseismic creep: Earth and Planetary Science Letters, v. 211, p. 97-110.

Motuza, G., 1998, Description to the geological map of the eastern part of Kvaløya, Troms county, northern Norway: Geological Survey of Norway Report, v. 111, p. 21.

Myers, J.S., and Krøner, A., 1994, Archean tectonics. In: Hancock, P.L. (ed.), Continental Deformation: Pergamon Press, Oxford, p. 355-369.

Naruk, S.J., 1987, Kinematic significance of mylonittic foliation: PhD thesis, University of Arizona.

Park, R.G., 2005, The Lewisian terrain model: a review: Scottish Journal of Geology, v. 791, p. 105-118.

Priesemann, F.D., 1984a, Summary report - 1983, Rombak project, Foldal Verk A/S: Bergvesenet rapport, v. 2953, p. 38 s.

Priesemann, F.D., 1984b, Summary report - 1984, Rombak project. Foldal Verk A/S: Bergvesenet rapport, v. 2949.

Ramsay, J.G., and Graham, R.H., 1970, Strain variation in shear belts: Canadian Journal of Earth Sciences, v. 7, p. 786-813.

Ramsay, J.G., and Hubert, M.I., 1987, The techniques of modern structural geology; Folds and fractures: Academic Press, New York, v. 2, p. 700.

Ring, U., 1998, Volume strain, strain type and flow path in a narrow shear zone: Geologische Rundschau, v. 86, p. 786-801.

Robin, P.-Y.F., and Cruden, A.R., 1994, Strain and vorticity patterns in ideally ductile transpressional zones: Journal of Structural Geology, v. 16, p. 447-466.

Rodionov, A., Ofstad, F., and Koziel, J., 2012, Helicopter-borne magnetic, electromagnetic and radiometric geophysical survey in Rombaken area, Narvik, Nordland: NGU report, v. 2012.022.

Romer, R.L., 1987, The geology, geochemistry and metamorphism of the Sjangeli area, a tectonic basement window in the Caledonides of Northern Sweden: Research Report University of Technology, Luleå, Sweden.

Romer, R.L., and Boundy, T.M., 1988, Lithologic and tectonic profile across the Muohtaguobla area, Rombak basement window, northern Norway: NGU report, v. 88.116.

Romer, R.L., 1989, Implications of isotope data on the metamorphism of basic volcanites from the Sjangeli Window, northern Sweden: NGU Bulletin, v. 415, p. 39–56.

Romer, R.L., Kjøsnes, B., Korneliussen, A., Lindahl, I., Stendal, H., and Sundvoll, B., 1992, The Archean-Proterozoic boundary beneath the Caledonides of northern Norway and Sweden:

U-Pb, Rb-Sr and Nd isotope data from the Rombak-Tysfjord area: Norges geologiske undersøkelse rapport, v. 91.225, p. 67.

Rykkelid, E., and Andresen, A., 1992, Basement-contraction, out-of-sequence thrusting and late-orogenic extension in the Rombak tectonic window, northern Scandinavian Caledonides. In: Rykkelid, E. Doctoral thesis, University of Oslo.

Sanderson, D.J., and Marchini, W.R.D., 1984, Transpression: Journal of Structural Geology, v. 6, p. 449-458.

Sawyer, E., 1986, Metamorphic assemblages and conditions in the Rombak basement window: Norges geologiske undersøkelse, v. Unpublished report no. 86.168.

Schrank, C.E., Boutelier, D.A., and Cruden, A.R., 2008, The analogue shear zone: From rheology to associated geometry: Journal of Structural Geology, v. 30, p. 177-193.

Sibson, R.H., 1977, Fault rocks and fault mechanisms: Journal of the Geological Society. London, v. 133, p. 191–213.

Simpson, C., and Paor, D.G.D., 1993, Strain and kinematric analysis in general shear zones: Journal of Structural Geology, v. 15, p. 1-20.

Skonseng, E.E., 1985, Berggrunnsgeologisk kartlegging i Gautelis området, Skjomen, Nordland: Feltrapport. NGU-rapport, v. 85.214, p. 16.

Sullivan, W.A., and Law, R.D., 2007, Deformation path partitioning within transpressional White Mountain shearzone, California and Nevada: Journal of Structural Geology, v. 29, p. 583-598.

Sylvester, A.G., and Smith, R.R., 1976, Tectonic transpression and basement-controlled deformation in San Andreas Fault Zone, Salton Trough, California: American Association of Pertoleum Geologists Bulletin, v. 60, p. 2081-2102.

Sylvester, A.G., and Smith, R.R., 1987, Structure section in Painted Canyon, Mecca Hills, southern California: in Cordilleran Section of the Geological Society of America, Hill, M. L., (ed.), Boulder, Colorado: Geological Society of America Centennial Field Guide, v. 1, p. 103-108.

Tavarnelli, E., Holdsworth, R.E., Clegg, P., Jones, R.R., and McCaffrey, K.J.W., 2004, The anatomy and evolution of a transpressional imbricate zone Southern Uplands, Scotland: Journal of Structural Geology, v. 26, p. 1341-1360.

Teyssier, C., Tikoff, B., and Markley, M., 1995, Oblique plate motion and continental tectonics: Geology, v. 23, p. 447– 450.

Tikoff, B., and Greene, D., 1997, Stretching lineations in transpressional shear zones: Journal of Structural Geology, v. 19, p. 29-40.

Tikoff, B. and Fossen, H., 1993. Simultaneous pure and simple shear; the unifying deformation matrix. Tectonophysics 217: 267-283.

Tull, J.F., 1977, Geology and structure of Vestvågøy. Lofoten, north Norway: Norges Geologiske Undersøkelse, v. 42, p. 109.

Vitale, S., and Mazzoli, S., 2009, Finite strain analysis of a natural ductile shear zone in limestones: insights into 3-D coaxial vs. non-coaxial deformation partitioning: Journal of Structural Geology, v. 31, p. 104-113.

Whitney, D.L., Teyssier, C., and Heizler, M.T., 2007, Gneiss domes, metamorphic core complexes, and wrench zones: Thermal and structural evolution of the Nigde Massif, central Anatolia: Tectonics, v. 26, p. 1315-1343.

Zoback, M.D., Zoback, M.L., S.Mount, V., Suppe, J., Eaton, J.P., Healy, J.H., Oppenheimer, D., Reasenberg, P., Jones, L.M., Raleigh, C.B., Wong, I.G., Scotti, O., and Wentworth, C.M., 1987, New evidence for the state of stress on the San Andreas fault system: Science, v. 238, p. 1105 – 1111.

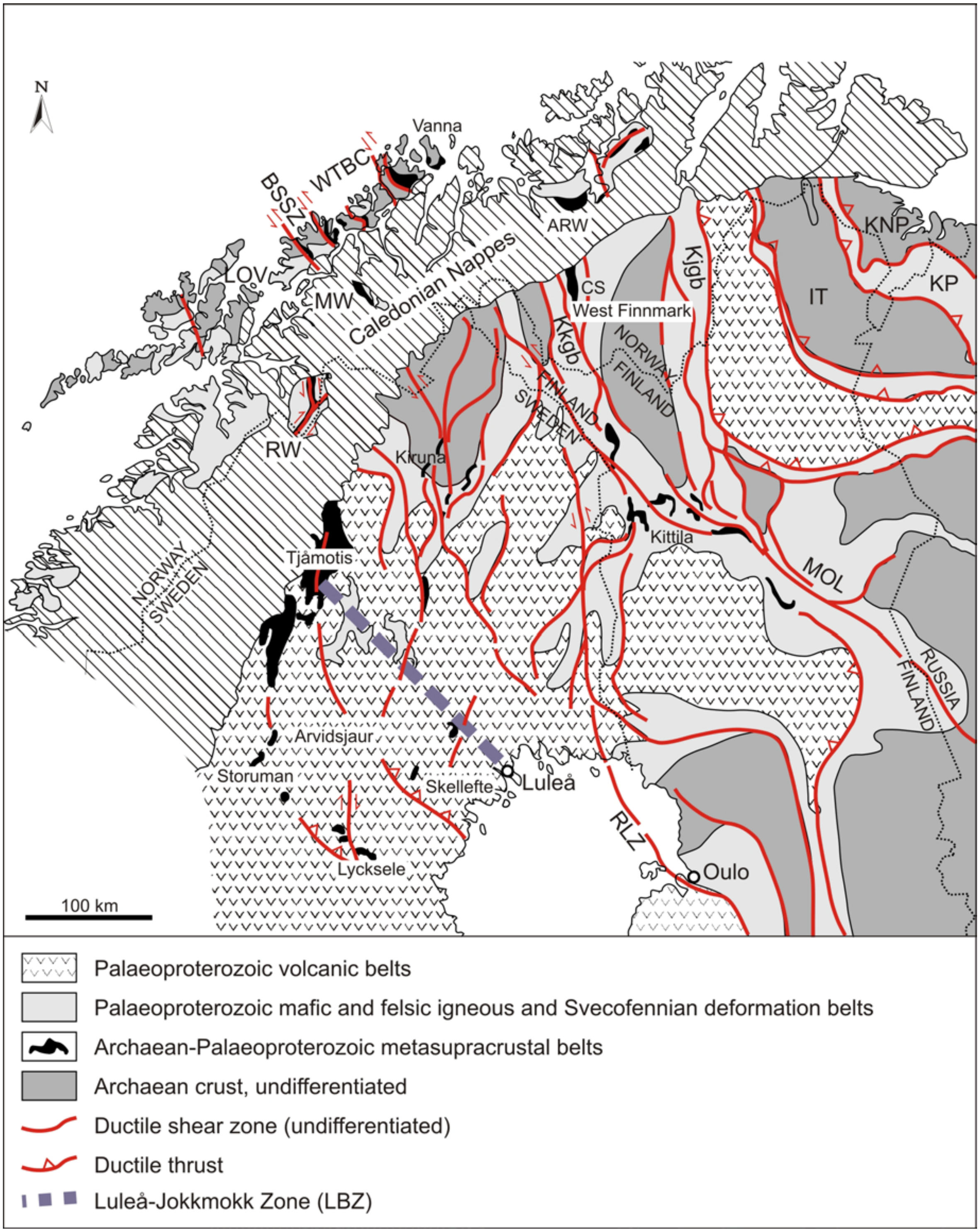

Fig. 1: Overview geological map of Fennoscandia shows the Orogenic domains and the location of Rombaken tectonic window (Fig. 2) in Northern Norway. Abbreviations: BSSZ=Bothnian-Senja shear zone, Kkjgb= Karasjokk Greenstone belt, Kkgb=Kautokeino Greenstone belt, KNP=Kola-Norwegian province, KP=Kola province, MW=Mauken Tectonic Window, NP=Norrbotten province, RW=Rombaken Tectonic Window, WTBC= West Troms Basement Complex, The map is modified from, Korsman et al 1997; Cagnard et al 2007; Bergh et al., 2012.

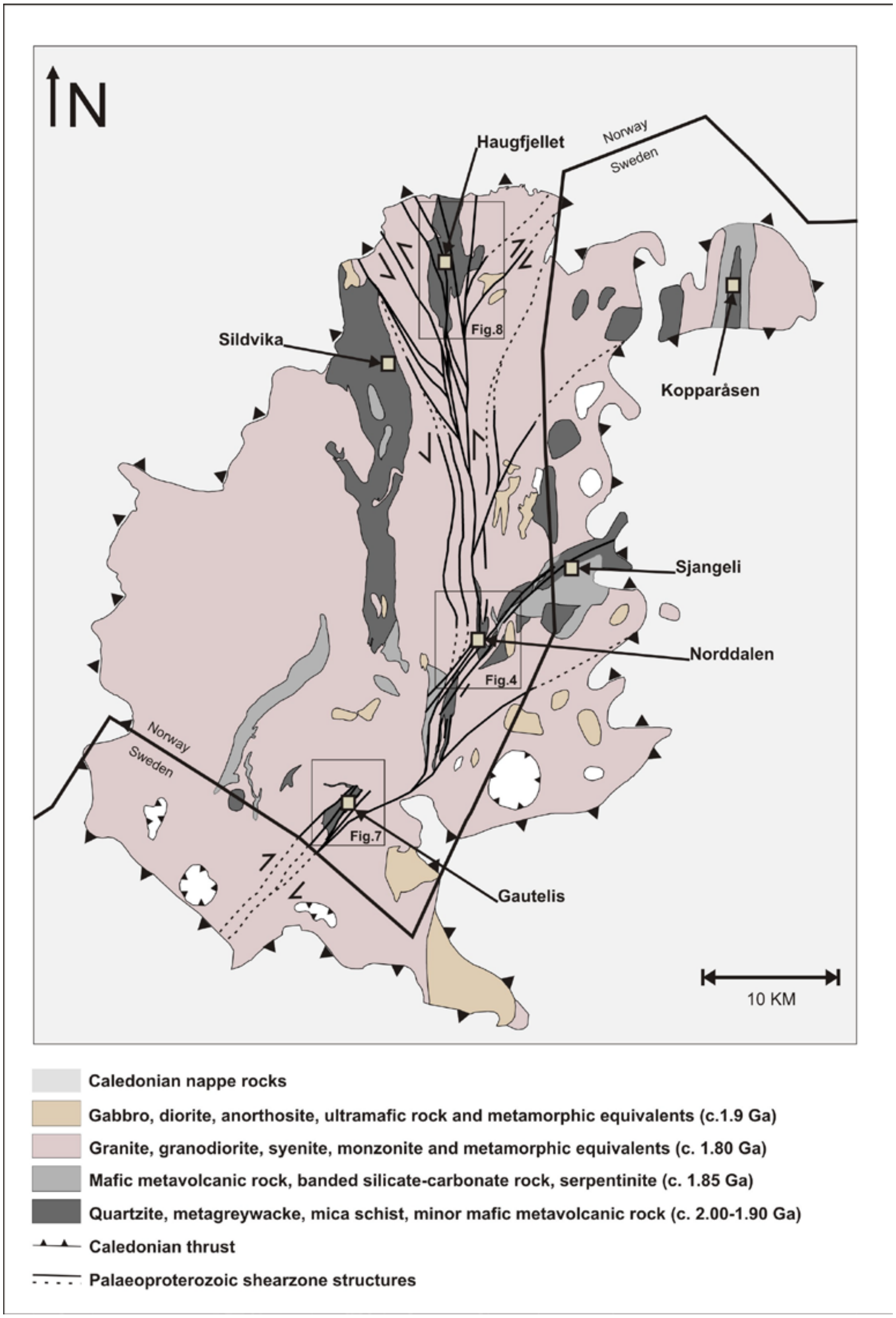

Fig. 2: Geological and tectonic map of Rombaken tectonic window, showing several N-S trending supracrustal belts with surrounding granitoid rocks, and the network of ductile shear zones (Rombak-Skjomen Shear Zone) that frame the window. The map also shows the location of the three main localities Haugfjellet (Fig. 8), Norddalen (Fig. 4) and Gautelis (Fig. 6) marked with a square and a point in addition to Sjangeli, Sildvika and Sjangeli, which are relevant localities for comparison. The map is modified from Arc GIS maps provided by SGU and NGU.

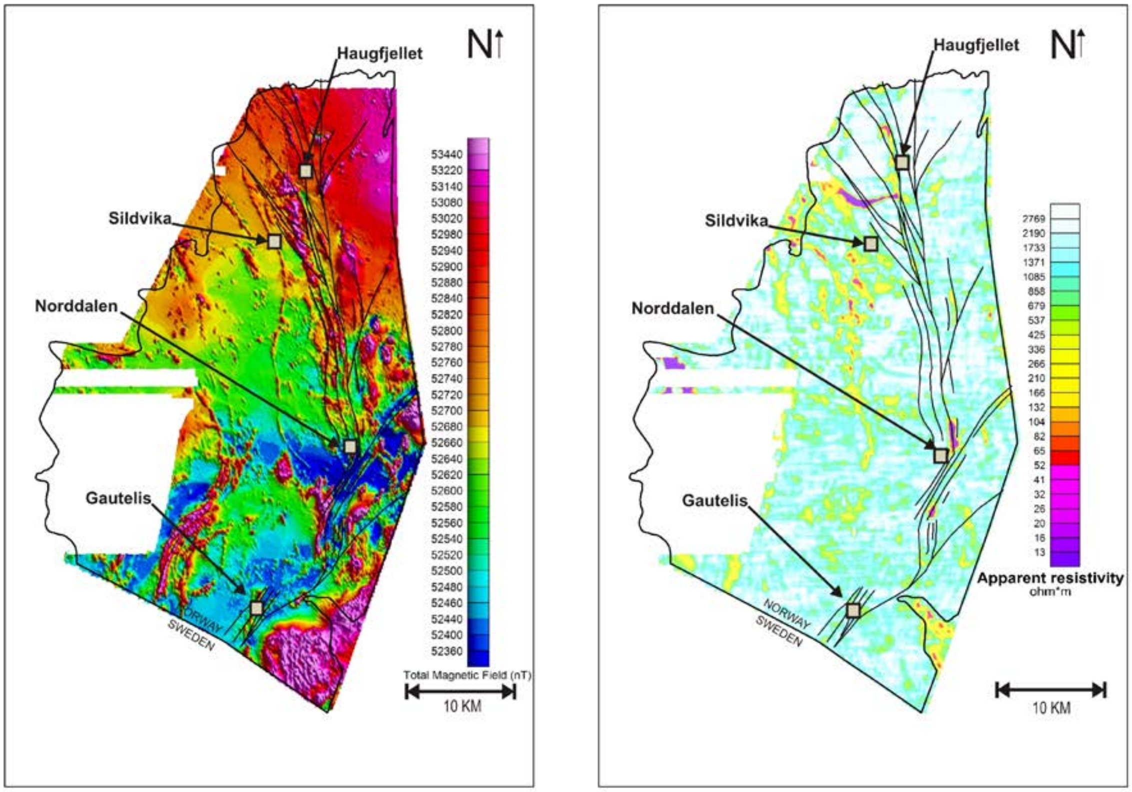

Fig. 3: A) Aeromagnetic map with structural interpretation. Note the presence of the N-S trending anomaly lineaments (shear zone arrays) that are truncated by NE-SW trending lineaments. B) EM gravity map showing N-S trending anomaly patterns that are displaced ca. 5 km by NE-SW trending lineaments (shear zones). The graphitic schist in Norddalen can be seen with its high anomaly and purple colour. Both the magnetic and EM data were collected from a helicopter based survey and flown with 200 m line spacing and line direction of 90° East West (Rodionov et al., 2012).

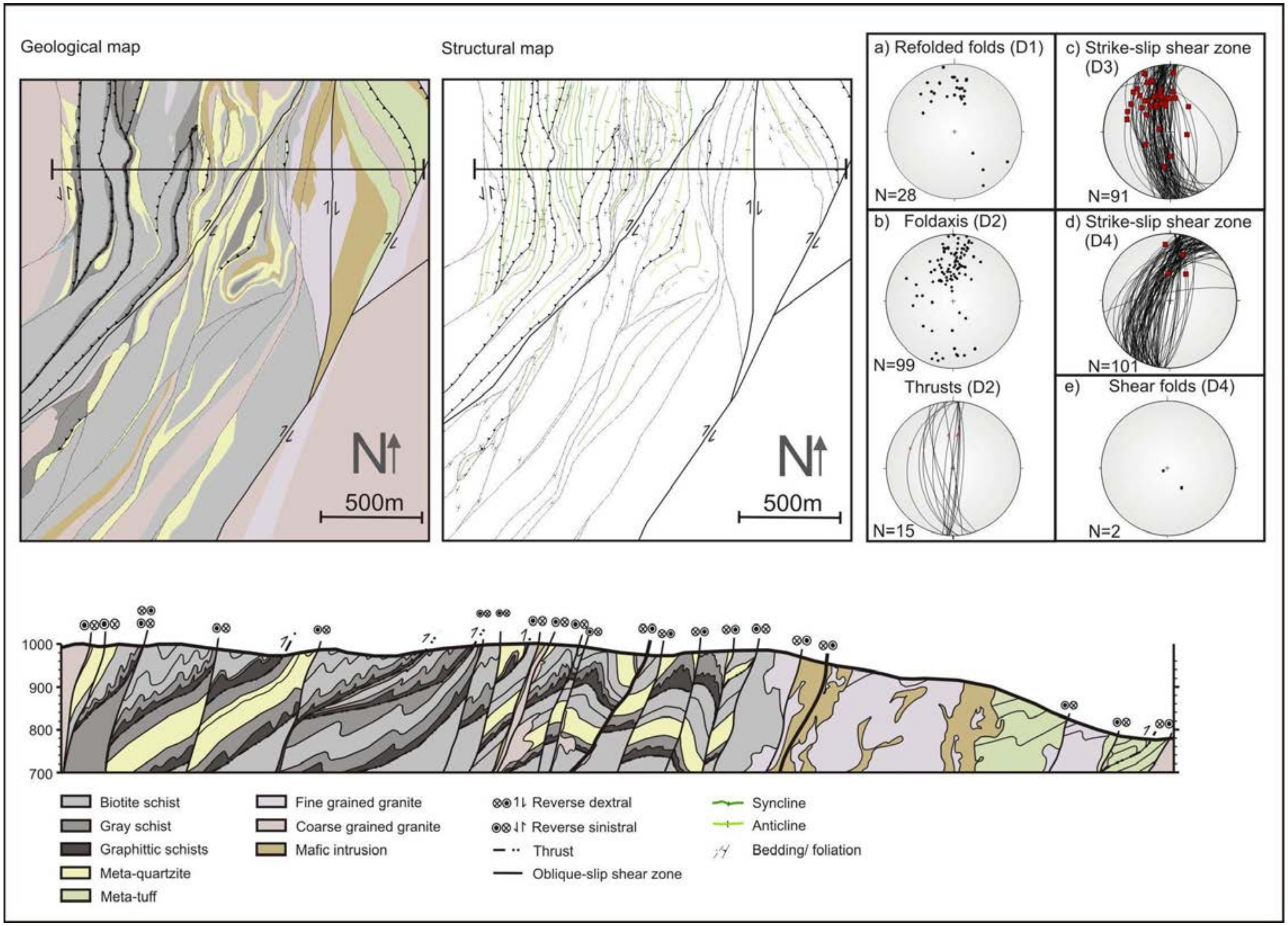

Fig. 4: Geological and structural map of the Norddalen fold-and thrust belt domain and a cross-section from the area. The stereo nets (Schmidt net, lower hemisphere) show the attitudes of: a) fold axes of refolded D_1 folds, b) D_2 fold axes in the dissected fold-thrust belt and its thrusts with lineations shown as great circle girdles with poles, c) N-S striking D_3 shear zones (as great circle girdles), d, e) NE-SW striking D_4 shear zones and e) steeply dipping fold axes (dots).

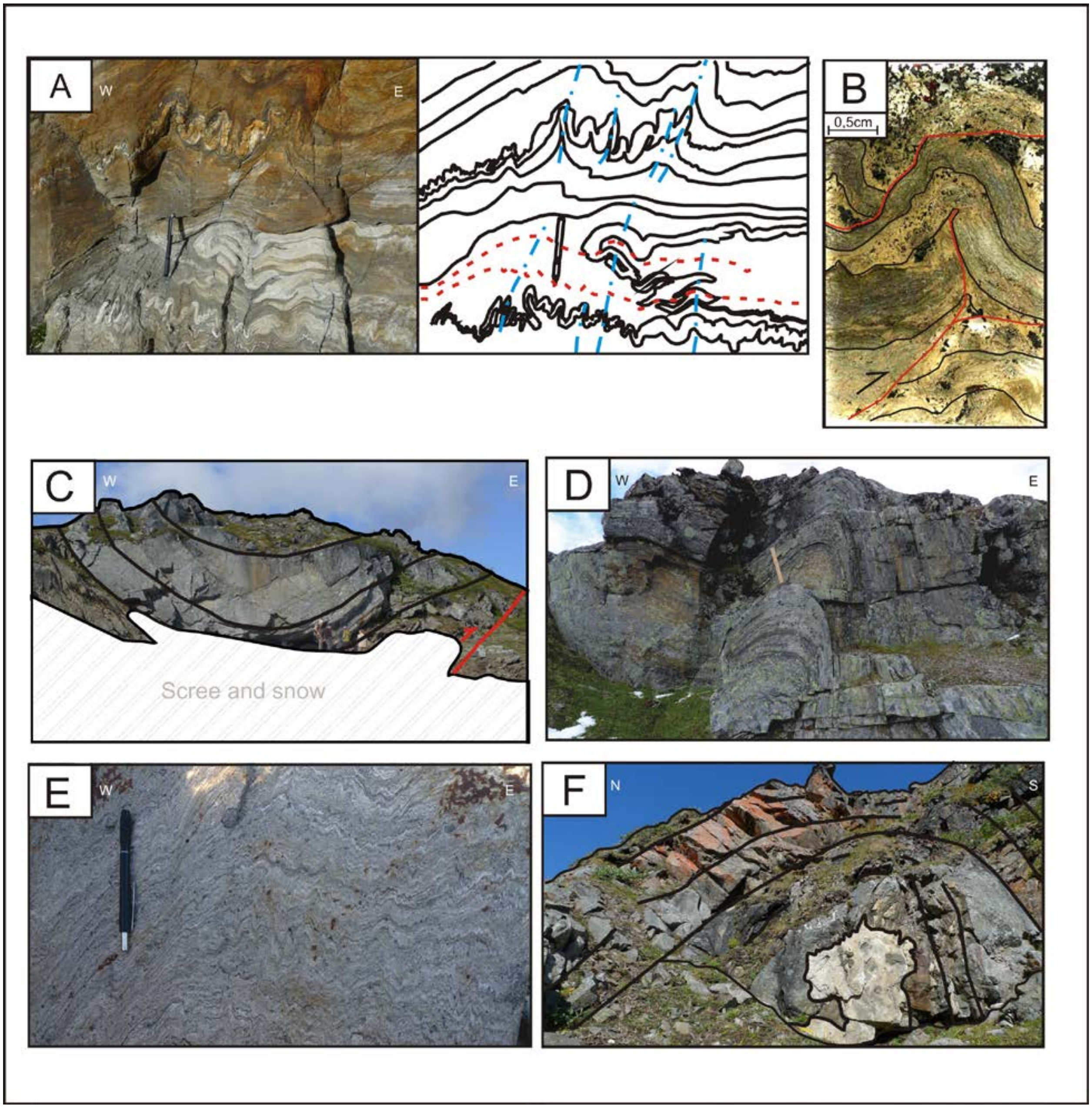

Fig. 5: Outcrop and microscale features of contractional (fold-thrust belt) structures with sketch interpretations from the Norddalen and Gautelis domain: A) Iron-rich mafic and felsic schists showing three generations of folds; the limbs and F_1 fold axial surfaces have been modified from a near-horizontal attitude parallel (red line) to the overlying and underlying enveloping surface of primary layers, into F_2-F_3 folds with nearly vertical axial surfaces (blue line). View is toward north. B) Microphotograph of thin section from the fold-thrust belt in Norddalen showing a complex fold and thrust pattern. C) A syncline in quartzittic conglomerate and sandstone on top of a thrust cutting through graphitic schist in Norddalen. D) Open asymmetric upright fold in Norddalen, verging east. E) S-Z-M shaped parasitic folds. F) Open asymmetric fold in Gautelis showing a thrust that cuts through and deforms the soft marble in the core.

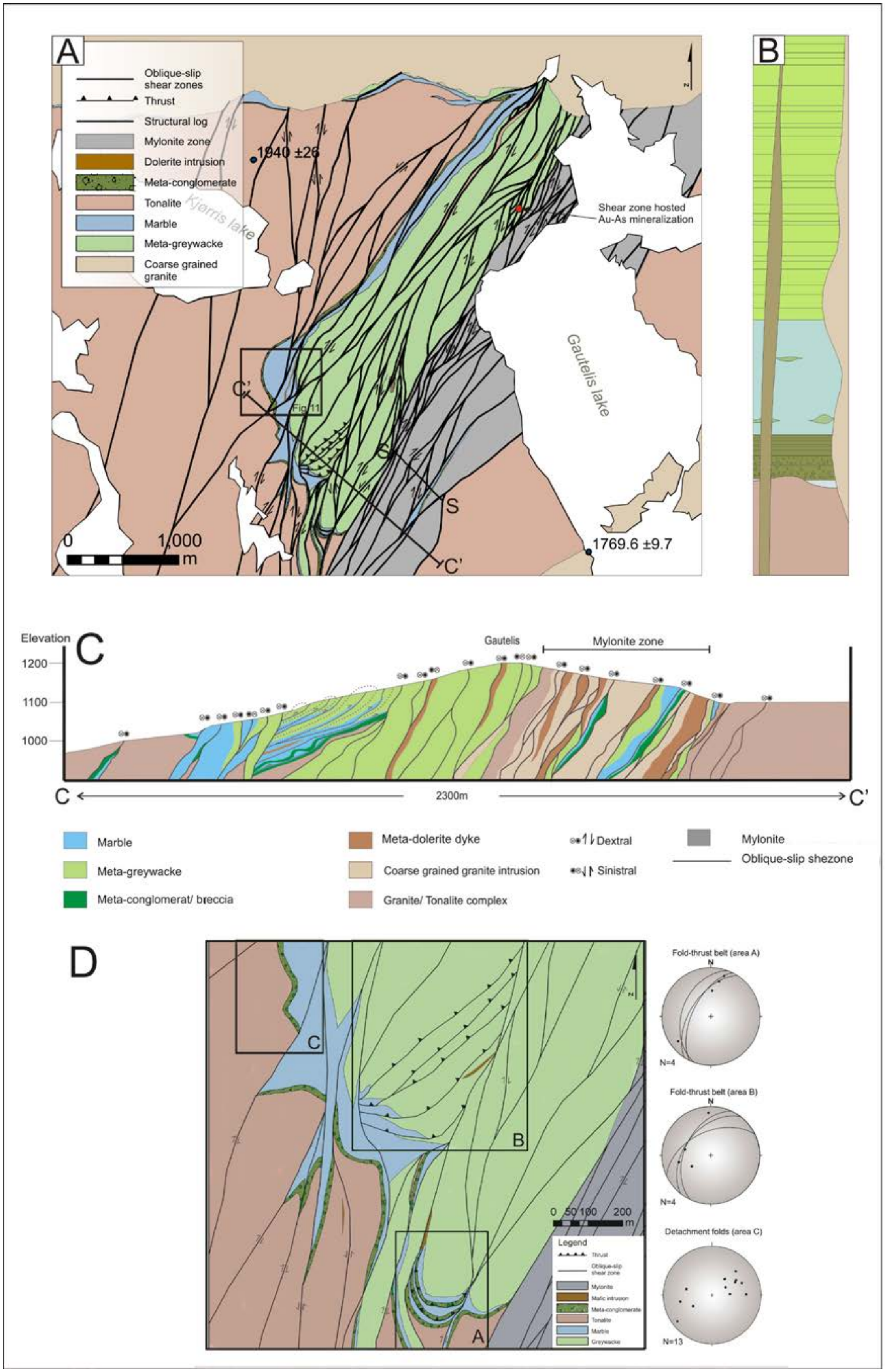
A
Oblique-slip shear zones
Thrust
Structural log
Mylonite zone
Dolerite intrusion
Meta-conglomerate
Tonalite
Marble
Meta-greywacke
Coarse grained granite
Kjørris lake
1940 ±26
Shear zone hosted Au-As mineralization
Gautelis lake
Fig 11
C'
S
C'
0
1,000
m
1769.6 ±9.7
B
C
Elevation
1200
1100
1000
Gautelis
Mylonite zone
C
2300m
C'
Marble
Meta-greywacke
Meta-conglomerat/ breccia
Meta-dolerite dyke
Coarse grained granite intrusion
Granite/ Tonalite complex
Dextral
Sinistral
Mylonite
Oblique-slip shezone
D
C
B
A
0 50 100 200
m
Legend
Fold-thrust belt (area A)
N
N=4
Fold-thrust belt (area B)
N
N=4
Detachment folds (area C)
N=13

Fig. 6: Geologic and structural map of the oblique-slip dominated Gautelis domain. A) Geological overview map of the Gautelis area. Location of cross-section lines (Fig. 6C; line C-C'), structural log (Fig. 11; line S'-S) and Fig 6D (frame) is marked on this map. The added radiometric ages are from Romer et al. (1992). B) Stratigraphic log of the Gautelis domain. C) Interpreted cross section of the main ductile shear zone of the Gautelis domain. D) Close-up geological map of the south-western part of the Gautelis domain, showing small remnants of the D_2 fold-thrust belt (in frames) with stereoplots showing the thrusts (great circles) and fold axis (poles) for each frame.

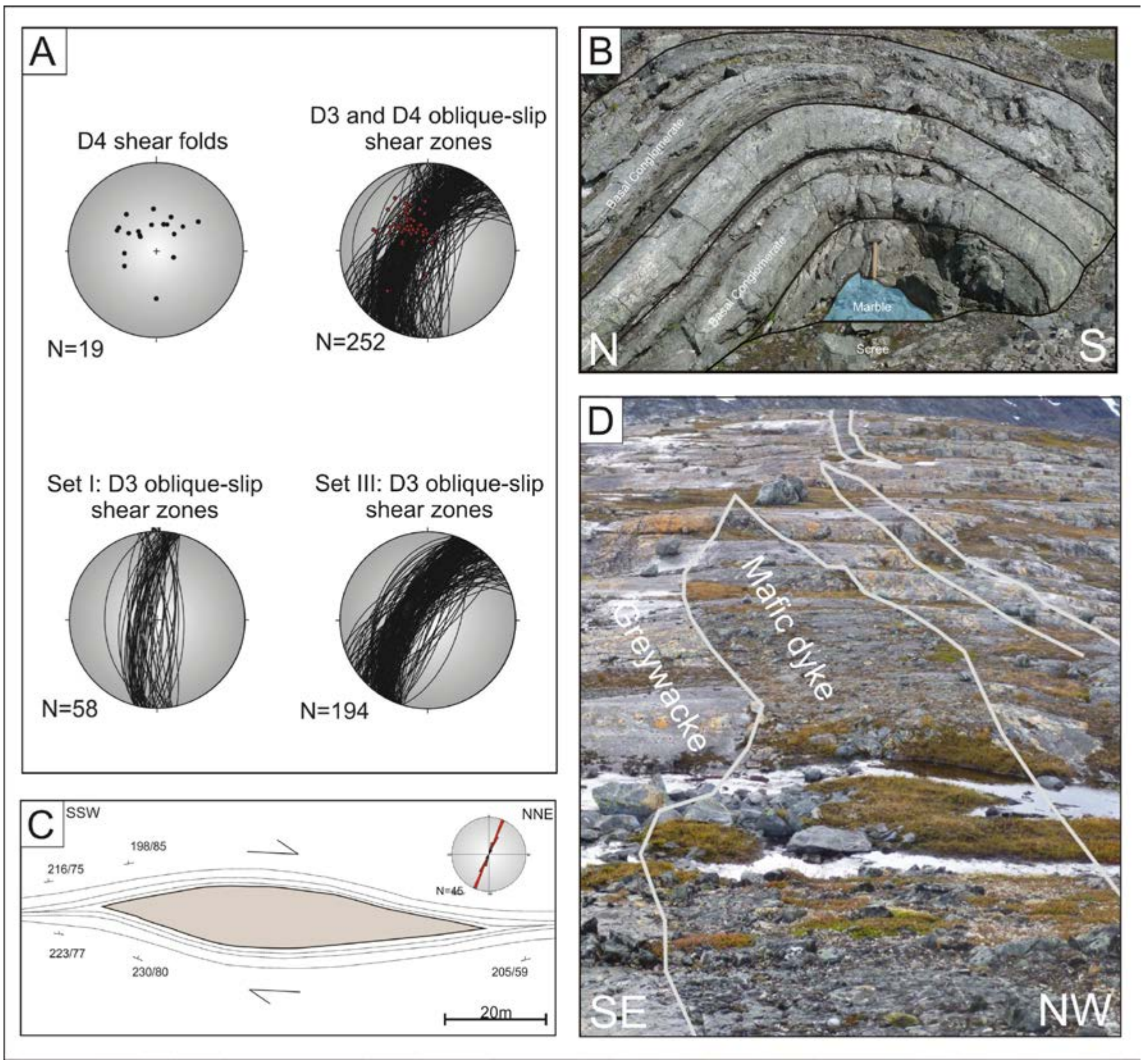

Fig. 7: A) Structural orientation data from the Gautelis domain shown as stereo plots: D_4 shear fold axes, D_3 oblique-slip shear zones (great circle girdles) and D_4 oblique-slip shear zones (great circles) with stretching lineations (dots). B) Slightly asymmetric upright fold in the basal conglomerate overlying the tonalittic basement rocks. The fold core consists of marble and shows that there is a possible detachment thrust in the tonalite below. C) The sketch shows a mafic dyke with D_4 shear zones bending around the dyke body. The sketch is from the same dykes as in the photograph. D) Mafic dykes are found as strike-parallel dykes within the D_4 shear zone.

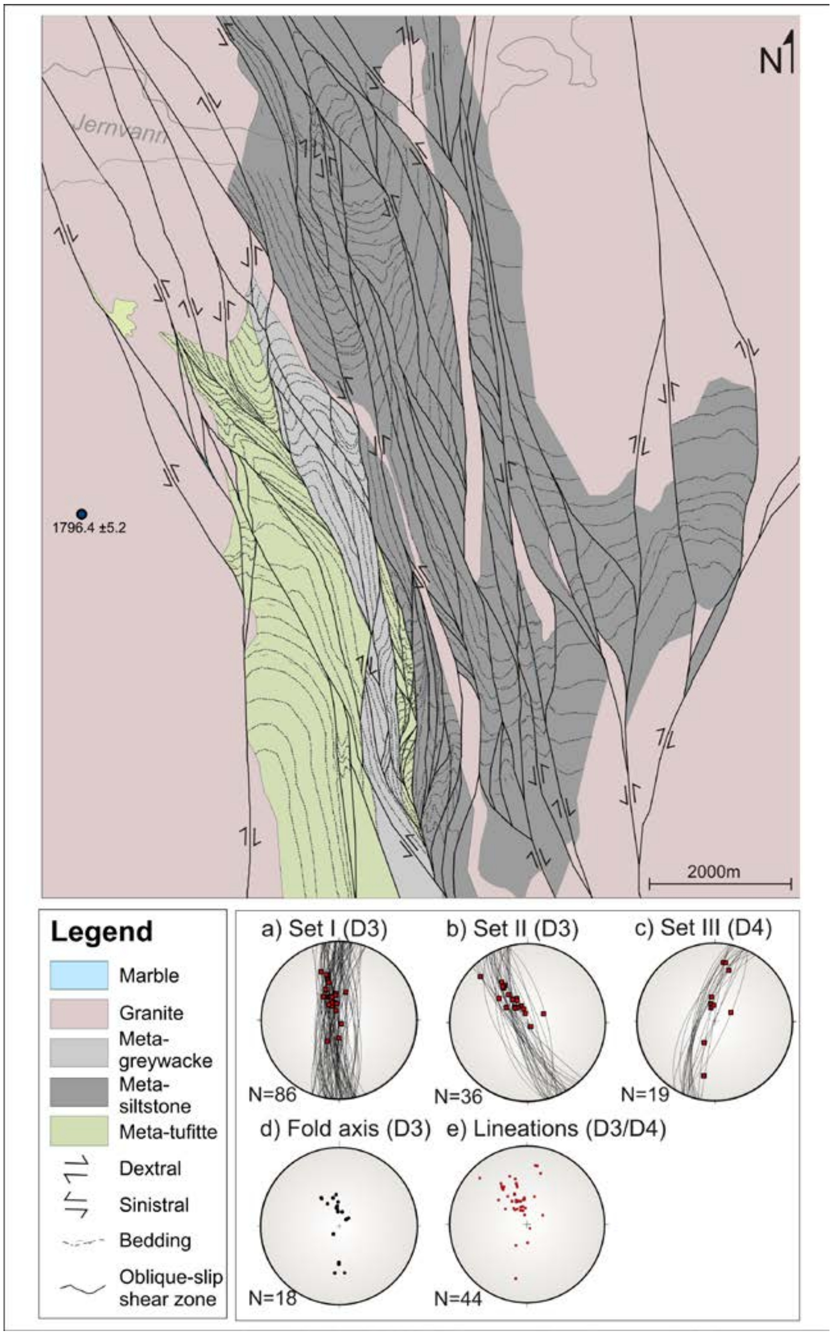

Fig. 8: Geologic and structural map of the combined contractional and oblique-slip dominated (transpressional) Jernvann-Haugfjellet domain with structural data. The map shows how the bedding (dotted line) are cut and folded by D_3-D_4 sinistral and dextral oblique-slip shear zones (black unbroken lines, arrows indicate sense-of-shear). The stereo plots a-c) show three differentiated oblique-slip shear zone sets (I-III; shown as great circles) with their belonging lineations (dots). d) Show stereo plots of steep plunging D_3 fold axis marked as dots. e) Stereo plot with all lineations from D_3-D_4 shear zones collected as dots in one stereo net. The zircon dated granite dated to 1796.4 ± 5.2 Ma, marked at the left of the map, is from Romer et al (1992).

Fig. 9: Outcrop photos of oblique-slip structures and related folds of the Gautelis, Norddalen and Jernvann-Haugfjellet domain. A) Steep N-plunging dextral asymmetric folds in a D_4 oblique-slip shear zone in Gautelis. View is on horizontal surface. B) Steep N-plunging folds in the greywacke sequence with a mafic intrusion along the cutting D_4 shear zone. View is from moderate dipping surface C) Steep plunging D_3 folds from Haugfjellet on horizontal surface. D) Steep plunging fold at Haugfjellet, segmented by D_3 oblique-slip shear zones on horizontal surface. E) Sinistral sigma clast of quartz in the greywacke D_3 oblique-slip shear zones in Norddalen. View is on horizontal surface. F) Steep, dextral duplex of D_4 oblique-slip shear zones in a granite dyke on a horizontal surface. G) Reverse sinistral oblique-slip shear zone south of Haugfjellet, here seen with a sinistral shear sense. Photo is taken on a vertical surface towards the south.

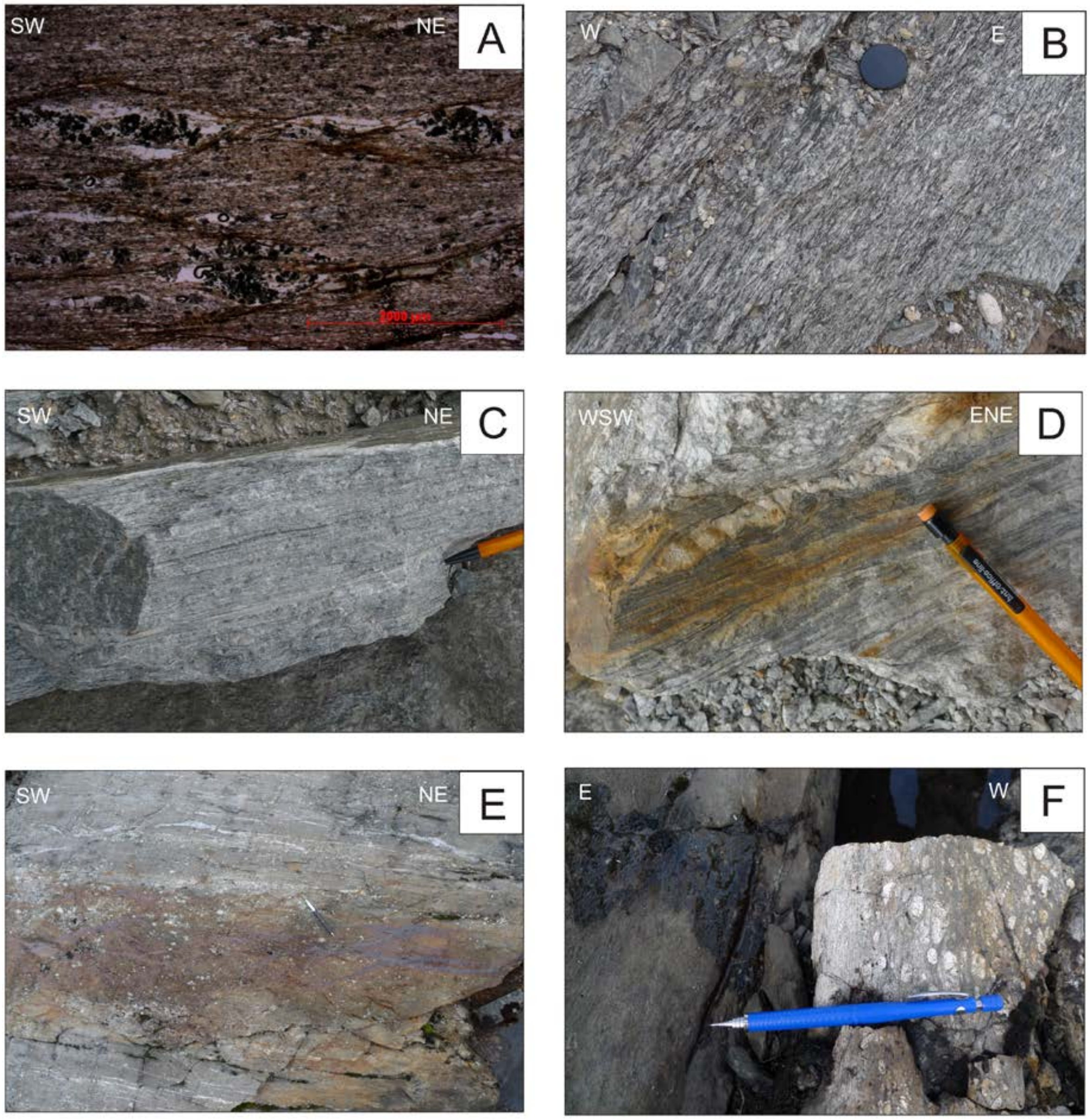

Fig. 10: Oblique-slip features from the Gautelis and Jernvann-Haugfjellet domain. A) Anastomosing shear zone pattern from a thin section of meta-greywacke from Gautelis. Note asymmetric clasts of ore minerals enclosed by Fe-enriched shear zone networks. B) D_4 Proto-mylonite in granite C) D_4 Ortho-mylonitic shear zone in granite D) D_4 Ultra-mylonitic granite in steep, localized shear zone. E) Anastomosing D_4 oblique-slip shear zone pattern from Gautelis carrying sulphides. C) Sheared granite (ultramylonitic) cutting steep plunging D_3 folds at Haugfjellet.

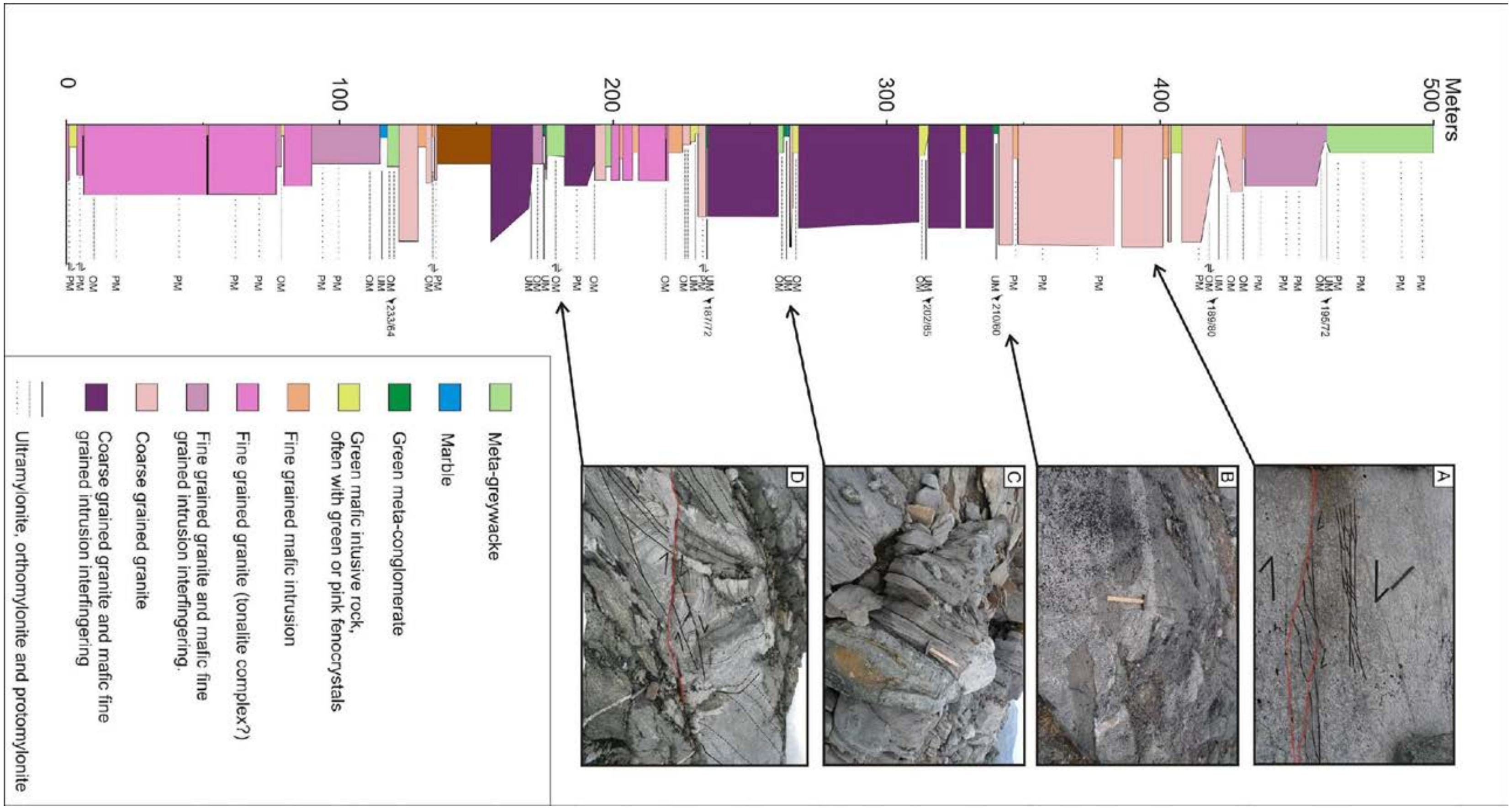

Fig. 11 Detailed structural log across the ca. 600 m thick D_4 mylonite shear zone in Gautelis (location line is shown in fig. 6A). Note the rapid variation in rock types across this anastomosing shear zone pattern suggesting high strain segmentation and formation of lens shaped units of the host rocks. The photographs show examples from the rapid variations of structures: A) Dextral duplex and extensional crenulation cleavage in the same outcrop of coarse grained granite seen on a horizontal surface. B) Greywacke rafts in coarse grained granite. View at horizontal surface. C) Strongly deformed marble with isoclinal folds in the lower right corner. D) A complex, dextral duplex (black line) with folded greywacke (dotted lines) and granite intrusions which are again cut by oblique-slip shear zones (red line). Photo is taken on moderate dipping surface. Abbreviations: OM: D_4 Proto-mylonite (Fig. 10B), PM: D_4 Ortho-mylonite (Fig. 10C) and UM: D_4 Ultra-mylonite (Fig. 10D).

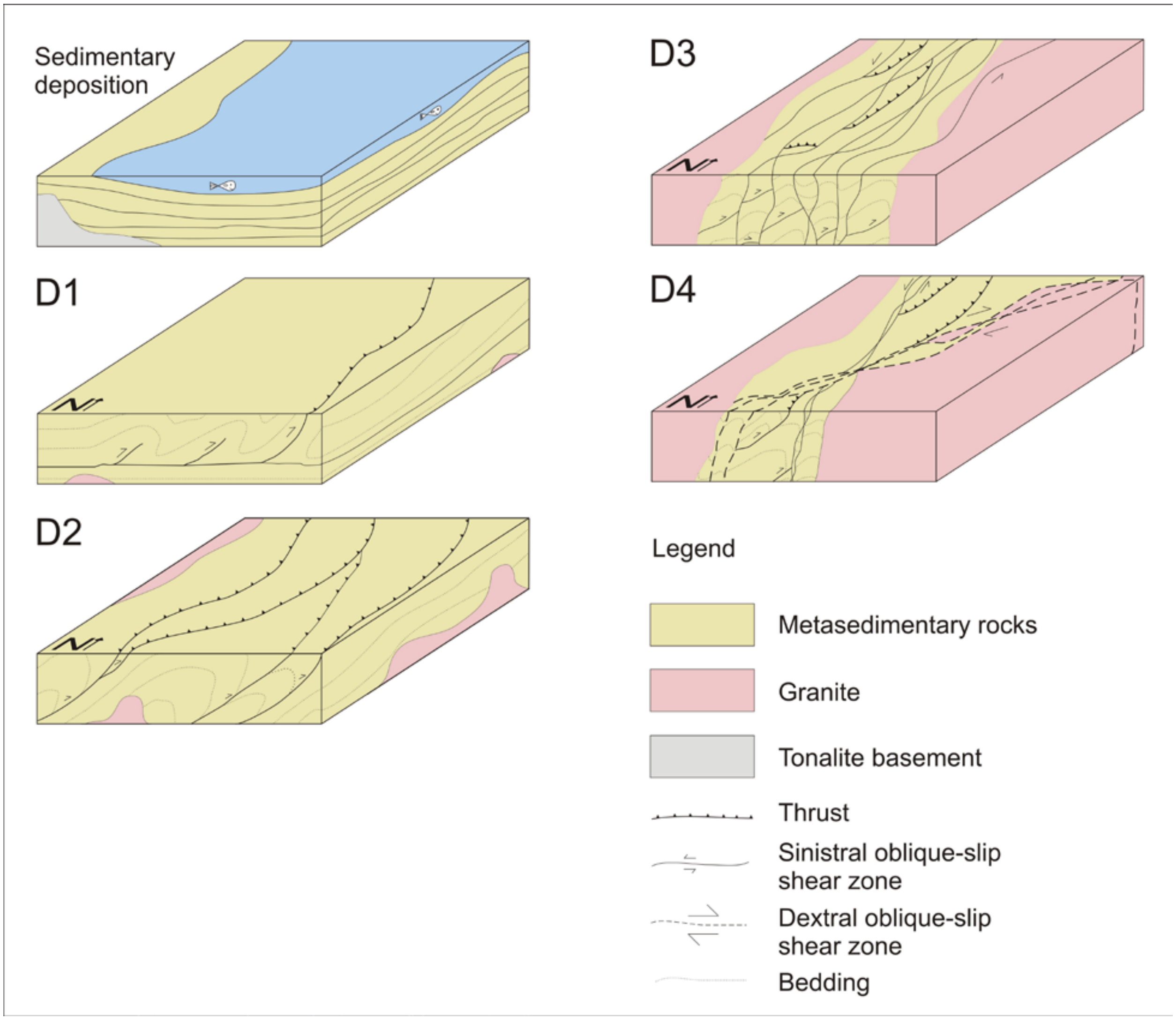

Fig. 12: A structural model with the four deformation stages. Formation of a sedimentary basin deposited on a stable, passive margin setting in the Paleoproterozoic (2.4-1.9 Ga) with deposition of strata on top of eroded tonalittic basement rocks. D_1) Initial E-W shortening of the sedimentary basin and formation of thrust detachments and related folds (Fig. 7B). D_2) Continued E-W shortening with folding and thrusting towards east in the sedimentary rocks. These structures refolded the D_1 structures coaxially (Fig. 5A and B). Granit started to intrude at this stage, syn-tectonic with D_2 folding and thrusting. D_3) N-S striking steep sinistral oblique-slip shear zones developed parallel to the steeply dipping forelimbs of D_2 folds, and granite dykes intruded into the sedimentary rocks and along the late-stage, steep shear zones. D_4) NE-SW striking steep dextral shear zones developed oblique to the N-S going lineament. This major structure cut and folds the metasedimentary belt at several places. The granite dykes intruded into and parallel with these shear zones, and also interfingering with mafic dykes.

Paper II

Tine Larsen Angvik, Leon Bagas, Are Korneliussen

Geochemical evidence for arc-related setting of Paleoproterozoic (1790 Ga) volcano-sedimentary and plutonic rocks of the Rombak Tectonic Window

(manuscript)

Geochemical evidence for arc-related setting of Paleoproterozoic (1790 Ga) volcano-sedimentary and plutonic rocks of the Rombak Tectonic Window

Tine L. Angvik [1, 2], Leon Bagas [3], Are Korneliussen [1]

[1] Norges Geologiske Undersøkelse, Postboks 6315 Sluppen, 7491 Trondheim.
[2] University of Tromsø, Dramsveien 201, 9037 Tromsø
[3] Centre for Exploration Targeting, ARC Centre of Excellence for Core to Crust Fluid Systems, The University of Western Australia, 35 Stirling Highway, Crawley, WA 6009, Australia

ABSTRACT

The Rombak Tectonic Window (RTW) of north-central Norway is an inlier exposed through Caledonian (ca. 500-400 Ma) nappes and represents a western-extension of the Proterozoic Fennoscandian Shield in Sweden and Finland to the east. Sensitive high-resolution ion-microprobe U–Pb dating of zircons from monzogranite samples collected for the study in the RTW yielded ages of ca. 1790 Ma, which are synchronous with granites in Sweden and Finland. Structurally, the granites cross-cut and are cross-cut by large north-going oblique-slip shear zones within the inlier that are associated with Au-sulfide mineralisation. Therefore, the ca. 1790 Ma age brackets both the timing of the deformation and the timing of the gold and sulfide mineralization.

The RTW has a complex geology with a strongly deformed metamorphosed succession of ca. 2000 – 1867 Ma turbidites (greywacke and shale), graphitic shale, quartzite, conglomerate and marble interbedded with metamorphosed ultramafic, mafic, intermediate and felsic volcanic.

Both the sedimentary and volcanic units have similar tectonic settings as indicated by geochemical discrimination affinities, with the sedimentary rocks having being deposited in an active continental margin or island-arc setting, and the ultramafic and mafic plotting in a continental to oceanic-arc settings. The geochemistry of the volcanic rocks also suggests that they were deposited in an island-arc setting over a tonalitic substrate. In addition, they are primitive and probably derived from the mantle. Therefore from the geochemical characteristics of the volcanic rocks, we suggest that the metasedimentary rocks in the RTW were deposited in an island arc to active continental margin setting, from a provenance dominated by mafic to intermediate and felsic volcanic rocks.

The ca. 1790 Ma granitic rocks are late-orogenic to anorogenic and associated with a volcanic-arc to within-plate tectonic setting, which is a similar tectonic setting as the metasedimentary and volcanic units they intrude. It is suggested that these granites are derived by similar rocks as those they intrude and were emplaced during or shortly after the ca. 1850-1800 Ma Svecofennian Orogeny. We also suggest the metamorphosed metasedimentary, volcanic and plutonic rocks in the inlier developed in a long-lived and progressive tectonic event spanning ~70 Ma in an island-arc setting. Through time, the island-arc progressively changed into a continental-arc with felsic volcanic rocks and granites being emplaced. This sedimentary, volcanic and plutonic succession then accreted on to the Baltic continent to the east.

Keywords: Rombak Tectonic Window, tectonic model, Paleoproterozoic, geochemistry, U-Pb zircon dating

1. Introduction

Precambrian rocks in the northern part of Norway are overlain extensively by Caledonian (ca. 500-450 Ma) thrust nappes, and are therefore known principally from geophysical investigations and the study of inliers or “tectonic windows” (e.g. Bergh et al., 2010; Larsen et al., 2013). Archaean and Paleoproterozoic units in these inliers in Norway, Sweden, Finland and northwest Russia are presently assigned to the northern part of the Fennoscandian Shield containing metasedimentary belts intruded by similar aged granites (Fig. 1; Bargel, et al., 1995). The granites are largely coeval and assigned to the Transscandinavian Igneous Belt (TIB; e.g. Romer et al., 1992; Larson & Berglund, 1992; Persson & Wikström, 1993; Wikström, 1996).

The Fennoscandian Shield is an important source for metals and despite centuries of exploration, new deposits are still being explored (e.g. Weihed et al., 2005). A more precise knowledge of the tectonic and metallogenic evolution of the shield is required for the understanding of ore-forming systems in the region leading to a better targeting tool for mineral exploration, and this requires accurate structural and geochronological investigations.

This contribution presents the results of structural, geochronological and integrated geochemical investigations (Korneliussen & Sawyer, 1989; Sawyer & Korneliussen, 1989) in RTW and a model for the crustal evolution of the Fennoscandian Shield in north-central Norway.

2. Regional geology of the Fennoscandian Shield

The RTW is an important Paleoproterozoic terrane in the Fennoscandian Shield containing metallic mineralization (Cu-Fe-Zn-Pb-As-Au) characterised by disseminated massive sulfides along bedding-parallel layers interpreted as possible sedimentary exhalative deposits, in gashes associated with folds and faults, and in steep late-stage anastomosing ductile shear zones (Coller, 2004; Larsen et al., 2010; Whitehead, 2010; Larsen et al., 2013).

The Fennoscandian Shield extends from at least Norway to Russia, and is likely to be a continuation of the Paleoproterozoic successions in the eastern part of Greenland (e.g. Bagas et al., 2013). Inliers of the shield are exposed in windows formed through allochtonous nappes of Paleozoic Caledonian rocks and situated near the southern margin of the Archaean component of the Precambrian Baltic Shield (Gaál and Gorbatschev, 1987; Gorbatschev, 1985; Gustavson and Gjelle, 1991; Romer et al., 1991; Myers and Kroner, 1994). The nappes are the products of collisional tectonics during the Early to Mid-Paleozoic that was followed by extensional collapse during ca. 400-350 Ma (e.g. Fossen, 2000). Four Caledonian nappes were thrust over the Baltoscandian Platform in Norway mainly to the southeast (e.g. Gee & Sturt, 1985). These structures are characterized by their flat lying nature as compared to the steeply dipping foliation within the inliers (e.g. Birkeland, 1976). Erosional processes gradually exposed the underlying tectonic inliers such as the RTW (Fig. 1).

RTW consists of a succession of metamorphosed volcanic and sedimentary rocks that formed parts of the Paleoproterozoic (ca. 2000 – 1867 Ma) Bothnian Basin located between central Sweden to the eastern part of Finland (Lindquist, 1987; Welin et al., 1993; Korneliussen and Sawyer, 1989). Mafic dykes, granodiorite, monzogranite and syenite, which are the predominant rock types in the inlier, intrude these basement rocks (Gaál and Gorbatschev, 1987; Nironen, 1997; Fig. 2).

RTW is an important transition between the autochthonous northeast and eastern part of the Fennoscandian Orogen and the exposed basement rocks located west of the Caledonides, such as the West Troms Basement Complex (WTBC) and Mauken Tectonic Window (Fig. 1). As yet, the relationship between the disparate windows in the orogen and the nature of the Paleoproterozoic crustal architecture related to the Svecofennian crustal scale shear zones are poorly understood.

Six narrow zones of north-trending amphibolite facies metasedimentary and metavolcanic rocks, including metamorphosed greywacke, quartzite, graphitic shale and carbonate, form linear rafts in granite in the RTW. The age of the rafts is not known, but they are younger than the ca. 1951 Ma tonalites and older than ca. 1800 Ma granites (Skyseth and Reitan, 1990; Romer et al., 1991). In addition, regional metamorphism took place in the tectonic windows during the ca. 1850-1800 Ma Svecofennian Orogeny (e.g. Korsman et al. 1984; Nironen, 1997), which was followed by greenschist-facies retrogression associated with folding and ductile faulting between (Sawyer, 1986; Korneliussen et al., 1989).

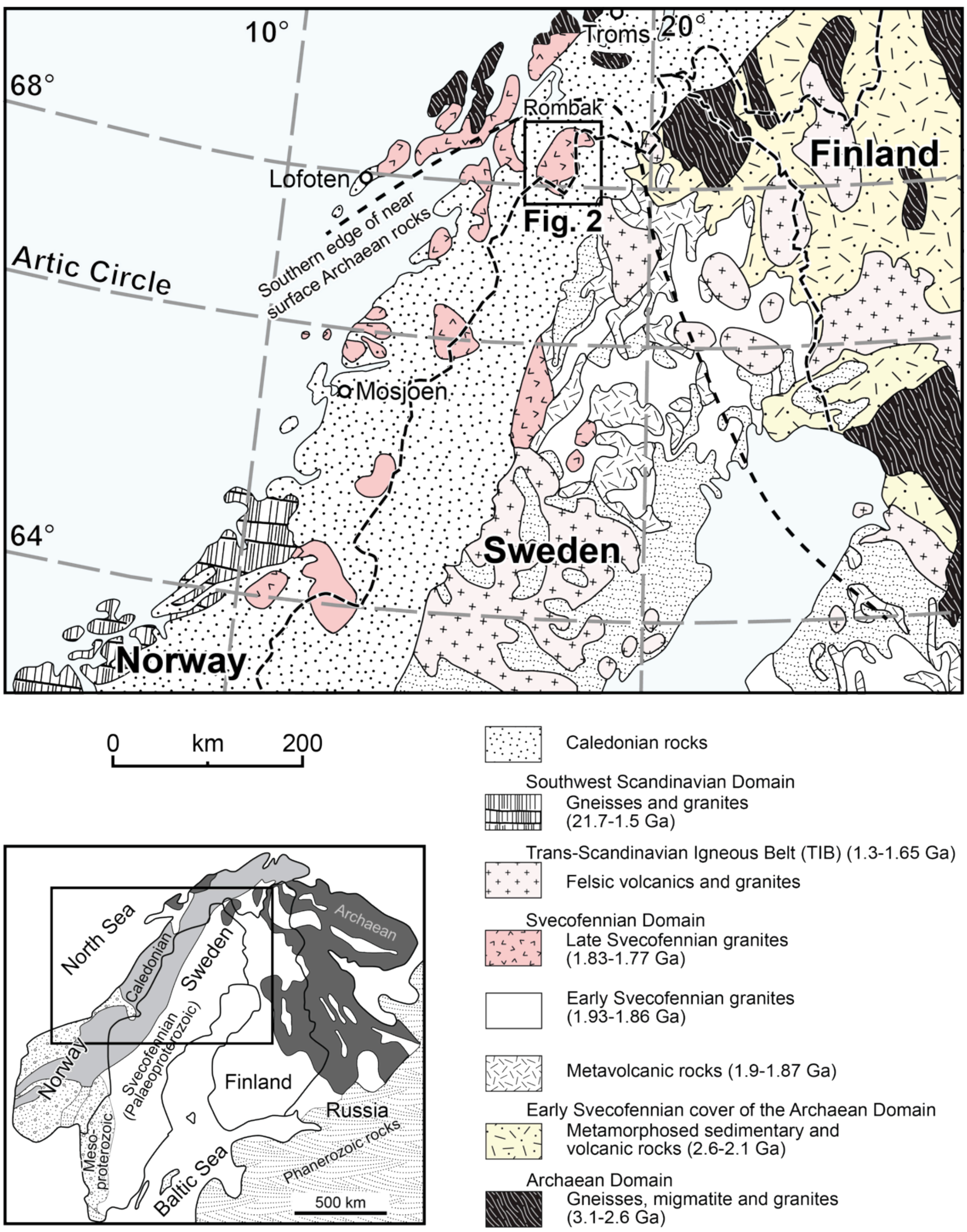

Fig. 1. Geology of the central part of Norway showing the location of the Rombak Tectonic Window shown in Fig. 2 (modified after Gaál and Gorbatschev, 1987).

3. Tectonic geology

3.1. Regional tectonics

Rocks in the Fennoscandian Shield have been deformed during the Svecofennian Orogeny associated with the collision or accretion of at least two continents (Nironen, 1997; Korja et al., 2006; Lahtinen et al., 2008).

Hietanen (1975) was the first person to suggest that the Svecofennian Orogen had an island-arc tectonic setting before the onset of collision. The orogen is still interpreted as a collage of microcontinents and island arcs accreted on to the Karelian microcontinent which itself was accreted onto the North Atlantic Craton (NAC) during ca. 1.8 Ga (Nironen, 1997; Korja et al., 2006). The geometry of these microcontinents is still unknown as the mappable continuity of the juxtaposing shear zones and lithologically units are masked by the overlying Caledonian sequences. Korja et al. (2006) proposed that the accretion of the microcontinents and island-arcs evolved in the following stages: 1) microcontinent accretion between ca. 1920 and 1880 Ma; 2) large-scale extension of the accreted crust between ca. 1870 and 1840 Ma; 3) continent-continent collision during ca. 1870-1790 Ma); and 4) gravitational collapse between ca. 1790 and 1770 Ma.

Nironen (1997) describes how convergent deformation associated with the collision of continent and island-arc complexes during the Svecofennian Orogeny resulted in partitioning of transpressional and ductile shear zones with the development of several crustal scale ductile shear zones within the Bothian Basin. The deformation events assigned to the orogeny have affected the basement and intrusive rocks in varying degrees across the RTW and other inliers in Norway and

Sweden (Fig. 1). On a shield scale, fabrics assigned to the deformation include early regional, north-trending and steeply dipping, dextral oblique and strike-slip shear zones (e.g. Lindh, 1987; Berthelsen and Marker, 1986; Nironen, 1997; Braathen and Davidsen, 2000; Olesen and Sandstad, 1993; Henderson and Kendrick, 2003). These shear zones have been locally sinistrally reactivated (Berthelsen and Marker, 1986; Kärki and Laajoki, 1995).

Bergh et al. (2010) provide the most comprehensive study of a complex set of anastomosing Paleoproterozoic shear zones in the WTBC, which are interpreted as part of a complex and multiphase Paleoproterozoic amalgamation of both Archaean and Paleoproterozoic microcontinents to the west of the Caledonides. They describe an initial orthogonal to oblique phase of NW-SE directed compression producing a NW-verging fold and thrust belt, which was subsequently transposed by a predominantly sinistral oblique set of steep ductile shear zones in a progressive transpressional orogen. Various authors interpret similar evolutionary tectonic events in the region (Braathen and Davidsen, 2000; Myhre et al., 2011, Henderson and Viola, 2013).

3.2 Local deformation in the Rombak Tectonic Window

Ductile shear zones in the RTW vary on a millimetre- to kilometre-scale and extend ≥60 km in length disappearing beneath Caledonian thrusts to the north and south (Fig. 2; Larsen et al., 2010, 2013). These structures have complex geometries and are observed as narrow, high-strain zones made up of anastomosing steep, northerly trending, oblique-slip ductile shear zones that segment and juxtapose zones of low-strain. The zones contain remnants of tight, upright, east-verging fold and thrust faults, which thicken and repeat the metasedimentary sequences. The high-strain oblique-slip shear zones are localized along the margins of the metamorphosed volcanic and sedimentary rocks and plutonic intrusions (Larsen et al., 2010; 2013).

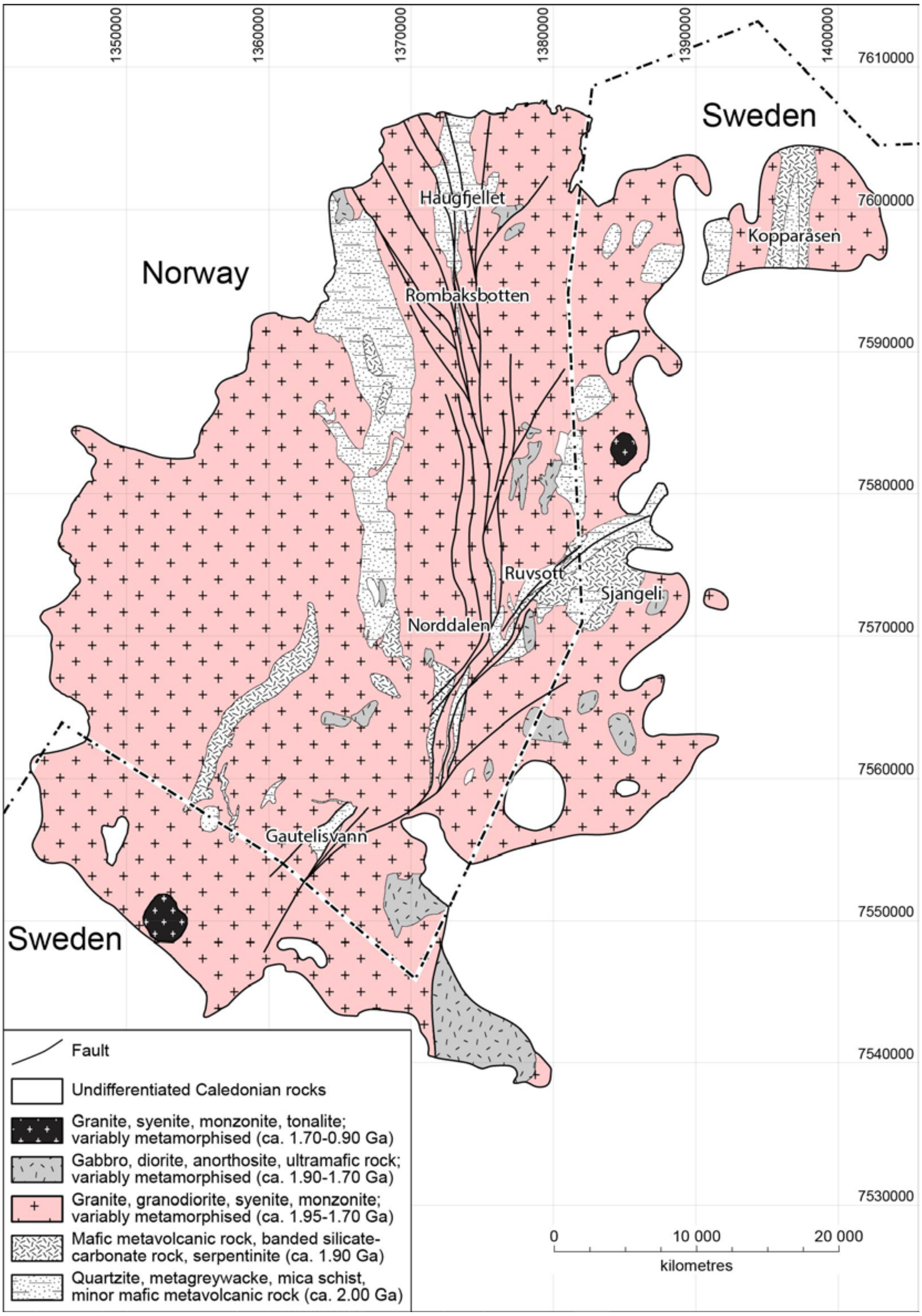

Fig. 2. Geology of the Rombak Tectonic Window (from Larsen et al., 2013 modified after Bargel et al., 1995).

The steeply dipping high-strain shear zones post-date and segment the earlier phase of dip-slip movement. These high-strain shear zones display a complex range of kinematics, including reverse dip-slip, dextral and sinistral oblique-slip, and ductile kinematic indicators including sigma clasts, crenulations cleavages, brittle-ductile tension gash fractures and asymmetric boudinaged that are suggestive of multiple periods of movement with an overall dextral transpressional sense of movement. From detailed kinematic studies, these structures are interpreted to represent a protracted, east-directed oblique transpression during Paleoproterozoic accretionary tectonics (Larsen et al., 2010).

A complex structural history of the accretionary system is interpreted to the following progressive stages: (1) formation of an orthogonal, east-verging fold and thrust belt with simple horizontal open, asymmetric F_1folds, and accompanying gently west-dipping thrusts; (2) coaxial refolding and formation of gently N-S plunging F_2 folds; (3) F_2 folds are cut by steeply dipping, N-trending, sinistral anastomosing and axial planar ductile oblique-slip shear zones; and (4) development of steeply dipping, dextral northeast-trending ductile oblique-slip shear zones. These late shear zones are associated with steep plunging F_4 folds and cut and complexly segmenting both the earlier formed upright fold and thrust belt structures and the sinistral ductile shear zones (Larsen et al., 2010; 2013).

Various granitic bodies intrude and are located close to the shear zones within this complex structural evolution. The shear zones cut the fold-and-thrust structures and some of the oblique-slip shear zones. Based on the structural and intrusive relationships, the structures have been interpreted to be coeval with syn- to late-orogenic intrusions (Larsen et al., 2013).

Here we present geochemical data from the rocks and U-Pb age dating study of these granitic bodies documenting a progressing tectonic evolution in the RTW during the Paleoproterozoic. The granitic bodies crosscut the late and steep oblique shear zones (D_4), which gives a minimum age for the Rombaken Skjomen Shear Zone (RSSZ) and a frame for understanding metallogenic processes in the region.

4. Methodology

4.1. Whole-rock geochemistry

The Norges Geologiske Undersøkelise (NGU, Norwegian Geological Survey) collected 46 samples of metasedimentary, metavolcanic and intrusive rocks from Haugfjellet, Rombak, Norddalen Ruvvsott, Sørdalen and Gautelisvann (Fig. 2; also see Korneliussen et al., 1986; Korneliussen and Sawyer, 1989; Sawyer and Korneliussen, 1989). The samples have been analysed by the NGU, Institute for Energy Technology and Midland Earth Science Associates.

Major oxides concentrations were determined using a wavelength-dispersive XRF on fused disks (after Norrish and Hutton, 1969). Trace elements Y, Zr, Nb, Rb, Ba, Sr Pb, V, Cu, Zn, and Ni were determined by wavelength-dispersive XRF on a pressed pellet (after Norrish and Chappell, 1997). Sc, Co, Cr, Cs, Hf, Ta, Th, U, La, Ce, Nd, Sm, Eu, Tb, Yb and Lu, were analysed by instrumental neutron activation analysis (NAA).

The geochemical data for these rocks are presented in the Appendix. Despite variable degrees of recrystallization, the mafic igneous rocks have consistent concentrations of immobile elements such as La, Nb, Y, and Zr. However, relatively mobile elements show wide variations in their analyses attributed to alteration and metamorphism, and interpretations based on elements such as Sr, Ba, Na, K, and Ca have thus been avoided.

4.2. SHRIMP U-Pb zircon dating

Zircon crystals are handpicked from the heavy mineral separate with the aid of a binocular microscope. In general, up to 200 representative crystals are selected from igneous and sedimentary rocks. Crystals are mounted in 25 mm diameter Epofix epoxy disks, and the mount surface polished to expose grain interiors.

Each mount contains zircons from three different samples, which are aligned in rows, together with BR266 and OGC1 used as U–Pb calibration standard zircons.

Mount-making and backscattered electron and cathodoluminescence (CL) imaging were completed at the Centre for Microscopy, Characterization and Analysis at the University of Western Australia. Gold coating of mounts were performed at the John de Laeter Centre, Curtin University in Western Australia.

Zircon grains were analysed using the SHRIMP-II facility housed within the John de Laeter Centre for Mass Spectrometry at Curtin University of Technology. Procedures for SHRIMP U–Pb isotopic analysis followed those described by Compston et al. (1984),and Stern (2009). Targeted grains were sputtered using an O_2^- primary beam with a 30 μm–diameter spot, and six cycles of sequential measurements of peaks in the secondary ion beam at mass stations 196 ($^{90}Zr_2O^+$), 204 ($^{204}Pb^+$), 204.1 (background), 206 ($^{206}Pb^+$), 207 ($^{207}Pb^+$), 208 ($^{208}Pb^+$), 238 ($^{238}U^+$), 248 ($^{232}ThO^+$) and 254 ($^{238}UO^+$) were made using an electron multiplier in pulse counting mode.

The effect of Pb/U fractionation in measurements of the unknowns was corrected by reference to interspersed analyses of the laboratory U–Pb standard zircon BR266 (U = 909 ppm, $^{207}Pb/^{206}Pb$ age = 559; Stern, 2001) and OGC1 ($^{207}Pb/^{206}Pb$ age = 3465 Ma; Stern et al., 2009).

The measured ^{204}Pb was used for common Pb correction. The data was compiled using the ISOPLOT 3.0 and Squid 1.0 programs (Ludwig, 2003, 2009). Individual analyses are reported with 2σ uncertainties; weighted averages of age are also reported at the confidence of 2σ.

5. Results

5.1 Geochronology

Three samples (NO13, GL19 and HF1) of granite were collected from the RTW for SHRIMP U-Pb zircon dating (Fig. 3). The aim of this exercise was to determine whether they represent a Paleoproterozoic or Caledonian (ca. 490-390 Ma) magmatism, and to help petrographically outline the tectonic events in the region.

Sample NO13 is a sample of monzogranite collected from Norddalen. Zircons analyzed are euhedral, elongated or stubby, most show oscillating zoning typical of magmatic zircons, and most have a homogeneous pool of ages with a weighted mean of 1786 ± 8 Ma (MSWD = 0.38, n = 16; Fig.3a).

Sample GL19 is from monzogranite collected from Gautelisvann. The zircons are similar in shape and zonation to sample NO13 and the main population yields an upper intercept age of 1789 ± 4 Ma (MSWD = 1.2, n =24), and there is a scatter of younger ages due to Pb loss (Fig. 3b).

Sample HF1 is of a monzogranite from Haugfjellet. The zircons are stubby to elongate (Fig. 4), and zircon analyses yield a weighted mean of 1790 ± 8 Ma (MSWD = 0.27, probability 0.99, n = 18; Fig. 3c). These three dates are the same within error and indicate a significant magmatic event of ca. 1790 Ma.

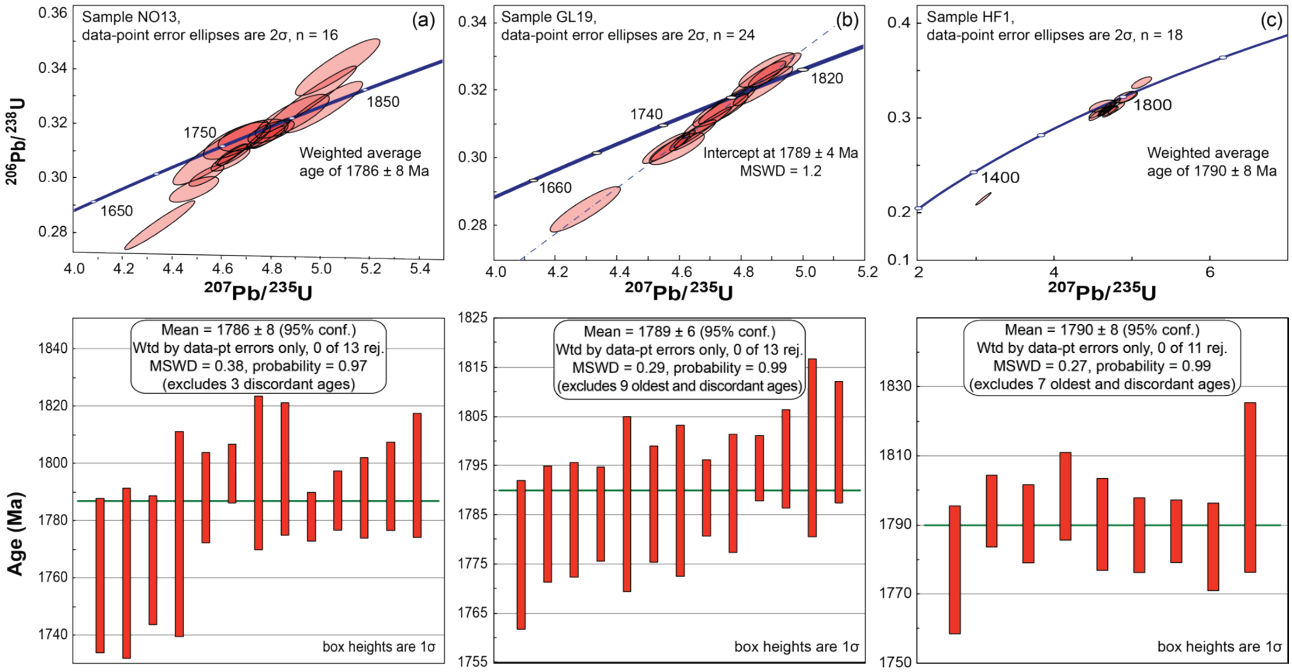

Fig. 3. U-Pb concordia diagrams for SHRIMP results and Weighted means for: (a) Sample NO13; (b) Sample GL19; and (c) Sample HF1; n is the number of zircon ages in the calculated age. Error ellipses represent 2 σ uncertainties.

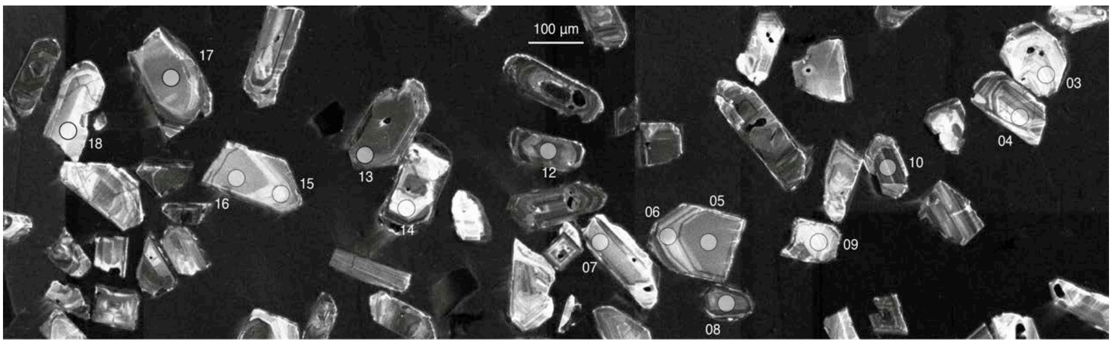

Fig. 4. Scanning electron microscopy cathodoluminescence (CL) image of zircons from Sample HF1 showing the location of spots with SHRIMP U-Pb analyses.

5.2. Geochemistry of greywacke and shale units

Sawyer and Korneliussen (1989) and the researchers of this study collected 18 samples of greenschist to amphibolite facies, siltstone, and fine- to medium-grained lithic sandstone. The samples came from surface exposures in the Rombaksbotten (6), Gautelisvann (4), Ruvssot (4) areas and were collected for geochemistry (Appendix A-1). Despite variable degrees of recrystallization, the rocks show relatively limited compositional variation.

It is assumed that rare earth element (REE) abundances and patterns in clastic sedimentary rocks trace the chemical evolution or development of the upper continental crust since Precambrian times. It is also that the average composition of the upper crust is not significantly different from the average composition of the Precambrian crust (e.g. Moorbath, 1977; Armstrong and Harmon, 1981; Taylor et al., 1981). These two hypotheses assume: (a) the REE have not experienced relative fractionation during weathering, erosion, deposition and diagenesis accompanying the transformation of source rocks into sediment; (b) metamorphism has not altered the whole-rock REE patterns of the samples; (c) the REEs in sedimentary rocks provide a broad average of available source areas at the time of sedimentation; and (d) the sampled units are representative of sediments deposited in the area.

Applying a geochemical classification plot (K_2O/Na_2O versus SiO_2/Al_2O_3) of Wimmenauer (1984), the Paleoproterozoic samples can be classified as greywackes, arkoses, and pelitic greywackes (Fig. 5).

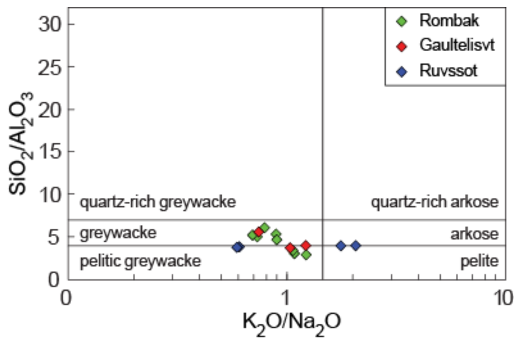

Fig. 5. Metagreywacke and pelite samples from Rombaksbotten, Gautelisvann and Ruvssot in the geochemical classification plot after Wimmenauer (1984).

The samples show a spectrum of chemical compositions resembling that of the upper crust (Fig. 6a; Rudnick and Gao, 2004), and have geochemical compositions that are free of anomalously high concentrations of Ti, Zr, Hf and Y (Fig. 6b and c). These elements would be concentrated by hydraulic sorting of heavy minerals during processes of transportation and deposition of detrital material obscuring relations to the sources of such material (e.g. Cullers et al., 1987).

The normalised geochemical pattern for the Paleoproterozoic sedimentary rocks in the study area broadly resemble the North American Shale Composite (NASC; Gromet et al., 1984), except for the elevated Cr values, Mn depletion, and elevate Na values (Fig. 6b and c). These characteristics suggest that there is a mafic or ultramafic input in the provenance for the rocks, alteration has lead to depletion in Mn, and the rocks might have been affected by saline solutions either as hydrothermal fluids or during deposition.

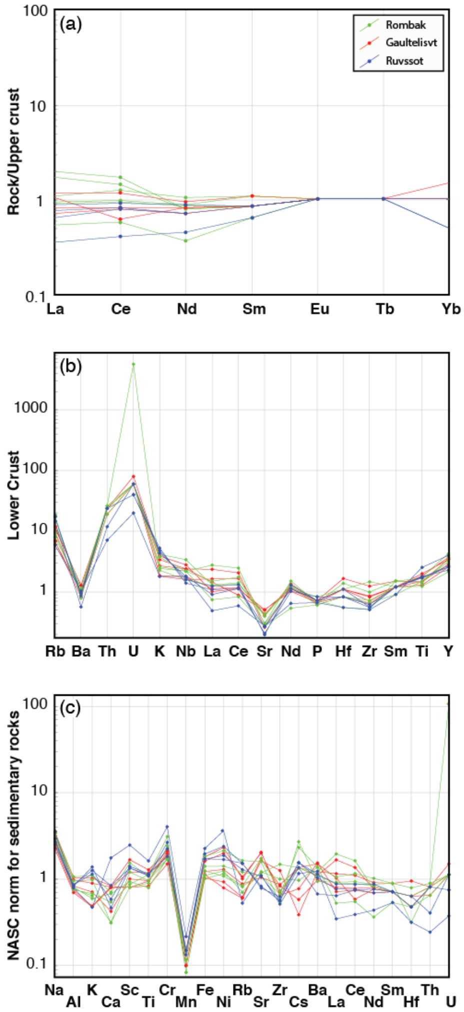

Fig. 6. Geochemical plots for sedimentary rocks in the Rombaksbotten, Gautelisvann and Ruvssot areas: (a) Upper crust normalized (Rudnick and Gao, 2004); (b) Lower Crust normalized (Weaver and Tarney, 1984) showing depletion in Sr and elevation in Th and Rb; and (c) North American Shale Composite normalized (after Gromet et al., 1984) showing depletion in Mn and enrichment in Na.

5.3. Geochemistry of mafic and ultramafic rocks

Basaltic magmatism is a feature of many geotectonic environments in modern intra-oceanic and intracontinental settings as well as at convergent and divergent plate margins (e.g. Wilson, 1989). Geochemical data for 12 mafic intrusive rocks from Gautelisvann and Norddalen, and five komatiites from Ruvssot collected by Korneliussen and Sawyer (1989) have been plotted on discrimination diagrams in an attempt to help determine what the tectonic environment was during their emplacement.

The spread in the K_2O verses MgO and Na_2O verses MgO plots in Fig. 7 indicates that hypogene alteration (presumably due to either amphibolite facies metamorphism or associated with hydrothermal events) has affected the more mobile elements that might be used as tectonic discriminators. In addition, samples with LOI values above 2% have been disgarded. In order to ascertain the geotectonic setting for mafic units the geochemical data presented in Appendix A-2 are compared against modern analogues of basaltic volcanic rocks using relatively immobile elements. The assumption is that hydrothermal alteration processes in the area did not involve very high fluid/rock ratios that lead to the mobility of where relatively immobile elements (e.g. Lesher et al., 1986; Schandl et al., 1995).

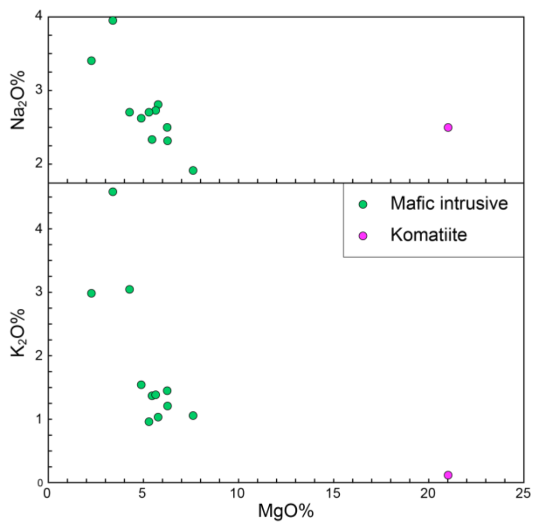

Fig. 7. Plots for mafic and ultramafic rocks from Gautelisvann and Ruvssot: (a) MgO verses Na_2O; and (b) MgO verses K_2O. The spread in the plots suggests that alteration has affected the more mobile elements.

From the Zr/TiO_2–Nb/V classification plot of Winchester and Floyd (1977) shown in Fig. 8, the mafic igneous rocks analysed from the study area predominantly have basaltic compositions.

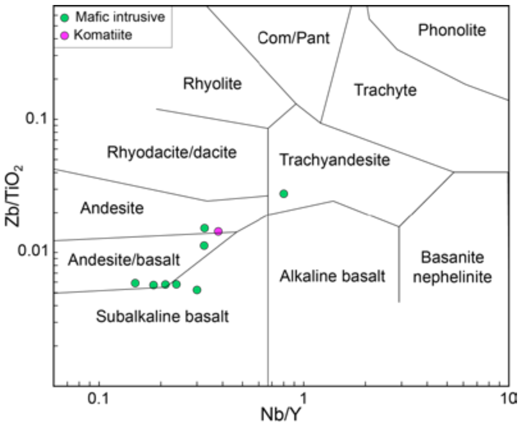

Fig. 8. The Zr/TiO**2**–Nb/V classification plot (after Winchester and Floyd, 1977) for mafic and ultramafic rocks analysed from the study area. These plots rely on relatively immobile elements under a range of alteration and metamorphic conditions. Such plots are commonly used for the classification of ancient or altered volcanic rocks.

On the AFM (Miyashiro 1974, Fig. 9a), FeO*/MgO versus SiO_2 (after Miyashiro, 1974; Fig. 9b), FeO*/MgO versus FeO* (after Miyashiro, 1974; Fig. 9d), and Zr versus Y (after Barrett and MacLean, 1999;l Fig. 9e) diagrams, the samples plot in the tholeiitic field (except for the komatiite samples).

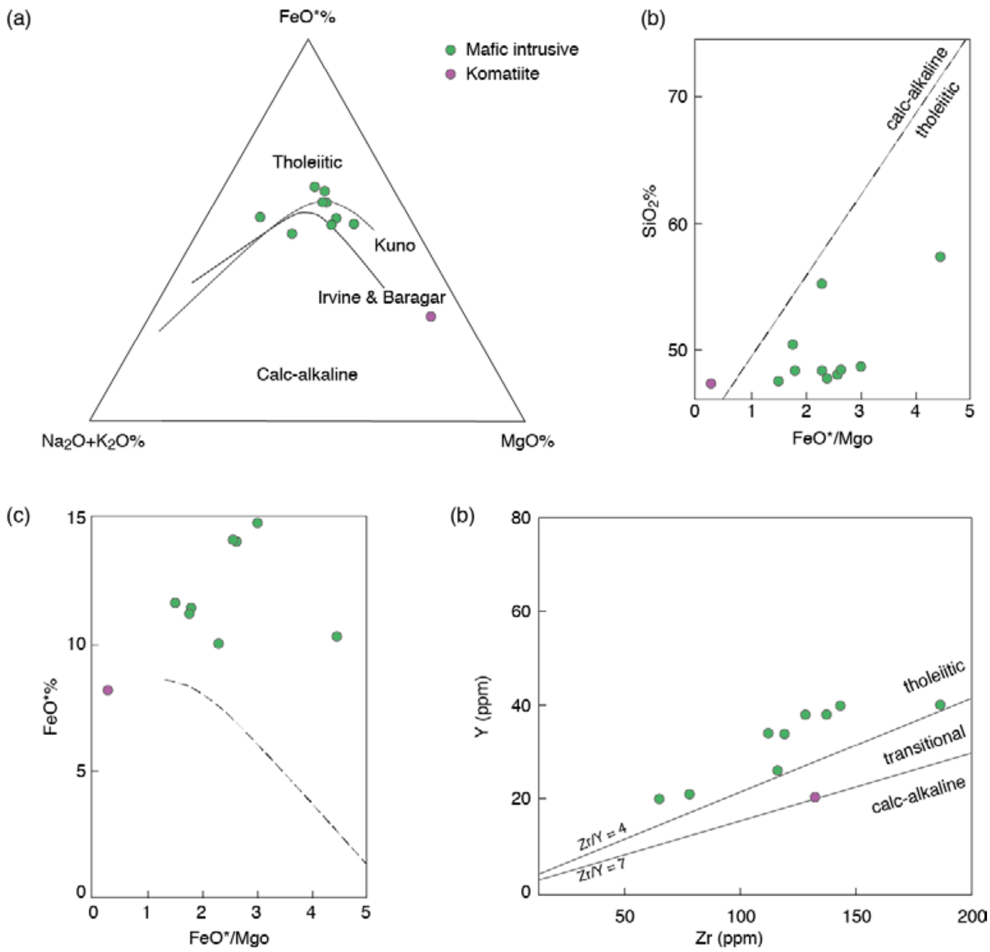

Fig. 9. Plots for mafic and ultramafic volcanics: (a) AFM diagram (after Miyashiro, 1974), (b) FeO*/MgO vs SiO_2% diagram (after Miyashiro, 1974), (c) FeO*/MgO vs FeO* diagram (after Miyashiro, 1974), and (d) Zr vs Y diagram showing that the bulk of the samples have a tholeiitic geochemical affinity. The total Fe is presented as wt % FeO (FeO*).

5.4. Geochemistry of the ca. 1790 Ma felsic igneous rocks in the Rombak Tectonic Window

In general, the ca. 1790 Ma granitic rocks in the Gautelisvann and Norddalen areas in the RTW range in composition from syenite to granodiorite and monzogranite, although monzogranite predominates (Fig. 10a, b). The aluminium saturation index of Barton and Young (2002) indicates that most of the granites have metaluminous to weakly peraluminous compositions (Fig. 10c). The samples have K_2O contents of 1.5-5.8% (with an average of 4.4%), with the data plotting in alkaline and subalkaline fields in Fig. 10a, in the medium-K calcalkaline and shoshonite series in the K_2O versus SiO_2 classification diagram of Peccerillo and Taylor (1976) in Fig. 10d, and form calc-alkaline trends in the AFM diagram of Fig. 10e (Rollinson, 1996). The rocks also have Al_2O_3 contents between 12.4 and 18.5% (with an average of 14.6%), and TiO_2 contents of 0.09-5.4% (with an average of 0.8%; Appendix A-3).

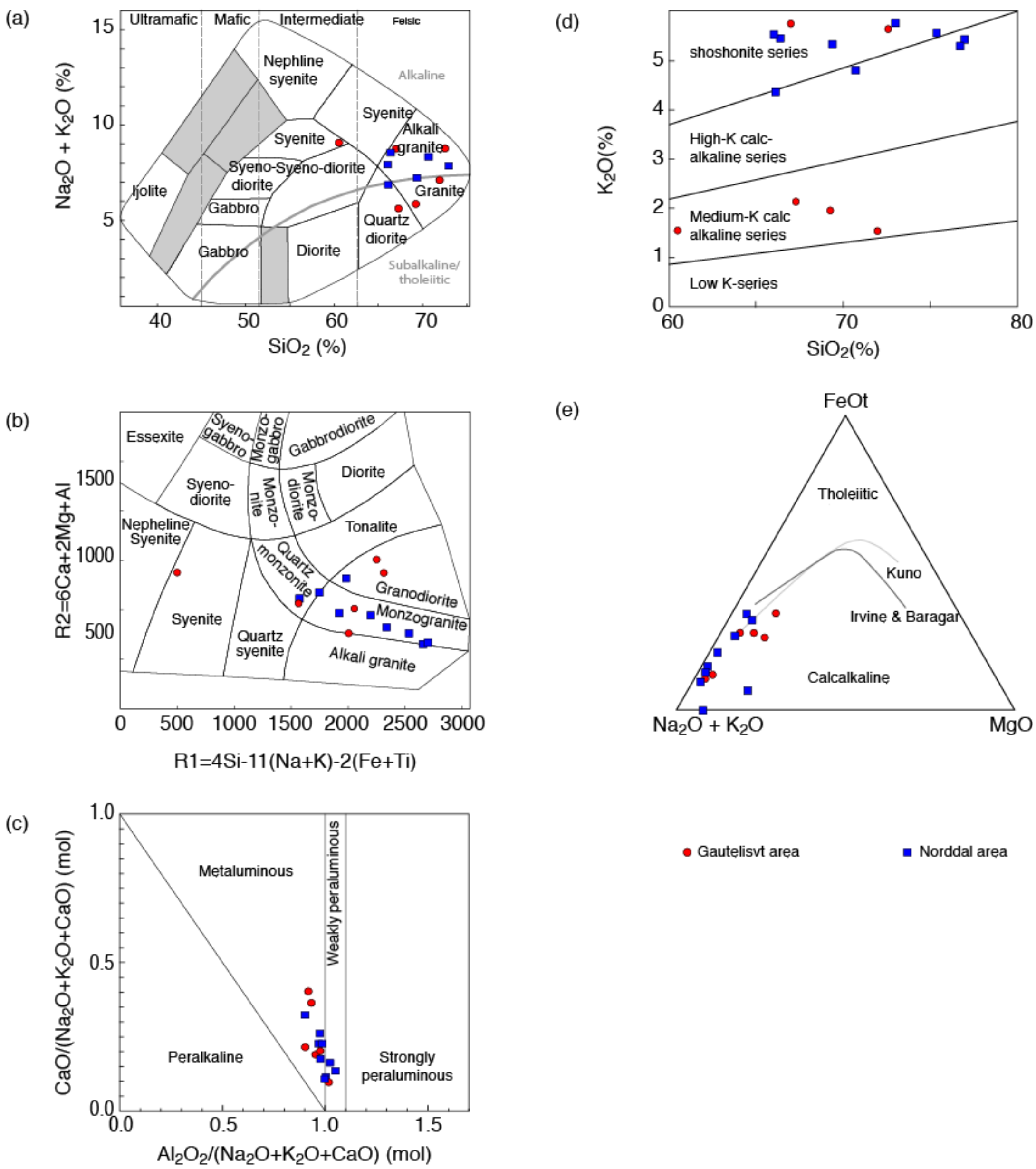

Fig. 10. Classification diagrams for the ca. 1790 Ma granitic rocks from the Gautelisvann and Norddalen areas of the Rombak Tectonic Window: (a) and (b) total alkali versus silica plutonic plot of Cox et al. (1979) and R1 versus R2 plutonic chemical plot of de la Roche et al. (1980) showing that the granites are predominantly monzogranites and granodiorites, with one syenite sample; (c) aluminia saturation of Barton and Young (2002) showing that the samples are metaluminous to weakly peraluminous; (d) K_2O versus SiO_2 classification diagram of Peccerillo and Taylor (1976) showing that the samples can be subdivided into medium-K alkaline series (predominantly from Gautelisvann) and shoshonite series; and (e) AFM diagram of Rollinson (1993) using curves after Irvine and Baragar (1971) and Kuno (1968) showing that the samples form calc-alkaline trend.

The samples also form a linear trend in the ternary diagram Al_2O_3 – CaO+Na_2O – K_2O of Nesbitt and Young (1989) in Fig. 11a. This linear trend indicates that: (i) there is a gradual change in the ratio of CaO + Na_2O to K_2O from the Gautelisvann area to the south to the Norddalen area to the north in the RTW; and (ii) weathering has had minimal overall effect on the samples collected. The plots in Fig. 11b define broad linear trends interpreted to reflect magmatic processes. The broad deviations from linearity in the various Harker (1909) diagrams are considered to reflect variations in initial bulk compositions and compositions of crystallizing phases (Fig. 11b).

The Harker plots in Fig. 11b indicate that: (i) the SiO_2 content varies between 60 and 77%, and the samples plot in the medium- to high-K and shoshonitic fields (also see Fig. 10d); (ii) the granites are heterogeneous; and (iii) the overall patterns of decreasing Ti, Fe, Mg, and Ca with increasing SiO_2 is typical of fractionating granitic systems (e.g. Drake and Weill, 1975; White and Chappell, 1983).

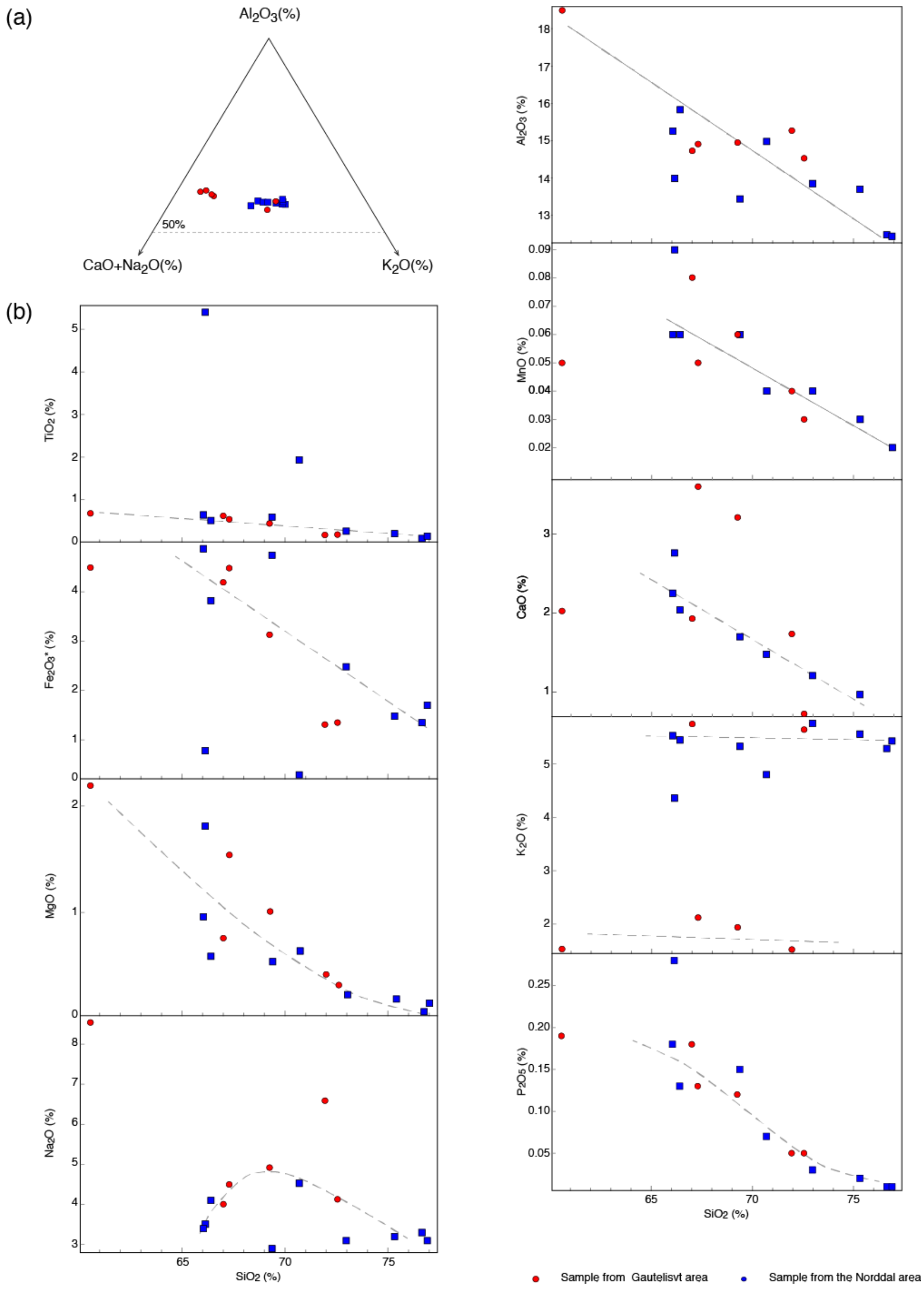

Fig. 11. Diagrams for granites from the Rombak Tectonic Window of Norway: (a) Al_2O_3 – $CaO+Na_2O$ – K_2O (modified from Nesbitt and Young, 1989); (b) Harker (1909) variation diagrams of the major element oxides. The legend is the same for all the diagrams.

Using the ACF diagram of Chappell and White (1974) and White and Chappell (1983), the major element compositions and petrographic observations of the granites noted are not consistent with S-type granites (i.e. of sedimentary origin; Fig. 12a). However, this “S-type” classification is genetic (e.g. Frost et al., 2001), and implies no magma mixing and no fractionation (Bonin, 2007). Furthermore, Fig. 12a assumes that the granites are neither fractionated I-types nor anorogenic (A-type), but most of the samples plot in the I-type granite field of Fig. 12b and the I-type and A-type fields of Fig. 12c indicating that these granites are I-type granites and most are A-types.

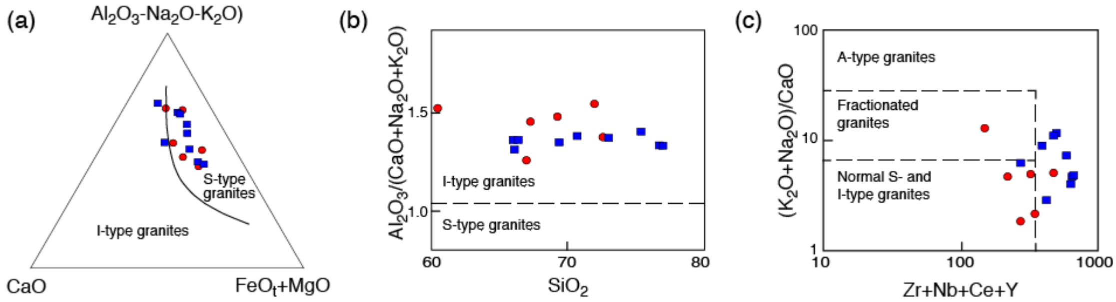

Fig. 12. Compositional diagrams for granites from Rombak Tectonic Window: (a) Al_2O_3-Na_2O-K_2O – CaO – FeO_t+MgO plot of White and Chappell (1983); (b) $A1_2O3$ / (CaO+Na_2O+ K_2O) versus SiO_2 plot of White and Chappell (1983); and (c) (K_2O + Na_2O)/CaO versus Zr + Nb + Ce + Y diagram after Whalen et al. (1987) for fractionated granites (the legend is the same as in Fig. 10).

The granitic rocks have downward-sloping primitive mantle-normalized ‘spidergram’ profiles with large ion lithophile (LILE) enrichment, relative negative Ba, Nb, Sr and Ti anomalies, and positive Th, U and Pb anomalies (Fig. 13a). On MORB normalized plots, Rb, Th, and Ce are anomalous (Fig. 13b). Sr is present in K-feldspar and plagioclase, and is relatively depleted in fractionating melts by the removal of K-feldspar and plagioclase from the system. Rb, however, is commonly present in K-feldspar, biotite and muscovite (McCarthy and Hasty, 1976). Ba is hosted by biotite and K-feldspar, and early fractionation of K-feldspar will deplete the residual melt in Ba once saturation is reached (McCarthy and Hasty, 1976). Thus, crystal fractionation involving feldspar leads to depletion of Ba and Sr, and enrichment in Rb. The observed patterns suggest that at least some of the granites in the RTW show evidence of fractionation of feldspar and, to a lesser extent, biotite (as is shown by the decreasing Ba and Sr in Fig. 13).

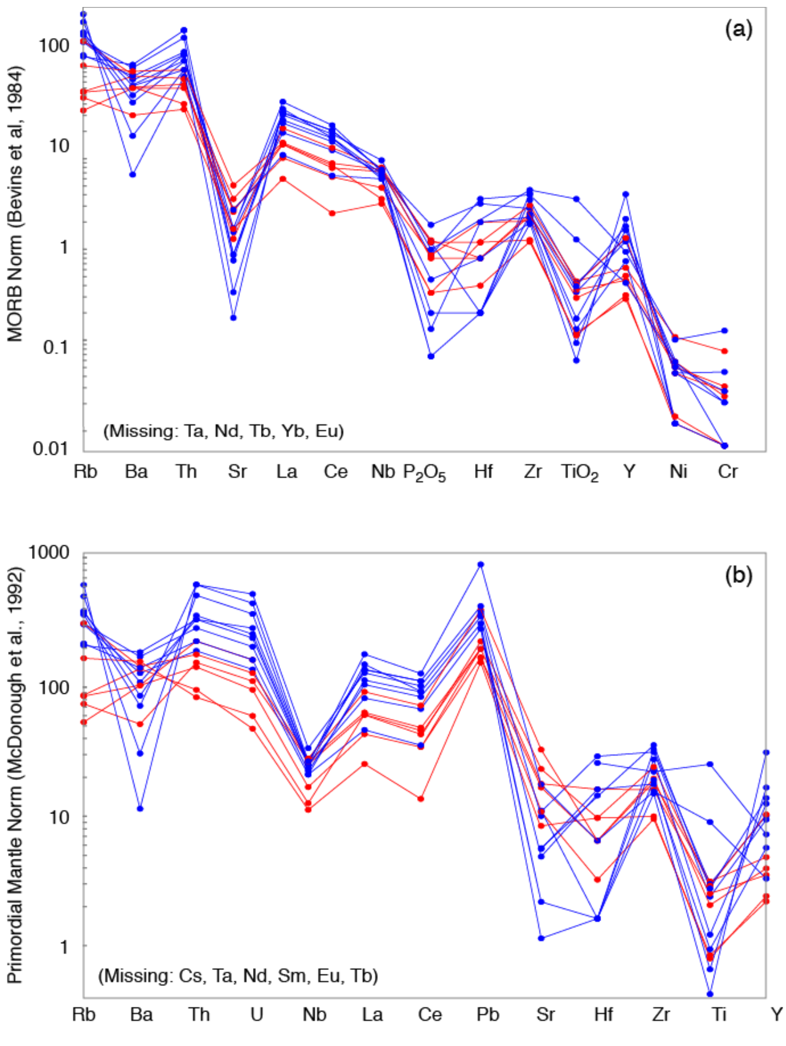

Fig. 13. REE and spider diagrams for granites from the Rombak Tectonic Window: (a) MORB normalized values from Bevins et al. (1984), and (b) Spider diagram for primitive mantle normalized values from McDonough et al. (1992). The legend is the same as in Fig. 10.

6. Paleoproterozoic tectonic setting

6.1. Tectonic setting for the turbiditic sandstone (greywacke) and shale units

Systematic variations in the geochemical compositions of greywackes have been in different tectonic environments to help determine their tectonic setting during deposition (e.g. Bhatia, 1983, 1985a, 1985b; Bhatia and Cook, 1986; Cullers et al., 1987; McLennan et al., 1993). Using such analyses with the least mobile elements, the samples from the Rombaksbotten, Gautelisvann and Ruvssot inliers plot in the continental- to oceanic-arc tectonic setting (Fig. 14a). A similar result is obtained in the general immobile elements Zr, Sc, Th, and La plots in Fig. 14b. These plots also suggest that the samples have possibly been enriched in iron causing them to spread further to the right in right in Fig. 14a, which is consistent with the presence of pyrite in the samples (as observed in thin section).

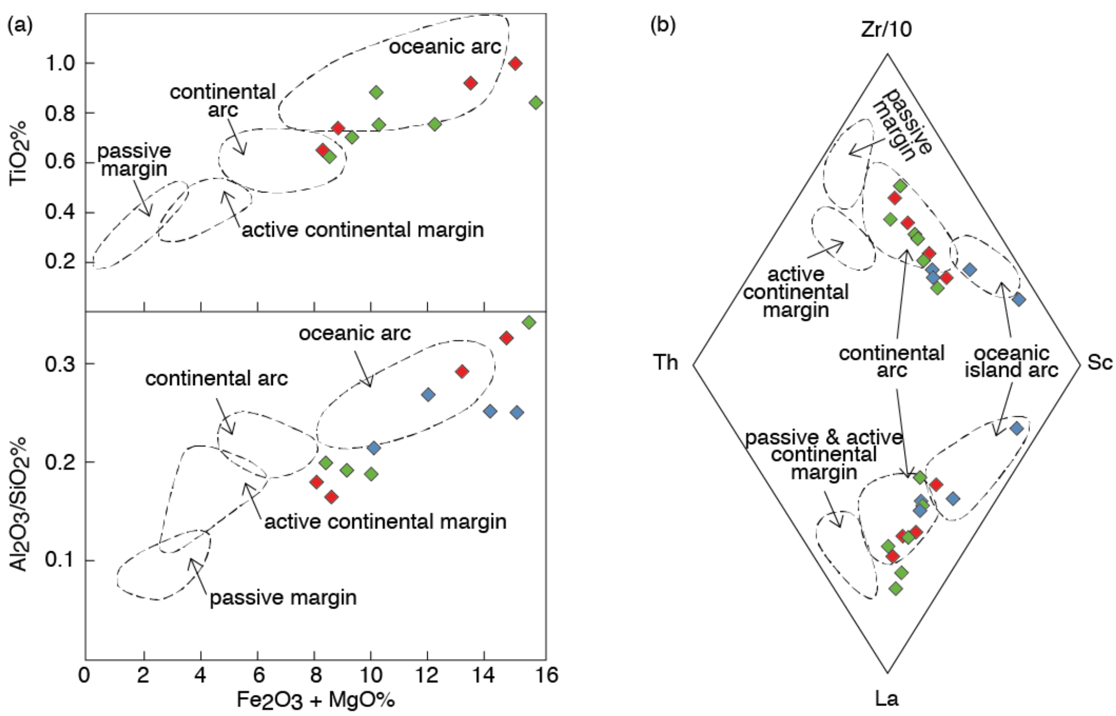

Fig. 14. Sedimentary samples from the Rombaksbotten, Gautelisvann and Ruvssot areas plotted on: (a) selected published discrimination diagrams emphasizing major element chemical variations (after

Bhatia, 1983); and (b) Sc-Th-Zr/10 discriminant plots (after Bhatia and Crook, 1986). These plots suggest that the sandstone was deposited in a continental island arc to oceanic arc tectonic setting. Symbol legend is the same as Fig. 9

A good tracer for mafic source components is the compatible element Sc, particularly when compared with Th, which is incompatible and enriched in felsic rocks. Both elements are generally immobile under surface conditions and therefore preserve the characteristics of their source, making the Th/Sc ratio a robust provenance indicator (Taylor and McLennan, 1985; McLennan et al., 1990). In sandstone from the study area, the Th/Sc ratios increase from 0.08 for sample ES131ac from Ruvssot to 0.92 for sample ES068.4R from RTW (Fig. 15a), whereas the Th/Sc ratio for the average upper continental crust is 0.79 (McLennan, 2001). The Th/Sc and Zr/Sc ratios can reveal compositional heterogeneity in provenances for the sandstone, if the samples show Th/Sc and Zr/Sc values along the trend from mantle to upper continental crust compositions (McLennan et al., 1993). The Zr/Sc ratio is commonly used as a measure of the degree of sediment recycling leading to the concentration of zircon in sedimentary rocks (McLennan, 1989; McLennan et al., 1993). Such a trend is present in Fig. 15a, suggesting input from a less evolved provenance.

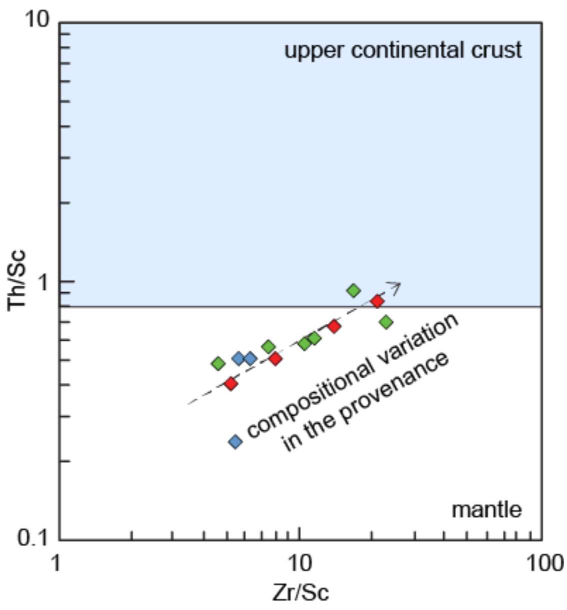

Fig. 15. Plot of turbiditic sandstone (greywacke) from the Rombaksbotten, Gautelisvann and Ruvssot areas on a Th/Sc versus Zr/Sc diagram (after McLennan et al., 1993), suggesting that the samples are sourced from ‘primitive’ material.

6.2. Tectonic setting for the mafic and ultramafic rocks

Most of the plots in Fig. 16 suggest mid-ocean ridge or arc affinities for the mafic and ultramafic units, which is similar to the continental- to island-arc tectonic setting for deposition of sandstone and shale units (discussed above). These similarities strengthen the suggestion that both the sedimentary and igneous rocks were emplaced during similar tectonic settings (~1900 Ma).

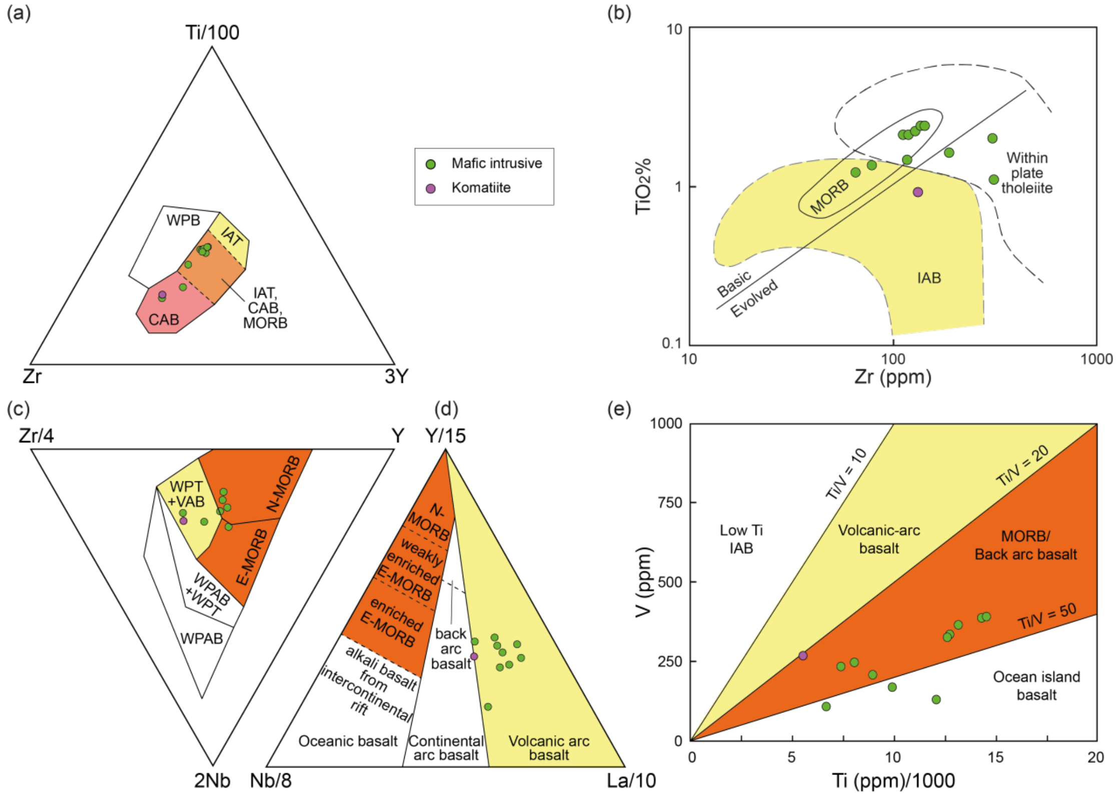

Fig. 16. Discriminations diagrams for mafic and ultramafic units plotted on: (a) Ti-Zr-Y diagram of Pearce and Cann (1973); (b) Ti–Zr diagram of Pearce (1982); (c) Nb–Zr–Y diagram of Meschede (1986); (d) La–Y–Nb diagram after Cabanis and Lecolle (1989); and (e) Ti–V diagram of Shervais (1982). These plots suggest that the mafic and ultramafic units have a mid-ocean ridge to volcanic arc setting.

6.3. Tectonic setting for the granitic rocks

On tectonic discriminant plots (Fig. 17), it is apparent that the granitic rocks in the RTW do not show a clear affinity towards a single, clearly isolated tectonic environment. Instead, they tend to overlap the boundaries of within plate and volcanic-arc granites, with most of the granites from Gautelisvann having a volcanic-arc affinity and most from Norddalen having a within-plate affinity (Fig. 17a, b). If we consider the R2 versus R1 discrimination plot of Batchelor and Bowden (1985), the granites can be interpreted predominantly as late orogenic granites (Fig. 17c).

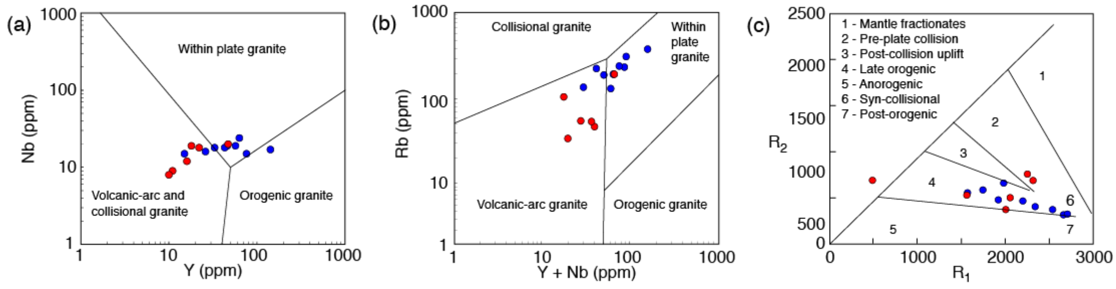

Fig. 17. Tectonic discrimination diagrams for of granites in the Rombak Tectonic Window: (a) Nb versus Y of Pearce et al. (1984); (b) Th/Yb versus Ta/Yb plot (after Pearce, 1982); and (c) R2 versus R1 of Batchelor and Bowden (1985; R1 = 4Si − 11(Na + K) − 2(Fe + Ti) and R2 = 6Ca + 2Mg + Al). Symbol legend same as in Fig. 10.

6.4. Progressive tectonic setting

On the primitive mantle plots of McDonough et al. (1992), which are normalized to the average greywacke composition in RTW (Fig. 18), the volcanic rocks, greywackes, granites, felsic and mafic intrusive rocks in the inlier plot in similar positions. In detail, the greywacke samples from Ruvsott and Rombaksbotten plot in similar positions as the mafic intrusives and intermediate volcanic rocks. Greywacke from Gautelisvann plots in a similar position as the tonalite and the felsic volcanic rock plots close to that of the granite from Gautelisvann. These similarities of the greywacke samples with the mafic and intermediate intrusions and volcanics suggest that they have developed in a similar tectonic setting and that the mafic intrusions and intermediate volcanic rocks are probable sources for the greywackes at Ruvsott and Rombaksbotten. Similarly, the greywacke samples from Gautelisvann plot in essentially the same positions as the underlying tonalite in Fig. 18, suggesting that the tonalite is a possible provenance for the greywacke in that location. Also the likeness of the felsic volcanic samples and the granite suggest that they may have developed from the same magma chamber, which is in accordance to what was suggested by

Korneliussen and Sawyer (1989). The mafic volcanic samples do not show similarities to any of the rocks in the area and suggest that they are either different magma chamber or not a source for the sedimentation of the studied rocks.

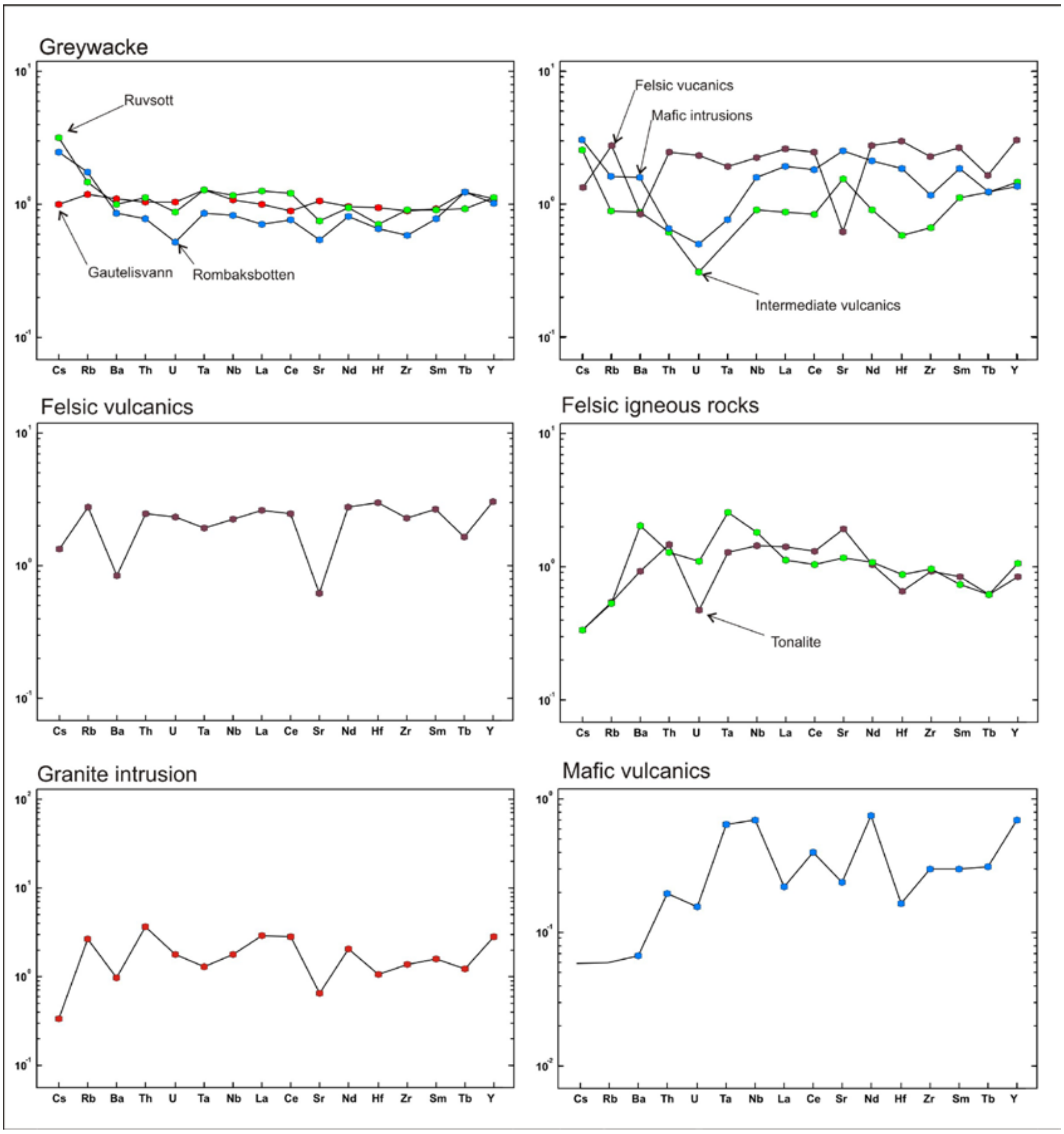

Fig. 18. Primitive mantle plots normalized to the average greywackes in the Rombak Tectonic Window (McDonough et al., 1992): a) the average of the metagreywacke from Rombaksbotten, Ruvsott and Gautelisvann; b) a plot showing the difference between the mean value from the felsic volcanic, intermediate volcanic and the mafic intrusions; c) the average of the felsic volcanic with high similarities to the average plot of the granite intrusions (e); d) the mean value of felsic igneous rocks and the tonalite rocks from Gautelisvann; e) the average of granite intrusion; and f) The average of the

mafic volcanic from Ruvsott that are different to the plots of felsic and intermediate volcanics. The diagrams are plotted based on the average of each category and shows the similarities between the metasedimentary rocks to the volcanic rocks and granites in the area.

7. Discussion and conclusions

The ca. 2000 – 1867 Ma metamorphosed greywacke and shale from RTW show some degree of variation from the east to the west, but in general, all samples plot within an active continental margin or island arc settings on discrimination diagrams (Fig. 3).

When the data is plotted in discrimination diagrams for clastic sediments, the plots for the sedimentary rocks vary with the sample location. For example, Fig. 3 (after Bhatia et al., 1983) shows that the samples from Ruvsott plot in an ocean arc field. The more westward located samples at Rombaksbotten and Gautelisvann plot on a line from oceanic arc to a continental-arc setting (Fig. 3). Similarly, the chemical variation diagram show that there are mafic and intermediate provenances for the metasedimentary rocks and that the samples taken from the east have an increased mafic (basaltic) provenance than those from the west, which appear to have an andesite provenance. Furthermore, the plot in Fig. 15 indicates that the felsic volcanic rocks are sourced largely from a primitive (mantle) source.

Therefore, based on the discrimination plots (Fig. 14), we suggest that the metasedimentary rocks in the RTW were deposited in an island arc to active continental margin setting, from a provenance dominated by mafic to intermediate compositions. A possible source could be erosion of the ~1900 Ma mafic to felsic volcanic rocks found in the study area.

The ca. 2000 – 1867 Ma mafic and ultramafic rocks in the RTW plot predominantly in the continental to oceanic arc fields of Fig. 14. This is consistent with the proposed island-arc to active continental margin setting for the sedimentary units discussed above, which confirms that these settings are probably valid for both the sedimentary and volcanic rocks in the RTW.

The ca. 1790 Ma felsic intrusive rocks can be classified as I-type or partially fractionated A-type granites (Fig. 12). These rocks plot in the late-orogenic to anorogenic fields associated with a volcanic-arc to within-plate tectonic setting (Figs. 12c and 17), which is not too dissimilar from that for the ca. 1900 Ma metasedimentary and volcanic units. This suggests that the granites intruded these metamorphosed sedimentary and volcanic rocks during accretion associated with the Svecofennian Orogeny.

The Na_2O+K_2O enrichment of A-type granitic rocks was also taken as a fundamental diagnostic parameter by Collins et al. (1982) and Whalen et al. (1987), who stressed other characteristics of such rocks. Other factors include high contents of Zr, Nb, W, Mo, REE, and the Ga:Al ratio. Pitcher (1983) and Brown et al. (1984) consider A-type granites to be related to alkaline and peralkaline monzogranites, granodiorites and syenites. Data presented by several researchers during the last decades indicate that most of these rocks are formed in late- to post-collisional settings (Harris et al., 1986; Sylvester, 1989; Bonin, 1990, 2007; Bitencourt and Nardi, 2000).

Because of the similarities in the geochemical characteristics of the rocks in RTW, we suggest these rocks developed in a progressive tectonic event starting with an island-arc setting for the mafic intrusions and intermediate volcanic rocks deposited over tonalite. The mafic and volcanic rocks were subsequently the provenance for the turbidite units at Ruvsott and Rombaksbotten, and the mafic intrusive, intermediate volcanics and tonalite are the provenance for the turbidite units at Gautelisvann. The tectonic setting progressed into a continental-arc setting with deposition of felsic volcanic units and the emplacement of granites during ca. 1820-1790 Ma. These successions were then accreted on to the Baltic continent. The tectonic setting for the Paleoproterozoic is here schematically summarized in Fig. 19, which covers a ~70 million year period.

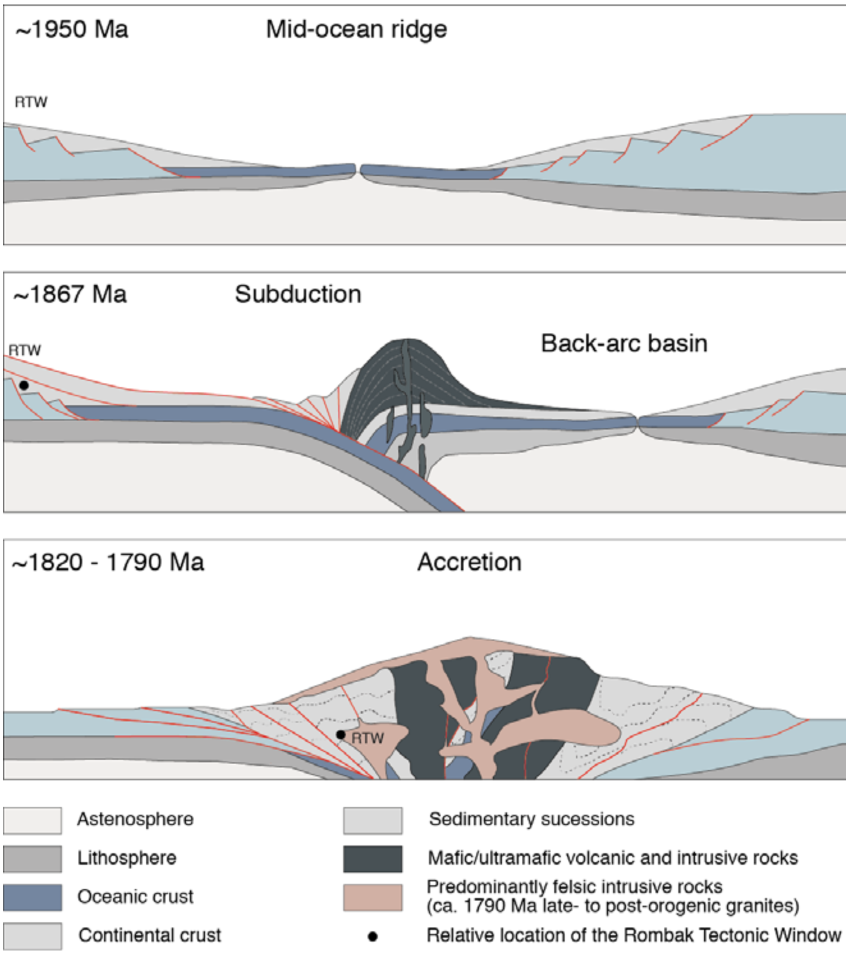

Fig. 19. Model for the tectonic setting during deposition of the ca. 2000 – 1867 Ma sedimentary and volcanic rocks in the Rombak Tectonic Window.

Acknowledgements

This contribution is part of the Rombaken and Skjomen project in northern Norway by the Geological Survey of Norway and University of Tromsø. We also acknowledge the Australian Research Council (ARC) Linkage Project LP110100667 and the ARC Centre of Excellence for Core to Crust Fluid Systems (CCFS). The constructive comments from Iain Henderson have significantly improved this manuscript.

References

Armstrong, R.L., Harmon, R.S., 1981. Radiogenic Isotopes: The Case for Crustal Recycling on a Near-Steady-State No-Continental-Growth Earth. Transactions of the Royal Society of London A301, 443–472.

Bargel, T.H., Bergstrøm, B., Boyd, R., Karlsen, T.A., 1995. Geologisk kart, Narvik kommune M 1:100.000: Norges geologiske undersøkelse.

Barton, M.D., Young, S., 2002. Non-pegmatitic deposits of beryllium: mineralogy, phase equilibria and origin. Reviews in Mineralogy and Geochemistry 50, 591–691.

Batchelor, R.A., Bowden, P., 1985. Petrogenetic interpretation of granitoid rock series using multicationic parameters. Chemical Geology 48, 43–55.

Bergh et al., 2010. Neoarchaean to Svecofennian tectono-magmatic evolution of the West Troms Basement Complex, North Norway. Norwegian Journal of Geology, 90, 21-48.

Berthelsen, A., Marker, M., 1986. 1.9-1.8 Ga old strike-slip megashear in the Baltic Shield, and their plate tectonic implications. Tectonophysics 128, 163–181.

Bevins, R.E., Kokelaar, B.P., Dunkley, P.N., 1984. Petrology and geochemistry of lower to middle Ordovician igneous rocks in Wales: a volcanic arc to marginal basin transition. Proceedings of the Geologists' Association 95, 337–347.

Bhatia, M.R., 1983. Plate tectonics and geochemical composition of sandstones. J. Geol. 91, 611–627.

Bhatia, M.R., 1985a. Composition and classification of Paleozoic flysch mudrocks of eastern Australia: implications in provenance and tectonic setting interpretation. Sed. Geol. 41, 249–268.

Bhatia, M.R., 1985b. Rare earth element geochemistry of Australian Paleozoic sandstones and mudrocks: provenance and tectonic control. Sed. Geol. 45, 97–113.

Bhatia, M.R., Crook, K.A.W., 1986. Trace elements characteristics of graywakes and tectonic setting discrimination of sedimentary basins. Contrib. Mineral. Petrol. 92, 181–193.

Bhatia, M.R., 1983. Plate tectonics and geochemical composition of sandstones. J. Geol. 91, 611–627.

Bhatia, M.R., Crook, K.A.W., 1986. Trace elements characteristics of graywakes and tectonic setting discrimination of sedimentary basins. Contrib. Mineral. Petrol. 92, 181–193.

Bitencourt, M.F., Nardi, L.V.S., 2000. Tectonic setting and sources of magmatism related to the Southern Brazilian Shear Belt. Revista Brasileira de Geociências 30, 184–187.

Bonin, B., 1990. From orogenic to anorogenic settings: evolution of granitoid suites after a major orogenesis. Geological Journal 25, 261–270.

Bonin, B., 2007. A-type granites and related rocks: evolution of a concept, problems and prospects. Lithos 97, 1–29.

Braathen, A., Davidsen, B., 2000. Structure and stratigraphy of the Paleoproterozoic Karasjok Greenstone Belt, north Norway – regional implications. Norsk Geologisk Tidsskrift 80, 33-50.

Brown, G.C., Thorpe, R.S., Webb, P.C., 1984. The geochemical characteristics of granitoids in contrasting arcs and comments on magma sources. Journal of the Geological Society London 141, 413–426.

Cabanis, B., Lecolle, M., 1989. Le diagramme La/10 -Y/15 -Nb/8: Un outil pour la discrimination des series volcaniques et la mise en evidence des procesus de melange et/ou de contamination crutale. Comptes Rendus de l'Académie des Sciences 309, 2023–2029.

Chappell, B.W., White, A.J.R., 1974. Two contrasting granite types. Pacific Geology 8, 173–174.

Coller, D., 2004. Varden Ridge Target Generation Report: Golden Chalice Resources Inc report, v. GT 04-18D-01.

Collins, W.J., Beams, S.D., White, A.J.R., Chappell, B.W., 1982. Nature and origin of A-type granites with particular reference to southeastern Australia. Contributions to Mineralogy and Petrology 80, 189–200.

Compston, W., Williams, I. S., Meyer, C., 1984. U–Pb geochronology of zircons from lunar breccia 73217 using a sensitive high mass-resolution ion microprobe. Journal of Geophysical Research 89, B252–B534.

Cox, K.G., Bell, J.D., Pankhurst, R.J., 1979. The interpretation of igneous rocks. George, Allen and Unwin, London, 464 pp.

Cullers, R.L., Barrett, T., Carlson, R., Robinson, B., 1987. Rare earth element and mineralogic changes in Holocene soil and stream sediment: a case study in the Wet Mountains, Colorado, USA. Chem. Geol. 63, 275–297.

de la Roche, H., Leterrier, J., Grandclaude, P., Marchal, M., 1980. A classification of volcanic and plutonic rocks using R1R2-diagram and major-element analyses: Its relationships with current nomenclature. Chemical Geology 29(1–4), 183–210.

Drake, M.J., Weill, D.F., 1975. Partition of Sr, Ba, Ca, Y, Eu2+, Eu3+, and other REE between plagioclase feldspar and magmatic liquid: an experimental study. Geochimica et Cosmochimica Acta 39, 689–712.

Eggins, S. M., Woodhead, J. D., Kinsley, L. P. J., Mortimer, G. E., Sylvester, P., McCulloch, M. T., Hergt, J. M., Handler, M. R., 1997. A simple method for the precise determination of >40 trace elements in geological samples by ICPMS using enriched isotope internal standardisation. Chemical Geology 134, 311–326.

Fossen, H., 2000. Extensional tectonics in the Caledonides: synorogenic or postorogenic? Tectonics 19, 213-224.

Frost, B.R., Barnes, C.G., Collins, W.J., Arculus, R.J., Ellis, D.J., Frost, C.D., 2001. A geochemical classification for granitic rocks. Journal of Petrology 42, 2033–2048.

Gaál, G., Gorbatschev, R., 1987. An outline of Precambrian evolution of the Baltic Shield. Precambrian Research 35, 15–52.

Gorbatschev, R., 1985. Precambrian basement of the Scandinavian Caledonides. In: Gee, D.G., Sturt, B.A. (Eds.), The Caledonide Orogen-Scandinavia and Related Areas. Wiley, Chichester, pp. 197–212.

Gromet, L.P., Dymek, R.F., Haskin, L.A., Korotev, R.L., 1984. The ‘North American Shale Composite’: its compilation, major and trace element characteristics. Geochimica et Cosmochimica Acta 48, 2469–2482.

Gustavson, M., Gjelle, S.T., 1991. Geological Map of Norway (1:250 000) Mo i Rana. Geological Survey of Norway.

Harris, N.W.B., Pearce, J.A., Tindle, A.G., 1986. Geochemical characteristics of collision-zone magmatism. In Coward, M.P., Ries, A.C. (Eds.), Collision Tectonics. Geological Society Special Paper 19, 115–158.

Henderson, I.H.C., Kendrick, M., 2003. Structural controls on graphite mineralisation, Senja, Troms. Geological Survey of Norway Report 2003.011, 16pp.

Henderson, I.H.C., Viola, G., 2013. Structural analysis of the Kautokeino Greenstone Belt from geophysical and field studies: Towards a refined understanding of its gold mineralisation. Proceedings of the Geological Society of Norway, Winter Conference, Oslo.

Hietanen, A., 1975. Generation of potassium-poor magmas in the northern Sierra Nevada and the Svecofennian in Finland. Journal of Resources U.S. Geological Survey 3(6), 631-645.

Harker, A., 1909. The natural history of igneous rocks. Methuen, London.

Irvine, T.N., Baragar, W.R.A., 1971. A guide to the chemical classification of the common volcanic rocks. Canadian Journal of Earth Science 8, 523–548.

Kärki A., Laajoki, K., 1995. An interlinked system of folds and ductile shear zones – late stage Svecokarelian deformation in the central Fennoscandian Shield, Finland. Journal of Structural Geology 17, 1233–1247.

Klein, A.C., Steltenpohl, M.G., Hames, W.E., Andresen, A., 1999. Ductile and brittle extension in the southern Lofoten Archipelago, northern Norway: implications for differences in tectonic style along an ancient collision margin. American Journal of Science 299, 69–89.

Korja, A., Lahtinen, R., Nironen, M., 2006. The Svecofennian orogen: a collage of microcontinents and island arcs, *in* Gee, D.G., Stephenson, R.A. (Eds.), European Lithosphere Dynamics. Geological Society, London, Memoirs 32, 561-578.

Korneliussen, A., Tollefsrud, J.I., Flood, B., Sawyer, E., 1986. Precambrian volcano-sedimentary sequences and related ore deposits, with special reference to the Gautelisfjell carbonate-hosted gold deposit, Rombaken basement window, Northern Norway. Geological Survey of Norway Report 86.193, 44p.

Korneliussen, A. and Sawyer, E. W. (1989). The geochemistry of Lower Proterozoic mafic to felsic igneous rocks, Rombak Window, North Norway. NGU Bulletin 415: 7-21.

Kuno, H., 1968. Differentiation of basalt magmas. In: Hess, H.H., Poldervaart, A. (Eds.), Basalts, the Poldervaart treatise on rocks of basaltic composition, vol. 2. Wiley and Sons, New York, p. 623-688.

Lahtinen, R., Garde, A.A., Melezhik, V.A., 2008. Paleoproterozoic evolution of Fennoscandia and Greenland. Episodes 31, 20-28.

Larsen, T., Bergh, S.G., Henderson, I.H.C., Korneliussen, A., Kullerud, K., 2010. Svecofennian structural development and metallogenesis of Paleoproterozoic volcano-sedimentary rocks of Rombak Tectonic widow: NGF abstract proceedings of the Geological Society of Norway, v. 1, 29th Nordic Geological winter meeting, Oslo.

Larsen, T., Sundblad, K., Henderson, I.H.C., Bergh, S.G., Bagas, L., Sandstad, J.S., Andersen, T., and Simonsen, S., 2013. Recognition of Svecofennian sulphide bearing crust in the Rombak region, northern Norway: NGF abstract proceedings of the Geological Society of Norway, v. 1, 32nd Nordic Geological winter meeting, Oslo.

Lesher, C.M., Gibson, H.L., Campbell, I.H., 1986. Composition-volume changes during hydrothermal alteration of andesite at Buttercup Hill, Noranda District, Quebec. Geochimica et Cosmochimica Acta 50, 2693–2705.

Lindh, A., 1987. Westward growth of the Baltic Shield. Precambrian Research 35, 53-70.

Ludwig, K. R., 2003. Isoplot/Ex version 3: A Geochronological Toolkit for Microsoft Excel, User’s Manual. Berkeley Geochronology Center Special Publications 4, 70 p.

Ludwig, K. R., 2009. SQUID 2: A User’s Manual. Berkeley Geochronology Center Special Publication 5, 110p.

Lundqvist, Th., 1987. Early Svecofennian stratigraphy of southern and central Norrland, Sweden, and possible existence of an Archaean basement west of the Svecokarelides. Precambrian Research 35, 343-352.

McCarthy, T.S., Hasty, R.A., 1976. Trace element distribution patterns and their relationship to the crystallization of granitic melts. Geochimica et Cosmochimica Acta 40, 1351–1358.

McDonough, W.F., Sun, S.-S., Ringwood, A.E., Jagoutz, E., Hofmann, A.W., 1992)\. Potassium, Rubidium and Cesium in the Earth and Moon and the evolution of the mantle of the Earth. Geochimica et Cosmochimica Acta 56, 1001–1012.

McLennan, S.M., 1989. Rare earth elements in sedimentary rocks: Influence of provenance and sedimentary process. Mineral. Soc. Am. Rev. Mineral. 21, 169–200.

McLennan, S.M., 2001. Relationships between the trace element composition of sedimentary rocks and upper continental crust. Geochem. Geophys. Geosyst. 2, 2000GC000109.

McLennan, S.M., Hemming, S., McDaniel, D.K., Hanson, G.N., 1993. Geochemical approaches to sedimentation, provenance, and tectonics. Geol. Soc. Am. Special Paper 284, 21–40.

McLennan, S.M., Taylor, S.R., McCulloch, M.T., Maynard, J.B., 1990. Geochemical and isotopic determination of deep sea turbidites: Crustal evolution and plate tectonic associations. Geochim. Cosmochim. Acta 54, 2015–2049.

Meschede, M., 1986. A method of discriminating between different types of mid-ocean ridge basalts and continental tholeiites with the Nb–Zr–Y diagram. Chemical Geology 83, 55–69

Moorbath, S., 1977. Ages, isotopes and evolution of Precambrian continental crust. Chemical Geology 20, 151-–187.

Myers, J.S., Kroner, A. 1994. Archaean tectonics. In: Hancock, P.L. (Ed.), Continental Deformation. Pergamon Press, Oxford.

Myhre, P.I., Corfu, F.C., Bergh, S., 2011. Paleoproterozoic (2.0–1.95 Ga) pre-orogenic supracrustal sequences in the West Troms Basement Complex, North Norway. Precambrian Research 186(1-4), 89-100.

Nesbitt, H.W., Young, G.M., 1989. Formation and diagenesis of weathering profiles. Journal of Geology 97, 129–147.

Nironen, M., 1997. The Svecofennian Orogen: a tectonic model. Precambrian Research 86, 21–44.

Norrish, K., Chappell, B.W., 1997. X-ray fluorescence spectrometry. In: Zussman, J. (Ed.), Physical Methods in Determinative Mineralogy, 2nd Edition. Academic Press, London, pp.201–272.

Norrish, K., Hutton, J.T., 1969. An accurate X-ray spectrographic method for the analysis of a wide range of geological samples. Geochim Cosmochim Acta 33, 431–453.

Olesen, O., Sandstad, J.S., 1993. Interpretation of the Proterozoic Kautokeino Greenstone Belt, Finnmark, Norway, from combined geophysical and geological data. Geological Survey of Norway Bulletin 425, 43–62.

Pearce, J.A., Cann, J.R., 1973. Tectonic setting of basic volcanic rocks determined using trace element analysis. Earth and Planetary Science Letters 19, 290–300.

Pearce, J.A., 1982. Trace element characteristics of lavas from destructive plate boundaries. In: Thorpe, R.S. (Ed.), Andesites. Wiley, New York, pp. 525–528.

Pearce, J.A., Harris, N.B.W., Tindle, A.G., 1984. Trace element discrimination diagrams for the tectonic interpretation of granitic rocks. Journal of Petrology 25, 956–983.

Peccerillo, A., Taylor, S.R., 1976. Geochemistry of Eocene calcalkaline volcanic rocks from the Kastamonu area, Northern Turkey. Contributions to Mineralogy and Petrology 58, 68–81.

Pidgeon, R.T., Furfaro, D., Kennedy, A. K., Nemchin, A.A., Van Bronswijk, W., 1994. Calibration of zircon standards for the Curtin SHRIMP II, *in* Eighth International Conference on Geochronology, Cosmochronology, and Isotope Geology - Abstracts. U.S. Geological Survey Circular 1107, p. 251.

Pitcher, W.S., 1983. Granite: typology, geological environment and melting relationships. In Atherton, M.P., Gribble, C.D. (Eds.), Migmatites, Melting and Metamorphism. Shiva Publishing Limited, Cheshire, U.K., p. 277–287.

Pyke, J., 2000. Mineral laboratory staff develops new ICP-MS preparation method. Australian Geological Survey Organisation Newsletter 333, 12–14.

Rollinson, H., 1996. Using Geochemical Data: Evaluation, Presentation, Interpretation. Longman Geochemistry Series, p. 75-76.

Rudnick, R., Gao, S., 2004. Composition of the continental crust. In: Holland, H.D., Turekian, K.K. (Eds.), Treatise on Geochemistry, Vol. 3. Elsevier, Amsterdam, pp. 1–64.

Sawyer, E., 1986. Metamorphic assemblages and conditions in the Rombak Basement Window. Geological Survey of Norway Report 86.168, 25pp.

Sawyer, E. W. and Korneliussen, A. (1989). The geochemistry of Lower Siliciclastic turbidites from the Rombak Window: implications for palaeogeography and tectonic settings. NGU Bulletin 415: 23-38.

Schandl, E.S., Gorton, M.P., Wateneys, H.A., 1995. Rare earth element geochemistry of the metamorphosed volcanogenic massive sulphide deposits of the Manitouwadge mining camp, Superior province, Canada: a potential exploration tool? Economic Geology 90, 1217–1236.

Stern, RA 2001, A new isotopic and trace-element standard for the ion microprobe: preliminary thermal ionization mass spectrometry (TIMS) U–Pb and electron-microprobe data: Geological Survey of Canada, Radiogenic Age and Isotopic Studies, Report 14, Current Research 2001-F1, 11p.

Stern, R. A., 2009. Measurement of SIMS instrumental mass fractionation of Pb isotopes during zircon dating. Geostandards and Geoanalytical Research 33(2), 145-168.

Shervais, J.W., 1982. Ti–V plots and the petrogenesis of modern and ophiolitic lavas. Earth and Planetary Science Letters 59, 101–118.

Sylvester, P.J., 1989. Post-collisional alkaline granites. Journal of Geology 97, 261–280.

Taylor, S.R., McLennan, S.M., 1985. The continental crust: its composition and evolution. Blackwell, Oxford, 312 pp.

Taylor, S.R., McLennan, S.M., Armstrong, R.L., Tarney, J., 1981. The Composition and Evolution of the Continental Crust: Rare Earth Element Evidence from Sedimentary Rocks. Philosophical Transactions of the Royal Society of London A301, 381–399.

Weaver, B.L., Tarney, J., 1984. Empirical approach to estimating the composition of the continental crust. Nature 310, 575–577.

Welin, E., Christansson, K., Kähr, A.-M. , 1993. Isotopic investigations of metasedimentary and igneous rocks in the Paleoproterozoic Bothnian Basin, central Sweden. Geologiska Föreningen i Stockholm Förhandlingar 115(4), 285-296.

Whalen, J.B., Currie, K.L., Chappell, B.W., 1987. A-type granites: geochemical characteristics, discrimination and petrogenesis. Contributions to Mineralogy and Petrology 95, 407–419.

White, A.J.R., Chappell, B.W., 1983. Granitoid types and their distribution in the Lachlan Fold Belt, southeastern Australia. Geological Society of America Memoir 159, 21–34.

White, A.J.R., Chappell, B.W., 1988. Some supracrustal (S-type) granites of the Lachlan Fold Belt. Transactions of the Royal Society of Edinburgh: Earth Sciences 79, 169–181.

Whitehead, D., 2010, Moraine as a Source of Gold in Stream Sediments and the Relationship to a Shear Zone in the Rombak-Skjomen Area of Norway: Master thesis from Luleå University of Technology, Department of Chemical Engineering and Geosciences.

Wilson, M., 1989. Igneous Petrogenesis: A Global Tectonic Approach. Chapman and Hall, London, UK, 465 pp.

Wimmenauer, W., 1984. Das prävaristische Kristallin im Schwarzwald. Fortschr. Miner. Beih. 62, 69–86.

Appendix

A-1. Geochemistry of greywacke and shale units (Sawyer and Korneliussen, 1989).

Id	SiO2	Al2O3	Fe2O3	FeO	TiO2	CaO	MgO	Na2O	K2O	MnO	P2O5	V	Sc	Co	Cr	Ni	Cu	Zn	Pb	Rb	Sr	Ba	Zr	Y	Nb	Cs	Th	U	Ta	Hf	La	Ce	Nd	Sm	Eu	Tb	Yb	Area
ES057.4G	71,35	11,68	0,63	5,66	0,73	2,67	2,33	2,27	1,80	0,06	0,13	137	12		262	46	84	111		75	231	778	252	20	8	2	10	3	1	6	36	74	25	5	1	1	2	Gautelisvann
ES058.4G	70,48	12,56	0,58	5,21	0,65	2,77	2,41	2,49	1,86	0,06	0,13	118	12		187	54	51	111		77	246	622	167	18	9	3	8	3	1	4	25	52	22	4	1	1	2	Gautelisvann
ES060.4G	57,84	16,78	0,93	8,32	0,93	2,78	4,27	3,23	3,45	0,09	0,12	223	18		229	116		190		133	285	959	143	26	12						32	39						Gautelisvann
ES061.4G	54,62	17,69	1,03	9,22	1,00	2,85	4,64	3,59	3,89	0,09	0,12	279	25		266	135	6	144		126	291	981	130	24	14	4	10	4	1	3	22	50	19	4	1	1	3	Gautelisvann
ES067.4R	66,46	14,13	0,70	6,28	0,75	1,45	3,28	3,01	2,71	0,06	0,13	144	15		245	75	6	103		110	149	704	173	24	12						52	91						Rombaksbotten
ES068.4R	68,98	13,14	0,62	5,59	0,70	1,06	2,99	3,48	2,42	0,05	0,12	131	12		301	72	11	82		88	173	873	201	25	11	5	11	283	1	5	33	77	28	5	1	1	2	Rombaksbotten
ES072.4R	68,80	13,62	0,57	5,13	0,62	2,30	2,77	3,08	2,26	0,05	0,11	112	14		215	67	59	86		105	247	697	147	15	8	7	8	3	1	3	28	59	23	4	1	-	2	Rombaksbotten
ES073.4R	68,09	12,72	0,70	6,31	0,88	1,84	3,06	2,89	2,58	0,07	0,15	155	13		387	63	35	91		102	168	775	297	30	11						61	109						Rombaksbotten
ES069.4R	53,44	18,15	1,05	9,40	0,84	2,41	5,35	3,41	4,19	0,08	0,13	198	23		212	124	109	147		205	227	598	106	18	17	14	11	3	1	2	29	62	24	5	1	1	2	Rombaksbotten
ES070.4R	60,73	16,22	0,81	7,24	0,76	1,07	4,24	3,63	3,76	0,07	0,11	158	18		210	82	18	23		151	155	876	134	22	11	12	10	3	1	3	16	37	10	3	1	1	2	Rombaksbotten
ES131AC	51,96	13,42	1,29	11,56	1,27	6,01	8,69	2,98	1,80	0,13	0,12	254	37	43	503	211	84	132	13	66	157	785	103	28	9	6	3	1	-	2	11	26	12	3	1	1	2	Ruvssot
ES132AC	56,31	14,04	1,12	10,03	0,85	1,59	6,78	2,56	5,30	0,09	0,15	141	20	35	332	139	67	62	9	190	118	660	112	19	7	8	10	2	1	3	24	51	19	4	1	1	1	Ruvssot
ES133C	58,45	14,54	0,96	8,66	0,90	1,99	5,65	3,57	4,36	0,08	0,13	128	21	30	279	109	76	47	10	161	153	429	114	16	9		5			4	0	50						Ruvssot
ES134AC	58,55	14,66	0,98	8,79	0,88	2,87	4,62	2,72	4,80	0,09	0,13	132	20	28	228	98	12	48	12	191	112	726	125	18	8	8	10	2	1	3	27	58	24	4	1	1	2	Ruvssot

A-2. Geochemistry of mafic and ultramafic rocks (Korneliussen and Sawyer, 1989)

Id	SiO2	Al2O3	Fe2O3	TiO2	CaO	MgO	Na2O	K2O	MnO	P2O5	V	Sc	Co	Cr	Ni	Cu	Zn	Pb	Rb	Sr	Ba	Zr	Y	Nb	Cs	Th	U	Ta	Hf	La	Ce	Nd	Sm	Eu	Tb	Yb	Area
G2.4GB	48,12	13,41	15,31	2,19	8,97	5,37	2,30	1,35	0,22	0,77	365	36	42	48	45	59	160	15	36	382	846	128	38	8						27	54						Gautelisvann
G4.4GB	47,60	15,99	12,59	1,23	9,81	7,55	1,90	1,05	0,18	0,34	234	28	62	103	121	65	127	13	39	392	433	65	20	6						13	19						Gautelisvann
G5.4GB	48,41	13,81	14,58	2,12	9,56	5,75	2,80	1,03	0,22	0,84	335	36	52	101	49	48	167	17	28	422	617	119	34							27	51						Gautelisvann
G6.4GB	48,75	12,51	16,12	2,38	8,74	4,84	2,60	1,53	0,23	0,95	387	33	41	18	30	49	222	14	43	371	872	137	38	7						40	72						Gautelisvann
G7.4GB	48,49	13,48	15,39	2,42	9,65	5,28	2,70	0,96	0,24	0,95	391	39	41	28	32	22	189	15	24	427	649	143	40	6						35	73						Gautelisvann
K133.4G	48,38	16,32	12,36	1,34	9,67	6,22	2,30	1,20	0,17	0,40	247	29	43	79	77	66	133	11	39	455	580	78	21	5	2	1	-	-	2	19	39	14	4	1	1	2	Gautelisvann
K071.85S	59,82	15,24	6,52	1,11	4,25	3,38	3,94	4,57	0,11	0,31	108	14	16	136	31	34	71	18	145	480	1220	309	25	20		18			5	46	99						Norddalen
K132A.4	53,28	15,63	12,73	2,21	4,16	4,39	1,10	3,37	0,13	0,43	401	27	38	45	38	152	137		151	207	715	192	37	10						40	68						Norddalen
K152.3GK2	47,79	13,53	14,71	2,10	9,21	5,58	2,70	1,37	0,20	0,83	326	34	38	103	55	23	120	15	55	397	574	112	34							32	65	37	9	2	1	2	Norddalen
K268.3N	50,50	14,94	12,19	1,49	8,88	6,25	2,50	1,45	0,18	0,35	208	31	42	134	31	15	142	16	64	387	483	116	26		2	2	1	-	3	25	52	21	5	1	1	2	Norddalen
K273.3N	55,27	14,29	10,83	1,65	6,15	4,26	2,70	3,04	0,15	0,62	169	20	34	91	24	13	131	20	144	378	938	186	40	13						44	88	44	10	2	1	3	Norddalen
K274.3N	57,46	13,80	11,17	2,01	5,09	2,26	3,40	2,98	0,15	0,89	130	18	22		6	10	143	16	86	332	1300	306	49	16						52	116						Norddalen
R001.3RT	48,57	9,88	13,04	1,30	6,86	7,75	4,10	0,17	0,09	0,12	213	21	36	277	90	11	38			107	56	93	13	6						14	25	16	3	1	-	1	Ruvssot
R004.3RT	48,81	9,63	10,05	0,92	6,20	21,04	2,50	0,12	0,13	0,10	268	24	74	550	234	16	43			107	80	132	21	8		6	1	1	3	16	23	18	4	1	1	2	Ruvssot
R016.3RT	47,40	6,92	8,74	0,20	6,70	28,76	0,01	0,01	0,18	0,02	154	27	55	3000	1400	45	46				42	21				-	-		-	0			-	-		1	Ruvssot
R022.3RT	45,55	7,49	10,63	0,25	8,85	20,56	0,50	0,03	0,16	0,02	168	26	89	2200	1 000	8	98			9	25	25	8			-		-	-	1			-	-	-	1	Ruvssot
R023.3RT	44,03	4,80	8,76	0,16	5,05	28,77	0,01	0,01	0,17	0,01	131	20	111	2600	1600	5	55			15	48	18				1				1						1	Ruvssot

Table A-3. Geochemistry of the ca. 1790 Ma felsic igneous rocks in the Rombak Tectonic Window (Korneliussen and Sawyer, 1989).

Id	SiO2	Al2O3	Fe2O3	TiO2	CaO	MgO	Na2O	K2O	MnO	P2O5	V	Sc	Co	Cr	Ni	Cu	Zn	Pb	Rb	Sr	Ba	Zr	Y	Nb	Th	U	Hf	La	Ce	Eu	Area
K142.85	60,55	18,49	4,49	0,67	2,03	2,19	8,54	1,53	0,05	0,19	63,00	9,00	7,00	22,00	15,00	3,00	43,00	16,00	47,00	353,00	361,00	206,00	22,00	18,00	13,00	2,33	2,00	43,00	79,00	0,50	Gautelisvann
ES083GR	66,04	15,26	4,87	0,64	2,25	0,96	3,40	5,53	0,06	0,18	43,00	8,00	11,00	13,00	6,00	8,00	81,00	20,00	197,00	234,00	1200,00	367,00	46,00	19,00	24,00	4,30	0,50	96,00	204,00	0,50	Norddalen
K063.85S	66,13	13,99	0,78	5,40	2,76	1,81	3,51	4,36	0,09	0,28	58,00	11,00	10,00	37,00	14,00	12,00	75,00	26,00	193,00	212,00	895,00	248,00	33,00	18,00	16,00	2,87	8,00	58,00	124,00	0,50	Norddalen
ES081GR	66,40	15,83	3,82	0,51	2,04	0,59	4,10	5,45	0,06	0,13	23,00	5,00	7,00	2,00		1,00	43,00	25,00	133,00	229,00	1300,00	352,00	43,00	18,00	28,00	6,00	9,00	127,00	233,00	2,00	Norddalen
K152.85	67,00	14,73	4,19	0,62	1,93	0,76	4,00	5,75	0,08	0,18	31,00	10,00	6,00	8,00	6,00	28,00	58,00	28,00	197,00	178,00	1008,00	270,00	47,00	20,00	15,00	2,69	3,00	65,00	132,00	0,50	Gautelisvann
K140.85	67,29	14,91	4,47	0,54	3,60	1,54	4,50	2,12	0,05	0,13	56,00	8,00	6,00	9,00	7,00	11,00	36,00	12,00	55,00	377,00	967,00	180,00	16,00	12,00	8,00	1,00	5,00	30,60	62,90	1,00	Gautelisvann
K144.85	69,25	14,95	3,13	0,44	3,21	1,01	4,92	1,94	0,06	0,12	34,00	8,00	3,00	7,00	8,00	2,00	31,00	12,00	54,00	692,00	722,00	219,00	18,00	19,00	19,00	3,41	2,00	45,00	89,00	0,50	Gautelisvann
K275.3N	69,37	13,44	4,74	0,59	1,70	0,54	2,90	5,33	0,06	0,15	30,00	8,00	7,00	6,00	6,00	6,00	90,00	25,00	239,00	120,00	760,00	398,00	63,00	24,00	28,00	5,02		91,00	187,00	0,50	Norddalen
K072.85S	70,69	14,98	0,29	1,93	1,48	0,64	4,53	4,80	0,04	0,07	32,00	3,00	3,00	6,00	8,00	5,00	21,00	14,00	138,00	372,00	983,00	174,00	15,00	15,00	19,00	3,41	2,00	33,00	65,00	0,50	Norddalen
K143.85	71,94	15,27	1,31	0,17	1,74	0,42	6,59	1,52	0,04	0,05	15,00	4,00	3,00	2,00	1,00	4,00	17,00	11,00	34,00	490,00	719,00	112,00	11,00	9,00	12,00	2,00	3,00	43,50	84,40	1,00	Gautelisvann
K145.85	72,55	14,53	1,35	0,18	0,76	0,32	4,13	5,64	0,03	0,05	19,00	4,00	1,00	2,00	2,00	2,00	34,00	14,00	106,00	229,00	1101,00	107,00	10,00	8,00	7,00	1,26	1,00	18,00	25,00	0,50	Gautelisvann
ES022GR	72,97	13,85	2,48	0,26	1,21	0,23	3,10	5,76	0,04	0,03	10,00	1,00	7,00	8,00	7,00	1,00	70,00	27,00	246,00	103,00	599,00	309,00	57,00	19,00	30,00	5,38	0,50	97,00	204,00	0,50	Norddalen
ES033GR	75,32	13,70	1,48	0,20	0,97	0,19	3,20	5,56	0,03	0,02	10,00	1,00	6,00	2,00	1,00	1,00	14,00	22,00	230,00	118,00	500,00	199,00	26,00	16,00	52,00	11,00	5,00	73,90	154,00	1,00	Norddalen
K272.3N	76,65	12,48	1,35	0,09	0,74	0,07	3,30	5,29	0,01	0,01	5,00	1,00	6,00	2,00	1,00	9,00	38,00	63,00	391,00	24,00	80,00	168,00	142,00	17,00	52,00	9,33	0,50	106,00	170,00	2,00	Norddalen
ES024GR	76,91	12,44	1,70	0,14	0,78	0,15	3,10	5,43	0,02	0,01	5,00	1,00	1,00	2,00	1,00	1,00	45,00	30,00	319,00	46,00	214,00	214,00	76,00	15,00	43,00	7,71	0,50	80,00	168,00	0,50	Norddalen

Paper III

Tine L. Angvik, Jan Sverre Sandstad

The timing of sulphide mineralisation in the Rombaken Tectonic Window and their spatial relation to the Rombaken-Skjomen Shear Zone, northern Norway

(manuscript)

The timing of sulphide mineralisation in the Rombaken Tectonic Window and their spatial relation to the Rombaken-Skjomen Shear Zone, northern Norway

Angvik, T.L. ([1, 2]) and Sandstad, J.S. ([1])

([1]) Geological Survey of Norway, Leiv Eirikssonsvei 39, 7040 Trondheim

([2]) Dept. of Geology, University of Tromsø, 9037 Tromsø

Abstract

The Rombaken Tectonic Window (RTW) is a Paleoproterozoic inlier within the Caledonian nappes of northern Norway. The bedrock consists of Svecofennian granites intruded into metasedimentary and metavolcanic rocks, which appear as N-S trending parallel belts widening and thickening along strike. Sulphide mineralisations in the RTW, including As-Au, Cu and Pb-Zn, have long been explored for gold in the area and the need for a better understanding of the geological evolution of the area has increased. Recent tectonic and structural models have verified a large scale Svecofennian Rombaken-Skjomen shear zone (RSSZ), which can be traced across the whole window and into Sweden. The model consists of four deformation events that includes two N-S striking, east verging fold-thrust (D_1-D_2) and two oblique-slip events with steep ductile N-S striking (D_3) and NE-SW (D_4) striking shear zones. Several known sulphide mineralisations are found along, within and near this regional shear zone. In the present study we have studied several of these for their genesis, timing and spatial relationship to the RSSZ. We found at least four stages of mineralisation including; 1) syngenetic bedding parallel Zn-Pb SEDEX deposits (D_0), 2) syntectonic metasomatic As-Au-Fe deposit (D_3-D_4) and 3) orogenic gold, both along the regional shear zone, including remobilisation of the SEDEX mineralisations (D_3-D_4) and as 4) Cu-Au in late Svecofennian quartz veins (D_3-D_4). The formation of most of the sulphide mineralisations in RTW is very complex with several stages of remobilisation and deformation, that are spatially and temporally linked to the development of RSSZ

Keywords: Rombaken Tectonic Window, Orogenic gold, SEDEX, Metasomatic, sulphides, Rombaken-Skjomen Shear zone.

1.0 Introduction

The Fennoscandian Shield is dissected by a network of major shear zones containing associated economic important deposits of gold and/or base metals (Eilu et al., 2003; Sundblad, 2003; Martinsson, 2004). In the northern part of the shield these regional fault structures developed and were reactivated during several tectonothermal events in conjunction with the Paleoproterozoic Svecofennian orogeny (1920-1790 Ma; Lahtinen et al., 2012). Recently, an additional member of this network has been defined in the Rombaken Tectonic Window (RTW) where the N-S trending Rombaken-Skjomen Shear Zone (RSSZ) intersects Paleoproterozoic basement rocks overthrusted during the Ordovician to early Devonian by Caledonian nappe complexes close to the eastern margin of the Caledonian orogen (Fig.1). The RTW is endowed with partly auriferous polymetallic sulphide mineralisations which are the theme of the present paper.

The RSSZ developed during the Svecofennian orogeny and is situated close to the boundary between the Karelian Craton with Archean-Paleoproterozoic granite-greenstone terrains (e.g. Rutland et al., 2001) and the Svecofennian arc-related volcano sedimentary sequences to the west and south. The boundary between these terrains is largely obliterated by the emplacement of granitic plutons comprising possibly the eastern margin of northern extension of the Transscandinavian Igneous Belt (TIB; Gorbatschev 2004). Thus the RSSZ may represent an important suture zone between crustal segments in the Fennoscandian shield. Several sulphide mineralisations have been known in this area for more than a century (Foslie, 1916; Korneliussen & Sawyer, 1986; Coller, 2004; Blomlie, 2011). However, the knowledge of their genesis has not been well understood. The importance of the present study is to show how the sulphide mineralisation in the Paleoproterozoic supracrustals in the RTW and along RSSZ may be part of a complex story involving several genetic types. The understanding of the metallogeny of the RSSZ is largely based on field and structural relationship as well as microscopic studies and geochemical analysis of the host rocks and the hydrothermal alteration associated with the mineralisations. The ultimate aim of the present paper is to place the development of the sulphide mineralisations in time and space within the geotectonic framework of the RSSZ.

2.0 Geological setting

The RTW consists mainly of Paleoproterozoic rocks exposed as an inlier surrounded by Caledonian thrust sheets of Phanerozoic rocks, and is a result of deep erosion and removal of the overlying Caledonian nappes. The geology of the area has previously been described by Gustavson et al. (1974), Priesemann (1984 a, b), Skonseng (1985), Korneliussen & Sawyer (1986) and Bargel (1995).

The RTW consists of plutonic rocks, comprising intrusions of granites and subordinate gabbros and several N-S trending belts of metasupracrustal rocks (Fig. 1). The oldest dated rock in the area is represented by a tonalitic basement rock found in the Sjangeli area (Sweden). It yields a U-Pb age of 2709 Ma and occurs as xenoliths in the Sjangeli granite (Romer et al., 1992) (Fig. 1). The metasupracrustal rocks in the Sjangeli area are dominated by mafic to ultramafic volcanic and volcano sedimentary units intercalated with metasedimentary rocks. The metasupracrustal rocks in the Sjangeli and Kopperåsen areas are assumed to have a depositional age of 2300-2000 Ma (Romer & Boundy, 1988; Romer, 1989), but is uncertain. They have previously been correlated to the Gautelis supracrustal belts in the southern part of the studied area (Fig. 1) (Romer, 1987). The metasedimentary rocks in Gautelis are assumed to be of younger age. The tonalite in the Gautelis area is the lowermost basement rock and is overlain by sedimentary breccias and conglomerates containing pebbles of the underlying tonalitic basement. Romer et al., (1992) dated a Paleoproterozoic tonalite, yielding an age of 1949±26 Ma (U-Pb). The basal conglomeratic sequence is overlain by marbles and metagreywacke with an assumed age of 1900-1880 Ma (Korneliussen & Sawyer, 1989). These metasedimentary rocks are thought to be deposited in a basin in an Andean-type setting and show large similarities to the supracrustal belts in the Haugfjellet-Sildvika and Norddalen areas (Fig.1.) (Korneliussen & Sawyer, 1989). The rocks in the RTW have undergone several stages of metamorphism. Peak metamorphism reached amphibolite-grade at 6kb and 575ºC, and is dated to ca. 1800 Ma (Sm-Nd) (Sawyer, 1986; Romer, 1989). Another metamorphic event was detected by U-Pb dating of zircons from a granite to the east of Gautelis giving an age of 1769.6±9.7Ma correlating with the Svecofennian orogeny (Romer et al, 1992). Uranitite, associated with Cu-Fe sulphides in Kopparåsen, have been dated and also associated to this age and metamorphic event (1780 Ma; Romer & Boundy, 1988). In the Sjangeli area (Fig. 1) the epigenetic Cu-Fe vein mineralisation is thought to be related to Proterozoic metamorphism with remobilsation of stratiform Fe-Zn sulphides during the Caledonian metamorphism (Romer, 1989). It has been furthermore documented that retrogression to greenschist facies metamorphism occurred in the Norddalen area (Fig. 1). Structure related gold occurrences have been documented locally from Haugfjellet (Fig. 1: Coller, 2004). The age of this event has both been interpreted as Proterozoic (Korneliussen & Sawyer, 1986) and as Caledonian (Romer, 1993). Korneliussen & Sawyer (1986) suggested that the retrogradation was linked to steep N-S trending shear zone and fold structures in Norddalen, whereas Romer (1993) argued that the presence of upright folds in combination with Pb-Pb isotope data suggested a Caledonian tectonothermal event. However, recent investigations show that the structures are Paleoproterozoic with approximately the same age as the Rombak granites in the Haugfjellet and Gautelis area (1786 ± 8 – 1790 ± 8 Ma; Angvik et al., 2014 included manuscript). They are found both to be segmented by and also crosscut the shear zone (Larsen et al., 2013). The shear zone cuts through variably deformed gabbros and metasupracrustal rocks, and it is interpreted as a dynamic and continuous transpressional event with strain partitioning (Larsen et al, 2013). The strain was first dominated by two events of N-S striking, upright and east verging folding and thrusting (D_1-$D_{2)}$ which progressively turned into thrust parallel, sub vertical, N-S orientated, mainly sinistral and slightly dextral oblique-slip shear zones (D_3) which were later drag folded and cut by a NE-SW dextral oblique-slip shear zone (D_4). The greenschist facies retrogression is strongly related to the transpressive RSSZ structures carrying associated sulphide mineralisation (Larsen et al., 2010; Larsen et al., 2013). Nevertheless, Caledonian reactivation cannot be entirely excluded (Larsen et al., 2013).

3.0 Sulphide mineralisation

Several sulphide deposits have been known in this area for more than a century (Foslie, 1917; Korneliussen & Sawyer, 1986; Skyseth, 1995; Coller, 2004; Blomlie, 2011). The genetic aspects of the deposits have not been treated in any detail including their relation to the RSSZ. The sulphide occurrences along the shear zone include a variety of polymetallic deposits. The supracrustal belts are generally very rusty in appearance as an indication of their contents of Fe-sulphides. There are several areas of interest in regard to auriferous sulphide deposits (Fig. 1), and two of these, the Haugfjellet-Sildvika and Gautelis areas have been emphasised in the present study (Fig. 1).

3.1 Haugfjellet-Sildvika area

The Haugfjellet-Sildvika area is located in the northern part of the RTW where the bedrock consists of granites with two large belts of metasedimentary rocks (Fig. 1). The bedrock in Sildvika is similar to Haugfjellet and consist of metagreywacke, marble, metatuffite, metasiltstone, graphitic schist and quartzitic rock (Fig. 2). The eastern part of the metasupracrustal belt at Haugfjellet is dominated by siltstones interbedded with metagreywacke, sandstones, volcanites and graphitic schists whereas the western part is mainly composed of metatuffite interbedded with metagreywackes, quartzites and graphitic schists (Bargel, et al. 1995; Coller, 2004). There are also some marble beds forming thin lens-shaped units elongated parallel to and within oblique-slip shear zones (Fig. 2). In the western part of Haugfjellet, some lenses of marble and metagreywacke are even found within a shear zone in the coarse-grained Rombak granite (Fig. 2). The Sildvika metasupracrustal belt is located SW of Haugfjellet (Fig. 1) and comprises the same type of lithologies as in the western part of the Haugfjellet belt. The rocks are less deformed than at Haugfjellet, and primary structures are commonly observed. The Haugfjellet metasupracrustal belt show more deformation with a pronounced N-S striking cleavage dipping steeply to the west (D_3). The surrounding Rombak granites are more or less undeformed with a slight foliation developed except along localised shear zones. The metasedimentary rocks at Haugfjellet are affected dominantly by steep to subvertical folds (D_3), plunging both to NNW and SSE (Larsen et al., 2013).The folds are bounded by steep ductile shear zones where low angle thrust planes being refolded (D_1-D_2), have only been identified by microscopy (Larsen et al., 2013). Several sub vertical N-S, NE-SW and NW-SE orientated (D_{3-} D_4) oblique-slip ductile shear zones cut and drag fold the primary sedimentary bedding. The shear zones are mm to several meters wide and seem to spread out and slightly bend of towards the NNW (Fig. 2). They show both dextral and sinistral shear senses as well as a pronounced moderate dipping lineation towards NW (Larsen et al., 2013). The structures of the Haugfjellet belt have been interpreted to be part of a pure-shear-dominated domain in a transpressive orogen with ductile strain partitioning developing from a fold-thrust belt (D_1-D_2) into steep oblique-slip ($D_{3-}D_4$) shear zones (Larsen et al., 2010).

Sulphide-rich metasedimentary rocks with a reddish brown, rusty colour appear frequently in the Haugfjellet supracrustal belt. Since the rocks in this area have been strongly deformed and segmented, the distribution of the sulphide mineralisation appears very irregular and complex. There is a visual difference between the eastern part of Haugfjellet, dominated by metasiltstones and the western part composed of oxidised red-coloured metatuffite and metagreywacke with more Fe sulphides (Fig. 2). There are several old showings in the Haugfjellet-Sildvika area from earlier exploration. Three main types of mineralisation can be differentiated: 1) Bedding parallel Fe and Zn-Pb sulphide mineralisations (D_0), 2) Shear-zone-hosted Cu-Au-As mineralisation, including remobilisation of Zn-Pb (D_3-D_4), and 3) quartz-vein-hosted Cu-Au mineralisation (D_3-D_4).

3.1.1 Bedding parallel Fe and Zn-Pb sulphide mineralisations

Sulphide mineralisations along primary sedimentary beds have been observed in the supracrustal belts at Haugfjellet, Jernvann and Sildvika (Fig. 1-2). The sulphides are found in a few centimeters thick beds, either as single or multiple, parallel beds that can be followed up to hundreds of meters (Fig. 3A). They are either cut by steep oblique-slip (D_3-D_4) shear zones, thin out or the sulphide content gradually decreases. Both on Haugfjellet and Jernvann occur beds with a high content of sulphides (Fig. 3) in areas where the rocks are weakly deformed and frequently contain primary sedimentary structures such as cross-bedding and graded bedding (Fig. 3B and D). The sulphides are commonly found along distinct beds of the darker, fine-grained silty beds with high quartz and mica content. The sulphide mineralisation comprises three different types, dominated by disseminated to semi-massive 1) pyrrhotite (Fig. 3C, 2), pyrite (Fig. 3E) and 3) sphalerite and galena (Fig. 3D).

The types 1 and 2 are very similar in appearance and can sometimes coexist as separate pyrrhotite- and pyrite-dominated beds in the same outcrop. These two types are mainly found in the oxidised red-coloured metatuffite and metagreywacke units in the western part of Haugfjellet and Jernvann. Pyrite beds are more commonly encountered in the metatuffites, whereas the pyrrhotite is more evenly distributed in all the metasedimentary units especially along metagreywackes.

Type 1 is the most common and occurs as dissemination of very fine-grained (10-150 µm) pyrrhotite in silty beds. Locally the dissemination grades into semi-massive pyrrhotite bands. Pyrrhotite is also intergrown with minor amounts of chalcopyrite, sphalerite and pyrite, which appear to have copercipitated with the pyrrhotite (Fig. 3C). The metagreywacke host-rocks consist mainly of quartz and K-feldspar together with some biotite and chlorite. In beds with alternating high chlorite and biotite content, the sulphide is more abundant in the chlorite dominated beds. The type 2, pyrite mineralisation (Fig. 3D) occurs commonly as the only sulphide in the metatuffite (Fig. 3E), although minor pyrrhotite is locally observed. Pyrite has a grain size in the range 10-150 µm and commonly occurs as minor segregations and thin (5-10 mm) semi-massive bands together with quartz. The gangue is dominated by biotite, chlorite, larger but fewer quartz grains than type 1 (10-500 µm) and with epidote aggregates (100-150 µm).

Type 3 consists of bedding parallel sphalerite and galena mineralisation (Fig 3F). It is found along undeformed greywacke beds in the Sildvika area and partly at Haugfjellet, where the mineralised rocks frequently retain their primary sedimentary structures and occur adjacent to areas affected by strong shear deformation. The sulphide mineralisation is found in the finer grained silty beds with large amounts of quartz and biotite and less of plagioclase. The sulphide minerals occur as dissemination locally grading into massive bands and lenses (1-50m long, 1-20cm thick) in the outcrops. The sulphide minerals coexist with coarse chlorite (50-1500 µm), calcite (50-500 µm) and quartz grains (10-1000 µm) which define weak foliation or hairline veining. Mineralisation of Sphalerite dominates and has grain sizes of 10-500 µm with small pyrite inclusions (<50 µm) (Fig 3F).

3.1.2 Shear-zone-hosted Cu-As-Au with remobilised Pb-Zn mineralisation

Several of the old showings in the Haugfjellet area show a complex development of shear zone-hosted sulphide mineralisation (Fig. 2). The sulphides are mixed and are slightly anomalous with uncommon metal association such as Pb-Zn together with As. The sulphide minerals of this category consists of pyrrhotite, sphalerite, galena and chalcopyrite, and locally minor arsenopyrite (Fig. 4) which have been interpreted to be of two different genetic types with typical metal assemblages 1) Cu-As-Au and 2) remobilised Pb-Zn.

The sulphide mineralisation at locality HF-235, in the western part of Haugfjellet, occurs in a metagreywacke sequence sandwiched between the tuffite-dominated and siltstone-dominated units (Fig. 2). At this locality there are two exploration pits worked on a 1.5 m wide, ductile dextral shear zone (Fig. 4A), which has been intersected by two core holes. This steep dipping shear zone (D_3), with a red, purple and black coloured oxidised surface, can be traced for hundreds of meters along strike and have been observed to join or spread into several shear zones along strike in an anastomosing pattern (Fig. 6B). The different segments of the shear zone cut and fold the surrounding sedimentary beds with different frequency and intensity. The weakly deformed host rocks outside the shear zone consist of approximately 10-20 cm thick folded beds of upwards fining metagreywackes. The primary bedding of the greywacke has been totally erased in the shear zone and appears as steep, foliated, dark silty schist. The shear foliation is steep with a NW-SE strike direction. The fine-grained schistose tectonites within the shear zone contain up to 30 cm thick massive sulphide layers. Quartz-filled micro-fractures mainly occur along the shear foliation, but may locally form small clusters of non-directional veins or quartz-cemented breccias filling the shear zone (6C). The mineralised and sheared metagreywacke is characterised by large amounts of biotite and quartz which occur intergrown with epidote, muscovite and plagioclase. The minerals do not show any strong planar orientation and may be recrystallised. Biotite is partly to fully chloritised and occurs abundantly along quartz filled micro-fractures enveloped by fine-grained biotite aggregates dimishing in abundance away from the fractures. Chlorite is commonly intergrown with the sulphides which comprise pyrrhotite, galena, sphalerite and chalcopyrite, and minor arsenopyrite (Fig. 4D,F,G). The pyrrhotite appears as disseminated grains, whereas galena, sphalerite and chalcopyrite are confined to microfractures or to the shear zones (Fig. 4E). The latter sulphides appear locally to replace grains of pyrrhotite, but do also form aggregates together with pyrrhotite.

Geochemical data on three samples from pit 1 (Fig. 4A and C) show that they are enriched in Zn, Pb and Cu along the zones of high strain when compared with data for one sample from the unmineralised and weakly deformed layered metagreywacke host rock (Fig. 4). When the analytical values of the samples are normalised to the average value of unmineralised and weakly deformed metagreywacke in the Haugfjellet area they confirm that the mineralisation is enriched in a number of metallic elements and especially Pb, Zn, Cu and Hg (Fig. 4B). The gold contents of the shear zone are generally low, but higher than in the weakly deformed surrounding metagreywacke where no gold was detected.

Comparable observations were also done by logging the cores from a 140 m long drill hole, BH-1 (Figs. 4-5). The drill hole crosscuts several shear bands and high-strain zones, as well as weakly deformed to undeformed metagreywackes (Fig. 5). The core confirms the observations found in the prospects at the surface. The sulphides occur strongly associated with zones showing strong ductile deformation (Fig. 5). Pyrrhotite is the most abundant sulphide throughout the length of the cores and occurs both in areas of low and high strain. Abundant sphalerite and galena (Fig. 5) are found both in ductile shear bands and along the bedding of the weakly deformed metagreywacke. Arsenopyrite is only observed in zones showing strong ductile shearing, where it occurs along hairline thin quartz veinlets cutting the shear foliation (Fig. 5). These veinlets show both sinistral and dextral displacements of the metagreywacke bedding and the ductile shear bands that locally show tendencies of developing quartz breccias, similar to what is seen in Fig. 6C. In the log of BH-1 (Fig. 5), the Zn-Pb mineralisation show strong similar enrichment patterns relatable to the ductile shear zones, whereas Cu and As shows a different enrichment pattern though still confined to zones of ductile shearing with hairline veinlets.

Locality HF-232 is located near HF-235 (Fig 2) within metagreywacke and also within a similar shear zone enriched in sulphide minerals. The sulphides in this locality are dominated by pyrrhotite, sphalerite and arsenopyrite. Pyrrhotite and sphalerite occur in micro shear zones filled with quartz as micro veins and lesser amounts of arsenopyrite. The arsenopyrite is intergrown with sericite and epidote. The normalised values of the analytical data for the samples from this locality (Fig. 6D,E) also confirm the general enrichment of most of the heavy metals when normalised to the weakly deformed and unmineralised metagreywacke wall rock, and especially Zn, Pb, As, Ag, Hg, Sb, and Mo.

The Varden locality is situated in the middle of a highly structurally segmented area in the metatuffite near the contact to metasiltstone (Fig. 2.). The sulphide mineralisation is found in a 2x1 meter blasted pit and is similar to the two other localities described above. The mineralisation occurs in metagreywacke and is located along a one meter wide ductile shear zone (D_3) that can be followed for at least tens of meters, and contains arsenopyrite, sphalerite, galena and minor chalcopyrite. Similar to the drill core at locality HF-235, the mineralisation contains clusters of non-directional quartz veins crosscutting and brecciating the shear zone (Fig. 6C). The geochemical data of these veins are marked with a green line, and the normalised values for the samples from the shear zone show that the mineralisation is enriched in W, Bi, Ag, Cd, Pb, Zn and to a less extent also Au (Figs. 6F, G).

3.1.3 Quartz-vein hosted Cu-Fe-Au mineralisation

Sulphide mineralisations are also found in quartz veins in the Haugfjellet area. The sulphide mineralised brittle-ductile quartz veins consist mainly of quartz (80%) some carbonate (2%) and 5-10% sulphides (Fig 7A). Only some veins contain sulphides. The veins are 1mm-1m thick and 10cm-5m long and occur widespread and occasionally in swarms (Fig 8). The brittle-ductile subvertical veins strike NW to NNE (Fig. 8) which suggests a NE-SW compression. They are found within the supracrustal rocks and in less extent within the coarse grained Rombak granite. Some quartz veins appear as an array of tension gashes which again have been sheared by the oblique-slip shear zones and some veins are also sheared along the boundary to the host rocks, which show that they are a late stage (D_3-D_4) of the development of the RSSZ (Fig.7; Larsen et al., 2010).

The sulphides are mainly comprised of chalcopyrite and pyrite (Fig. 7C) with minor arsenopyrite and accessory galena. Some veins contain epidote, chlorite and Mg-rich biotite (Fig 7B and 7D) which occur most abundantly along the walls of the veins and may even form separate veins of biotite and epidote. The geochemical data, normalised to the average host rock in the Haugfjellet area, shows that the quartz veins are enriched in Cu, Au, Bi, Ag and W (Fig. 7G; appendix 1). The gold content in the samples from the mineralized veins is up to 10ppm, but no gold grains have been observed in the microscopic studies and are probably refractory grains.

3.2 Gautelis area

The Gautelis area is located in the southernmost part of the RTW (Fig. 1). The metasediments rocks comprise metagreywacke, sedimentary breccia/conglomerate and dolomitic marble which are truncated by sub-parallel bodies of sub-volcanic metadolerite, as well as coarse- and fine-grained granites (e.g. Korneliussen & Sawyer, 1986) (Figs. 1 and 9). The metasupracrustal rocks are deposited on a tonalitic basement dated to 1940 Ma (Romer et al. 1992). Korneliussen & Sawyer (1989) and Korneliussen et al. (1986) have previously described this granite/tonalite as part of the Gautelis Tonalite Complex. The supracrustals have been intruded by metadolerite and granites (Korneliussen & Sawyer, 1986). The basal metasedimentary breccias and conglomerates comprise the lowermost unit. The rock fines upwards from coarse grained breccias with fragments of the underlying tonalite to metaconglomerates and metasandstones. The basal succession is about 5-8m thick and varies laterally. Locally the basal breccia/conglomerate is missing, and metasandstone, green bedded metatuffite or marble lie directly on top of the tonalitic complex. The basal marble is locally strongly deformed with thinning and thickening and occurs especially in areas with detachment folds. It may indicate the existence of a former thin continuous marble unit that has thinned out caused by a detachment horizon at the base. The metabreccia/conglomerate/sandstone sequence is overlain by another marble succession (Fig. 9) that varies from a few cm to several 100m thick. The marble is strongly deformed with formation of tight, isoclinal folds which lead to increased thickness of the unit. In areas with low deformation, and primary bedding have been preserved, the marble is about 2-3m thick. Korneliussen et al. (1986) describes two different types of marble from this area. The stratigraphically lower member comprises impure, brownish dolomitic marble that is overlain by an upper member of pure white calcitic marble (Korneliussen et al., 1986). The dolomitic marble contains widespread bands and veins of pale green tremolite which decrease in abundance as moving upwards through the stratigraphy. Metagreywacke comprises the uppermost unit in the metasedimentary belt and consists of an upwards fining metaturbidite sequence with bedding in 2-20 cm scale (Korneliussen & Sawyer, 1986; Korneliussen et al., 1986; Sawyer & Korneliussen, 1989). The metagreywacke sequence at Gautelis is very similar in composition to that occurring further north at Haugfjellet and the sediments are assumed to be derived from the mafic to intermediate metavolcanites rocks occurring in the Ruvsott and Sjangeli area of the RTW (Korneliussen et al., 1986; Sawyer & Korneliussen, 1989).

The metasedimentary sequence and its tonalitic basement are intruded by granites and gabbroic dolerite. The granites comprise two major bodies of coarse-grained S-type Rombak granites (Korneliussen et al., 1986). The granite along the eastern margin of the tonalites (Fig. 9) has been dated to 1769 Ma (Romer et al., 1992). The porphyritic, high-K granite dominating the area to the north (Fig. 9) of the tonalite and the supracrustal rocks, is medium- to coarse-grained (Korneliussen et al., 1986). This granite, which cuts across the supracrustal belt and the ductile shear zones, yields U-Pb isotope ages in the range 1.786-1.790 Ga (Larsen et al., 2010; Larsen et al., 2013). This slightly older granite can be followed from the main body developing into dykes parallel to the shear zones, i.e. comparable to observations at Haugfjellet (Fig. 2 and 10). These dykes are a few cm to several meters thick and are partly affected by shear deformation. The major granite massif, crosscutting the ductile shear zone in the northern part of Gautelis, appears very little deformed with only weak foliation. The gabbroic intrusions are dominated by coarse-grained metadolerites intruding the supracrustals parallel to the ductile shear zones. They are 0.2-1m thick and 2-50m long, sub vertical dykes which intersect the tonalite, supracrustals and also the younger coarse-grained granite in the east part of the area. However, in some localities the metadolerites are also intruded by the same coarse grained Rombak granite, which makes the granite, shear zones and metadolerite to be more or less of the same age. The conflicting contact relationships between the granite and metadolerites is possibly caused by the presence of several generations of dykes as suggested by Korneliussen et al. (1986).

The approximately 4 km wide belt of individual shear zones cutting the tonalite complex and the overlying supracrustal rocks developed during several tectonic events giving rise to shear zones with different shear senses and strain regimes in the wall rocks. Thus the general NE-SW trending foliation and bedding of the wall rocks is on a local scale variably orientated and the foliation in the rocks is somewhat dependent on lithology. The micaceous metagreywacke is commonly penetratively foliated, and the marble is highly internal deformed with development of flow-banding with associated multi-directional plunging folds. The strongest deformation is found associated with the mylonite zone along the eastern part of the Gautelis supracrustal belt (Fig. 9) where the zone is approximately 800m wide and comprising a mélange of variably mylonitised sedimentary and intrusive rocks (Fig. 10). A characteristic feature for all the lithologies is that they form elongated lens shaped bodies bordered by high strain zones (Figs. 9 and 10).

The Gautelis area comprises two different structural styles, which include one with remnants of an early fold-thrust belt and another characterised by several oblique-slip ductile shear zones segmenting the fold-thrust belt (Fig.9; Larsen et al., 2013). The rocks of the fold-thrust domain are affected by upright folds with low angle thrust structures. The folds are usual open SE verging and plunging at a low angle towards the NNE and SSW. These folds can be found at several levels in the stratigraphy from the basal conglomerate resting on lower marble detachment horizon on top of the tonalitic basement, and to higher levels where the upper marble and metagreywacke sequences show bedding repetitions in conjunction with folds above low angle thrusts. The SSE-striking thrusts are parallel to the hanging wall beds which show moderate dips towards the NW. These fold-and-thrust belts are typically found in areas of weak deformation and are bound by steep oblique-slip ductile shear zones (Priesemann, 1984b; Larsen, 2010). The oblique-slip shear zones are cutting and segmenting the sedimentary beds and are therefore good indicators of displacement and movement directions. The main foliation developed during the ductile oblique-slip shearing is N-S to NE-SW (Fig. 9) and forms an anastomosing pattern with zones of higher and lower strain including the supracrustals and the mylonite zone. The high strain zones comprise lens-shaped rocks of metagreywacke, conglomerate, marble and igneous dykes separated by mylonites. The rocks in the low strain zones still retain their original sedimentary structures and textures (Larsen et al., 2013). The oblique-slip shear sense is mainly reverse dextral, but in some outcrops both reverse sinistral and dextral shear sense can be observed (Larsen et al., 2010). The orientation of the oblique-slip shear zones can be separated into N-S striking (D_3), moderate to sub vertical, equal sinistral, and dextral shear zones, dipping towards the west and are found most frequently within the tonalite complex, or NE-SW striking (D_4), steep to sub vertical, predominantly dextral shear zones. The latter type of shear zones are the dominating regional structures in Fig. 1 and are oriented parallel to the main foliation of the area, especially along the major mylonite zone (Larsen et al., 2010). They are also closely related to the dolerite that follows the shear zones and to the sulphide mineralisation mainly observed in the localities of this set. The shear zone lineation is similarly orientated in both directions of shear zones where the lineation plunges moderately to steeply NNW to NW in a reverse oblique slip manner. Within the mylonite zones, the folds comprise tight to isoclinal asymmetric drag folds with hinge thickening and limb thinning and multidirectional plunge. In the low-strain domains of the shear belt, the folds are open to tight similar folds with slight limb thinning and steep plunge. The belt of oblique-slip shear zones extends into Sweden in the south, whereas to the north they are abruptly cut by the coarse-grained granite with the exception of the eastern mylonite zone which appears to continue northeastwards along the eastern margin of the northern granite towards the Swedish border (Fig.2; Skonseng 1985; Larsen et al., 2010).

Two main types of sulphide mineralisations are found within the two sets of structures and are either hosted or related to the steep oblique-slip shear zones (D_3-D_4): 1) Shear zone hosted Au-As mineralisation and 2) Metasomatic As-Au-Fe mineralisation.

3.2.1 Shear zone-hosted Au-As mineralisation

Numerous up to 2 meter wide and hundreds of meters long rusty sulphidic bands occur along a number of the individual high strain zones among the large anastomosing system of shear zones (D_3-D_4) in the Gautelis belt. These rust bands are strongly developed in the greywacke, but similar bands can also be found in the marble and the granite dykes (Fig. 11A). The rusty bands commonly represent mylonite zones, characterised as D_3-D_4 by Angvik et al. (included manuscript I), in the greywacke or occasionally in the granite lenses. The sulphides are especially enriched in areas where dilation has occurred within the individual shear zones (Fig. 11B). For example in zones where the shear zones bifurcate in duplex structures (Fig. 9A) and along shear bands following the boundary of two lithologies like metagreywacke/metadolerite or metagreywacke/granite. The mylonite bands in the metagreywacke follow the finer grained silty beds when the orientation of the bedding is parallel to the shear zone, these beds tend to be enriched in sulphides. The mineralisation occurs mainly as semi massive thin (0.2-1cm) bands and lenses, or dissemination along wider deformation bands (10-20cm)

One of these rusty bands found in the middle of the metagreywacke sequence (Fig. 9A) was chosen for detailed investigations of mineralisation. An approximately one meter thick dextral oblique-slip shear zone, characterised as D_3-D_4 by Angvik et al. (included manuscript I), striking NE-SW can be followed for hundreds of meter with several bifurcations of other shear zones along strike. It follows the contacts around a 4 meters wide and 60 meters long metadolerite. The sulphide-bearing metagreywacke is strongly ductily deformed with a pronounced micaceous foliation (Fig 11B and C). It is composed dominantly of quartz forming a very fine-grained matrix (1-20µm) together with subordinate plagioclase, epidote and biotite. The D_3-D_4 shear foliation is defined by epidote stringers and parallel orientated aggregates and crystals (1-60µm) of chlorite, biotite and/or muscovite which locally fill pressure shadows (Fig. 11 C). The sulphides which occur disseminated in the fine-grained matrix comprise arsenopyrite and chalcopyrite, as well as minor pyrrhotite, sphalerite and accessory galena and native gold. The arsenopyrite occurs as cataclastic crystals intergrown with chlorite and epidote. It contains abundant micro-fractures filled with chalcopyrite and/or quartz as well as occasional micrometer-sized grains of galena and native gold (Fig. 11 D and E). Some of the cataclastic arsenopyrite grains appear as rotated sigmaclasts with pressure shadows filled with biotite and chlorite. The orientation of these indicate both sinistral and dextral shear senses on micro-scale with chlorite and biotite aligned along the shear band (Fig. 11C).

Eight samples were collected for chemical analyses across the rusty sulphide-bearing shear zones in the metagreywacke. They were taken from lithologies showing different degrees of strain, i.e. from fine-grained weakly strained medium-grained metagreywackes to fine-grained highly strained greywacke and dark mylonitic grey schists. The normalised metal distribution shows that the high-strain zones contain more sulphides and metals than the zones of lower strain (Fig. 11G). The shear zone is mainly enriched in Au, As, Bi, Sb, Cu and Pb (± Se, Te, Co, Ag, Cd and Zn) compared to a sample of the weakly deformed, layered and unmineralised greywacke.

The metamorphic grade in the shear zones and around the metasomatic deposit is interpreted to be of greenschist facies based on the mineral assemblages associated with the D_3-D_4 metadolerite: chlorite- actinolite (Fig.14G), Metagreywacke: quartz- K-felspar-albite-chlorite, chloritized biotite-muscovite-scapolite (14C) Marble: calcite- tremolite- quartz- muscovite (Fig 14B)

3.2.2 Metasomatic As-Au-Fe deposit

In the early 1900'es, the Gautelis As-Au-Fe deposit was subject to test mining for gold and arsenic (Foslie, 1917; Blomlie, 2011). Since then, a series of companies have explored the area for gold and base metals (e.g. Pedersen, 1984; Flood, 1985; Tollefsrud, 1986). The mine appears today as a several meter deep water-filled inclined adit measuring 1.5m x 2.0m horizontally (Fig 12).

The mined ore zone occurs at the segmented, and strongly sheared and folded contact zone between the upper calcitic marble, a sub-vertical metadolerite and overlying layered metagreywacke. The metasedimentary units are less affected by the shear deformation away from the metadolerite. The mineralisation is mainly hosted by the high-strain zones in the metagreywacke and some in the marble. A mélange at the transition from greywacke to marble consist of the metagreywacke enclosing tectonic lenses of the marble (mix zone in Fig. 12A and 13A). The foliation is parallel to the NE-SW trending shear zone and is sub vertically dipping towards the west. A sub vertical metadolerite dyke has intruded along the mix zone parallel to the marble contact and represents one of several dykes that are parallel to the main NE-SW shear foliation in the Gautelis belt (Larsen et al., 2013). The dyke at the mine is approximately 15m long and 1.5m thick, is more competent and show little deformation. The metadolerite shows a typical magmatic texture and the contact to the surrounding rocks are sharp and strongly sheared. It is composed of plagioclase and actinolite, as well as aggregates of quartz, sericite and epidote related to retrogression (Fig. 14G).

The main ore zone occurs in the metagreywacke close to the metadolerite dyke (Zone 2 and 3; Fig. 12A and 13). It is recognised by its supergene alteration giving rusty to dark bluish surface coatings (Fig. 12A). The rusty colour is very extensive in this area and can be followed for tens of meters northwards and several meters east as a thick lens shaped body parallel to the shear zone, and are bounded by the marble in the south. The sulphide mineralisation is composed of pyrrhotite, sphalerite, arsenopyrite, chalcopyrite, pyrite and locally magnetite which occur as dissemination to massive zones. Eight zones have been identified with different proportions and types of gangue minerals, sulphides and magnetite (Fig. 12, 13, 14 and 15). The main sulphide zones are found in metagreywacke and the mixed zones on each side and close to the metadolerite dyke (Fig. 13A). Zone 1 of the mineralisation comprises scattered grains of pyrrhotite occurring in penetratively foliated metagreywacke in the eastern periphery of the mine area (Fig. 12, 13 and 14A). The metagreywacke is medium- to fine-grained and is composed of quartz, feldspar, muscovite, biotite and variably chloritised biotite. The minerals comprise bands with granoblastic texture (Fig. 14A) separated by foliation planes defined by aggregates of chlorite and mica. The quartz frequently forms micro-veinlets parallel to the foliation. Fine-grained pyrrhotite, chalcopyrite and arsenopyrite occur as disseminated grains and aggregates constituting about 5 volume % of the rock. The sulphide content increases in Zone 2 (up to 40 volume %) (Fig. 14C and 14D). The sulphides appear as semi-massive to massive, irregular segregations of pyrrhotite which occurs intergrown with some irregular grains and segregations of chalcopyrite and disseminated arsenopyrite (Fig. 14D). These sulphides occur intergrown with tremolite, quartz, scapolite, epidote and sericite (Fig 14C). The arsenopyrite is anhedral to euhedral and intergrown with tremolite which shows that the minerals have been deposited synchronous. The epidote and sericite occur as irregular aggregates along the foliation and quartz micro-veins. Zone 3 occurs immediately adjacent to the eastern contact of the metadolerite dyke (Fig. 13A). The zone comprises disseminated to massive sulphides composed of arsenopyrite and minor irregular grains of pyrrhotite, chalcopyrite and sphalerite (Fig. 14E and F). The zone is approximately one meter thick and probably tens of meters long. The sulphides occur as bands parallel to the micaceous foliation which are intersected by quartz veins and tremolite veinlets. The arsenopyrite which occasionally occurs along quartz veins is often found as strongly fractured cataclastic crystals in the fine-grained matrix of the metagreywacke where it occurs intergrown with pyrrhotite, chalcopyrite and tremolite (Fig.14E). The three latter minerals also occur as separate aggregates containing sphalerite. Zone 4 comprises the metadolerite (Fig. 12 and 13), and the sulphide mineralisation is weak and comprises fine-grained dissemination of irregular minor pyrrhotite and accessory grains of arsenopyrite (Fig. 14G,H). Along the boundary of the dyke and the marble, clinopyroxen have been identified together with large aggregates of quartz which may indicate a higher temperature caused by the dyke. The mineralisation in Zone 5 is comparable with semi-massive ores in Zone 3 on the opposite side of the metadolerite. (Fig. 13 and 15A). The sulphides occur as semi-massive to massive irregular aggregates and bands. They consist mainly of cataclastic arsenopyrite with strongly ductily deformed pyrrhotite and chalcopyrite intergrown with tremolite, quartz, calcite, muscovite and feldspar (Fig. 15B). Chalcopyrite and gold can be found along micro-fractures in cataclastic grains of arsenopyrite (Fig. 15B). Sericite and epidote has overgrown the other minerals. Zone 6 is located in folded calcitic marble west of the strongly deformed mix zone (Fig. 12A and 13A) and are composed of disseminated to semi-massive magnetite intergrown with tremolite and calcite, as well as minor epidote (Fig. 15C). Magnetite occurs as irregular aggregates and bands that have been folded. The magnetite mineralisation coexists with scattered grains of chalcopyrite pyrite and quartz. The weak pyrrhotite chalcopyrite and arsenopyrite dissemination in Zone 7 is hosted by a weakly deformed calcite marble carrying parallel orientated stringers of sericite-epidote, tremolite- and/or quartz defining the foliation (Fig. 15E and 15F). Zone 8 represents the non-mineralised marble close to the top of the underlying weakly deformed conglomerate beds (Fig. 12). The marble is part of the lower dolomitic marble member and consists mainly of dolomite/calcite with some quartz veins and aggregates of tremolite, chlorite, muscovite and epidote along the foliation (Fig. 14B).

Similar metasomatic occurrences can be found scattered elsewhere in the Gautelis area and show typical skarn occurrences with magnetite and pyrrhotite together with garnet, diopside and epidote along contacts of marble and greywacke (Fig. 15G). In this setting no intrusion can be found in direct contact to the marble, but metadolerites occurs nearby, within <100m.

4.0 Discussion

4.1 Genesis of the sulphide deposits in RTW

Based on field work mapping and sampling we suggest that the studied mineralisations along the Rombaken-Skjomen Shear Zone (RSSZ) can be divided into 1) pre-orogenic SEDEX deposits along distinct metasedimentary beds, locally remobilised during tectonic events, 2) syn-orogenic metasomatic deposit affected by shear zones and parallel dolerites and 3) late orogenic gold deposits following the deformation zones. The RSSZ is a progressive result of a Svecofennian orogenic transpressive event incorporating Paleoproterozoic volcanic and sedimentary rocks (Larsen et al., 2013), that we strongly connect to the mineralisations with distribution and genesis.

4.1.1 Haugfjellet SEDEX deposits

The stratiform Zn-Pb and pyrite or pyrrhotite mineralisations occurring in undeformed metagreywacke in Sildvika, Jernvann and Haugfjellet areas mineralisation are interpreted to represent low-grade sedimentary exhalative type deposits (SEDEX). These deposits are believed to form by hydrothermal fluids in extensional sedimentary basins, resulting in precipitation of stratiform mineralisation. It is commonly referred to as laminated, bedding-parallel, Pb-Zn rich siltstones appearing as a series of stacked mineralised lenses interbedded with pyritic and carbonaceous siltstones. These sulphides are hosted of fine grained, organic bearing, dolomitic siliciclastic siltstones and shales, and the mineralisation is located close to major basin-scale faults acting as fluid channels (Gustafson & Williams, 1981; Solomon & Groves, 2000; Large et al., 2005). SEDEX deposits are thought to be a Paleoproterozoic worldwide event and to be caused by the global ocean chemistry at the time (Lyons et al., 2006).

SEDEX type of deposits on Haugfjellet have been mentioned by several authors (Flood, 1984; Flood 1985; Korneliussen & Sawyer, 1986; Coller, 2004) although Flood (1984, 1985) considered the Pb-Zn to be associated with the As and Au mineralisation. Coller (2004) suggested a SEDEX type deposit, however, he did not include the Pb-Zn, but the enrichment of pyrite and pyrrhotite. Because of the nature of these sulphides following distinct beds, we suggest that the SEDEX mineralisation consist of Pb-Zn and also the pyrite and pyrrhotite mineralisation which have been deposited syn-sedimentary during the opening of the basin and the transition to the island arc setting, which is in accordance to the tectonic setting of the greywackes (Sawyer et al., 1989). The Fe sulphides could represent a more distal facies to the Pb-Zn mineralisation.

A syngenetic deposition of the Pb-Zn mineralisation is supported by ore lead systematics, with a population of 206Pb/204Pb isotopes that have been found at Sildvika and Haugfjellet to have a Svecofennian signature (Larsen et al., 2013). They found local changes with less and less radiogenic lead from west (Sildvika) to east (Haugfjellet), suggesting that the galena either have deposited in a further distance from the mantle source, caused by the progressive change from mantle derived (mafic) magmatism to more continental derived (felsic) magmatism. Similarly may also different stratigraphic levels explain the change where the more radiogenic values are higher in the stratigraphy when the island arc (mafic and radiogenic) has developed into a more continental system (felsic and less radiogenic). They further showed how the values from RTW was similar to the Proterozoic Pb/Pb signatures values from Tjåmotis-Skuppe area, and that they fit on a line and show the relative distance (either by stratigraphy or tectonic progression). This tectonic model is supported by the study of Korneliussen & Sawyer (1989) and Sawyer & Korneliussen (1989), which suggested a similar development. Similarly did Larsen et al., (2013) present a structural based tectonic model which confirm the structural development of the sedimentary layers and that the sedimentation is of Paleoproterozoic age.

We suggest that these deposits have been overridden by fold-thrust belts and steep ductile shear zones which have caused remobilisation of the Fe and Pb-Zn mineralisations as discussed in section 4.1.3.

4.1.2 Gautelis metasomatic deposit

In this study there was recognised several metasomatic deposits in the Gautelis area with a zonation, where one was studied in detail. Metasomatic deposits have been described from numerous authors (e.g. Einaudi et al., 1981; Burt, 1982), and are referred to as either contact or regional metamorphic processes with calc-silicate minerals metasomatic replacing of carbonate rocks (Robb, 2005). In addition, the zonation replacement pattern are typical for skarns (e.g. Einaudi & Bart, 1982).

Eight different zones were identified (Fig. 12, 13) and the ore in the Gautelis mine is interpreted to be an As-Au metasomatic deposit related to the sub-vertical metadolerite crosscutting the folded marble and greywacke. The deposit show complexities because of the syn-genetic relationship between the metadolerite and the late orogen sub-vertical shear zones. The metadolerite has intruded parallel to the weakness zones. It has therefore been interpreted to be syn- or late tectonic with strong relation to these shear zones, with a weakly overprinting by late shear zones that may have caused remobilisation of minerals. This metasomatic deposit probably has formed by fluids transported in the shear zone.

Similar minor skarn occurrences in the Gautelis area have been described by Korneliussen et al. (1986) as irregular, fine grained aggregates or lenses/boudins occurring up to a few meters wide with chalk silicates with sulphides and magnetite. The lenses show a small zoning with a rim of diopside/tremolite and a core of grossular and epidote and the skarn occurrences are strongly deformed and folded which is consistent with the present study (op cit.). Similar observations have also been done by other authors, but interpreted the genesis differently. Bugge & Foslie (1922) characterised the deposit as a vein-type, formed by metasomatic processes. They describe the mineralisation as a metasomathic deposit between hornblende schist (here described as metadolerite) and the marble. Arsenopyrite occurs in quartz veins together with biotite and pyroxene, and pyrrhotite and chalcopyrite are locally/occasionally observed in the marble (op cit.). They also describe the deposit to be thickened and folded, but do not direct link the deposit to the structures. Priesemann (1984b) interpreted the mineralisation to be related to a volcanic explosive hydrothermal vent because of the brecciation of the arsenopyrite and the boudinaged and laminated bands. Boudinage structures are common in ductile deformation (e.g. Davis & Reynolds; 1996) and we have therefore interpreted the deposits to be related to the shear zone development.

Skyseth & Reitan (1995) showed in their study of fluid inclusions that the deposit is derived from high saline fluids and suggested that the fluids got trapped along the barrier between low and high competency rocks. They interpreted the structures to be of Caledonian age, while Larsen et al. (2013) have demonstrated that the structures are Paleoproterozoic. The high saline fluids may have its source from the syn tectonic Rombak granite (Larsen et al., 2013) The role of the metadolerite is not fully understood and may have co-acted as a local heating or fluid source when crosscutting the marble changing the pH and releasing fluids.

Because the syn orogenic metadolerite in the Gautelis deposits are closely related to the sulphides, it is therefore reasonable to believe that the metadolerite may have had an important role in the process. Metasomatic deposits associated with metadolerites are not as well understood as connected to felsic intrusions. However, similar metasomatic deposits to Gautelis have been described. A gold skarn deposit from British Columbia (Dawson, 1981) is associated with metadolerites and show several stages of overprinting deformation and that they acted as fluid conduits. Spooner (1993) showed how metadolerite intrusives in Archean terrain could be a gold-skarn target caused by their high volatile content before sulphide loss.

The formation of the metasomatic Gautelis deposits is assumed to be associated to the intrusion of dolerite along regional shear zones, with contemporaneous granites as probable fluid source. The combination of a dolerite heat source, a regional shear zone structure and a possible change in pH when crosscutting the marble, are contributing to this type of metasomatic deposit.

4.1.3 Rombaken-Skjomen orogen deposits

Several classifications of orogenic gold deposits exist (e.g. Groves et al.,1998; McCuaig and Kerrich 1998). Groves et al.(1998) suggested a classification scheme including late Archean to Phanerozoic rocks on a deformed continental margin with structural highs in late stage of deformation, mafic volcanics, intrusive or greywacke rocks mainly in greenschist facies metamorphism, associated with intrusions of felsic to lamprophyre dykes or continental batholits, variable and late tectonic mineralisation style with structurally complexity, strong overprinting in larger deposits, Au-Ag ± As ± B ± Bi ± Sb ± Te ± W metal association, cryptic lateral and vertical zoning, low salinity with P: 0.5–4.5 kbars and T: 220º–600ºC, metal sources are thought to be from subducted crust, supracrustal rocks or granitoids and heat source from granitoids. Based on these parameters compared to the geological evolution of the RTW, we propose an orogenic gold ore-genesis for deposits occurring within the RSSZ. The Paleoproterozoic age range (Larsen et al., 2013), the Andean type accretion tectonic setting with greywacke and marble as the host rock (Sawyer & Korneliussen, 1989) and the steep anastomosing transpressional structural setting with a syn orogenic granite intrusion as the heat source (Larsen et al., 2010) of the RTW, all correspond to what Groves et al. (1998) suggested.

The metamorphic grade in the host rock has earlier been discussed from the RTW (Korneliussen et al., 1986; Sawyer, 1986; Skyseth & Reitan, 1995). We have shown that the rocks within the shear zone are of greenschist facies. The main metamorphism in the RTW is thought to be amphibolite facies (Sawyer, 1986), but Korneliussen et al. (1986) also found that the N-S going shear zones (D_3) in Norddalen (Fig. 2) show evidence of retrogradation from amphibolite facies to greenschist facies metamorphism. He explained this change to be caused by fluids transported along the Paleoproterozoic shear zones. Similarly, Skyseth & Reitan (1995) documented a retrogradation to greenschist facies metamorphism in the Gautelis area. However, they linked the metamorphism and gold deposition to the Caledonian orogeny. We suggest that this retrogressive of the metamorphic event is linked to the Paleoproterozoic development of the regional shear zone (D_3-D_4) running from Gautelis, through Norddalen and Sjangeli, and covered by the Caledonian nappes to the east (Larsen et al., 2013). The N-S trending shear zone at Haugfjellet shows a similar retrogression where the chlorite is present within the quartz veins occurring as a late event of deformation.

The mineralisation styles for orogenic gold deposits may occur in a large variety (Groves et al., 2003). However, strong overprinting and veining are typical for orogenic gold. In the RTW are the structural overprint of earlier-formed deposits are extensive, where shear zones cut through SEDEX deposits and metasomatic deposits that can be seen with sericite overprinting other mineral assemblages and deposit together with As and Au in particular. In addition, the quartz veins are thought to be a late stage of the orogen (D_3-D_4) as they cut the fold structures and shear zones, but are slightly sheared themselves (Larsen et al., 2013). Similarly, Coller (2004) suggested that the gold values were related to the quartz-veins and silica alteration in the Haugfjellet area and that the shear zone were responsible for transporting the silica. The Au, Cu, Bi, Ag, Pb mineralisations are therefore believed to be the latest stage of sulphide mineralisation in the orogenic deposits.

Orogenic gold deposits are believed to be characterised by low saline fluid (Groves et al.. 1998; 2000; 2003). However, in a fluid inclusion study carried out by Skyseth & Reitan (1995) nearby the metasomatic As-Au deposits at the Gautelis mine, they found that the mineralising fluids where highly saline. High saline fluids have been reported from several gold provinces classified as orogenic gold (e.g. Tyler & Tyler, 1996; Khin et al., 1994; Rowins et al., 1997; Eilu et al, 2007). The high saline fluids can be explained with rocks developing in a basinal setting, the pore water may stay within the original rock until melting occurs (Yardley, 1997). However, the fluid inclusion study does not show if the fluids are connected directly to the metasomatic deposit or to the shear zones (D_3-D_4).

The suggested ore-genesis of orogenic gold, defined by Groves et al. (1998; 2000; 2003). is supported by work of Larsen et al., (2013) that related RTW and the gold line in central Sweden, to the north coast of Norway. The RSSZ is linked to major Paleoproterozoic shear zone systems across the whole of the Fennoscandian shield (Bergh et al., 2013; Larsen et al., 2013). This large system is known for its gold deposits in Northern Norway, Finland and Sweden (e.g. Eilu & Weihed, 2005) which now can be extended underneath the Caledonian nappe complex to include the RTW, (Larsen et al., 2013).

4.2 Timing and spatial relationship of the sulphide deposits along the RSSZ

Several stages of sulphide mineralisation have been found and can be either pre-dated or structurally linked to the RSSZ. In this paper we are able to put the investigated mineralisation into four stages of mineralisation (Fig. 16); 1) pre-orogen SEDEX deposits (D_0), 2) syn-orogenic metasomatic deposit, 3) Syn-orogenic shear zone overprinting metasomatic deposit and with a signatures of orogen- type Au-As deposits (D_3-D_4) and 4) late, syn-orogenic quartz veins (D_3-D_4).

It is well known from the Fennoscandian shield that in the early Paleoproterozoic, the continent was characterised by extension, breakup and basin development (e.g. Gorbatschev & Bogdanova, 1993; Nironen, 1997). In the RTW, the basin gradually changed into an Andean type setting (Korneliussen & Sawyer, 1989) with development of the Sjangeli island arc (Romer et al., 1992). Greywacke sediment infill continued in the RTW (Sawyer & Korneliussen, 1989) before closure, accretion and intrusion of granite plutons.

We have identified SEDEX occurrences in the lower deformation zones and within the same rocks that Sawyer & Korneliussen (1989) suggested to be turbiditic greywacke sequences deposited in an Andean-type setting which again put the SEDEX deposit in a setting developing from an extensional basin regime into an island arc system (Fig. 16). The SEDEX deposits are mainly found along beds with low deformation and are remobilised in areas of high deformation. Cu-Fe sulphides from island arc rocks in Sjangeli are similarly found to be stratabound and syngenetic with the deposition of the tuffs (Romer, 1989).

The metasomatic deposits in Gautelis are interpreted to have developed within a shear zone (D_3-D_4) in association with metadolerites. Metadolerites in an accretionary regime are thought to develop from an early stage of subduction where the magma is derived from the mantle and have not been contaminated by melting of the continental crust (e.g. Hall & Hughes, 1993). This is also according to Korneliussen & Sawyer (1989) which interpreted the igneous rocks in RTW as a continuous change from ultramafic/mafic to felsic magma series through the Paleoproterozoic. Because of the metadolerite dykes that crosscut the already folded strata and stratigraphy, and that they have intruded along steep dipping weakness zones or shear zones. We suggest an early D_3-D_4 syn-orogenic metasomatic development is found where marbles, large ductile oblique-slip shear zones and dolerite s are present (Fig. 16).

Larsen et al. (2013) presented a model of two folding (D_1-D_2) and two oblique-slip syn-orogenic (D_3-D_4) events; one sinistral (D_3) overprinted by a dextral event (D_4). They furthermore suggested that all four events were a result from progressive syn-orogenic transpressive strain partitioning. The interpreted orogenic gold is found in deformation zones either within ductile oblique-slip deformation zones or with brittle-ductile fractures (D_3-D_4), both within the shear zone. The orogenic gold found within the shear zone is only found within the steep ductile oblique-slip shear zones and not in the fold-thrust belt (D_1-D_2). The brittle ductile fractures (D_3-

D_4) cuts these shear zones and represent the last event of gold formation. The D_1-D_4 shear zones in RTW are believed to be part of a large regional scale tectonic event (e.g. Nironen, 1997; Larsen et al., 2013) and are interpreted to be directly linked to Sjangeli, Kopparåsen, Tjåmotis, the Bothnian basin and the southern part Skellefte district in Sweden (Fig. 16) and to the western Precambrian provinces in North Norway (Larsen et al., 2013). For example are Cu-U mineralisations found along large deformation zones at Kopperåsen, dated to 1.780 Ma (Adamek, 1975; Romer, 1988). Orogenic gold is actively mined from the gold line, in similar aged and type of greywacke rocks, in the southern part of the Skellefte district (Bark & Weihed, 2007). Svecofennian shear zones described from Finland and Russia have shown to be carriers of large amounts of orogenic gold (e.g. Sundblad & Ihlen, 1995; Sundblad, 2003; Goldfarb et al., 2001; Ojala, 2007).We hereby suggest that the RTW is part of this large regional juvenile event during the Svecofennian orogeny and orogenic gold is likely to be found along the late stage shear zone structures (D_3-D_4) as found in quartz veins, microstructures and weakness zones.

5.0 Conclusions

- Three genetic types of principally sulphide mineralisations have been identified within the rocks and structures of Rombaken Tectonic Window; 1) Syn-sedimentary Pb-Zn and Fe-sulphide SEDEX deposit (D_0), 2) Syn-orogenic intrusion related metasomatic As-Au-Cu deposit (D_3-D_4) and 3) Orogenic gold deposits with Au-As enrichments along shear zones (D_3-D_4) and 4) late orogenic Cu-Au quartz veins (D_3-D_4).

- The SEDEX deposits vary between pyrite, pyrrhotite and galena-sphalerite dominated layers within the greywacke sequence.

- The metasomatic Au-As-Cu deposit is related to metadolerites crosscutting the folded beds of marble and greywacke. The metadolerites are probably an important heat source. They are also syn-orogenic and might be a source for fluids, and together with the shear zones that may have acted as carriers of the fluids.

- The orogenic gold deposits are related to regional structures, continuing into Northern Norway, Finland and Sweden, that indicate mineral potential in large areas. The RSSZ crosscuts several of the pre orogenic localised zones of sulphide deposits which makes the orogen deposits differ slightly from the definition by Groves et al., (1998) with atypical mineralisation caused by remobilisation.

- We propose a regional model developing through time (D_0-D_4) which incorporates several mineralisation events. They are developing from a syngenetic stage of sediment deposition and basin development (D_0), to volcanic rocks and deposits related to an active margin turning into a stage of orogeny (D_1-D_2) and all deposits are accreted into the large regional scale orogeny (D_3-D_4)

- The spatial relationship between the sulphide deposits and the large structures are closely related. The SEDEX are syngenetic (D_0) found along undeformed greywacke beds in low deformation zones, but also redistributed along ductile shear zones D_3-D_4. The metasomatic deposits are found in locations where metadolerites, marbles and steep ductile shear zones exist (D_3-D_4). The orogenic gold and their related sulphides are found in dilatational structures and weakness zones along the large scale shear zones including quartz veins and steep ductile oblique-slip structures (D_3-D_4).

References

Adamek, P. M. (1975). Geology and Mineralogy of the Kopparåsen Uraninite-sulphide Mineralisation: Norrbotten County, Sweden. Avhandlingar och uppsatser - Sveriges Geologiska Undersökning ; serie C 712.

Bargel, T. H., Bergstrøm, B., Boyd, R. and Karlsen, T. A. (1995). Geologisk kart, Narvik kommune M 1:100.000. Norges geologiske undersøkelse.

Bark, G. and Weihed, P. (2007). Orogenic gold in the Lycksele - Storuman ore province, northern Sweden; the Paleoproterozoic Fäboliden deposits. Ore Geology Reviews 32: 431-451.

Bergh, S. G., Kullerud, K., Myhre, P. I., Corfu, F., Armitage, P. E. B. and Zwaan, K. B. (2014). Archean Elements of the Basement Outliers West of the Scandinavian Caledonides in Northern Norway: Architecture, Evolution and Possible Correlation with Fennoscandia. Springer 2014 7: 103 - 126.

Blomlie, T. (2011). Skatter i fjell - På tur i bergverkshistorien til Ballangen, Evenes, Narvik og Tysfjord. Museum Nord.

Bugge, C. and Foslie, S. (1922). Norsk Arsenmalm og arsenikfremstilling. NGU Tidsskrift 106.

Burt, D. M. (1982). Skarn Deposits - Historical Bibliography through 1970. Economic Geology 77: 755-763.

Coller, D. (2004). Varden Ridge Target Generation Report. Golden Chalice Resources Inc report GT 04-18D-01.

Davis, G. H. and Reynolds, S. J. (1996). Structural Geology og rocks and regions. John Wiley & sons, inc second edition.

Dawson, G. L. (1981). Geological setting of the Hedley gold skarn camp with spesific reference to the french mine, south-censtral British Columbia. M.Sc. thesis, Department of geological Sciences, The University of British Columbia.

Eilu, P., Pankka, H., Keinänen, V., Kortelainen, V., Niiranen, T. and Pulkkinen, E. (2007). Characteristics of gold mineralisation in the greenstone belts of northern Finland. Geological Survey of Finland, Special Paper 44: 57−106.

Eilu, P., Sorjonen-Ward, P., Nurmi, P. and Niiranen, T. (2003). A Review of Gold Mineralisation Styles in Finland. Economic Geology 98(7): 1329-1353

Einaudi, M. T. and Burt, D. M. (1982). A special issue devoted to Skarn deposits - Introduction - Terminology, Classification and Composition of Skarn Deposits. Economic Geology 77: 745-754.

Einaudi, M. T., Meinert, L. D. and Newberry, R. J. (1981). Skarn deposits. Economic Geology 75th anniversary volume: 317-391.

Flood, B. (1984). The Rombak project area, North Norway. Summary of work done 1983 and work program proposal for 1984. Arco Norway Inc, Hard Mineral section 84-670-19.

Flood, B. (1985). The Rombaken Gold-basemetal project, Northern Norway. A participation offer. Arco Norway. Bergvesenet rapport BV 4185.

Foslie, S. (1916). Avskrift av statsgeolog Steinar Foslies dagboksopptegnelse angående Sjangeli 1916. NGU Ba-rapport 3336: 19 s.

Goldfarb, R. J., Groves, D. I. and Gardoll, S. (2001). Orogenic gold and geologic time: a global synthesis. Ore Geology Reviews 18: 1–75.

Gorbatschev, R. (2004). The Transscandinavian Igneous Belt – introduction and background. In: Högdahl, K., Andersson, U. B., and Eklund, O., 2004. Geological Survey of Finland, Special Paper 37.

Gorbatschev, R. and Bogdanova, S. (1993). Frontiers in the Baltic. Precambrian Research 64: 3-21.

Groves, D. I., Goldfarb, R. J., Gebre-Mariam, M., Hagemann, S. G. and Robert, F. (1998). Orogenic gold deposits: a proposed classification in the context of their crustal distribution and relationship to other gold deposit types. Ore Geology Reviews 13: 7-27.

Groves, D. I., Goldfarb, R. J., Knox-Robinson, C. M., Ojala, J., Gardoll, S., Yun, G. Y. and Holyland, P. (2000). Late-kinematic timing of orogenic gold deposits and significance for compute-based exploration techniques with emphasis on the Yilgarn Block, Western Australia. Ore Geology Reviews 17: 1-38.

Groves, D. I., Goldfarb, R. J., Robert, F. and Hart, C. J. R. (2003). Gold deposits in metamorphic belts: Overview of current understanding, outstanding problems, future research, and exploration significance. Economic Geology 98: 1-29.

Gustafson, L. B. and Williams, N. (1981). Sediment-hosted stratiform deposits of copper, lead, and zinc. Economic Geology Seventy-Fifth Anniversary Volume: 139-178.

Gustavson, M., Foslie, S., Birkeland, T., Vogt, T., Bøe, P., Lund, P. R., Mitsem, T., Mortensen, A. H., Kalsbeek, F. and Olesen, N. Ø. (1974). Geologisk kart over Narvik. Norges geologiske undersøkelse.

Hall, R. P. and Hughes, D. J. (1995). Early Precambrian crustal development: changing styles of mafic magmatism. In: Le Bas, M. J. (ed.), 1995, Milestones in Geology. Geological Society, London, Memoir NO 16: 25-35.

Kerrich, R. and Fryer, B. J. (1981). The separation of rare elements from abundant base metals, in Archean lode gold deposits: Implications of low water/rock source regions. Economic Geology 76(160-165).

Khin, Z., Huston, D. L., Large, R. R., Mernagh, T. and Hoffmann, C. F. (1994). Microthermometry and geochemistry of fluid inclusions from the Tennant Creek gold-copper deposits: implications for ore deposition and exploration. Mineral Deposita 29: 288-300.

Korneliussen, A. and Sawyer, E. (1986). Berggrunns- og malmgeologi med særlig vekt på muligheter for gull, sydlige deler av Rombakvinduet, Nordland. NGU Ba-rapport 86.167.

Korneliussen, A. and Sawyer, E. W. (1989). The geochemistry of Lower Proterozoic mafic to felsic igneous rocks, Rombak Window, North Norway. NGU Bulletin 415: 7-21.

Korneliussen, A., Tollefsrud, J. I., Flood, B. and Sawyer, E. (1986). Precambrian volcano-sedimentary sequences and related ore deposits, with special reference to the Gautelisfjell carbonate-hosted gold deposit, Rombaken basement window, Northern Norway. NGU report 86(193): 44.

Lahtinen, R., Hallberg, A., Korsakova, M., Sandstad, J. S. and Eilu, P. (2012). Main Metallogenic events in Fennoscandia: Summary. In: Eilu, P. (ed.), Mineral deposits and metallogeny of Fennoscandia. Geological Survey of Finland Special Paper 53.

Large, R. S., Bull, S. W., McGoldrick, P. J. and Walters, S. (2005). Stratiform and strata-bound Zn-Pb-Ag Deposits in Proterozoic Sedimentary basins, Northern Australia. Economic Geology 100th Anniversary Volume: 931-963.

Larsen, T., Bergh, S. G., Henderson, I., Korneliussen, A. and Kullerud, K. (2010). Svecofennian structural development and metallogenesis of Paleoproterozoic volcano-sedimentary rocks of Rombak Tectonic widow. NGF abstract proceedings of the Geological Society of Norway 1, 2010, 29th Nordic Geological winter meeting, Oslo.

Larsen, T., Sundblad, K., Henderson, I., Bergh, S. G., Bagas, L., Sandstad, J. S., Andersen, T. and Simonsen, S. (2013). Recognition of Svecofennian sulphide bearing crust in the Rombak region, northern Norway. NGF abstract proceedings of the Geological Society of Norway 1, 2013, 32nd Nordic Geological winter meeting, Oslo.

Lyons, T. W., Gellatly, A. M., McGoldrick, P. J. and Kah, L. C. (2006). Proterozoic sedimentary exhalative (SEDEX) deposits and links to evolving global ocean chemistry. Geological Society of America Memoir 198: 169-184.

Martinsson, O. (2004). Geology and Metallogeny of the Northern Norrbotten Fe-Cu-Au Province. Society of economic geologists guidebook series 33: 131-148.

McCuaig, T. C. and Kerrich, R. (1998). P-T-t-deformation-fluid characteristics of lode gold deposits: evidence from alteration systematics. Ore Geology Reviews 12: 381–453.

Nironen, M. (1997). The Svecofennian Orogen: a tectonic model. Precambrian Research 86: 21-44.

Ojala, J. V. (2007). Gold in the Central Lapland Greenstone Belt. Geological Survey of Finland, Special Paper 44.

Pedersen, F. D. (1984). Report on geological field work in the Rombak-Storfjord areas in Ofoten. Norsk Hydro.

Priesemann, F. D. (1984a). Summary report - 1983, Rombak project, Foldal Verk A/S. Bergvesenet rapport 2953: 38 s.

Priesemann, F. D. (1984b). Summary report - 1984, Rombak project. Foldal Verk A/S. Bergvesenet rapport BV 2949.

Robb, L. J. (2005). Introduction to Ore-Forming Processes. Blackwell Publishing.

Romer, R. L. (1987). The geology, geochemistry and metamorphism of the Sjangeli area, a tectonic window in the Caledonides of northern Sweden. Research report Luleå University Tulea 1987:16: 124.

Romer, R. L. (1989). Implications of isotope data on the metamorphism of basic volcanites from the Sjangeli Window, northern Sweden. NGU Bulletin 415: 39–56.

Romer, R. L. (1989). Interpretation of the lead isotopic composition from sulfide mineralisations in the Proterozoic Sjangeli area, northern Sweden. NGU Bulletin 415: 57-69.

Romer, R. L. and Boundy, T. M. (1988). Interpretation of lead isotope data from the uraniferous Cu-Fe-sulphide mineralisations in the Proterozoic greenstone belt at Kopparåsen, northern Sweden. Mineral Deposita 23: 256-261.

Romer, R. L., Kjøsnes, B., Korneliussen, A., Lindahl, I., Stendal, H. and Sundvoll, B. (1992). The Archean-Proterozoic boundary beneath the Caledonides of northern Norway and Sweden: U-Pb, Rb-Sr and eNd isotope data from the Rombak-Tysfjord area. Norges geologiske undersøkelse rapport 91.225: 67.

Romer, R. L. and Wright, J. E. (1993). Lead mobilization during tectonic reactivation of the western Baltic Shield Geochimica et Cosmochimica Acta 57(11): 2555-2570

Rutland, R. W. R., Kero, L., Nilsson, G. and Stølen, L. K. (2001). Nature of a major tectonic discontinuity in the Svecofennian province of northern Sweden. Precambrian Research 112: 211–237.

Sawyer, E. (1986). Metamorphic assemblages and conditions in the Rombak basement window. Norges geologiske undersøkelse Unpublished report no. 86.168.

Sawyer, E. W. and Korneliussen, A. (1989). The geochemistry of Lower Siliciclastic turbidites from the Rombak Window: implications for palaeogeography and tectonic settings. NGU Bulletin 415: 23-38.

Skonseng, E. E. (1985). Berggrunnsgeologisk kartlegging i Gautelis området, Skjomen, Nordland. Feltrapport. NGU-rapport 85.214: 16.

Skyseth, T. and Reitan, P. (1995). Geology and genesis of Gautelisfjell gold deposit, Rombak window, Northern Norway: A link between retrograde Caledonian metamorphism and saline fluids. In: Ihlen et al., 1995 (eds.) Gold mineralisation in the Nordic countries and Greenland. Grønlands Geologiske Undersøkelse, Open File Series 95/10.

Solomon, M. and Groves, D. I. (2000). The Geology and Origin of Australia's Mineral Deposits. Centre for Ore Deposit Research and Centre for Global Metallogeny 32: 1002 pp.

Spooner, E. T. C. (1993). Magmatic sulphide/volatile interaction as a mechanism for producing chalcophile element enriched, Archean Au-quartz, epithermal Au-Ag and Au skarn hydrothermal ore fluids. Ore Geology Reviews 7(5): 359–379.

Sundblad, K., 2003. Metallogeny of gold in the Precambrian of northern Europe. Economic Geology 98, 1271-1289.

Sundblad, K. and Ihlen, P. M. (1995). Gold mineralisation in Fennoscandia: An overview. In: Ihlen, P., Pedersen and Stendal, H., (eds.). Gold mineralisation in the Nordic countries and Greenland. GEUS Open file series, extended abstracts and field trip guide 95/10.

Tollefsrud, J. I. (1986). Rombak prosjekt. Bergvesnet rapport(3152).

Tyler, R. and Tyler, N. (1996). Stratigraphic and structural controls on goldmineralisation in the Pilgrim's Rest goldfield, eastern Transvaal, South Africa. Precambrian Research 79: 141-169.

Yardley, B. W. D. (1997). The evolution of fluids through the metamorphic cycle: In: Jamtveit, B. Yardley, B.W.D. (Eds.), Fluid Flow and Transport in Rocks. Chapman & Hill, London: 99-121.

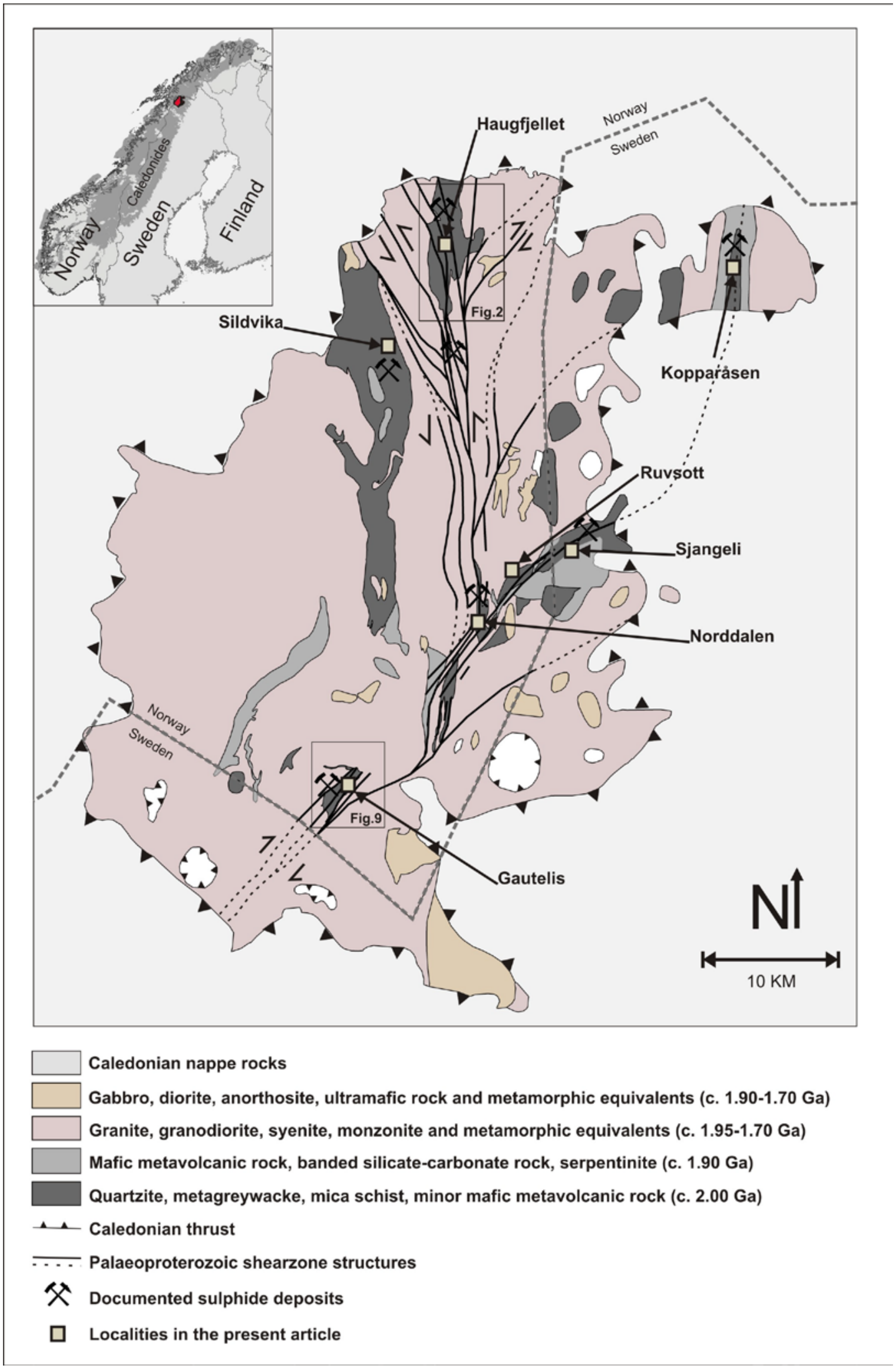

Fig. 1. Geological and structural map over the Rombaken Tectonic Window with sulphide deposits marked along the Rombaken-Skjomen Shear Zone.

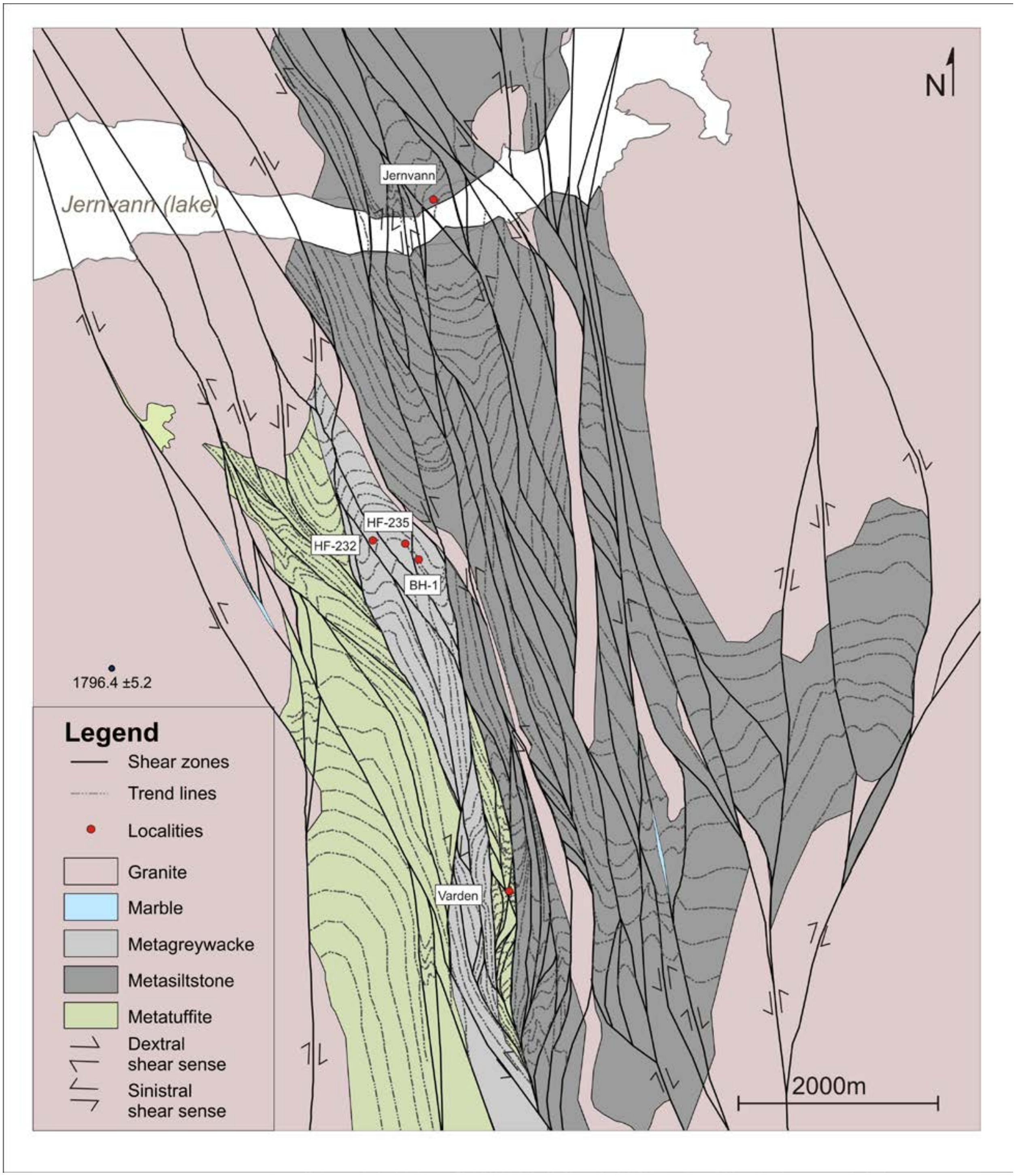

Fig. 2. Geological and structural map of the Haugfjellet area showing the localities of samples and drill hole. The marble is only found as narrow bands or lenses smeared out along the shear zones.

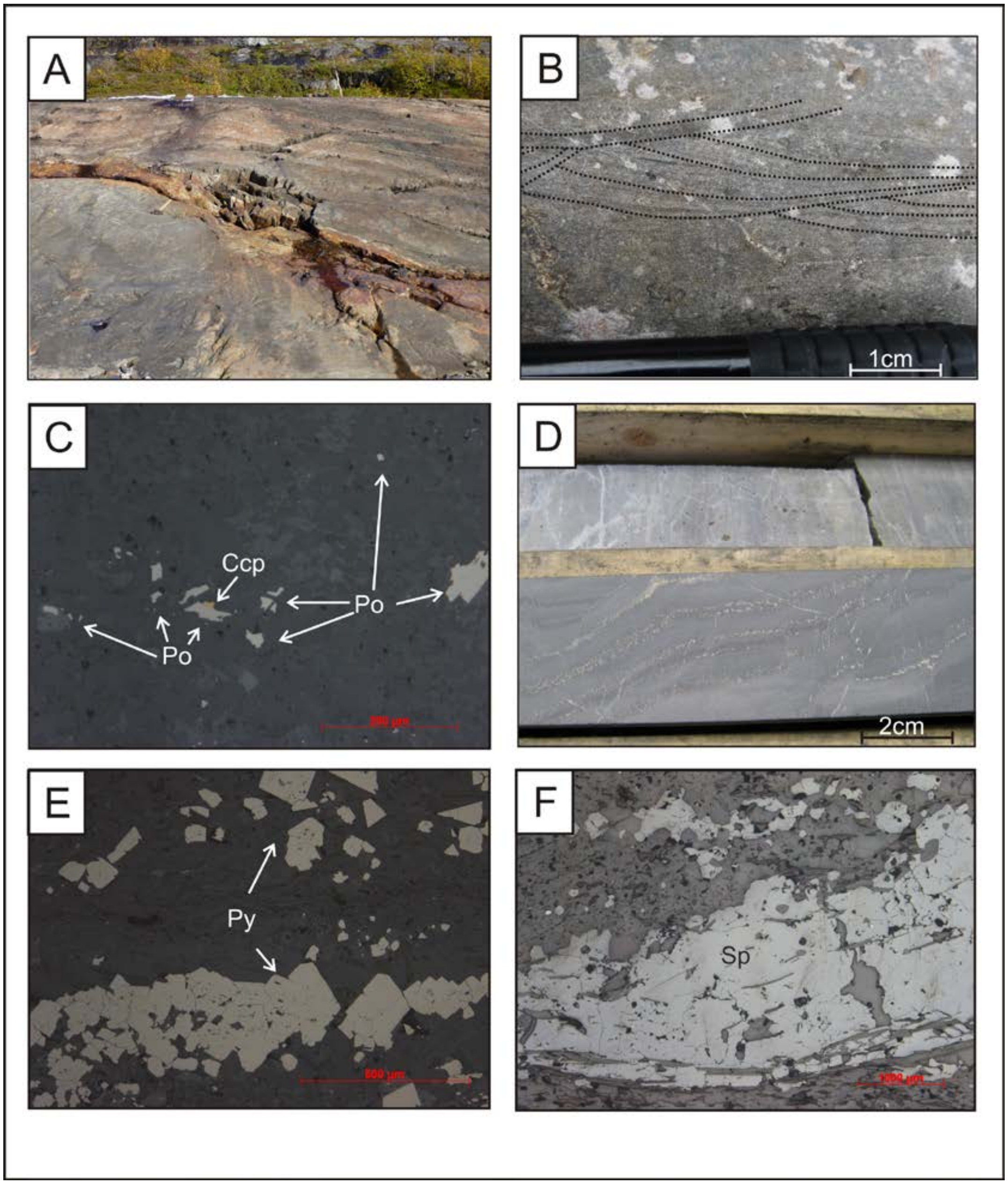

Fig. 3. Undeformed and layerparalell mineralisations at Haugfjellet and Sildvika. A) Layer parallel pyrrhotite along greywacke beds at the Jernvann locality (Fig. 2). B) Primary structures with trough cross-bedding found in the greywacke sequences at Sildvika implying very little deformation. C) Type 1: Photomicrograph of disseminated pyrrhotite accompanied by chalcopyrite (reflected light). D) Typical bedding parallel pyrite within Haugfjellet drill core (Photo: Jan Sverre Sandstad). E) Type 2: Photomicrograph of semi-massive pyrite bands in metatuffite from Haugfjellet (reflected light). F) Type 3: Photomicrograph of semi-massive sphalerite in the undeformed metagreywacke in the Sildvika locality (reflected light). Abbreviations: Po - pyrrhotite, Ccp - chalcopyrite, Sp - sphalerite

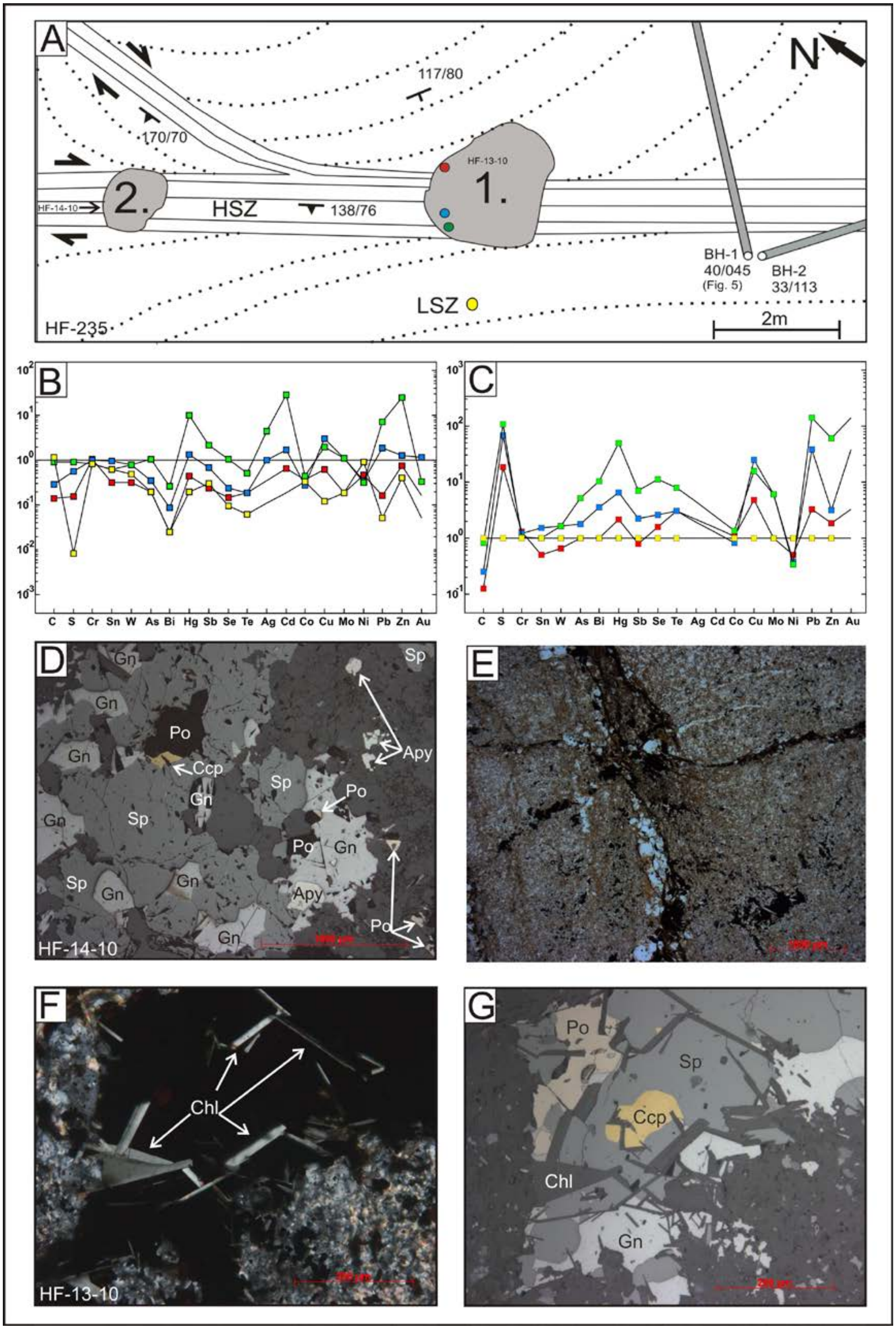
A
N
117/80
170/70
HF-13-10
1.
2.
HF-14-10
HSZ
138/76
BH-1
40/045
(Fig. 5)
BH-2
33/113
LSZ
HF-235
2m
B
C
C S Cr Sn W As Bi Hg Sb Se Te Ag Cd Co Cu Mo Ni Pb Zn Au
D
Gn
Sp
Po
Ccp
Apy
HF-14-10
E
F
Chl
HF-13-10
G
Po
Sp
Ccp
Chl
Gn

Fig. 4. A) Sketch of locality HF-235 found as an old working at Haugfjellet (Fig. 2). The old working is located along a dextral shear zone in metagreywacke and consist of two blasted holes (1 and 2) and two drill holes (Fig. 6) B) Spider plot of geochemical data of samples from locality HF-235 (colouring of samples as in Figure A). The analytical data are normalised to the average composition of unmineralised and undeformed metagreywacke sampled in different localities at Haugfjellet. C) Geochemical data of samples from locality HF-235 in a spider plot seen in Figure A with the same colours. The data are normalised to the host rock in the undeformed and unmineralised area seen as the yellow plots. D) Photomicrograph of a massive sulphide with unusual mineral assemblages, mainly sphalerite and galena together with minor amount of chalcopyrite, pyrrhotite and arsenopyrite (HF-14-10) from locality HF-235 (reflected light). E) Photomicrograph of sulphide accumulation along veins and fractures (HF-13-10) (cross-polarised, transmitted light). Abbreviations: LSZ - Low strain zone, HSZ - High strain zone. F) Photomicrograph of section HF-13-10 (cross-polarised, transmitted light) that shows intergrown chlorite and sulphide minerals G) As F, showing sphalerite, galena, chalcopyrite and pyrrhotite together, intergrown with chlorite (reflected light). Abbreviations: Gn - galena, Sp - sphalerite, Po - pyrrhotite, Apy - arsenopyrite, Ccp - chalcopyrite, Chl - chlorite.

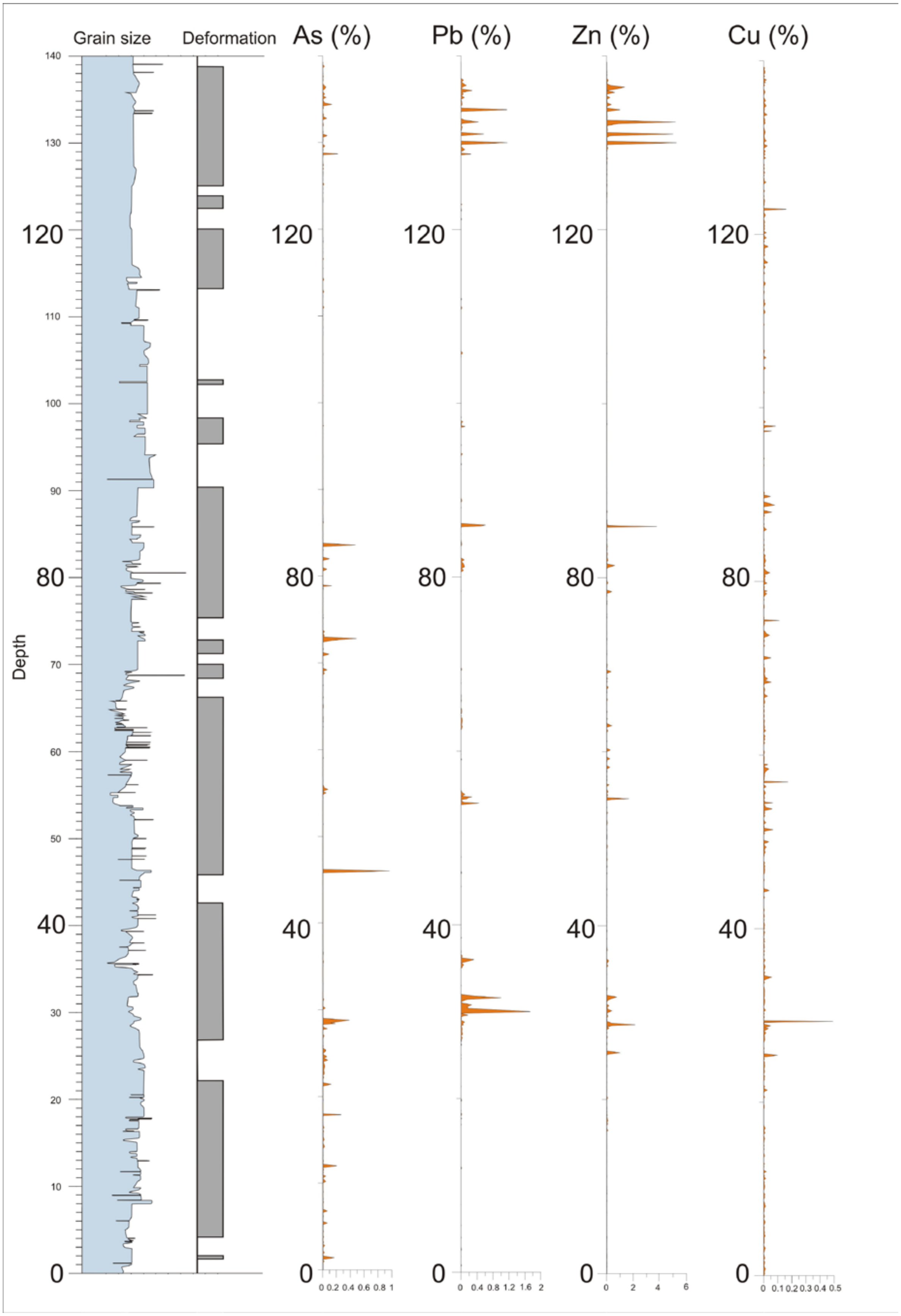
Grain size
Deformation
As (%)
Pb (%)
Zn (%)
Cu (%)
Depth
0
10
20
30
40
50
60
70
80
90
100
110
120
130
140
0 0.2 0.4 0.6 0.8 1
0 0.4 0.8 1.2 1.6 2
0 2 4 6
0 0.1 0.2 0.3 0.4 0.5

Fig. 5. BH-1 is an old drill core from an earlier prospect (Laundrum, 1995) in the Haugfjellet area. The result of the blue bar demonstrates the optical grain size through the core. The finer grained beds are more frequent deformed. The grey bar indicates where the rocks are deformed. However, the small details of the deformation cutting through the finer grained beds within coarser grained domains cannot be seen in the figure as the scale is too large. The orange graph represents the contents of As, Pb, Zn and Cu in % measured by portable XRF (Niton XL3t 900 Gold). The results are calculated average of three measurements for every second centimeter.

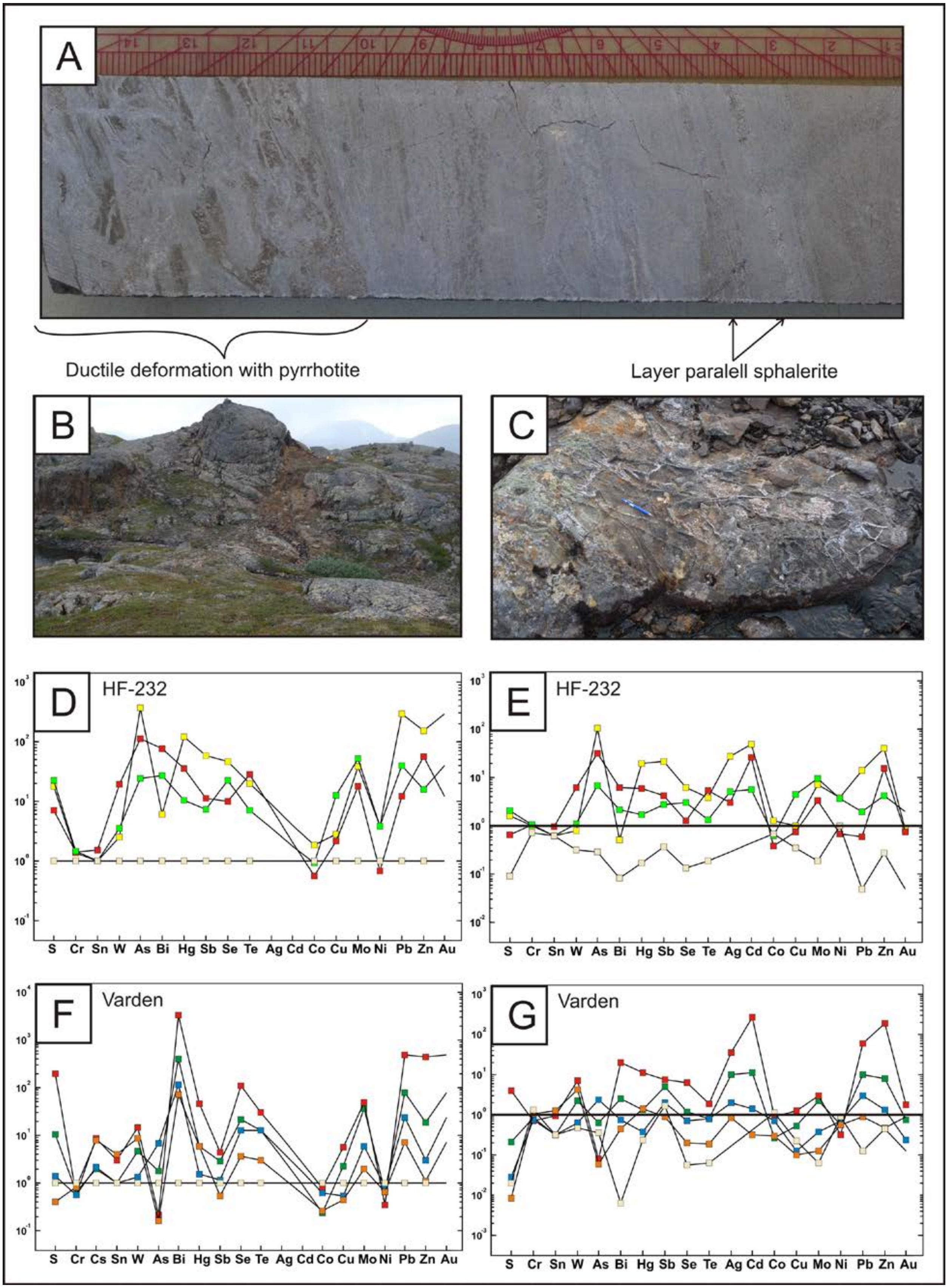

A
Ductile deformation with pyrrhotite
Layer paralell sphalerite
B
C
D
HF-232
S Cr Sn W As Bi Hg Sb Se Te Ag Cd Co Cu Mo Ni Pb Zn Au
E
HF-232
S Cr Sn W As Bi Hg Sb Se Te Ag Cd Co Cu Mo Ni Pb Zn Au
F
Varden
S Cr Cs Sn W As Bi Hg Sb Se Te Ag Cd Co Cu Mo Ni Pb Zn Au
G
Varden
S Cr Sn W As Bi Hg Sb Se Te Ag Cd Co Cu Mo Ni Pb Zn Au

Fig. 6. Shear-zone-hosted/related Cu-As-Au and remobilised Pb-Zn mineralisation from Haugfjellet area. A) A photo of a drill core (BH-1) with both ductily deformation metagreywacke with pyrrhotite and non deformed layer parallel sphalerite. B) Rusty coloured shear zone (locality HF-235) that can be followed for hundreds of meters to the right of the knob. C) Quartz vein brecciation at Varden locality often found together with Pb-Zn mineralisation. D) Geochemical data of samples from locality HF-232 in a spider plot. The data are normalised to the host rock in the undeformed and unmineralised area next to the shear zone. E) Geochemical data of samples from locality HF-232 in a spider plot. The data are normalised to the average of undeformed metagreywacke rocks found in Haugfjellet. The beige colour is the undeformed sample at the locality F) Geochemical data of samples from the Varden locality in a spider plot. The data are normalised to the host rock in the undeformed and unmineralised area next to the shear zone. G) Geochemical data of samples from the Varden locality in a spider plot. The data are normalised to the average of undeformed greywacke sediments found at different areas in Haugfjellet. The beige colour is the undeformed sample.

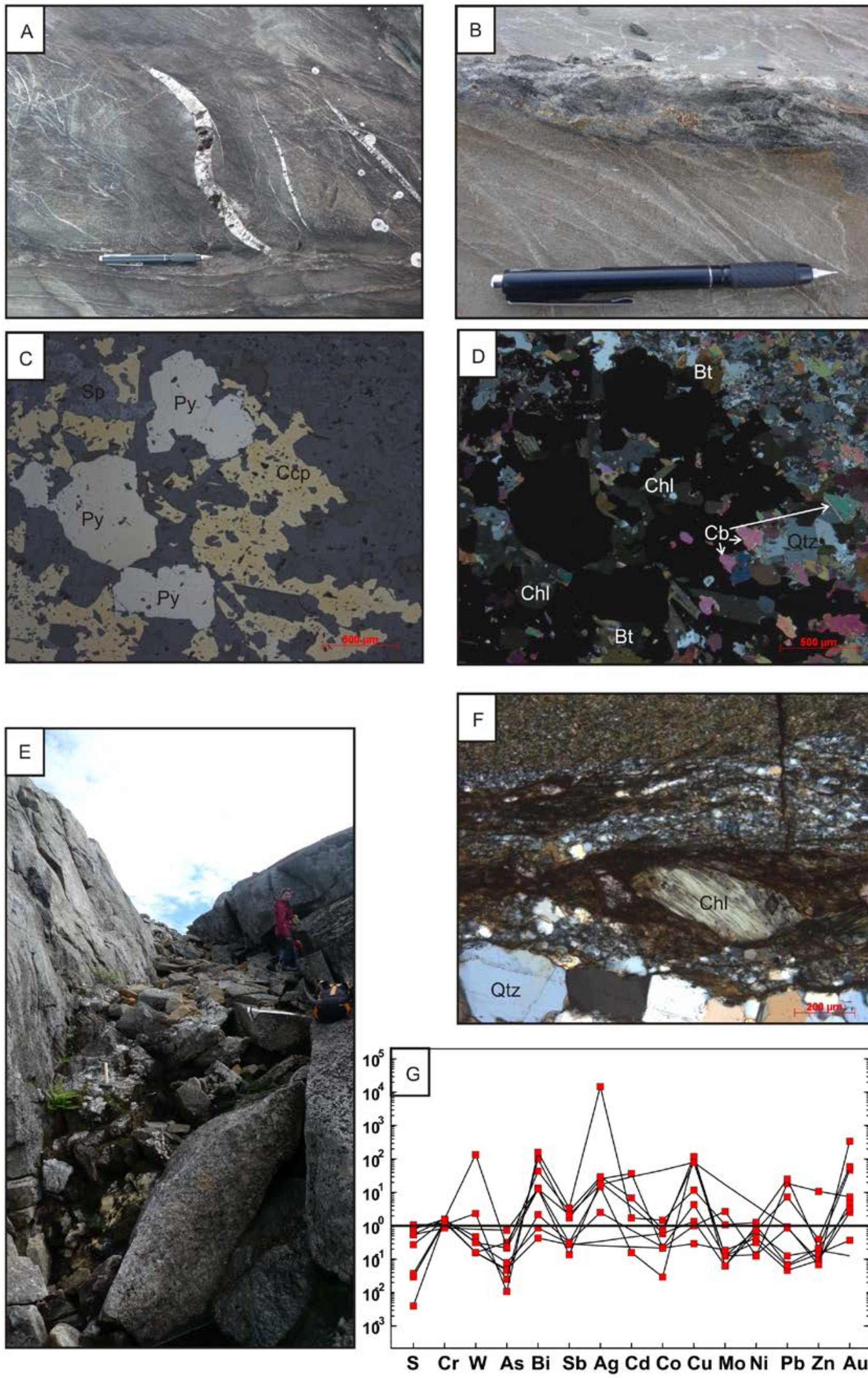

A
B
C
Sp
Py
Ccp
500 µm
D
Bt
Chl
Cb
Qtz
500 µm
E
F
Chl
Qtz
200 µm
G
S Cr W As Bi Sb Ag Cd Co Cu Mo Ni Pb Zn Au

Fig. 7. Brittle-ductile quartz veins in the Haugfjellet area. A) En echelon quartz vein ductily deformed into sigmoidal quartz veins defining a dextral shear sense. There are also thin non-directional veins occurring close to those veins B) Chalcopyrite and pyrite rich quartz vein with minor chlorite and biotite. C) Photomicrograph with reflected light of chalcopyrite and pyrite in quartz vein shown in Fig. 7B D) Photomicrograph with (cross-polarised, transmitted light) of quartz, chlorite, biotite and a minor calcite in quartz vein as Fig. C. E) A major quartz vein found in the middle of a 2 meter wide mylonite zone. The quartz vein is filling most of the gully, ca two meters wide. F) Photomicrograph with the sheared contact along a quartz vein seen at the bottom of the photo. The shear zones are also parallel to and together with minor micro quartz veins. A large chlorite grain is seen as a sinistral sigmaclasts. (cross-polarised, transmitted light). G) Geochemical data of quartz vein samples in a spider diagram which are normalised to the average greywacke values. Note the high Bi, Cu and Au content. Abbreviations: Sp - sphalerite, Py - pyrite, Ccp - chalcopyrite, Chl - chlorite, Bt - biotite, Qtz - quartz, Cb - carbonate.

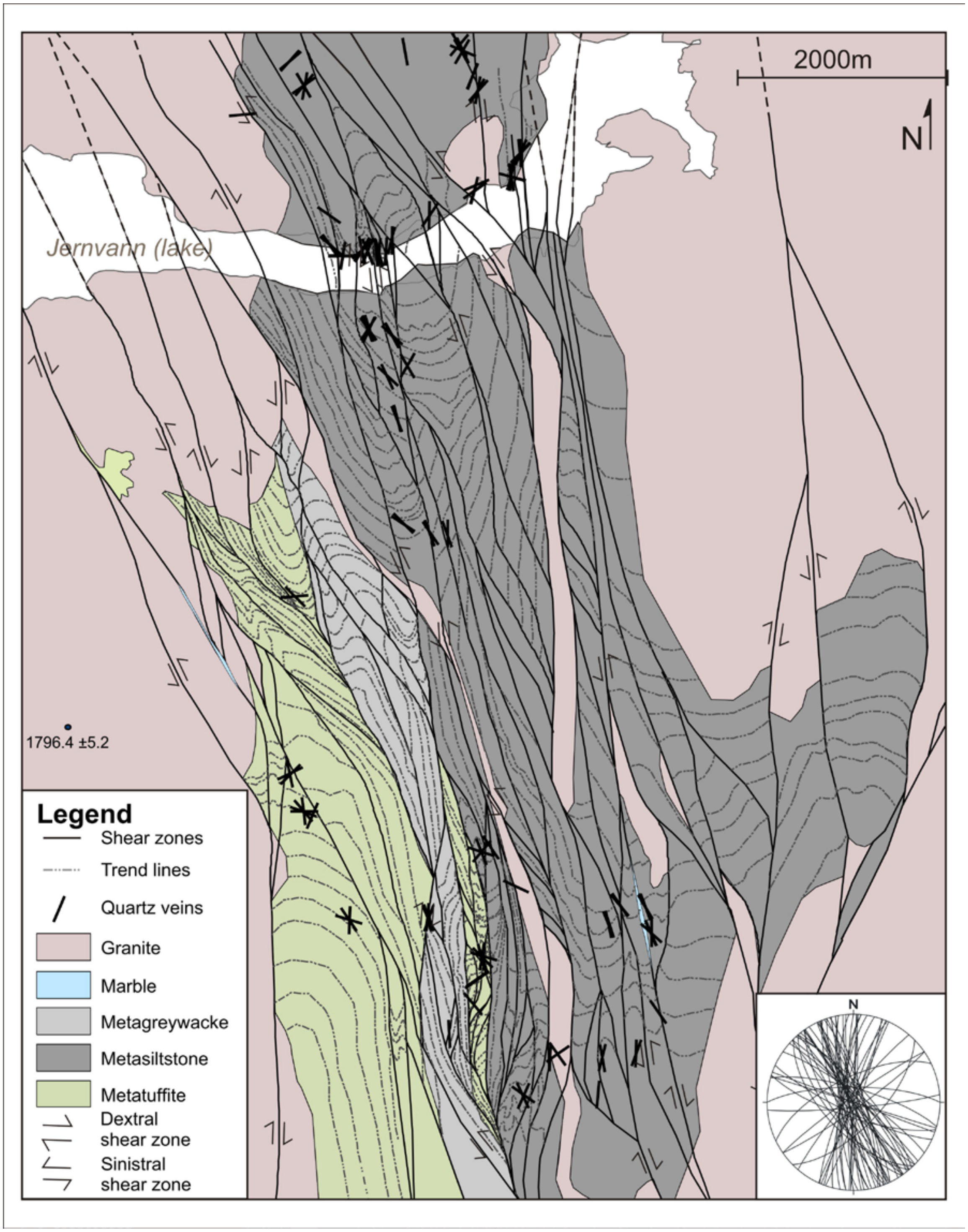

Fig. 8. Geologic and structural map of the Haugfjellet as Fig. 2 showing the orientation of the studied brittle-ductile quartz veins that are commonly found with Cu-Au sulphides. The map is the same as in Figure 2 but shows the measured brittle ductile quartz veins. The stereo plot shows the orientation of the veins.

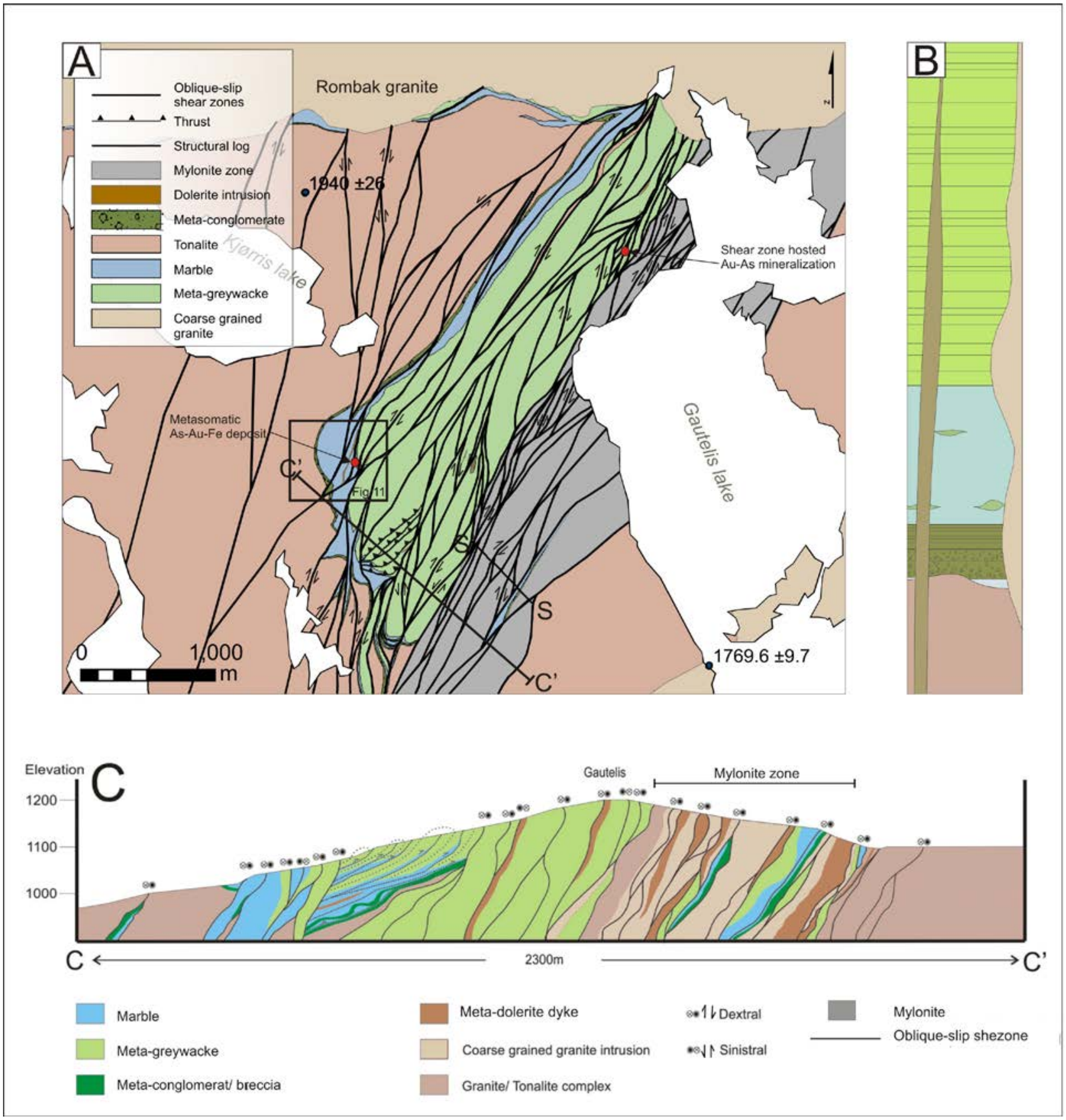

Fig. 9. Geologic and structural map of the oblique-slip dominated Gautelisvann area. A) Geological overview map of the Gautelis area. Location of cross-section profile (Fig. 9C; line C-C'), structural log (Fig. 10; line S'-S) and frame of Figure 11B are marked. Radiometric ages are from Romer et al. (1992). B) Schematic stratigraphic column of the Gautelis area. C) Interpreted cross section of the main ductile shear zone of the Gautelis domain.

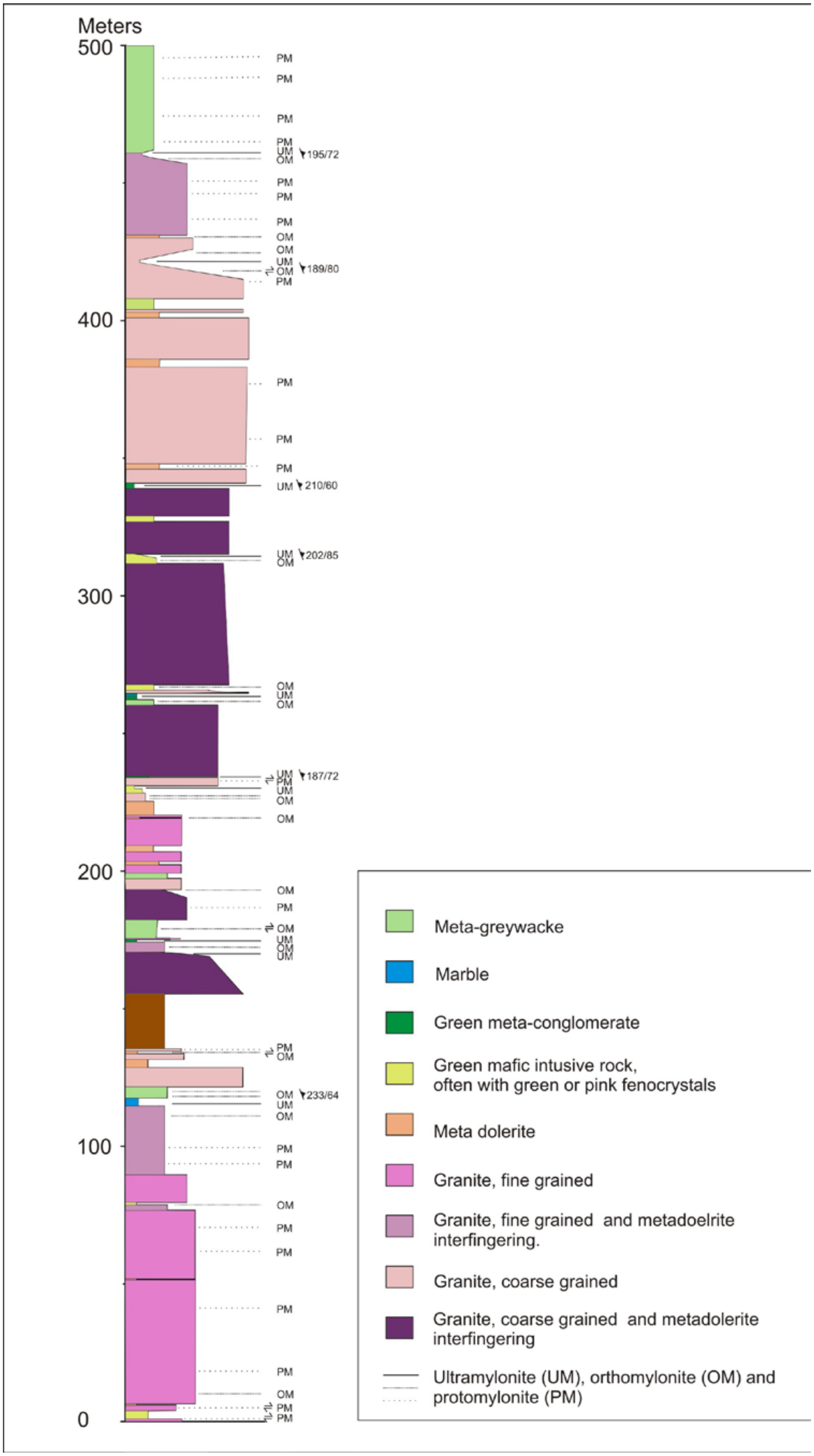
Meters
500
400
300
200
100
0
PM
UM
OM
195/72
189/80
210/60
202/85
187/72
233/64
Meta-greywacke
Marble
Green meta-conglomerate
Green mafic intusive rock,
often with green or pink fenocrystals
Meta dolerite
Granite, fine grained
Granite, fine grained and metadoelrite
interfingering.
Granite, coarse grained
Granite, coarse grained and metadolerite
interfingering
Ultramylonite (UM), orthomylonite (OM) and
protomylonite (PM)

Fig. 10. Detailed structural log across the ca. 600 m thick D_4 mylonite shear zone in Gautelis (location line is shown in fig. 9A). Note the rapid variation in rock types across this anastomosing shear zone pattern suggesting high strain segmentation and formation of lens shaped units of the host rocks (modified from Larsen et al., structural manuscript).

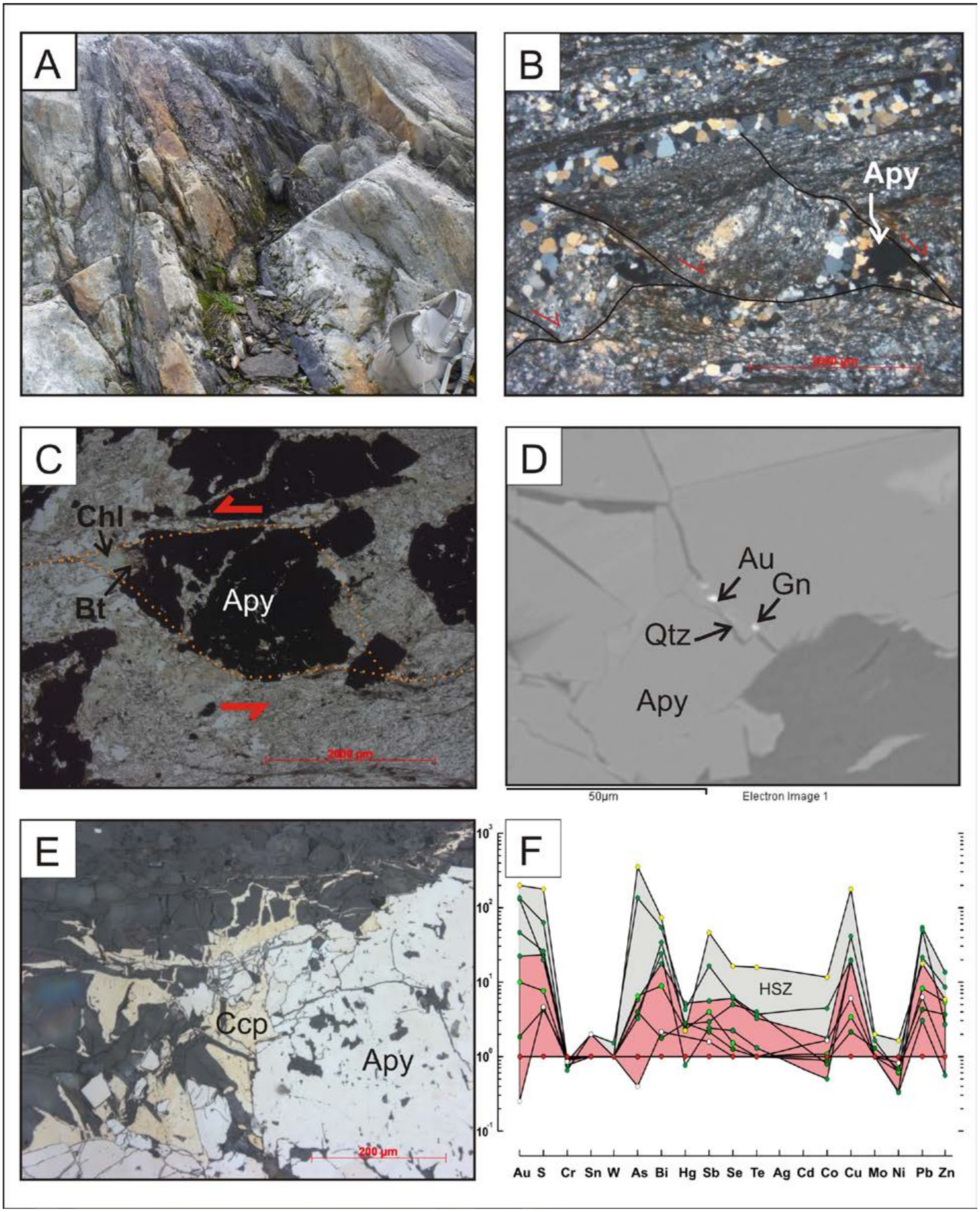

Fig. 11. Photos and diagram illustrating shear zone hosted sulfide and gold occurrences in the Gautelis area. A) Typical sulphides parallel to the mylonite in the Gautelis shear zone. Photo is taken on the eastern side of Gautelisfjell towards the south. B) Photomicrograph of a thin section from the shear zone hosted As-Au

mineralisation near the Gautelisvann showing the clear relationship between the mineralisation and deformation zones on micro scale. The sulphides have deposited in areas of dilation. C) Photomicrograph of a thin section from a ductile shear zone close to the Gautelis mine area that demonstrate that the arsenopyrite act cataclastic as a sigmaclast rotating creating pressure shadows filled with chlorite and biotite. D) Free gold found in fractures of the arsenopyrite together with quartz and galena. The section is from same area is in B. E) Photomicrograph of chalcopyrite are commonly found as fracture fill in the cataclastic deformed arsenopyrite. The sample is from same area as B. F), same location as B. Geochemical data of eight samples collected are across a shear zone hosted As-Au mineralisation plotted in a spider diagram normalised to the host rock samples which has no deformation and visible bedding. The LSZ (Low strain zone) and HSZ (High strain zone) fields have been subdivided based on their deformation observed in field.

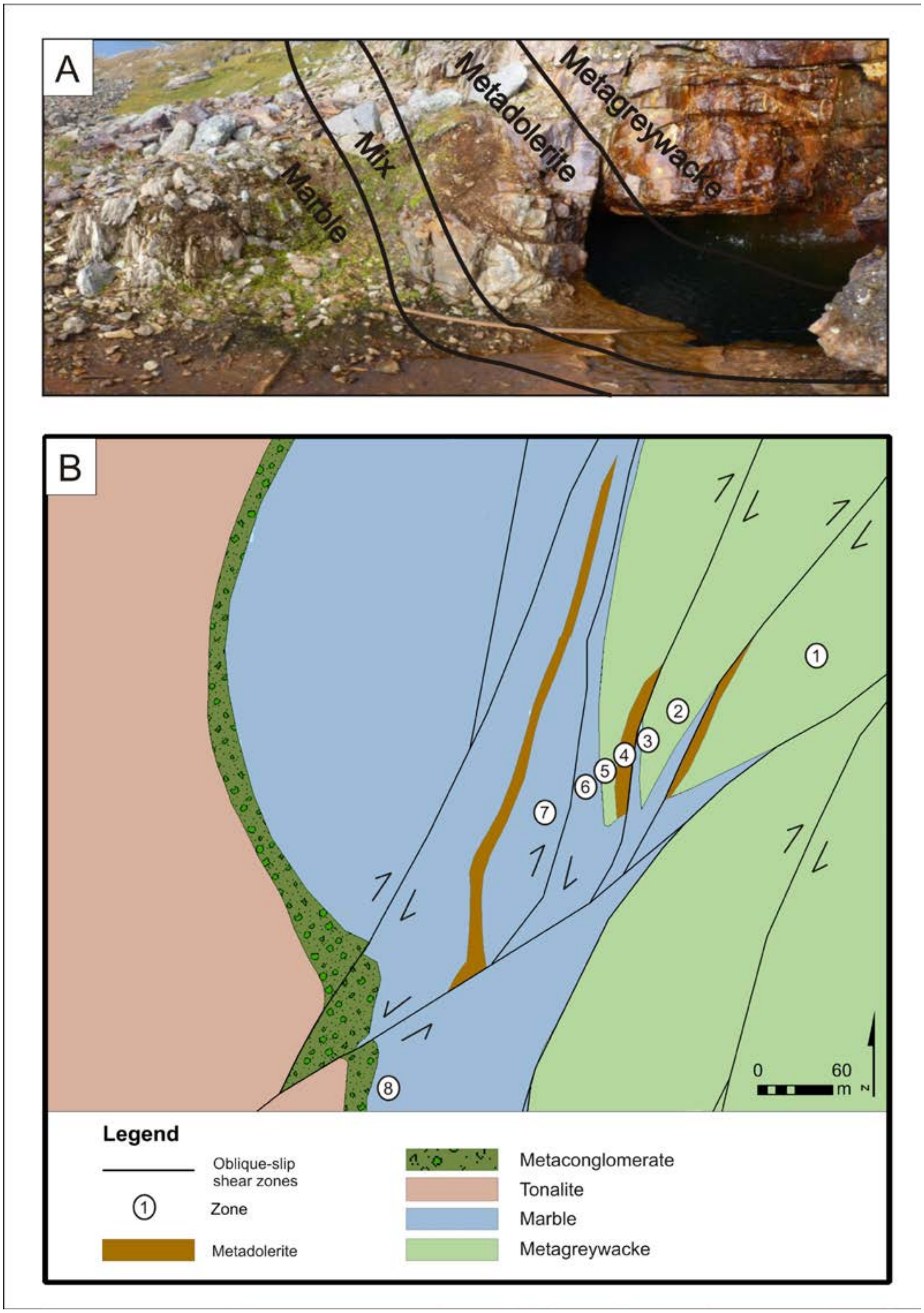

Fig. 12. The Gautelis metasomatic As-Au deposit. A) A photo of the mine area with the contacts between the different units/zones marked. B) A geological map of the mine area showing where the samples and the different zones are located. The scale of the metadolerite is exaggerated to make the dykes more visible in the figure. The real thickness of the dykes is approximately one meter.

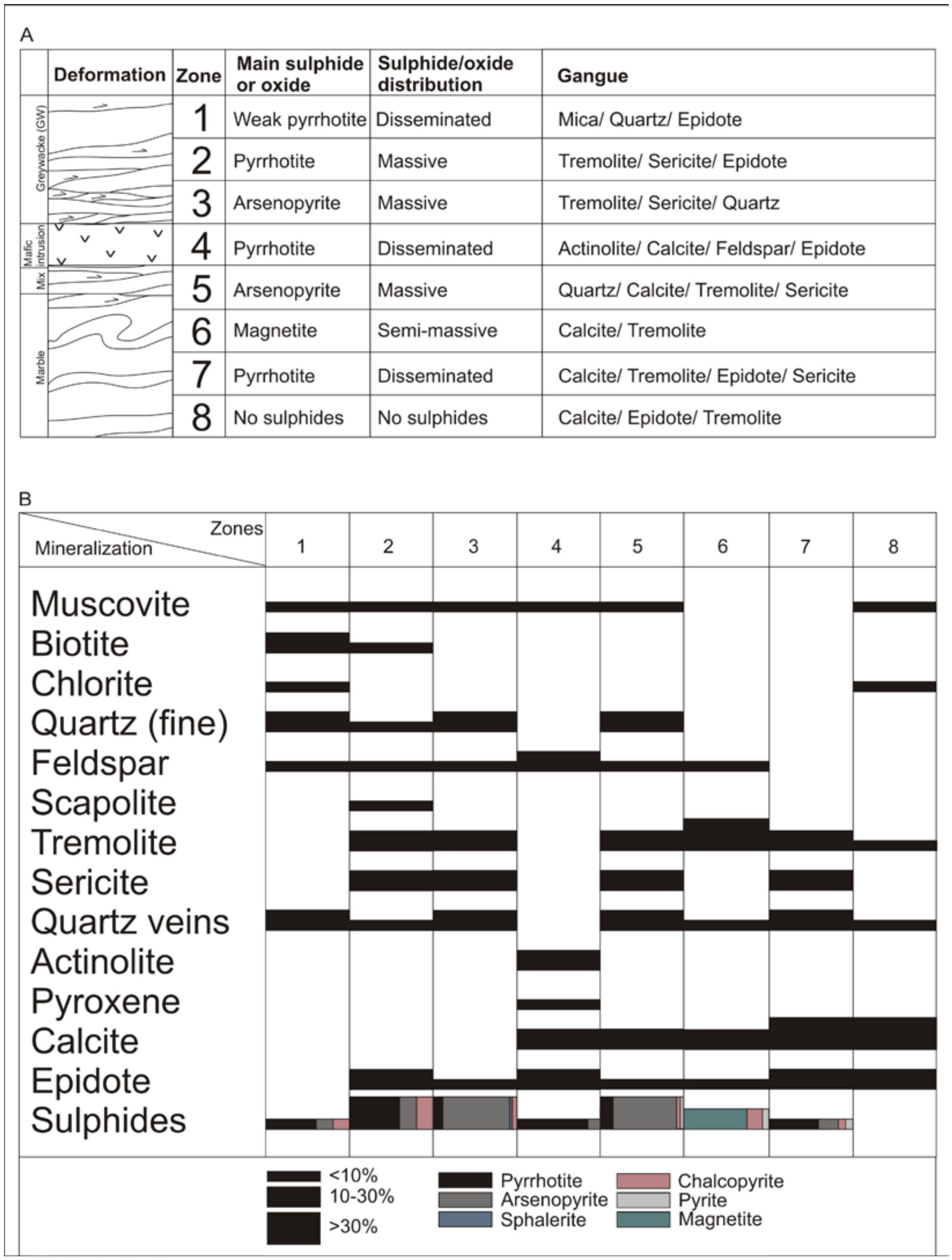

Fig. 13 Sulphide mineralisation zones at the Gautelis metasomatic deposit and their relation to deformation and their mineral assemblages. A) Shows the eight differentiated zones of mineralisation with the rock types, deformation style and intensity, sulphides and their gangue minerals. B) A diagram that shows the mineralisation of each zones. The thickness indicate the amount (three levels) and the colour indicates the type of sulphide or oxide minerals and the approximately percentage amount of the total sulphide bar.

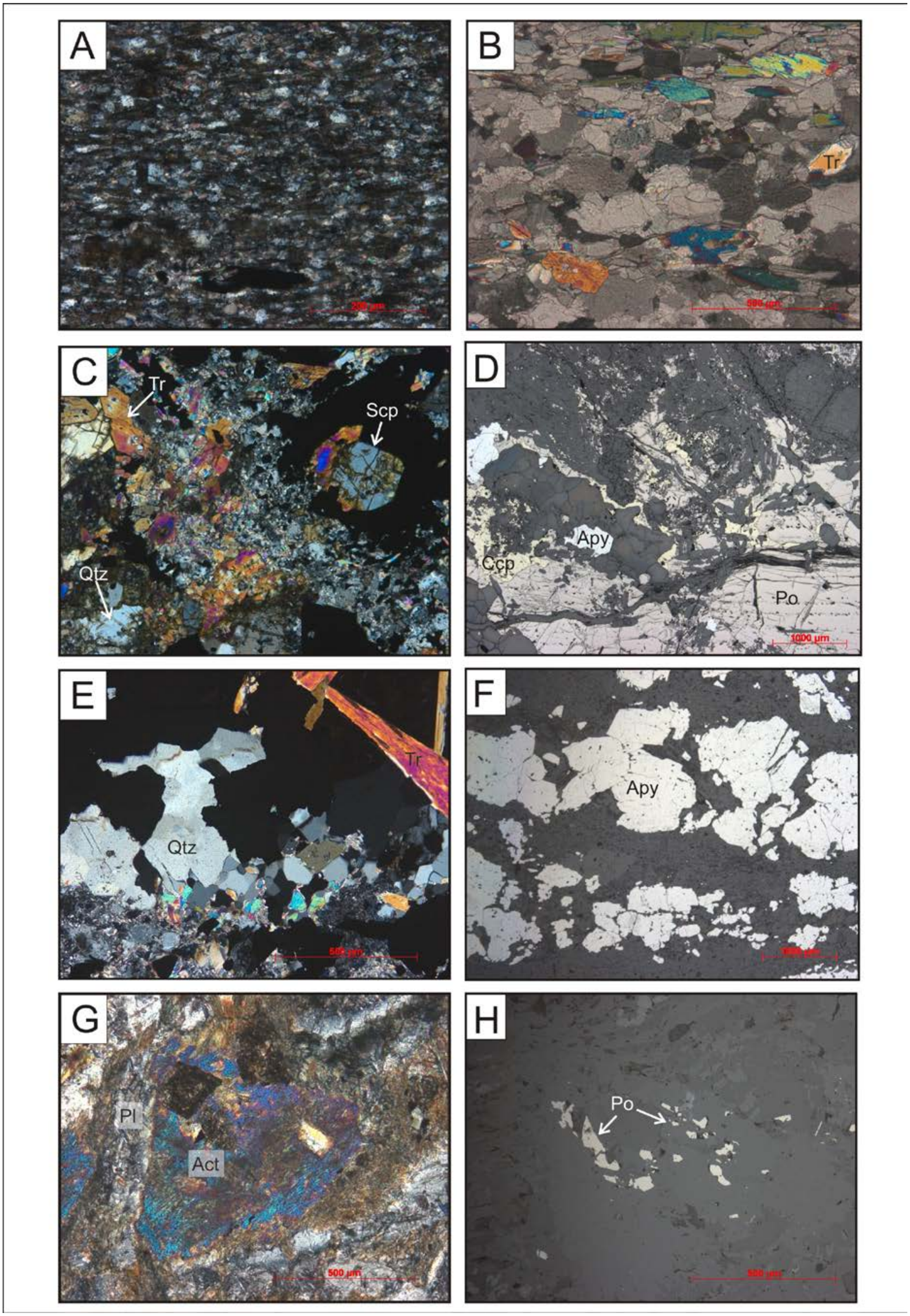
A
B
Tr
C
Tr
Scp
Qtz
D
Apy
Ccp
Po
1000 µm
E
Tr
Qtz
500 µm
F
Apy
G
Pl
Act
500 µm
H
Po

Fig. 14 Photomicrographs of zone 1-4 and 8 from the metasomatic sulphide deposit at Gautelis. A) Zone 1, weakly deformed metagreywacke with mica defining the foliation together with quartz, plagioclase and with scattered grains of pyrrhotite (cross-polarised, transmitted light). B) Zone 8, Weakly deformed and non-mineralised marble consist mainly of dolomite/calcite with some quartz veins and aggregates of tremolite, chlorite, muscovite and epidote along the foliation. (cross-polarised, transmitted light). C) Zone 2: Metagreywacke with semi-massive to massive pyrrhotite, intergrown with non-directional tremolite, quartz, scapolite, epidote and sericite. (cross-polarised, transmitted light). D) Zone 2: Strongly deformed, irregular segregations of pyrrhotite which occurs intergrown with some irregular grains and segregations of chalcopyrite and disseminated euhedral arsenopyrite. (reflected light) E) Zone 3: Metagreywacke found next to the eastern contact of the meta-dolerite dyke. The sulphides are intersected by recrystallised quartz veins and tremolite veinlets. (cross-polarised, transmitted light). F) Zone 3, disseminated to semi-massive arsenopyrite. (reflected light) G) Zone 4: the meta-dolerite dyke have a magmatic texture and weak deformation. The photomicrograph show plagioclase, actinolite and epidote minerals. (cross-polarised, transmitted light) H) Zone 4: The sulphide mineralisation comprises fine-grained dissemination of irregular minor pyrrhotite and accessory grains of arsenopyrite. (reflected light). Abbreviations: Scp - scapolite, Tr - Tremolite, Pl - plagioclase, Act - actinolite, Apy - arsenopyrite, Ccp - chalcopyrite, Po - pyrrhotite.

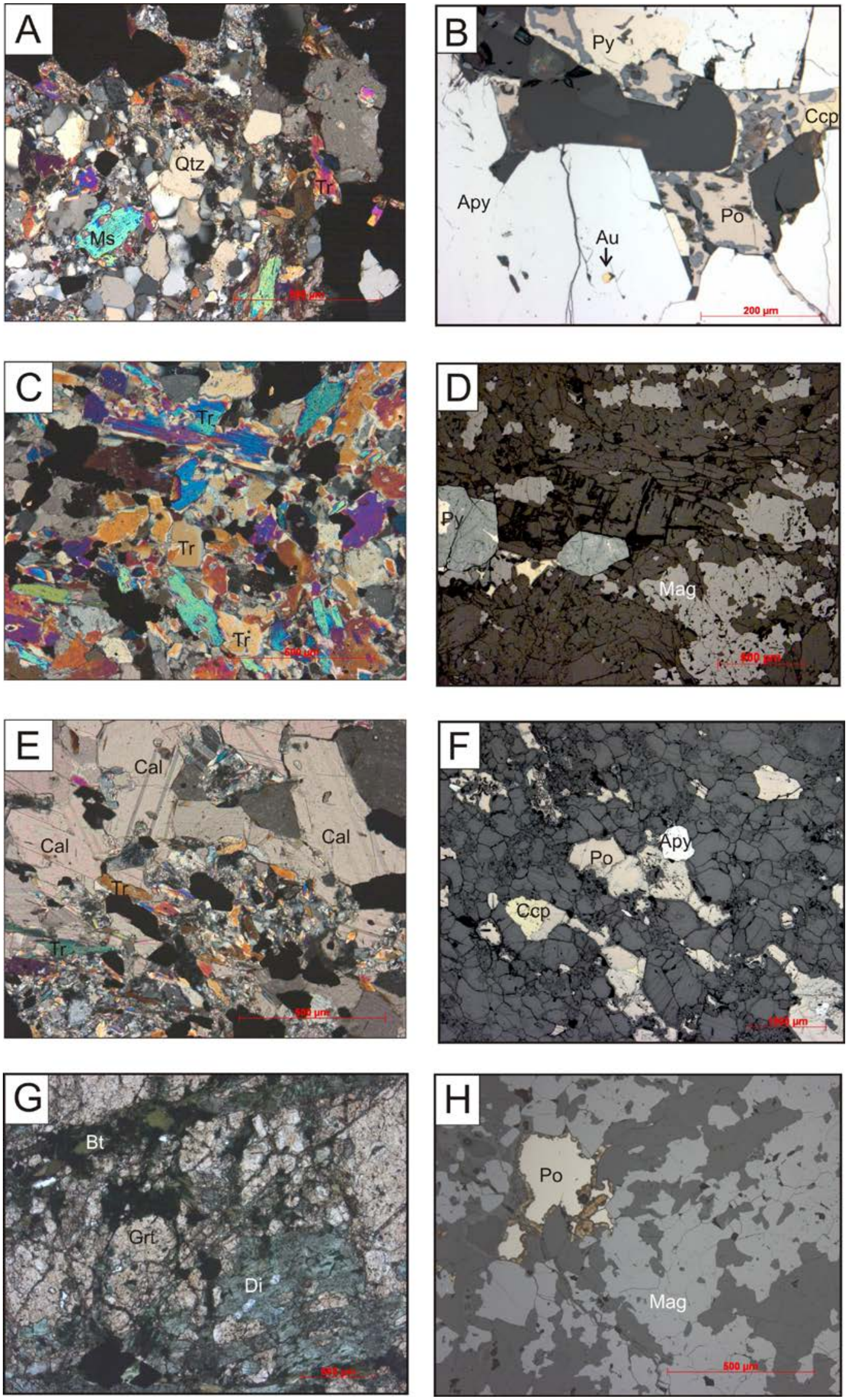
A
Qtz
Tr
Ms
B
Py
Ccp
Apy
Au
Po
200 μm
C
Tr
Tr
Tr
D
Py
Mag
E
Cal
Cal
Cal
Tr
Tr
F
Apy
Po
Ccp
G
Bt
Grt
Di
H
Po
Mag
500 μm

Fig. 15. Photomicrographs of zone 5-7from the metasomatic sulphide deposit at Gautelis and from a similar metasomatic occurrence nearby A) Zone 5, Sulphide minerals are intergrown with tremolite, quartz, calcite, muscovite and feldspar (cross-polarised, transmitted light). B) Zone 5, The sulphides occur as semi-massive to massive irregular aggregates and bands. They consist mainly of cataclastic arsenopyrite with strongly deformed pyrrhotite and chalcopyrite intergrown. Chalcopyrite and gold can be found along micro-fractures in cataclastic grains of arsenopyrite. (reflected light) C) Zone 6, calcitic marble with high content of tremolite and minor epidote intergrown with magnetite and pyrite. (cross-polarised, transmitted light). D) Zone 6, disseminated to semi massive magnetite and pyrite found in the strong deformed marble. E) Zone 7, calcite marble carrying stringers of sericite-epidote, tremolite, quartz and weak pyrrhotite dissemination. (cross-polarised, transmitted light). F) Zone 7, disseminated pyrrhotite with minor chalcopyrite and arsenopyrite. (reflected light). G) Diopside and garnet from a metasomatic deposit to the north in Gautelis. (cross-polarised, transmitted light). H) Magnetite and pyrrhotite from same location as G. (reflected light). Abbreviations: Tr - Tremolite, Qtz - Quartz, Ms - muscovite, Apy - arsenopyrite, Ccp - chalcopyrite, Bi - biotite, Di - diopside, Grt - garnet, Po - pyrrhotite, Au - Gold, Mag - magnetite.

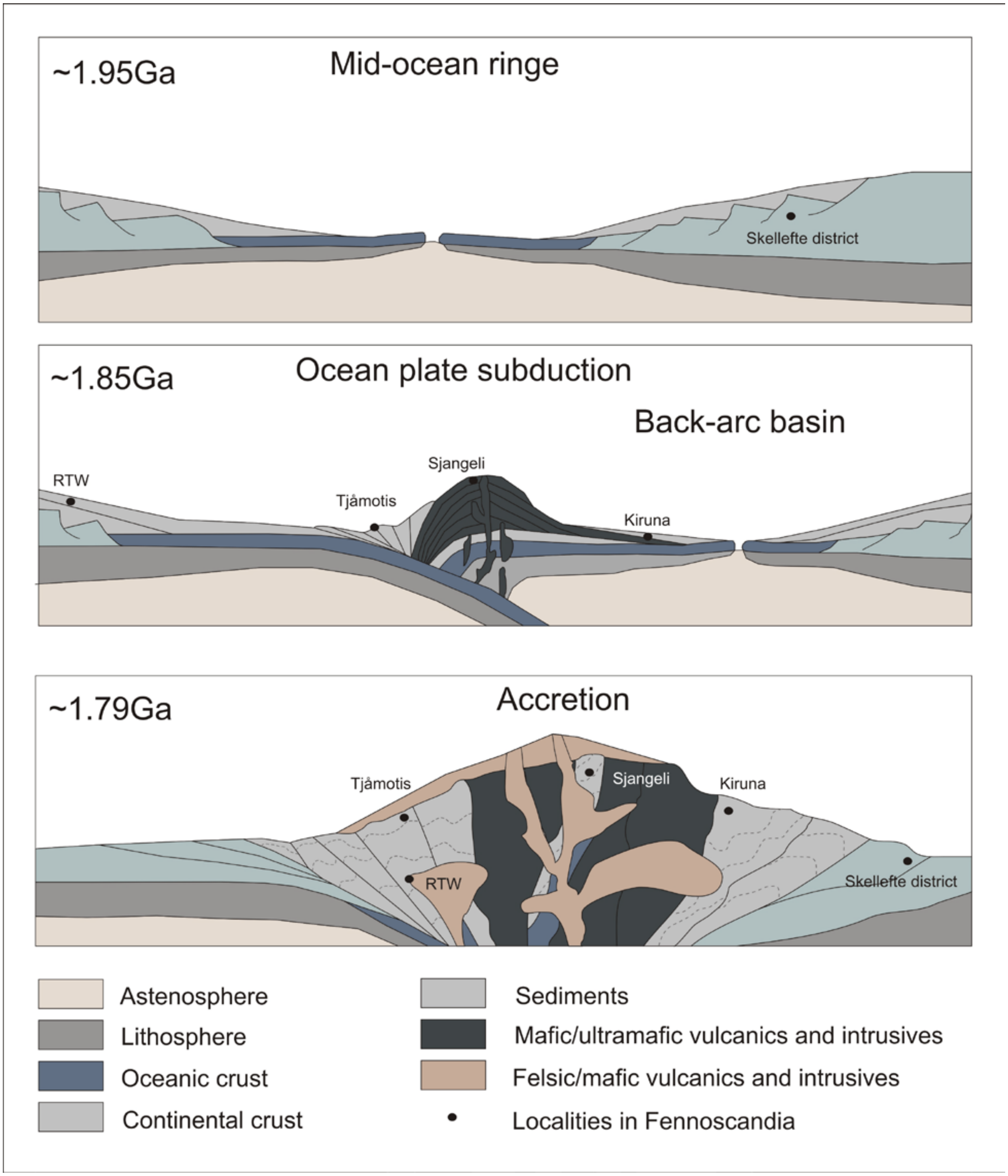

Fig. 16. Tectonic model of the Svecofennian orogeny with timing and spatial relationship to the sulphide and gold deposits in RTW and nearby in Sweden. The model demonstrates the different stages of a progressive development from basin on an active margin to the accretion and orogeny.

Paper IV

Tine Larsen Angvik, Iain C. Henderson and Steffen G. Bergh

Svecofennian shear zone networks of the Rombak Tectonic Window, North Norway: Structural architecture and regional correlation with the Fennoscandian shield

(manuscript)

Svecofennian shear zone networks of the Rombak Tectonic Window, North Norway: Structural architecture and regional correlation with the Fennoscandian shield

Tine L. Angvik[1 and 2], Iain H.C. Henderson[1] and Steffen G.Bergh[2]

1. The Geological Survey of Norway
2. University of Tromsø

Abstract

The northern part of the Fennoscandian shield comprises several domains of Archean to Paleoproterozoic age. These domains include the Kola province in Russia, the Kola-Lapland and Kittilä provinces farther west, and the Norrbotten province in northern Sweden. The evolution of these domains was extremely complex and involved continental break ups, development of micro continents, island arcs and later closing of oceans (Kola ocean) accompanied by subduction, accretion and continent-continent collision. The Archean and Paleoproterozoic crust is commonly juvenile and the Fennoscandian shield has a high potential for mineral and ore deposits.

Archean and Paleoproterozoic basement rocks are also present as inliers and outliers beneath and west of the Scandinavian Caledonides, and these provinces in general, have not been included in previous regional studies of the Fennoscandian Shield. Because of new knowledge of the stratigraphy, composition, age, structural relationship, and widespread sulphide mineralisation in the Rombak Tectonic Window and the similarities of these rocks with provinces farther north (inliers) and east, we consider them to be directly correlated with the basement rocks in northern Sweden, Norway and Finland. These provinces all show evidence of the same break-up activity in the Archean (2.5-1.9 Ga) that formed one or several micro continents filled in with Paleoproterozoic basin sediments and the development of island arcs and back arc basins and volcano-sedimentary deposits, terminating with the Svecofennian orogeny (1.92-1.79 Ga) which produced fold-thrust belts and regional ductile shear zones. One such shear zone is outlined by the Archean and Paleoproterozoic boundary, termed the Luleå-Jokkmokk zone, and can be traced beneath the Caledonian nappes in a bend to link up with the RTW and farther north to join the Senja shear zone west of the Caledonides. Correspondingly, the volcano-sedimentary deposits of the Bothnian basin, including a variety

of basins, can be traced all the way north to the Rombak Tectonic Window (RTW). These shear zones, and inter-related volcano-sedimentary belts, define portions of the Svecofennian Orogenic belt in northern Sweden and Finland. In the RTW the Svecofennian structures include early-formed fold-thrust structures that were later overprinted by steep strike-slip and/or oblique-slip ductile shear zones. These shear zones follow an overall NW-SE trend, but bend and merge into more N-S trending shear zones when approaching the Caledonides in the north. In addition, several steep NE-SW striking shear zones crosscut both the earlier-formed fold-thrust belt and the N-S trending shear zones, developing during the final stage of the Svecofennian, orogeny. The bend of the orogeny suggest an secondary orocline. This orocline geometry of the shear zone system and associated basement gneisses, volcano-sedimentary belts and intrusive and magmatic components, had a major and complex impact on the juvenile Fennoscandian crust and was responsible for remobilisation of several ore deposits. By comparing and correlating different domains with respect to tectono-magmatic evolution in the northern Fennoscandian Shield, we may be able to better understand the processes of ore genesis and tectonic remobilisation, as well as to locate regions with a high potential for economic valuable ore bodies.

Keywords: Rombak Tectonic Window, Svecofennian orogeny, srocline, Structural architecture, correlation, shear zone.

1) Introduction

Mineral occurrences may be structurally controlled when they are carried with fluids or magma and become remobilized along shear zones and/or crustal weakness zones (e.g. Goldfarb et al., 2001; Groves et al. 2003). However, mineral deposits can be part of a complex geological history involving sedimentation, volcanism, magma intrusion and multiple generations of tectono-metamorphic development (e.g. Groves et al 2003; Eilu, 2012: Larsen et al., 2013), and thus, the mineral deposits may be of a varied character and genesis. Attempts to regionally correlate tectono-magmatic events and their relation to ore genesis and known mineral occurrences within the Svecofennian domains of the Fennoscandian shield, including the basement tectonic inliers of the Caledonides to the west, has not yet been done. However, in recent years tectono-magmatic similarities have been pointed out across the borders and a new regional tectonic understanding has been developed (e.g. Nironen, 1997; Bergh et al. 2012, 2014).

The Paleoproterozoic Svecofennian domain of the Fennoscandian shield (Fig. 1) is defined as a wide irregular belt running from southern Finland/ Russia, through central and northern Sweden and into Norway (e.g. Gaàl & Gorbatschev, 1987; Korsman et al., 1997; Cagnard et al., 2007; Lahtinen et al. 2008). The domain is thought to be the result of protracted extension/rifting and formation of the Kola ocean (2.5-2.1 Ga), followed by arc-magmatism (2.1-1.79 Ga), island-arc accretion and subduction (1.95-1.86) and continent-continent collision (1.94-1.79 Ga) (e.g. Gaàl & Gorbatschev 1987; Nironen 1997; Korsman et al. 1997; Cagnard et al.2007; Lahtinen et al. 2008). The Svecofennian orogen (1.92-1.79 Ga) is characterised by a complex network of interacting ductile thrusts and oblique strike-slip shear zones (Fig. 1) that formed when the Kola ocean closed and formed large volumes of Paleoproterozoic crust (Lahtinen et al. 2005, 2008; Daly et al. 2006). The regional extent of the orogen, varied composition (e.g. metallogenic potential), structural architecture in different regions, and the nature of crustal growth during the Svecofennian orogen are still issues of great controversy (Skiöld & Rutland 2006; Högdahl et al. 2007; Hermansson et al. 2007).

The Rombak Tectonic Window (RTW) is located within the Caledonides of NW Scandinavia (Fig. 1). This basement province is composed of Paleoproterozoic meta-volcanic and sedimentary rocks (<2.3 Ga) intruded by mafic to intermediate 1.9-1.7 Ga granitic batholiths, and affected by ductile shear zone deformation and related metallogenesis (Korneliussen et al. 1986; Romer 1987, Korneliussen & Sawyer 1989; Bargel et al. 1995; Larsen et al. 2010, 2013). Because the RTW is an inlier, largely unaffected by Caledonian reworking (Larsen et al., 2013), and the excellent exposure of Paleoproterozoic rocks and tectonic structures, this province provides an important link for understanding such controversies as cratonic-marginal structural architecture and regional correlation (cf. Romer 1987; Cashman 1990; Bergh et al. 2010; Larsen et al., 2013).

This paper reviews the current knowledge of Paleoproterozoic metavolcano-sedimentary belts and Svecofennian structures in the RTW and discusses and compare the evolution in relation to other basement tectonic inliers and outliers in the Caledonides (e.g. Corfu 2003; Armitage & Bergh 2005; Bergh et al. 2010; Myhre et al. , 2011, Henderson & Viola, 2013), and within the autochthonous Fennoscandian shield of northern Sweden and Finland (e.g. Bergmann Weihed, 2001; Bark & Weihed, 2007). We will focus on the complex shear zone network of the RTW which resembles a regional-scale orocline structure (Carey 1958) or curved orogeny, and discuss how it may correspond and/or differ geometrically from similar shear zone networks in Norway, Sweden and Finland. In addition we will discuss the nature of the structural evolution and geometries and their relevance for metallogenic occurrences. The study focuses on meta-volcanic and sedimentary sequences (2.5-1.87 Ga), fold-thrust belt structures, regional oblique-slip shear zones (Larsen et al. 2010, 2013) and arc-related plutons (2.0-1.75 Ga) formed during the Svecofennian orogeny (1.92-1.79 Ga; e.g. Romer 1988), and attempts to unravel the processes of formation of metallogenic deposits in the main Paleoproterozoic rifting events and later reworking (e.g. Romer, 1988; Korneliussen & Sawyer, 1989; Larsen et al., 2013).

2) Regional setting of the *Svecofennian* domain

The Fennoscandian shield can be subdivided into three main crustal domains (Fig. 1): (i) Archean crustal provinces in the northeast, (ii) Paleoproterozoic cover units farther south, including the Karelian domain of Finland and the Svecofennian domain in the central part, and (iii) Mesoproterozoic rocks with the Gothian and Sveconorwegian orogenic belts in the southwest (Gaàl & Gorbatschev 1987; Gorbatschev & Bogdanova 1993; Korsman et al. 1997; Cagnard et al. 2007).

The Svecofennian domain is composed of sedimentary and volcanic sequences, and magmatic-intrusive rocks that are formed in the Paleoproterozoic time span (2.5-2.1 Ga), whereas the Svecofennian deformation (orogen) is confined to the compressional deformation from1.92-1.79 Ga (Lahtinen et al. 2008). The extent, boundary conditions, and tectono-magmatic and metamorphic signature of the complex and multi-phase Svecofennian deformation that affected these older Archean components in the Fennoscandian shield, are still relatively unresolved issues. It is possible that the Svecofennian domain contains older Archean micro continents, volcano-sedimentary belts and accretionary terrains from intra-oceanic, arc-related or subduction zone settings of the rifted Archean craton (i.e. the Kola Ocean, Berthelsen & Marker, 1986; Zhao et al., 2002; Daly et al., 2006). In this context the Svecofennian domain is determined from rocks that formed as a result of long-term break-up of the Archean cratonic margin by rifting and formation of the Kola Ocean from 2.5-2.1 Ga (e.g. Gaàl & Gorbatschev 1987; Nironen et al. 1997). Most of these rift-related rocks are usually referred to as Paleoproterozoic greenstone belts that include meta-volcanic, metasedimentary and some intrusive rocks that formed in separate basins, and with the overlying sedimentary units deposited on a stable platform (Lindquist, 1987; Martinsson, 1997; Hanski et al., 2001; Bergh et al., 2007). Initial break-up of the Archean supercontinent (2.5-2.4 Ga) is thought to have involved smaller continents with sedimentation of marine and deltaic sediments along their margins (e.g. Martinsson, 1997; Strachan & Holstworth, 2000). In southern Finland, the Archean continental break-up occurred later, between 1.91-1.87 Ga (Nironen 1997).

The main rifting event produced one or more large basins along a traverse from central Sweden into the Finnmark area of northern Norway (Fig. 1; Koistinen et al., 2001). These basins (Fig. 1) can be inferred from the presence of metasedimentary units (or greenstone belts) in the autochthonous shield areas as well as in tectonic inliers of the Caledonides (Figs. 1 and 3). These units include those of the Rombaken Tectonic Window (RTW) (Korneliussen et al., 1986), the Mauken Tectonic Window (Vognsen, 2010), West Troms Basement Complex (WTBC) and the Lofoten-Vesterålen province (Corfu et al. 2007; Bergh et al. 2010, 2012), the Alta-Kautokeino-Kittilä, Komagfjord-Repparfjord and Karasjok greenstone belts of central and eastern Finnmark (e.g. Pharaoh & Pearce 1984), the Tjåmotis and Lycksele-Storuman districts of northern Sweden (Ödman, 1957) and the Bothnian Basin in the central part of the Fennoscandian shield (Lindquist, 1987).

The magmatic and metasedimentary units of all these regions were variably deformed during the Svecofennian Orogeny (Korja et al., 2006; Bark & Weihed, 2007; Lahtinen et al., 2008), and several of these regions suffered only limited reworking during the Caledonian orogenic event (Corfu et al. 2003; Viola et al 2008; Bergh et al. 2010; Larsen et al. 2010). Thus, they provide a good framework for regional correlation. The Svecofennian Orogeny initiated with formation of island-arcs and arc-magmatism (2.1-1.79 Ga), and was followed by island-arc accretion, local subduction (1.95-1.86) and/or continent-continent collision (1.94-1.79 Ga) (e.g. Gaàl & Gorbatschev 1987; Nironen 1997; Korsman et al. 1997; Cagnard et al.2007; Lahtinen et al. 2008). Hietanen (1975) was the first to present an island-arc plate tectonic interpretation of the Svecofennian orogeny, in which micro-continents and island arcs were accreted onto the Karelian micro-continent adjacent to the Archean craton in the east, and onto Laurentia on the Greenland side of the margin. This model has been largely verified by a number of workers (Nironen, 1997; Zhao et al, 2002; Korja et al. 2006). Notably important, island-arc plate tectonics is known to carry a high potential for mineral deposits, for example the Kuruku type volcanic massive sulphide (VMS) deposits described from the Skellefte district in Sweden (Allen et al. 1996).

However, the transition from the Archean craton to Paleoproterozoic crust in the Svecofennian domain is not well constrained. In northern Sweden there is no definite boundary or boundary zones, but the Luleå-Jokkmokk zone (Fig. 3; Nironen, 1997), is a tentatively boundary proposed from a gradual shift and inter-fingering relationships between Archean and Paleoproterozoic components.

Structurally, the Svecofennian orogen in Fennoscandia delimits a network of N-S and NE-SW trending mylonitic shear zones, including fold-thrust zones and steep oblique- and strike-slip shear zones (Fig. 1) that formed when the Kola ocean closed (e.g. Berthelsen & Marker 1986; Nironen, 1997; Lahtinen et al. 2005, 2008; Daly et al. 2006). This closure event involved both lower and upper crust accretion and locally, high P/low T metamorphism (Gaàl & Gorbatschev 1987; Weihed et al. 1992; Weihed et al. 2002). The metamorphic grade seldom exceeded upper amphibolite facies in the metasedimentary units (Allen et al. 1996; Lundström et al.,1998; Bark 2005), and the pressure conditions averaged 5 ±1-2 kbar (Nironen, 1997). Metallogenic and ore deposits in the supracrustal units and contacts between arc-magmatic complexes were highly reworked and mobilized during these tectono-metamorphic events (e.g. Weihed et al., 2005). In addition, the meta-supracrustal units were intruded by mafic dykes and granitoid plutons during and late in the Svecofennian Orogeny throughout the Fennoscandian shield (Gaál & Gorbatschev 1987; Nironen 1997; Korneliussen & Sawyer 1989; Larsen et al. 2013).

In order to propose valid correlations of Svecofennian domains and delimiting structures (shear zones) in the northern Fennoscandian shield we will focus on the composition, internal structural architecture, metallogenic deposits and magmatic-metamorphic evolution in different provinces in the northern part of the Fennoscandian shield (Fig. 3), using the RTW (Fig 4) as a framework for regional correlations (Table 1).

3) Structural architecture and evolution of the Rombak Tectonic Window

The RTW is an inlier within the middle allochthon of the Caledonian nappes (Fig. 1) and consists of several N-S trending meta-sedimentary and volcanic belts surrounded by dominantly Paleoproterozoic granitic rocks (Fig. 4; Korneliussen & Sawyer, 1989; Sawyer & Korneliussen, 1989). These belts consist of conglomerates, greywacke, sandstone, marble, biotite schist and graphite schist (Birkeland, 1976; Korneliussen et al., 1986; Korneliussen & Sawyer, 1989; Sawyer Korneliussen, 1989), and these rocks were interpreted to be deposited on an active margin (Sawyer & Korneliussen, 1989). The most easterly sedimentary rocks within the RTW have a intra-oceanic signature whereas the sedimentary belts in the central and western parts of the window display an Andean-type setting (Sawyer & Korneliussen, 1989). The volcanic rocks consist of three main suites; Mg-rich basalts, potassium-rich mafic to felsic volcanites showing calc - alkaline relation, and a low-potassium, calc - alkaline felsic volcanites (Korneliussen & Sawyer, op.cit.). In addition, Romer (1988) described more mafic to ultramafic volcanites at Sjangeli in the easternmost parts of the RTW within Sweden (Fig. 4). Granitic rocks dominate the RTW and consist mainly of monzogranites of Svecofennian age (Gunner, 1981; Romer et al, 1992; Larsen et al., 2013). However, younger 1.71 Ga granites are found in the Norddalen area. The geochemical signature shows that the 1.8 Ga granites are orogenic with magmatic arc affinity and the 1.7 Ga is post-orogenic of within plate affinity from an eastward dipping subduction zone (Romer et al., 1992). A tonalitic complex located in the southern extremity of the RTW (Korneliussen & Sawyer, 1989, Romer et al., 1992) gives an age of 1.95 Ga. This is thought to be the basement for the overlying meta-sedimentary units in the southern part of the RTW at Gautelis.

Ductile shear zones and mylonite zones have been reported from several localities in the RTW (Priesemann, 1984; Skonseng, 1985; Korneliussen et al., 1986; Naruk, 1987; Coller, 2004). However, until recently, systematic structural studies have not been carried out. Larsen et al. (2010, 2012) identified a N-S striking, crustal scale shear zone extending the complete length of the RTW, nucleating on one of the N-S striking metasedimentary packages. This was termed the Rombaken-Skjomen Shear Zone (RSSZ) (Fig. 4). A complex model of Svecofennian transpression was proposed including an early phase of east-directed, N-S trending fold-thrust belt formation (D_1-D_2), followed by a phase of sub-vertical ductile sinistral shearing along steep fold limbs which attenuated and segmented the fold-thrust belt

(D_3). Finally, a phase of steep, NE-SW dextral ductile shearing, diagonally dissected the meta-sedimentary belt into a mega-scale transtensional duplex geometry (D_4). These structures further segmented and attenuated the fold-thrust belt resulting in a highly complex multiphase ductile deformation zone (Figs. 4 and 5).

Metamorphic conditions were interpreted to be at amphibolite facies in most of the RTW (Korneliussen at al., 1986; Romer, 1989). However, Korneliussen et al., (1986) described early-stage amphibolite facies metamorphism in the N-S trending ductile shear zone in the Norddalen area (Fig. 4) followed by greenschist facies retrogression. Furthermore, he described a major shear zone at Gautelis (Fig. 4), composed of ultramylonites, locally displaying high-strain deformation with amphibolites facies metamorphism. Larsen et al. (2013) demonstrated that the entire portion of the RSSZ displayed a high-strain phase with peak amphibolite facies metamorphic conditions followed by greenschist facies retrogression.

Sulphide and gold deposits have been variably documented in the RTW (e.g. Korneliussen et al., 1986; Flood, 1984; Coller, 2004; Korneliussen & Nilsson, 2008). The most important mineralisation includes numerous small Pb-Zn deposits (Lindahl, 1979; Romer, 1989; Coller et al; 2004), in addition to the Gautelis Au-As deposit (Korneliussen & Sawyer, 1986) and the Haugfjellet Pb-Zn-Cu-Au deposit (Coller, 2004). Larsen et al., (2012) constructed a spatial and temporal metallogenetic model to explain the tectonic setting and ore genetic processes and of syn-sedimentary pyrite, pyrrhotite or lead-galena as predominatly SEDEX, a syn-tectonic As-Au-Fe metasomatic deposit and Au-As-Cu orogenic type deposits associated with the RSSZ (Fig. 6; Pb-Pb isotope studies from the SEDEX deposit (Larsen, et al. 2013)), confirmed a syn-sedimentary genesis. Romer (1989) also demonstrated that Cu-Fe-Zn mineralisation within volcanoclastic rocks in the Sjangeli area in Sweden (Fig. 4) are syn-sedimentary. Romer (op.cit.) also described two contamination events from Pb-Pb isotope studies suggesting remobilisation during both the Svecofennian orogeny (Romer, 1989: Svekokarelian) and the Caledonian Orogeny. Larsen et al.(2013) also documented Pb-Pb signatures with a Caledonian influence in the eastern part of the RTW, close to the base of the Caledonian nappes.

Sjangeli and Kopparåsen are the two easternmost supracrustal belts in the RTW and outcrop in Sweden (Fig. 4).They differ slightly to the main part of the RTW but are strongly correlative with respect to similar meta-arkosic sedimentary rock types, orientation/trend and sulphide ore deposits. The rocks in Sjangeli and Kopparåsen consist of meta-sedimentary rocks intruded by Svecofennian granites, however they are thought to be slightly older (2.3-2.0 Ga) and comprise in addition mafic to ultramafic meta-volcanic rocks (Romer & Boundy, 1988; Romer, 1989). Kopparåsen consists of greywacke, meta-tuff, biotite- and graphitic schist, carbonate rocks, breccia, quartzite and conglomerate and mafic lava flows that are believed to be c. 2.3 Ga (Adamek 1975) intruded by a 1.7Ga Lina-type granite (Gunner, 1981; Adamek 1975). In the Sjangeli area the rocks are dominated by Paleoproterozoic volcano-sedimentary rocks intercalated with mafic and ultramafic volcanic rocks. The contact between these two lithologies is commonly mylonitized. The sedimentary rocks resemble those in the Gautelis area (Fig. 4) consisting of mafic tuffs, silicate-banded carbonates and meta-pelites (Romer, 1987).The volcanic units consist of lava flows, high magnesium mafic to ultramafic volcanic rocks and mafic pillow lavas (Romer, 1987). These meta-sedimentary and volcanic units were intruded by a 1.8 Ga granite (Romer et al., 1992). Tonalitic gneisses occur as xenoliths and crustal remnants of Archean TTG (tonalite–trondhjemite–granodiorite) gneisses (2.7 Ga) within the 1.8 Ga granite and have the same composition as the Gautelis tonalite (1.95Ga). Both are assumed to have formed close to a destructive plate margin but at slightly different times (Romer et al., 1992).

Previous descriptions of structures in the Kopperåsen area are sparse. However, faults and mylonite zones are documented along strike with steeply dipping N-S striking sedimentary layers (Adamek, 1973; Romer & Boundy, 1988). Strata of the Sjangeli area have been more strongly metamorphosed and deformed with bedding-parallel ductile shear zones, mylonites and isoclinal folds (Romer 1987). The marbles show bed thickening caused by a major NE-SW dextral ductile shear zone (Romer 1987). Also sinistral post granite but pre-Caledonian mylonitic ENE-WSW trending sinistral shear zones have also been documented. The RSSZ(Fig 4) is interpreted to continue into the Sjangeli area and possibly continues below the Caledonian nappes as far north as the Kuokkel tectonic window (Larsen et al., 2013).

The metamorphic grade in the meta-supracrustal units of the Kopperåsen and Sjangeli areas is upper greenschist facies to lower amphibolite facies, the peak metamorphism likely associated with the Svecofennian Orogenic event. Romer (1987) interpreted the Greenschist facies retrogression as being of Caledonian age (Romer, 1987).

The mineralisation in both the Kopparåsen and Sjangeli areas has been a target for mineral exploration for many years, and the ore-hosting rocks have been sporadically mined for copper in the past (e.g. Hallberg et al.,, 2012). The mineralisation in the Kopparåsen area occurs in volcano-sedimentary rocks and consist of elongated narrow zones of uraninite, magnetite, pyrite, pyrrhotite, chalcopyrite, bornite, galena, sphalerite, gersdoffite, arsenopyrite and molybdenite along bedding (Adamek, 1975). By contrast, Cu-Fe-sulfide mineralisation is found in mylonitic shear zones within mafic meta-tuffaceous rocks and graphite-bearing mica schists. Sulphide mineralisation is believed to be syn-depositional, however, the genesis of the uranium mineralisation may be, in part, hydrothermal, transported by metamorphic fluids along permeable zones during the Svecofennian orogeny (1.78 Ga; Romer & Boundy, 1988). Mineralisation in the Sjangeli area is comprised of mainly bornite, chalcopyrite and chalcocite present as bedding-parallel veins along the strike of the host rocks (Romer, 1987). The bornite is stratiform in bands and lenses along the mafic meta-tuffites together with some chalcopyrite and magnetite. Bornite is also present within quartz veins enriched with magnetite and lamellas of chalcocite. Chalcopyrite occurs as small strata-bound veins in actinolite-rich amphibolites. The mineralisation is interpreted to be of syn-genetic origin, with some potential Caledonian reactivation (Romer, 1987).

4) Structural architecture of other basement inliers within the northernmost Scandinavian Caledonides

4.1) West Troms basement complex

The West Troms Basement Complex (WTBC) is located in the coastal region of western Troms, North Norway, extending from Lofoten-Vesterålen through the island of Senja in the southwest to Vannøya in the northeast (Fig. 3). This basement province is separated from the Caledonian nappes by thrust faults (locally) and regional-scale Mesozoic normal faults. Therefore it is difficult to directly link this province to the autochthonous Fennoscandian shield (Bergh et al. 2012), although a correlation is previously inferred from gravity and magnetic data (Henkel, 1991; Olesen et al. 1997).

The dominant rock types in the WTBC consist of Neoarchean TTG-gneisses (2.9-2.6 Ga) and some intercalations of meta-volcanic and sedimentary units (Ringvassøya greenstone belt) dated at ca. 2.68 Ga (Bergh et al. 2010; Myhre et al. 2011). These Neoarchean rocks were deformed and metamorphosed prior to the intrusion of a major mafic dyke swarm (2.4 Ga: Kullerud et al. 2006) and overlain by Paleoproterozoic volcanic and sedimentary rocks (2.4 – 1.9 Ga), now present in NW-SE trending linear belts (Bergh et al. 2007, 2010, 2012). These belts and the remains of Neoarchean rocks were then intruded by proposed arc-related large felsic/granitic and locally, mafic plutons, at ca. 1.79 Ga (Bergh et al. 2010). They were subsequently deformed and metamorphosed during the Svecofennian orogeny at c. 1.78-1.67 Ga (Corfu et al. 2003; Bergh et al. 2010).

The Svecofennian high-strain deformation zones are crustal scale shear zones enveloping segments of Neoarchean mega-blocks surrounded by metasedimentary belts and anastomosing ductile shear zones confined to the boundaries between metasedimentary rocks and the TTG gneisses, e.g. the Svanfjellet shear zone (Zwaan 1995; Henderson & Kendrick 2003), Astridal shear zone (Pedersen 1997), Torsnes belt (Zwaan et al. 1992; Nyheim et al. 1994) and Mjelde-Skorelvvatn belt (Armitage, 2004; Armitage & Bergh 2005), and the Ringvassøya greenstone belt and the Vanna group in the north (Zwaan 1989; Bergh et al. 2007). The Svecofennian deformation in the WTBC was multi-phased and involved shear zone evolution throughout the region in the time span between 1.78 and 1.67 Ga (Fig. 7; Bergh et al. 2010). The Svanfjellet shear zone in the WTBC (Fig. 3) continues SE below the Caledonian nappes to link up with the Bothnian-Senja shear zone (Fig. 3: Henkel, 1991; Olesen et al. 1997), and this shear zone provides a basis for regional comparison with the Fennoscandian shield (see below). This crustal-scale shear zone displays dominantly sinistral shear sense (Armitage 2001; Henderson & Kendrick, 2003; Armitage 2004; Bergh et al. 2010). Svecofennian deformation in the WTBC is characterised by a strong NNW-SSE trending mylonitic fabric, isoclinal folds, and subsequent upright large-scale folds, associated with top to the NE thrusts formed in the earliest stages of the deformation. These structures were subsequently segmented and overprinted by oblique and orogen-parallel ductile strike-slip shear zones, mainly sinistral but some with a component of dextral shear and additional SE-directed thrusts (Fig. 7). The SE-directed thrust structures are better preserved in the north of the WTBC (for example on Ringvassøya and Vanna) where the effect of the later strike-slip segmentation of the orogen was minimal. Bergh et al. (2010) interpreted all these structures to have formed as a result of NE-SW contraction, with the strike-slip shear zones representing an increased strain partitioning and oblique transpression.

Metamorphism during the Svecofennian tectono-magmatic event in the south-western part of the WTBC mostly occurred at amphibolite facies conditions, with locally upper-amphibolite grade in the Svanfjellet shear zone belt (Zwaan 1990, 1992; Zwaan 1995), whereas greenschist facies conditions prevailed in the metasedimentary units in the north-eastern domains (i.e. Vanna) and the late-Svecofennian shear zones throughout the region (Bergh et al. 2007, 2010).

A number of workers have addressed the potential for Cu, Zn, Au deposits in the WTBC. In particular, gold occurrences are documented in the Ringvassøya greenstone belt (Sandstad & Nilsson 1998). In addition, stratiform ore bodies and also possibly VMS-deposits may be linked to iron-enriched meta-sedimentary rocks and in quartz-veins associated with the shear zones, intrusive bodies and felsic volcanic units (Ihlen & Furuhaug 2000; Henderson & Kendrick 2003). Notably, in the Ringvassøya greenstone belt, stratiform sulphide and gold quartz deposits have been remobilized and enriched along the youngest Svecofennian-aged, low-angle thrusts and steep strike-slip shear zones (Bergh et al. 2010). Gold has been found to positively correlate to Cu and Ag in quartz veins within volcanic rocks in the contact zone between the TTG-gneisses and the greenstone belt or in relation to quartz diorite intrusions. The quartz veins are commonly boudinaged. Enrichment of Au, Ag and Zn also found within a volcanoclastic schist horizon (Sandstad & Nilsson, 1998).

4.2) Mauken tectonic window

The Mauken Tectonic Window (MTW) to the north of the RTW is a small, elongated tectonic window surrounded by Caledonian thrust nappes (Fig. 3). Previous work from this area describes a geographically limited (10km wide and ca 50km long), WNW-ESE striking, strongly deformed greenstone belt, dominated by greenschist facies metamorphosed basalts, amphibolites, schist and meta-psammites intruded by 1.8–1.7 Ga granodiorites (Vognsen, 2010). Recent prospecting activity within the meta-supracrustal unit shows that gold is enriched within a NW-SE trending, steep ductile strike-slip shear zone that trends parallel to the strike of the MTW. However, no further kinematics or structural data allow comparison with the RTW (Vognsen 2010). This shear zone is thought to be linked with the regional-scale NW-SE trending Bothnian - Senja fault zone (Fig. 1, 3) Regional comparison of the MTW deposits with similar gold deposits along the same structural trend as this shear zone suggests that they are structurally controlled (Almås 2013).

4.3) Alta-Kvænangen, Altenes and Komagfjord-Repparfjord tectonic windows

The Alta-Kvænangen, Altenes and Komagfjord-Repparfjord tectonic windows are located in the Finnmark region in Northern Norway, and consist of various meta-volcanic and sedimentary rocks (greenstone belts). These apparently similar greenstone belts are part of a chain of basement culminations within the Kalak Nappe Complex of the Finnmark Caledonides (Fig. 3), and are thought to be the northwards continuation of the Kautokeino greenstone belt exposed to the east of the Caledonian thrust nappes (e.g. Pharaoh & Pearce 1984).

In the Alta-Kvænangen area, the greenstone belt consists of low-grade tholeiitic volcanics, carbonates/dolomites and clastic sedimentary rocks of the Raipas Group (Gautier, 1975; Zwaan & Gautier 1980; Vik 1985; Bergh & Torske 1988) dated as Paleoproterozoic (Krill et al. 1985; Sandstad et al., 2012) and interpreted to have formed in a rift basin correlated with the Kautokeino greenstone belt (Bergh & Torske, 1988). The rocks are then intruded by mafic, ultramafic and felsic rocks and overlain by a thin Neoproterozoic cover (Pharaoh & Pearce 1984; Gautier et al., 1986). The lower Raipas Group consists of the Kvenvik and Storviknes Formations and can be correlated to both the Repparfjord and Altenes Windows (Jensen, 1996). In the Altenes area, the windows consist of two internal volcano-sedimentary sequences, the oldest Brattholmen Group of calk-alkaline composition and the youngest of meta-tholeiitic composition. These are overlain by clastic conglomerates, shales and carbonates of the Sagelv Group. The volcanites are thought to be part of an arc-derived volcanic-sedimentary sequence that resembles the Kiruna and the Skellefte district (Jensen 1996). Similarly, the Komangfjord-Repparfjord window consists of the Holmvatn- Saltvatn , Nussir and Porsa Group metavolcanic and metasedimentary rocks of Paleoproterozoic age, overlain by Neoproterozoic sedimentary rocks intruded by mafic, ultramafic and felsic intrusive rocks (e.g. Jensen, 1996; Nilsen & Nilsson, 1996; Pharaoh et al., 1983). Specific horizons of meta-arenites, conglomerates, dolomites and siltstones (Ulveryggen, Djupelv and Stangvatn Formations) comprise the extensive copper deposits of the Nussir mine (Pharaoh et al. 1983).

The Alta-Kvænangen, Altenes and Komagfjord-Repparfjord Tectonic Windows are largely similar with respect to lithology, stratigraphy, age, composition and metamorphic grade of the rocks. However, the structural trends (Fig. 8) differ and show a lack of continuation (e.g. Gautier, 1975; Pratt, 1989;). In the Alta-Kvænangen area, N-S trending open asymmetric, upright folds affected the Raipas Group rocks (Zwaan & Gautier 1980). In the Altenes area, there are imbricated fold-thrust structures that show a NE-SW trend similar to the Komangfjord-Repparfjord window (e.g. Pratt, 1989; Jensen 1996; Rodinov et al., 2012), which is believed to be the northern continuation of the Altenes Window where the Alta-Kvænangen window is thrusted on top of the Altenes window (e.g. Pratt, 1989). The overall structure is a regional-scale ENE-WSW trending upright fold system where the lowermost Holmvatn Group occurs in the core of an antiform (Viola et al., 2008; Ofstad et al., 2013). Three different Precambrian folding events have been defined (Viola et al., 2008), including early ENE-WSW trending upright and open to tight folds (D_1) affecting only the Saltvatn Group, then SW-NE trending, upright to inclined, tight to isoclinal folds with a moderate plunge with axial surfaces dipping to the NW (D_2), and finally open folds trending SSW-NNE and plunging moderately to the NE (D_3). The D_3-folds are of kilometric scale and are linked to NE-SW trending strike-slip shear zones with a dextral shear sense. These folds also largely affected the upper Saltvatn and Nussir Groups (Viola et al., 2008; Torgersen et al., 2013). Viola et al (2008) interpreted D_1-D_3 to represent a regional transpressive event involving strain partitioning due to overall NW-SE shortening, as supported by the study of (Torgersen et al. 2013). There are no age constraints for these structures.

The metamorphic grade of the meta-volcanic/sedimentary rocks is generally low and of lower to upper greenschist facies. Primary structures are well preserved in the Alta Window (Gautier, 1975; Gautier et al., 1979; Zwaan & Gautier, 1980; Jensen, 1996; Torgersen et al., 2013). The metamorphic grade in the Komagfjord-Repparfjord Window increases southwards to amphibolite grade in the Altenes Window, where the Svecofennian deformation is more pervasive (Bergh & Torske, 1988; Jensen, 1996).

All of these windows are characterised by Gold-Copper deposits and have been a frequent target for mineral exploration and mining since the early 1800s (Sandstad et al., 2012). Mineral deposits are hosted by metasedimentary and volcanic rocks, both of a epigenetic and syngenetic origin (e.g. Bjørlykke et al., 1985; Sandstad, 1986). The Alta-Kvænangen window hosts two significant Cu deposits; the Kåfjord and Raipas deposits. The Kåfjord deposit is found in quartz-carbonate veins in brecciated metagabbro and basalts in the Kvenvik Formation of the lower Raipas Group. The deposit has been interpreted to be epigenetic with respect to a sub-horizontal shear zone (Mørk, 1970). The Raipas deposit is mainly located in the matrix of karst breccias of dolomite above the Kvenvik Formation and is related to red-bed copper or karst-related lead-zinc deposits (Vik, 1985). In the Komangfjord-Repparfjord Tectonic Window there are several copper deposits with a high potential for new discoveries. At least five deposits are significant including the Repparfjord, Nussir, Porsa, Bache and Vesterdalen deposits (Sandstad et al., 2012). The Repparfjord copper deposit is found in sandstones and conglomerates of the Ulveryggen Formation in the Saltvatten group and consists mainly of ENE-WSW trending and stratiform lens-shaped bodies. The Nussir copper deposit is also found in schist, sandstone and dolomite of the Saltvatten group and the mineralisation is localised along a ENE-trending lens with a steep to moderate dip (Sandstad et al., 2012). The Porscha copper deposit is hosted by two parallel carbonate-quartz veins within greenstones of the Svartfjell Formation in the Nussir Group. The veins are steeply-dipping, E-W trending and located within a larger semi-ductile shear zone trending NE-SW (Viola et al., 2008). The Bachke copper deposit is similar to the Porcha deposit, but is found in steeply-dipping carbonate veins in greenstones trending NW-SE (Sandstad et al., 2012). The Vesterdalen gold-copper deposit is not well understood (Sandstad et al., 2012) but is defined by veinlets, aggregates and disseminations of mineralisation hosted by sandstone and impure dolomite and is overlying the Nussir Group.

5) Structural architecture of Svecofennian provinces in autochthonous parts of northern Sweden and Finland

Meta-supracrustal units located to the east of the Caledonian thrust front in northern Norway, Sweden and Finland have been regarded as autochthonous as they were generally deposited directly onto the underlying Archean basement in Paleoproterozoic sedimentary basins (e.g. Melezhik & Sturt 1994; Torske & Bergh, 2004).

5.1.) Karasjok greenstone belt

The Karasjok Greenstone Belt (KjGB) is located in the north-eastern part of Finnmark, and is bounded by the Caledonian thrust front (Fig 3). It is a N-S trending belt that can be traced southward to link up with the Kittilä greenstone belt of central Finland (e.g. Patison, 2007) (Fig. 3). The KjGB (Marker, 1985; Braathen & Davidsen, 2000) is assumed to be of Paleoproterozoic age and consists mainly of meta-basalts, meta-sedimentary rocks, komatites and gneisses with intrusions of meta-gabbros (Siedlecka & Roberts, 1996). The contact to the assumed Archean basement is unconformable and tectonically bounded by a thrust (Braathen & Davidsen, 2000).

The northern part of the KjGB is an inlier termed the Karasjok-Levajok tectonic belt, and is an east dipping tectonic wedge with several, repeated fold- and thrust nappes juxtaposed with the surrounding basement provinces to the east and composed of granulite facies gneisses and migmatites (Siedlecka et al. 1985) (Fig. 9). Braathen & Davidsen (2000) suggested a four stage structural evolution with initial west-directed thrusting (D_1) (Fig. 8), followed by SSE-verging folding and thrusting associated with NNE-SSW shortening and generation of dextral and oblique thrust-related strike-slip faults (D_2). These structures were later refolded into N-S trending upright folds as a result of E-W shortening (D_3). All these thrusts were cut by dextral NW-SE and NE-SW striking subvertical, strike-slip semi-brittle faults which are thought to be post-Svecofennian (D_4), but older than the Caledonian deformation (Braathen & Davidsen, 2000).

The KjGB underwent regional amphibolite facies metamorphism during the Svecofennian fold-thrusting events (Sandstad et al., 2012). However, remnants of Archean tectono-thermal events have been inferred from the presence of granulite facies metamorphic assemblages (Marker, 1985).

The greenstone belt hosts several important deposits, including placer gold, komatites and associated BIF in the volcano-sedimentary rocks and Ni-Cu-PGE deposits in ultramafic and mafic intrusions (Sandstad et al., 2012). Placer gold has been extensively explored and is found mainly in superficial river sediments and basal till deposits. However, the bed rock source of the gold is yet unknown (Often, 1985; Sandstad et al., 2012). Several low grade metamorphosed gold-hosted lithologies with associated copper deposits, have been detected along the basal thrust zone to the west. These have been suggested to have formed both as stratiform, syngenetic and/or epigenetic relative to the Svecofennian fold-thrust event (Often, 1985; Bjørlykke et al., 1985; Sandstad et al., 2012).

5.2) The Kautokeino greenstone belt

The Kautokeino greenstone belt (KkGB) is located west of the KjGB and can be traced from the Caledonian nappe front in Finnmark southward across the border into Northern Finland. The KkGB is linked with the Central Lapland greenstone belt, which is well known for its orogenic gold ore deposits (e.g. Härkönen et al., 1999; Eilu et al., 2003; Hanski & Huma, 2005 Patison, 2007) (Fig. 1). The KkGB is also assumed to be the southwards continuation of the Alta-Kvænangen Tectonic Window underneath the Caledonian nappes. The lithologies in the KkGB consist of Paleoproterozoic volcano-sedimentary rocks comprising the Caskejas, overlain by the Bickkacåkka and Caravarri Formations (e.g. Siedlecka et al., 1985; Torske & Bergh 2004). These Formations overly the Archean Raisadno Gneiss Complex which is thought to be the basement even though no sedimentary contact has been documented. The Kautokeino greenstone belt has traditionally been interpreted as an early Paleoproterozoic rift basin containing shallow marine sediments and volcanics formed during crustal extension subsequently subjected to crustal collision associated with the Svecofennian orogeny (1.92-1.79 Ga; Siedlecka et al., 1985; Olesen & Sandstad, 1993; Lahtinen et al., 2012).

Despite extensive bedrock mapping during the 1980's (Seidlecka et al., 1985) the structural geology and tectonic development of the KkGB has remained enigmatic, mainly due to a paucity of data in an area with very limited outcrop. Reprocessing of high resolution aeromagnetic data allowed Henderson & Viola (2013) to propose a structural model for the KkGB, including an early phase of top-to-the west thrusting and folding with subsequent ductile sinistral NNW-SSE trending strike-slip shearing along the Bothnian-Kvænangen Fault Complex (Olesen & Sandstad, 1993).

The metamorphic grade of the KkGB is generally low, from upper greenschist to lower amphibolite facies increasing towards the outer boundaries of the greenstone belt (Sandstad, 1983; Olesen & Sandstad, 1993). The gold and copper mineralisation in the KkGB is thought to be associated with the latest phase of post peak metamorphism accompanying Svecofennian strike-slip deformation (Henderson & Viola 2013; Ettner et al., 1993; Ettner et al., 1996; Sandstad et al., 2012). However, the tectonic and metallogenic relationship of the KkGB, to the adjacent KjGB and also to the Central Lapland greenstone belt and Alta-Kvænangen Tectonic window is still poorly understood. The Bidjovagge gold-copper deposit located in the NW of the KkGB, is the only exploited deposit and operated between 1952-1991. The ore bodies are found within altered volcanic rocks (albite felsites) interbedded with graphitic schist and dolerite in the lowermost Caskejas Formation (Nilsen & Bjørlykke, 1991). Three mineralisation types were recognized, comprising copper and sulphide rich carbonate veins, gold in sheared and brecciated albite felsites as disseminations and in quartz veins, and gold in tellurides in brecciated albite felsites (Ekberg & Sotka, 1991). The ore deposits are lens shaped and found within shear zones cutting the limbs of an upright antiform

(Bjørlykke et al., 1993), and are classified as orogenic gold with atypical metal associations (Sandstad et al., 2012).

5.3.) Tjåmotis district

The Tjåmotis District, occur south of the RTW and east of the Caledonian nappes, and is a N-S trending meta-sedimentary belt extending southward from beneath the frontal part of the Caledonian nappes (Fig. 3). The meta-sedimentary belt consist of two main groups termed the Arvidsjaur Group and Snavva-Sjöfalls Group (1.9-1.8 Ga; Ödman, 1957; Quesada & Niva, 1981; Carlon, 1984 Bergström, 2001; Kathol et al., 2011; Kathol et al., 2012). The Arvidsjaur Group is the stratigraphic lowermost part and consists of basaltic to rhyolitic volcanoclastic rocks and sandstones interpreted to have formed in back-arc related and/or mature craton-marginal basins (e.g. Allen et al. 1996). It is thought to be partly equivalent to the Vargfors Group found in the Skellefte district (Bergman & Weihed, 2001). The Snavva-Sjöfalls Group was mainly deposited to the west of the Arvidsjaur group and consists of meta-arkoses, quartzite, siltstone, mudstone, micaschist and greywacke (Ödman, 1957). The meta-sedimentary rocks are intruded by the younger coarse grained Lina granite of monzonitic composition (Quesada & Niva, 1981; Carlon, 1984), and is thought to be of early Svecofennian in age (or Svekokarelian; c. 1.8 Ga) (e.g. Carlon, 1984; Kathol et al., 2011). The meta-sedimentary rocks are surrounded by felsic volcanics to the east and west which are andesitic and dacitic. These were recently dated to 1.88-1.86 Ga age (Perdahl & Einarsson, 1994; Kathol et al., 2008; Kathol et al., 2011).

The large-scale structure of the Tjåmotis metasedimentary belt is poorly understood. The main foliation trends NNE-SSW, parallel to the margins of the belt, with a varying dip from 20-90º (Quesada & Niva, 1981; Carlon, 1984; Kathol et al., 2012). Foliation-parallel mylonitic shear zones are observed in alternation with partly folded primary units. Three groups of folds were described (Carlon, 1984); early macro-and mesocale synformal and antiformal isoclinal folding, with horizontal fold axes and steep east dipping axial surfaces (F_1), were followed by sub vertical folding around steep NE-SW plunging axes (F_2). Finally an event of open folding and/or doming related to granite intrusions (F_3). Sets of NW-SE and NE-SW trending, semi-brittle lineaments crosscut all of the fold structures. NNE-SSW trending lineaments were interpreted from aeromagnetic investigations (Quesada & Niva, 1981), and considered to be older than the NW-SE and NE-SW lineament sets (Nylund & Nisca, 1981). Major lineaments on aeromagnetic surveys in the Arvidsjaur area (fig. 10), were interpreted as an array of late ductile shear zones trending NNE-SSW (Rutland et al., 2001). The metamorphic grade during these deformation events reached locally, amphibolite facies conditions (Carlon 1984).

Several mineralisation occurrences are described in the Tjåmotis area. For example, Mo-W minerals are present in relation to deformed acidic volcanic rocks in skarn deposits at the border between meta-volcanics and the Snavva-Sjöfalls Group (Theolin & Wikström 1979; Holmquist et al., 1982). Theolin & Wikström (1979) described a As-Zn occurrence in skarn marbles of the Snavva-Sjöfalls Group, Cu-Pb-Zn deposits in rusty granites, and Ti enriched in mafic rocks. In addition, chalcopyrite, bornite, pyrite, sphalerite, galena, chalcocite, magnetite and gold occur in quartz- biotite- and amphibole-bearing meta-sediments of the Snavva-Sjöfalls Group, the felsic volcanics of Arvidsjaur Group and feldspar-biotite gneisses (Kathol et al., 2012; Billström et al., 1997). Billström et al., (1997) demonstrated that Pb-isotopes in galena from the Tjåmotis area differed from the Svecofennian arc terrains to the south-east and display a pre-Svecofennian age signature of 2.0 Ga or earlier. This confirmed the work of Sundblad (1986) and Sundblad (1991) from Pb-Pb isotope data that demonstrated two mineralisation events, one related to the Paleoproterozoic basin development and the second related to the volcanic arc-forming event.

5.4.) Skellefte district

The Skellefte district in northern Sweden lies to the north of the Bothnian basin and southwest of the Archean- Proterozoic boundary (Fig. 3). The boundaries of the metasedimentary units is poorly exposed, but it is assumed to be close to the city of Skellefteå and traceable westwards.

The rocks in the Skellefte district consist of two sequences; the underlying Skellefte group composed of subaqueous volcanic rocks that have been associated with an extensive Paleoproterozoic rifting event (Vivallo and Claesson, 1987), overlain by the Vargfors group which consists of 1.875Ga (Billström & Weihed, 1996), shallow-water meta-sedimentary, greywacke and volcanic rocks with a MORB tholeiitic composition (Bergman & Weihed, 2001; Bergström, 2001). These were intruded by several generations of granitic plutons; the 1.89-1.88 Ga Jörn granite (Wilson et al., 1987; Weihed & Schönberg, 1991), 1.88 Ga Sikträsk granite (Weihed et al., 2002) and 1.81-1.77Ga Revsund Granite (Claesson & Lunquist, 1995; Billström & Weihed, 1996; Weihed et al., 2002). The metasedimentary rocks in the Skellefte district are interpreted to have been formed in a volcanic arc-setting that marked the onset of later Svecofennian accretion (Weihed et al. 2002; Juhlin et al. 2002).

Three deformation structures are described from the Skellefte district; as a main sub horizontal foliation (D_1) that is later overprinted by tight to isoclinal folds (D_2), and followed by more open folds and subsequent steep ductile shear zones (D_3). The two latter deformation features are an integrated part of a major ductile shear zone, the Skellefte Shear Zone (Bergmann & Weihed, 2001; Malehmir et al., 2007). The isoclinal folds display gentle N-dipping, axial surfaces, present in the eastern and western part of the Skellefte district, whereas in the central part, the foliation is more NW-SE striking (Bergmann & Weihed, 2001). The D_3 deformation is characterised by steep approximately N-S striking ductile strike-slip shear zones which cross-cut and displaced the older foliation and isoclinal D_2-fold structures both dextrally and sinistrally. These structures are associated with more open folds with steep axial surfaces striking N-NE and with associated oblique-slip shear zones. The D_2 fabric was the result of NW-SE directed crustal shortening and foliation-parallel thrusting with top-to-the south movement (D_2; Bergmann & Weihed, 2001). This is in contrast to Malehmir et al (2007) who introduced the Skellefte shear zone to include two major WNW-ESE striking and N-dipping thrust faults, with associated hanging wall anticline structures, and in which the Skellefte volcanic rocks were thrusted over the rocks in the Bothnian basin. This model was confirmed by Rodriguez-Tablante et al. (2007) and Hübert et al. (2009).
D_3 was interpreted to be a result of E-W convergence with possible transpression (Bergmann Weihed, 2001; Weihed et al., 2002). The timing of D_2 is interpreted to be older than the 1.81-1.77 Ga Revsund Granite (Claesson & Lunquist, 1995; Billström & Weihed, 1996; Weihed et al., 2002) but younger than the Sikträsk granite age of 1.88 Ga (Weihed et al., 2002). The D_3 event is interpreted to be syn- to post intrusion of the Revsund granite, as the granite is partially affected by D_3 shear zones (Bergmann & Weihed, 2001; Rutland et al., 2001; Weihed, 2003).

The Skellefte district suffered greenschist to lower amphibolite facies metamorphism, with increasing grade southwards towards the Bothnian basin. Peak metamorphism occurred at 1.84-1.8 Ga (Bergström, 2001; Weihed et al., 1992).

The Skellefte ore district is known for its long mining history (see Hallberg et al., 2012). The mineralisation occurrences in the area have been divided into at least three types. These are gold-rich VMS, Porphyry copper and Orogenic gold deposits. However, their age and nature is not well constrained and they potentially display several episodes of mineralisation and remobilisation (Billström & Weihed, 1996; Allen, 2008; Hallberg et al., 2012). Billström & Weihed (1996) suggested a two stage depositional model for the VMS deposits occurring at ca. 1885 to 1880 Ma and at ca. 1875 Ma. Lahtinen et al. (2012) interpreted the Boliden VMS deposits in a 1.9-1.88 Ga volcanic arc setting and the Björkdal orogenic gold deposit in a 1.89-1.88 Ga collisional setting. Remobilisation of the ore deposits in the Skellefte District is interpreted to have occurred during the Svecofennian Orogeny.

5.5.) The Bothnian basin (Lycksele-Storuman district)

The Bothnian basin covers a large area from the Transscandinavian igneous belt in south-western Sweden, through Bergslagen, and northward to the Skellefte district (Fig. 1). The boundary to the Svecofennian province of central/western Finland is marked by a transition between high grade metamorphic marine mudstones of the Bothnian basin to low grade volcanic rocks and shallow water to sub aerial rocks of the Arvidsjaur Group (Weihed et al., 1992). The dominant bedrock of the entire Bothnian basin area consists of an estimated 10km thick succession of mainly meta-greywacke and mudstones deposited in a continental margin environment (Lundquist, 1987). The Bothnian basin developed in the time period between c. 2.45 and 1.95 Ga, by rifting of the Archean continent (Nironen, 1997). The depositional timing of the meta-greywacke succession is interpreted to be pre-1.95 Ga to approximately 1.87.Ga (Claesson et al., 1993; Nironen, 1997; Lunquist et al., 1998). Igneous rocks such as gabbros and granitoids intruded during the Svekokarelian event at 1.9-1.8 Ga (Claesson & Lunquist, 1995).

This large continental basin has been subdivided into four sub-areas based on assumed differences in lithology; the Loos-, Naggen-, Central Norrland- and Lycksele-Storuman sub-areas (Kumpulainen, 2009). This description will focus on the Lycksele-Storuman sub-area, which differs from the southern Central Norrland sub-area by containing up to 50% graphitic schists (Eliasson et al., 2001; Kumpulainen, 2009), commonly with pyrrhotite dissemination. The main successions of the Bothnian basin in the Lycksele-Storuman sub-area include meta-conglomerates, sandstones, greywackes and schists interbedded with some volcanic units (Kumpulainen, 2009). A lower meta-volcanic unit has a MORB-basaltic signature (ca. 1.95Ga), and is overlain by a younger sequence of meta-sedimentary rocks interpreted to be deposited in a continental arc setting (Bergström, 2001). The intercalated basalt-rhyolite volcanic rocks are interpreted as island arc basalts (Bergström, 2001; Bark & Weihed, 2007). In the Lycksele-Storuman sub-area, the metasedimentary rocks were intruded by I-type granites at 1.95-1.85 Ga, by S-type granites at1.82-1.80 Ga and by alkali-calcic granites at 1.81-1.77 Ga (Claesson & Lunquist, 1995; Billström & Weihed, 1996; Weihed et al., 2002). These granites are transitional between volcanic-arc granite and syn-collisional granite (Ahl et al., 2001; Bark & Weihed, 2007).

Structurally, the meta-sedimentary rocks of the Lycksele-Storuman sub-area are similar to that of the Skellefte District (Fig. 10; Rutland et al. 2001) and were folded and thrusted along major E-W striking ductile shear zones, and overprinted by WNW-ESE to NE-SW trending steeply dipping oblique-slip shear zones (Rutland et al., 2001; Bark, 2005; Bark & Weihed, 2007; Kumpulainen, 2009; Samskog, 2011). In contrast to the Skellefte District, the main foliation in the Lycksele-Storuman area formed during the D_1 event, axial-planar to sub-horizontal isoclinal folds (Bark, 2005). Later E-W trending ductile D_2 thrust zones formed at the boundary to the Skellefte district (Fig. 10) as part of the Skellefte sub-zone (Rutland et al., 2001). The main foliation was described as steep NW-SE to NE-SW striking ductile shear zones with a transpressive oblique reverse and dextral shear sense (Bark & Weihed, 2007). On the other hand, Rutland et al., (2001) described the same structures as regional D_3 structures.

The meta-sedimentary rocks in the Bothnian basin are amphibolite facies (Allen et al., 1996; Bark, 2005) and locally granulitic (Hallberg, 1994; Lundström, 1998), with peak metamorphism dated at c. 1.85 to 1.80 Ga (Weihed et al., 1992; Billström & Weihed, 1996; Weihed et al., 2002; Bark et al., 2007).

The structures are spatially linked to the common gold occurrences in the area. The gold mineralisation in the area is closely associated to arsenopyrite- löllingite and stibnite in boudinaged quartz veins parallel to the oblique-slip dextral and reverse shear zones (Bark & Weihed, 2007). In addition, Bark et al. (2007) links the mineralisation in the Fäboliden gold deposit to the peak metamorphism in the area, and suggest the mineralisation to be of an orogenic type deposit (Bark & Weihed, 2007).

6) Discussion

The regional extent and correlation of volcano-sedimentary sequences associated with the Svecofennian orogen across the northern Fennoscandian shield is widely discussed and is not particularly well understood (Skiöld & Rutland 2006; Høgdal et al. 2007; Hermansson et al. 2007). This paper addresses general similarities of basement tectonic inliers of the Caledonides and the Fennoscandian Shield east of the Caledonides with respect to lithology, tectono-stratigraphy, composition, volcano-sedimentary and magmatic history, and the relationship to Svecofennian tectono-metamorphic evolution (See table 1). We further apply mineralisation as a tool to correlate the different areas and events, in order to present a regional tectonic-metallogenic model. Most of the mineralised deposits present in the Fennoscandian Shield formed within rift-related meta-volcanic and sedimentary deposits (2.1-1.9 Ga), when the Kola ocean opened (e.g. Marker, 1985,). These deposits were later segmented or remobilised during the Svecofennian Orogeny, i.e. closure of the Kola Ocean with subduction-accretion and final continent-continent collision. Therefore a thorough understanding of the initiation (rifting) of the Kola Ocean and later, Svecofennian convergent tectonism and remobilisation history will ultimately lead to a better understanding of the processes responsible for the genesis of the mineral deposits.

The sections in this chapter will discuss the similarities and differences across the Fennoscandian shield in light of rock types, structures, metamorphism and mineral deposits. We first discuss correlation of the RTW and other tectonic inliers of the Caledonides with provinces and events elsewhere in the Fennoscandian Shield. Subsequently we discuss the Paleoproterozoic rifting and magmatic events leading to formation of the Kola Ocean (2.5-1.9 Ga), and finally, establish a framework for the Svecofennian components and structural architectures. Although similar regional correlation efforts have been done in Finland and Sweden (e.g. Nironen et al., 1997), few studies have included structural details from the basement inliers of the northernmost Scandinavian Caledonides.

6.1. Archean and Paleoproterozoic basement and 2.5-1.88 Ga rifted continental margin (Kola Ocean)

Despite its location as a Caledonian inlier, the RTW shows strong similarities on a regional scale with Fennoscandian provinces east of the Caledonides, notably in the Norrbotten craton. This correlation is most notable in terms of lithology, composition, age, volcano-sedimentary and magmatic history (Table 1), and therefore a direct link can be inferred between the inliers and the autochthonous Fennoscandian Shield of Sweden and Finland. The rocks in the RTW are dominated by Paleoproterozoic metavolcanic and metasedimentary rocks overlying tonalitic basement rocks, and intruded by granitic plutonic rocks (1.8. Ga). Similar basement-cover and magmatic rock associations are present in the Skellefte, Tjåmotis and the Lycksele-Storuman districts and the Bothnian basin in Sweden, and in other tectonic inliers of the Caledonides in northern Norway. The similarities between the RTW (Larsen et al. 2013) and the Tjåmotis, Skellefte and Lycksele-Storuman districts (Quesada & Niva, 1981; Lundquist, 1987; Billström & Weihed, 1996) suggest that the RTW, and possibly also the West Troms Basement Complex (Bergh et al. 2010, 2014) and related inliers farther north (Mauken, Alta, Altenes and Repparfjord-Komagfjord units) belong to the westernmost part of the Norrbotten craton, which is part of the northern margin of the Bothnian basin in Finland and Sweden. Such a regional connection of the RTW was earlier indicated by Korneliussen & Sawyer (1989), but not verified by regional and detailed data across the Caledonian thrust cover.

In the following sections we will discuss the basement rocks that provide the sub-stratum for the overlying meta-volcanic and metasedimentary (greenstone belt), rifted continental margin deposits.

>2.5-1.94 Ga Archean basement rocks

The studied basement provinces in the north, including the WTBC, Mauken, Altenes-Komagfjord-Repparfjord, Alta, Kautokeino and Karasjok provinces, are all characterised by Archean gneisses and components below the Paleoproterozoic (greenstone belt) cover sequences, and therefore, all provinces belong to the Fennoscandian Archean craton. For example, the basement rocks in WTBC represent Meso-Neoarchean rocks (Bergh et al., 2012) and the Kautokeino Greenstone belt is assumed to be underlain by Archean gneiss complexes (Olesen & Solli, 1985; Sandstad et al., 2012). In addition, the Karasjok Greenstone Belt is tectonically bounded to the Archean basement suites by thrust faults.

The RTW, however, is presumed to be located just southwest of the western edge of the Archean craton (fig. 2), since obvious Archean basement rocks are absent.

The basement rocks of the RTW consist of a tonalite complex found at Gautelis (fig. 4), dated to 1940±26 Ma (Romer et al. 1992), corresponding in age (c. 1959 Ma; Eliasson & Sträng,

1998) and composition with the felsic magmatic complex in the southern part of the Skellefte and Lycksele-Storuman districts (fig. 3) (Korneliussen & Sawyer, 1989). The tonalitic gneiss complex is geographically constrained to the Gautelis locality and may only occur as an incorporated basement-lens within the major Rombak-Skjomen shear zone (e.g. Larsen et al., 2013).The similar aged tonalitic lithologies documented in the Bothnian group south of Skellefte district in the Lycksele-Storuman area, supports this correlation. The lower, MORB-basaltic rocks of the Bothnian group may be the basement to the overlying arc-related volcanic and sedimentary rocks (Bergström, 2001) and thus, probably also the local sub-stratum to the RTW greywacke succession..

2.5-1.9 Ga rift-related metasedimentary and volcanic rocks

Break-up of the Archean craton in the Paleoproterozoic (2.5-1.9 Ga) caused rifting and basin-formation across a wide NW-SE trending zone along the south-western margin of the craton. Based on correlative volcano-sedimentary units in the Tjåmotis, Skellefte and Lycksele-Storuman districts in Sweden (Table 1), we believe the margin boundary zone between the Archean and Paleoproterozoic basement continued northwards from the Luleå-Jokkmokk zone to link up with the RTW.

The metasedimentary rocks in the RTW show many similarities to the greywacke/schist units described in the Snavva-Sjöfalls group from the Tjåmotis district (Fig. 1), the Bothnian group in the Lycksele-Storuman region (Fig. 1) and the Vargfors Group overlying the Skellefte Group to the west of the Skellefte district. They consist of marine to shallow water continental margin-like mudstone deposits and volcanoclastic sediments linked to the Bothnian basin margin (e.g. Ödman, 1957; Korneliussen & Sawyer, 1989; Sawyer & Korneliussen, 1989; Bergström 2001; Bark, 2005).

The metasedimentary units in the RTW were deposited on top of a 1.95 Ga tonalite basement rock and are intruded by a younger, 1.79 Ga granite. Recent radiometric age Pb-Pb dating show that greywackes in the Tjåmotis district in Sweden and from Sildvika in the RTW (fig. 1) were all derived from a Svecofennian source (Larsen et al. 2013). The Pb-signatures in Galena from the Tjåmotis district within the Snavva-Sjöfalls group are of pre-Svecofennian age (Sundblad, 1991). The Tjåmotis meta-sedimentary units were likely deposited in the time period 2.5-2.0 Ga (Billström et al., 1997; Martinsson, 1997). However, the Vargfors Group, which is believed to be an equivalent to the Arvidsjaur group is also found in the Tjåmotis and

Skellefte districts, and is dominated by greywacke dated to 1.875Ga (Billström, 2001; Weihed, 1996). This suggests that greywacke sequences in the Tjåmotis and Skellefte districts are part of the same greywacke belt and of similar age to the RTW greywackes, possibly incorporated or overlain by slightly older units from the Snavva-Sjöfalls Group.

Similarly, the metasedimentary and volcanic rocks in the Lycksele-Storuman district are believed to have been deposited in a continent-margin arc-setting, confirmed by the presence of calk-alkaline volcanic rocks (Bark & Weihed, 2007). Geochemical studies of volcanic rocks in the RTW show that the mafic to calk-alkaline components of the volcanic rocks and also the mafic detritals within the greywacke sequences increased in volume from west to east and developed progressively from mafic to felsic compositions through time (Korneliussen et al., 2013). This supports the presence of an arc system along this presumed Archean-Paleoproterozoic boundary zone in transition from an island arc into a continental arc (e.g. Korneliussen & Sawyer, 1989; Larsen et al., 2013).

Several Paleoproterozoic metasedimentary belts are also found in basement windows in northern Norway. For example, the sedimentary belts in the WTBC (Bergh et al. 2010) and the Lofoten-Vesterålen areas (e.g. Griffin et al. 1978; Corfu 2004) show similarities to the RTW. In the WTBC the metasedimentary belts span in age from c. 2.7 Ga in the Ringvassøya greenstone belt (Motuza, 1998), 2.4-2.2 Ga in the Vanna Group (Bergh et al. 2007) to c. 1.97 Ga in the Torsnes belt (Myhre et al. 2011). The Torsnes metasedimentary belt consists of basal conglomerates deposited on a Neoarchean basement, and overlain by meta-psammites and mafic metavocanic rocks with a maximum deposition age of 1970±14Ma (Myhre et al., 2011). The metasedimentary rocks in the Mjelde-Skorevatn belt consist of volcanoclastic deposits, mudstones/schists, meta-psammites and some marble intercalations (Armitage & Bergh 2005), with a maximum age of 1992± Ma (Myhre et al., 2011). These meta-sedimentary belts are interpreted to represent different stages in the development from a cratonic-marginal rift-basin (passive margin) in the 2.5-1.9 Ga period (Bergh et al. 2010), to the onset, of arc development along an active margin of the Svecofennian orogeny (Bergh et al. 2010; Myhre et al., 2011). The Senja Shear Belt of the WTBC (Zwaan 1995; Bergh et al. 2010) is potential the northernmost boundary zone between the Archean and Paleoproterozoic domains. We tentatively suggests a link the with the Tjåmotis, Lycksele-Storuman and Skellefte districts farther south. Direct correlation of the Senja Shear Belt with the Luleå-Jokkmokk zone is problematic as the sub-stratum for the supracrustal rocks is different in both areas. The basement rocks in the WTBC is largely of Archean age, whereas they are Paleoproterozoic in the south. Margin-lateral changes from north to south, location relative to the magmatic arc, and/or presence of Neoarchean micro-continents relative to the frontal deformation zone, may explain the basement differences. The eastward extent of the continent-margin boundary zone, however, is unknown, but can be inferred from comparison with volcano-sedimentary belts of the Alta, Altenes, Repparfjord-Komagfjord, Kautokeino and Karasjok greenstone belts in Finnmark (Fig. 3). All of these belts comprise Paleoproterozoic rift- and arc-related volcanics and clastic sedimentary rocks (Bergh & Torske 1988; Jensen 1996; Viola et al. 2008) which supports their continental-marginal basin affinity. A direct correlation of greenstone belts in the WTBC with the Kautokeino- and Karasjok belts farther south is difficult. They may rather, reflect sub-basin of the Kola ocean deposited in a broad transition zone between the Archean craton to the east, and the Bothnian basin to the west. In this perspective, the Karasjok greenstone belt may be further linked southwards to the Kittilä greenstone belt in central Finland (e.g. Marker, 1988; Braathen & Davidsen, 2000), which is a molasse-type meta-sedimentary unit with c1asts dated at 1.9 Ga (Räsänen et al. 1995, Hanski et al., 2001, Lehtonen et al. 1998). Such a correlation is supported by similarity of the clastic Caravarri formation of the Karasjok greenstone belt with the Kumpu group (<1.88 Ga) which overlies the Kittilä greenstone belt (Torske & Bergh, 2004).

This means that the metasedimentary rocks of the RTW, Tjåmotis, Lycksele-Storuman and Skellefte districts and the northern part of the Bothnian basin successions show a similar tectonic setting and appear with volcanic and sedimentary rocks which are deposited in the same time interval, marking a possible link between the breakup of the Archean continent and the deposition of the sedimentary rocks prior to the development of an active Svecofennian margin. Therefore, we tentatively link the autochthonous volcano-sedimentary belts of Fennoscandia to successions inside tectonic windows of the north Norwegian Caledonides, including the WTBC, the Alta, Altenes and Repparfjord-Komagfjord areas. They show a similar development of rift-related basins followed by arc-related volcanism/magmatism and sedimentation, deposited on basement rocks varying in age from Archean to Paleoproterozoic, indicating a very broad and complex boundary zone.

6.2 The onset of an active continental margin and the Svecofennian orogeny (1.88-1.79 Ga)

In the following sections we will discuss the successions from an Andean type active margin developing into a collision and progressive structural styles across the Fennoscandian shield.

1.88-1.87 Ga active margin development and arc-volcanics

Volcano-sedimentary successions that formed during the active margin evolution (1.88-1.79 Ga) are present in the RTW as N-S striking belts (e.g. Bargel et al., 1995). These volcanic units are consistently overlain by meta-greywacke. The composition of the volcanic rocks changes from felsic-mafic in the west, to mafic-ultramafic in the east, suggesting a continuous evolution from island-arc to a continental arc setting (Korneliussen & Sawyer, 1989). Similar rocks are found further south in Sweden, in the Tjåmotis district, where felsic volcanic rocks (Table 1) from the Arvidsjaur Group (1876±3 and 1878±2Ma; Skiöld et al., 1993) is overlain by a thick greywacke sequence (Ödman, 1957; Carlon, 1985). Correspondingly, in the Skellefte district, the Arvidsjaur group consists of sub-aerial basaltic to rhyolitic volcanic rocks formed in a mature, convergent continental margin arc (Bergström; 2001), whereas the Skellefte Group (1.88Ga; Welin, 1987; Billström & Weihed, 1996), with MORB basaltic to rhyolitic volcanic rocks, is interpreted to have formed in an extensional continental margin arc, or back-arc basin setting (Karig et al, 1978; Bergström, 2001; Larter et al., 2003). The overlap in radiometric ages of synchronously formed island arc and extensional margin volcanic rocks both in the RTW, Tjåmotis and Skellefte districts suggest a correlative, but complex, tectono-magmatic history during this time period.

1.88-1.79Ga accretion and syn- post Svecofennian granites

Granitic plutons dominate the RTW and they show clear mutual cross-cutting relationships with the Svecofennian (D_2) folded sedimentary units and the oblique-slip shear zones (D_3 and D_4), (Larsen et al., 2013). This suggest they are syn-to post-tectonic relative to the Svecofennian deformation and likely were injected in multiple phases. These granites are dated to 1789±6Ma (Larsen et al., 2013), and similar aged granites have been found in a wide belt trending from southern Sweden northward to Lofoten in northern Norway (Fig.1) (e.g. Carlon, 1984; Wilson et al., 1987; Weihed & Schönberg, 1991; Romer et al., 1992; Åhall& Larson, 2000; Corfu et al., 2003), collectively described as the Trans-Scandinavian Igneous Belt (TIB) (Gaal & Gorbatschev, 1987; Romer et al., 1992). The Tysfjord granite located south of RTW has been dated at 1706±15Ma (Andresen, 1980) and 1779±19Ma (Romer et al., 1992), and the Ersfjord Granite in the WTBC (1.792±5 Ma) farther north, (Corfu et al., 2003). These age variations suggest two stages of granitic intrusions in the basement west of the Caledonides in Norway, changing from magmatic arc affinity to the younger, within plate affinity from an eastern-dipping subduction zone (Romer et al., 1992). However, in Sweden there is a continuous belt of similar aged granitic plutons that can be traced southwards into Finland (Fig. 1). For example, the Lina granite series in Tjåmotis is assumed to be approximately 1.80 Ga (Carlon, 1984), the Jörn granite in Skellefte has been dated to 1.88Ga related to a third stage of plutonism (Wilson et al., 1987; Weihed & Schönberg, 1991). This is in accordance with the three stage granite intrusion evolution of the TIB (Gorbachev, 2004).

6.3. Svecofennian structures and structural architectures

The Svecofennian orogeny affected a large part of the Archean and Paleoproterozoic domains of northern Fennoscandia, including the Kola, Belomarian and Karelian provinces (Gaàl & Gorbatschev, 1987; Bogdanova & Bibikova, 1993), and additionally all of the areas presented in this paper (Table 1; RTW: Larsen et al., 2013 Karasjok: Braathen & Davidsen 2000; Kautokeino: Henderson & Viola, 2013; WTBC: Bergh et al., 2010; Skellefte district: Bergmann Weihed, 2001; Malehmir et al., 2007; Lycksele-Storuman: Bark, 2005). This orogenic event produced a variety of crustal-scale structures, including fold-thrust belt domains and networks of anastomosing, N-S and NE-SW trending ductile shear zones (e.g. Lindh 1987; Berthelsen & Marker 1986; Nironen, 1997; Lahtinen et al. 2005, 2008; Daly et al. 2006). Moreover, these structures localized extensive metallogenic mineralisation and ore deposits in Sweden and Finland (e.g. Lahtinen et al., 2012).

The Svecofennian tectonic evolution of the RTW involved four stages of deformation (Larsen et al., 2010; 2013), characterised by two initial stages of folding and thrusting (D_1-D_2) localized within the metasedimentary rocks (fold-thrust belt) and two later stages of steep ductile oblique-slip shear zone development (D_3-D_4; Larsen et al., 2012). D_1 involved the development of detachment and isoclinal folds due to E-W shortening and the generation of fold-thrust belt geometries. D_2 produced folds are more open to tight asymmetric east-verging folds that refolded the first generation isoclinal folds. This fold-thrust belt was subsequently segmented and cut by steep, ductile, sinistral oblique-slip shear zones that followed the N-S trend of the metasedimentary belts, whereas a later set of dextral NE-SW trending ductile oblique-slip shear zones obliquely truncated the fold-thrust belt structures (Larsen et al.

2013). In conjunction, these elements together displayed the character of a major, complex shear zone system, the RSSZ that formed as a result of continued oblique transpression and strain partitioning during the Svecofennian orogen. Syn-tectonic granitoids have an intimate spatial and temporal relationship to the structural elements of the RSSZ as the granites interact with the oblique-slip shear zones by following the structure and acted as pathways for fluids and ore deposits (see below), displaying complex mutual cross-cutting relationships with the RSSZ (Larsen et al., 2010, 2013).

The Svecofennian structures of the RTW show many remarkable structural similarities to Svecofennian deformed provinces elsewhere (the WTBC, Alta-Kvænangen, Altaneset, Repparfjord, KjGB, Skellefte district and Lycksele-Storuman districts). All of these areas display an early fold-thrust belt generation, and one (or more) later stage(s) of strike- or oblique-slip ductile shearing (see Table 1). In the KJGB and Skellefte district fold-thrust belt structures predominate, while in portions of the WTBC, KkGB and Sjangeli areas, the later stages of ductile shear zones are more predominant.
The fold-thrust belts and steep ductile shear zones commonly interact to form an arcuate structural pattern. For example, the trend of the early stage fold-thrust belt in Lycksele-Storuman and the Skellefte district strike generally E-W and top to the south (Bergmann Weihed, 2001; Rutland et al., 2001; Bark & Weihed, 2007; Malehmir et al., 2007), while similar belts in the RTW, WTBC, KkGB and KjGB, all trend in an approximately N-S to NW-SE direction (Torske, 1997; Braathen & Davidsen, 2000; Torske & Bergh, 2005; Bergh et al., 2010; Larsen et al., 2013; Henderson & Viola, 2013) with the top to the east (Torske & Bergh, 2005; Bergh et al., 2010; Larsen et al., 2013) or NE side up in the Skellefte district (Braathen & Davidsen, 2000; Henderson & Viola, 2013). Another such arcuate system can be seen within the meta-sedimentary rocks of the Bothnian basin and Arvidsjaur group in the Skellefte district, where a thick succession thins out and disappears northwards into the RTW. This suggests further that the WNW trending mega-scale Luleå-Jokkmokk shear zone (Melquist et al., 1999), marking the Archean- Paleoproterozoic transition, can be followed northwards and continues north of the RTW and south of WTBC (Fig. 3).

A common feature for all these curved domains is that the localization of the steep strike- or oblique-slip ductile shear zones (D_3-D_4) on the steep fold limbs and along steepened thrusts in the fold-thrust belt (e.g. Bergh et al., 2010; Larsen et al., 2013). D_3-D_4 have been interpreted to be part of the same NE-SW directed progressive shortening event as D_1-D_2, with a dominant overall transport direction towards the NE, forming as a result of strain partitioning on the two different sets (D_1-D_2 and D_3-D_4) of structures. This resulted in more or less coeval Svecofennian folds, thrusts, and dextral and sinistral oblique and strike-slip shear zones. In addition, late stage Svecofennian steep dextral oblique shear zones (D_4) which diagonally crosscut the N-S striking fold-thrust belt structures (Larsen et al., 2013), are also observed along the Archean-Paleoproterozoic boundary (Luleå-Jokkmokk zone). For example, in the Lycksele-Storuman area, late steep NW to NE striking ductile transpressive shear zones truncate earlier fold structures (Rutland et al., 2001; Bark & Weihed, 2007) thought to be syn- to post intrusion of the Revsund granite. This is similar to the timing relationships of the Rombak granite of the RTW (Bergmann Weihed, 2001; Rutland et al., 2001; Larsen et al., 2013). In the WTBC late Svecofennian N-S to NE-SW trending strike-slip shear zones also cross cut all earlier NW-SE trending folds and thrusts of the Ringvassøya greenstone belt (Bergh et al., 2010). In the Skellefte area, similar ductile shear zones trend ENE-WSW, and are responsible for a significant dextral component of movement between the major fold-thrust structures of the sub-zones to the north and south (cf. Romer & Nisca, 1995). In the KJGB the dominant fold-thrust system was cut by sub-vertical dextral NW-SE and NE-SW striking semi-brittle faults (Braathen & Davidsen, 2000), which may be analogous to late-stage Svecofennian structures. The Svecofennian structures of the Repparfjord-Komangfjord and Altanes tectonic windows shows anomalous NE-SW trends relative to the N-S structural trend in the adjacent Alta area, which may indicating a flexure and dextral displacement of the N-S structures into NE-orientations (Pratt, 1989; Viola, 2008; Ofstad et al., 2013; Torgersen et al., 2013; Rodinov et al., 2013).

These geometrical differences in different domains show that the Svecofennian crustal shortening directions changed from dominantly N-S to more E-W and NE-SW with time. The overall result of such progressive shortening and oblique/strike-slip shearing due to strain partitioning (e.g. Skyttä et al., 2006; Bergh et al. 2010), is an arcuate structural pattern, or an orocline geometry (e.g. Johnston et al., 2013) The change and bend in orientations of the structures and the thinning shape NW-ward of the Paleoproterozoic Bothnian basin rocks, suggest that the pattern reflects a consistent, scale-independent structural trend compared to the regional-scale Svecofennian orogeny, i.e. producing an overall secondary oroclinal geometry (Fig. 11), which is an extra-orogen or a curvature developed in relation to orogen parallel stress applied to a pre-existing orogen (Johnston et al., 2013).

Such a geometric model is also supported from the structural study in the WTBC, where the shortening axis switched from an orthogonal NE-SW translation to a more oblique NW-SE trend, becoming a more transpressional geometry with time. (Bergh et al., 2010). In the Skellefte district, early N-S crustal shortening changed to a more E-W direction during the orogeny (Bergmann Weihed, 2001).

The understanding of the similarities and differences across and laterally in the orogen provides the key to understand the large scale architecture. The correlation of provinces across a wide region of Fennoscandia is important because it could provide a better understanding of the regional versus local strain fields and, notably, wide implications for ore exploration.

6.4. Correlation of ore deposits and genesis

From the discussion of Paleoproterozoic volcano-sedimentary and magmatic history and the subsequent Svecofennian tectono-metamorphic evolution, we now address more specifically the tectonic setting and potential linkage of ore deposits in northern Fennoscandia, based on data from the RTW (Larsen et al. 2012, 2013). We have argued for a three-stage Paleoproterozoic evolution (Fig. 12) involving break-up of the Archean craton margin (2.5-2.0 Ga, i.e. Kola ocean) followed by intra-oceanic and continental-margin like arc accretion/subduction, and finally, closure of the marginal ocean leading to the Svecofennian accretion and continent-continent collision (e.g. Gaal & Gorbatschev 1987; Pharaoh & Brewer 1990; Larsen et al. 2013).

In this tectonic scenario, the sulphide mineralisation within the RTW can be considered as both pre- and syn orogenic (Larsen et al. 2013), i.e. they formed as syn-sedimentary SEDEX deposits (Flood, 1984; Flood, 1985; Coller, 2004) in a volcano-sedimentary basin (1.90-1.88 Ga) that subsequently became remobilized and redistributed in the Svecofennian structures (1.80 Ga). Notably, orogenic gold was found both within regional shear zones in meta-supracrustal rocks of the RTW and along the RSSZ in the form of metasomatic sulphides related to the syn orogenic mafic intrusions. Similar syn-orogenic sulphide and gold mineralisation that formed within accretionary or metamorphic belts and suffered overprinting and remobilisation by convergent tectonism were described by Goldfarb et al. (2001) and Groves et al. (2003).

A number of volcano-sedimentary hosted greywacke-hosted deposits (2.5-1.88 Ga), with large amounts of gold, are present throughout Fennoscandia (Sundblad & Ihlen 1995; Lahtinen et al., 2012; Eilu, 2012), and many of these deposits resemble those of the RTW (Larsen et al., 2013). In particular, the ore deposits of the Lycksele-Storuman and Skellefte districts appear to have a similar genesis (Bark & Weihed, 2007).

In the RTW the sedimentary units were deposited on a tonalitic basement complex in an extensional regime as is also the case in the Skellefte district (Korneliussen & Sawyer, 1986). In both areas the sedimentary rocks are thought to have been deposited in an Andean type margin and island arc system (Korneliussen & Sawyer, 1989; Sawyer & Korneliussen, 1989; Allen et al., 1996). The sedimentary strata of the RTW, Tjåmotis and Lycksele-Storuman districts all consist of volcanoclastic turbeditic sediments (Ödman, 1957; Sawyer & Korneliussen, 1989; Bark, 2005) which most likely were derived from adjacent volcanic activity that included both mafic to ultramafic and felsic rocks (Sawyer & Korneliussen, 1989). One such source area may have been the Sjangeli region just to the east in the RTW, consisting of mafic to ultramafic volcanic and intrusive rocks (Romer, 1988) indicating genesis in an early-stage of intra-oceanic subduction (Romer, 1988; Korneliussen & Sawyer, 1989) (Fig. 12). Syn-genetic and bedding parallel Zn-Pb sulphide mineralisation in the greywacke successions of the RTW (Larsen et al., 2012) and Cu- mineralisation in the Sjangeli area, support this interpretation. Provenance studies using Pb-Pb isotope data from the Tjåmotis area show that the lead minerals in the SEDEX deposit were derived from a Paleoproterozoic source (e.g. Sundblad, 1991). In the RTW the Pb-isotopes are mantle-sourced and therefore more radiogenic in the east and less radiogenic (indicating a continental source) in the west, (Larsen et al., 2013). This variation may be explained by the distance from the source, a different stratigraphic level (early or later in the sedimentation), or mixed erosion products from volcanic arc (more radiogenic) and continental rocks (less radiogenic). The change from a dominant mafic and ultramafic lithology in the east to more felsic and mafic volcanic rocks and intrusives in the west is probably a result of gradually evolving of the magma suite (Korneliussen & Sawyer 1989). This implies that the geotectonic setting transformed from an intra-oceanic subduction setting, which was highly Pb-radiogenic, to an ocean-continent subduction setting with a lower Pb-radiogenic signature and was followed by accretion and continent-continent collision and/or, accretion of microcontinents (Fig. 12). During the later collisional stages the greywacke sediments were folded and accreted on to the

island arc or the continent margin and a giant system of convergent and transpressive ductile shear zones as part of the Svecofennian orogen within the Fennoscandian shield (fig. 3).
The Svecofennian shear zone network may have provided a frame for later hydrothermal remobilisation of sedimentary-hosted ore deposits. This is confirmed by the numerous occurrences of syn-tectonic ore deposits within major shear zones such as the Jokkmokk zone and the RSSZ within the Archean and Paleoproterozoic domains. Similarly, gold mineralisation in the Häme belt in southern Finland can be linked to late-Svecofennian dextral oblique ductile shear zones (Saalmann et al., 2009), similar to those of the RTW. In addition to remobilisation of the SEDEX sulphides, the Svecofennian shear zones also give more opportunities for new mineralisation (Larsen et al. 2012; Groves et al. 2003). For example, in the Gautelis area of the RTW (Fig. 3), syn-orogenic and shear zone-parallel mafic dykes cut thick marble layers and contain As-Au rich metasomatic deposit distributed along the intrusive contacts which were then modified and mixed with what was interpreted as orogenic gold. In Haugfjellet (Fig. 3), similar oblique-slip shear-zones are enriched with As-Au-Pb-Zn-Bi-W, while syn- and post- orogen quartz veins are enriched with Au-Cu.
Although the source of the pre-Svecofennian gold deposits can be varied, the source of most syn-genetic orogenic gold deposits are commonly believed to be from granitic plutons (e.g. Groves et al., 2003) Presumed arc-related Svecofennian plutons, including the Transscandinavian igneous belt, where most of the intrusions are believed to be of a similar age and syn-to late-orogenic (e.g. Kathol et al., 2011), they may be regarded as an important source for gold mineralisation in the larger system.

In summary, the overall geometry of the Svecofennian orogeny (1.92-1.79 Ga) is that of an orocline (Carey, 1955; Johnston et al., 2013), formed through a succession of tectono-magmatic events that are remarkably similar in all scales and all parts of northern Fennoscandia. This also includes basement tectonic windows (inliers) of the Caledonides of Norway and Sweden, and in autochthonous positions east of the Caledonides in Finland and Russia (Fig. 1, 2.) (e.g. Gaàl & Gorbatschev, 1987; Nironen, 1997; Beunk & Page, 2001; Weihed, et al., 2005; Cagnard et al., 2007). All of these Svecofennian deformed provinces share many features in common with respect to occurrence of ore deposits and ore genesis (e.g. Lahtinen et al., 2011). One main implication of the orocline model with respect to ore genesis discussed in this paper, is that it may explain both the irregular distribution, occurrence and variety of ore deposit-types, i.e. volcano-sedimentary hosted deposits versus numerous syn-and post orogenic (tectonically remobilized) ore deposits. The irregularity of the Archean-Paleoproterozoic boundary zone and the wide extent of the presumed Kola Ocean assemblages, may have caused different strain fields across the shield from west to east and furthermore may have caused changing physical conditions for pressure and fluid flow/remobilisation of ore deposits. This is essential knowledge in the process of understand an ore deposit. With this tectonic model in mind, we conclude that mineral deposits within the Svecofennian orogeny have been formed during several processes and therefore may show complex structural and geochemical patterns. However, by understanding the tectonic history and understand of how the Svecofennian deformation can remobilize and overprint other deposits, we may be able to predict undiscovered valuable deposits in the future.

6.5 Summary

The RTW is an important transition between the Paleoproterozoic rocks to the west of the Caledonides in Norway and the similar rocks in Sweden Finland and Russia. Excellent exposure provide good data for correlation and regional interpretation. The RTW show many similarities in the development of the rocks from the Archean break-up of the continent to the Paleoproterozoic basin infill and the development of the active margin to the Svecofennian orogeny. The RTW can be correlated by the rocks, metamorphic conditions, a poly-stage structural development and complex evolution of mineral deposits, both to the inliers and outliers in the NW and to Sweden and Finland to the east. Such correlation lead to an large scale tectonic model developing in several stages ending in the Svecofennian orogeny (Fig. 12).

The breakup, of the Archean rocks lead to a rifted continental margin during the Paleoproterozoic. The margin was separated into multiple microcontinents with several basin, that gradually was filled with sediments. These basins and micro continents show strong correlations across the Fennoscandian shield and can be found in Finland, Sweden and in inliers/outliers in the Caledonian rocks of Norway as Paleoproterozoic metasedimentary belts alternating with belts of Archean rocks (Koistinen et al., 2001) The margin of the Archean rocks is therefore transitional and are found as the Luleå-Jokkmokk zone bending northwards from Luleå in Sweden into the north of the RTW and across the WTBC (Fig 3). The RTW is thus part of the Bothnian basin and located close to the final margin of the Archean continents. The margin changed to an active continental margin during the Paleoproterozoic which produced mafic to ultramafic melts and which also can be found as eroded greywacke sediments in the basins especially with similarities between RTW and Lycksele-Storuman region in the southern part of the Skellefte district. During the ongoing progressive accretion the melts changed gradually into more continental mafic to felsic melts and became the Svecofennian orogeny. This orogeny accreted all the basins and microcontinents into one large system of domains of greenchistfacies ductile fold-thrust belts and oblique/strike-slip, steep, ductile shear zones produced as an anastomosing pattern in a W-NW-N-NE direction in Finland, Sweden, Norway and Russia developed by transpression from the N-S and NE-SW (Fig. 1). This structural history and pattern from these areas together with the geometry of the Bothnian basin suggest that the orogeny is an orocline resulting from N-S contraction changing into a NE-SW to E-W contraction (Fig. 11). The mineral deposits located within the Fennoscandian shield is very complex and are commonly a results of reactivation and remobilisation. However, the mineral deposits are strongly connected to the structures of the Svecofennian orogeny which have acted as carriers of juvenile fluids regardless if the source is from pre-existing deposits or from mantle derivate melts releasing fluids. These large scale structures do show evidence for a large tectonic system of orogenic gold. Further understanding of the geological evolution will help us to predict possible future deposits and is therefore essential.

7.0) Conclusions

- Archean and Paleoproterozoic basement rocks make up the autochthonous Fennoscandian Shield of northern Russia, Finland and Sweden, and also occur as inliers and outliers beneath and west of the Scandinavian Caledonides. Basement rocks of the Rombak Tectonic Window in northern Sweden and elsewhere in Norway provides the basis for comparison and correlation of provinces with respect to internal stratigraphy, composition, age, structural relationship, and mineralisation potential. The reviewed provinces include the RTW, WTBC, Alta-Kvænangen, Altenes, Komagfjord-Repparfjord, Kautokeino, Karasjok in northern Norway, and Tjåmotis, Lycksele-Storuman and Skellefte district in Sweden.

- All the reviewed provinces show evidence of the same break-up activity in the Archean (2.5-1.9 Ga) that formed micro continents and Paleoproterozoic basins, island arc-related volcano-sedimentary deposits, and the Svecofennian continent-continent collision (1.92-1.79 Ga) producing fold-thrust belts and regional ductile shear zones.

- The main Archean and Paleoproterozoic boundary is outlined by the Luleå-Jokkmokk zone that can be traced northwards to the RSSZ of the RTW and the Senja shear belt west of the Caledonides. Similar Svecofennian shear zone networks are also present farther east.

- The Svecofennian orogenic belt in northern Sweden, Finland and Norway, is overall characterised by early-formed fold-thrust belt structures segmented by later steep strike-slip and/or oblique-slip ductile shear zones. These belts and shear zones have a general NW-SE trend, but curve into N-S trending late-Svecofennian shear zones making a zigzag pattern that resembles an overall orocline geometry.

- The tectonic processes leading to the Svecofennian orocline and juxtaposition of pre-orogenic components, e.g. rifted basement gneisses, volcano-sedimentary belts and intrusive and magmatic components, were likely responsible for remobilisation of several ore deposits. By comparing different domains and correlating with respect to tectono-magmatic evolution in the northern Fennoscandian Shield, we may be able to better understand the processes of ore genesis and tectonic remobilisation, as well as to locate regions with a higher potential for economically valuable ore bodies.

- The RTW, WTBC, Tjåmotis and the Lycksele-Storuman regions marks the transition from an Archean basement for Paleoproterozoic metasedimentary rocks deposited in intracontinental extensional basins to the N, to Paleoproterozoic basement rocks deposited on an extensional margin in the RTW and Skellefte district in an 1.95-1.88Ga extensional continental margin.

- The similar ages of island arc and extensional basins suggest a complex but similar tectonic history of the RTW, Tjåmotis and the Skellefte district during 1.88-1.87 Ga. Extensional back arc basins explain the complexity of the rocks simultaneously with evidence from island arc environment and MORB.

- The metasedimentary rocks of the RTW, the Tjåmotis area and the northern part of the Bothnian basin show a similar tectonic setting and reflect the volcanic rocks which are deposited in the same time interval and is the boundary zone between the fragmented Archean continent margin and the Paleoproterozoic passive margin deposition of sedimentary rocks turning into an Andean type island arc margin. The meta-sedimentary belts from the WTBC and from the Finnmark area show development of similar basins but differ in the way that they occur as intracontinental basins within the Archean continent and the metasedimentary rocks are deposited on Archean basement rocks.

- The similarity of the meta-volcanic rocks in the RTW, Tjåmotis and the Lycksele-Storuman areas and their mutually tectonic history, with continuous development from an extensional regime to subduction, island arc, continental arc and finally the compressional regime, suggests that they are part of the same Norrbotten craton.

- The granites within the RTW and Northern Sweden are part of the Transscandinavian belt (TIB) forming during 1.88-1.79Ga (TIB1) which is the same aged granite found in the Lycksele-Storuman area.

- We demonstrate that there are remarkably similar regional structural evolution and trends within the geographically widely separate domains that constitutes the Svecofennian orogeny. Early Svecofennian structural evolution consists of an earlier stage of fold-thrust belt development segmented and attenuated by later events of mainly steep sinistral oblique- and strike-slip shear zones being cut by steep dextral oblique- and strike-slip shear zones, identical to those documented in detail from the RTW.

- Due to the bending of the E-W striking shear zones in Sweden into N-S trending shear zones in Norway, the disappearance and thinning of the Svecofennian rocks from Sweden into RTW and the late dextral NE-SW shear zones cutting the structures, we suggest that the late Svecofennian orogen was transformed into a secondary orocline as a late event of the orogenic development caused by a possible change of plate flow direction of the North-American or the Baltic shield.

- Based on the complex metallogenic history from the RTW (Angvik et al. included manuscript III), we suggest a three stage tectono-metallogenic model for the Svecofennian orogeny with already known mineralisation classified in terms of tectonic context (Fig. 12)

- Intra-continental extension with development of tonalitic complex, deposition of conglomerate, sandstone, shale and marble and possible the BIF located within the WTBC.
- Intra-oceanic subduction with ultramafic and mafic volcanic rocks developing in an island arc system. Deposition of turbeditic greywacke sediments with syn-sedimentary SEDEX deposits and possible VMS-deposits at Sjangeli and possible Kiruna
- Continent-continent collision or accretion on to the continent with developing regional shear zones opening for fluid migration and orogenic gold in the Lycksele-Storuman region, RTW and possibly the Finnmark region. Orogen related intrusion of mafic and felsic intrusives may have produced the metasomatic Au deposit in the RTW

- An implication of the secondary orocline model may be that the western part of the Svecofennian orogen differs in strain and stress to the east part and therefore also may show a more complex metallogenic history with more remobilisation in the west.

8.0) References

Adamek, P. M. (1973). Kopparåsen Uranium Project; Results of prospection work carried out during the years 1968-1970. SGU Malmbyrån BRAP 00907.

Adamek, P. M. (1975). Geology and Mineralogy of the Kopparåsen Uraninite-sulphide Mineralization: Norrbotten County, Sweden. Avhandlingar och uppsatser - Sveriges Geologiska Undersökning ; serie C 712.

Ahl, M., Bergman, S., Bergström, U., Eliasson, T., Ripa, M. and Weihed, P. (2001). Geochemical classification of plutonic rocks in central and northern Sweden. , 106: 82 Sveriges Geologiska Undersökning Rapporter och meddelanden 106: 82.

Allen, A. (2008). Geology and exploration of the Renström volcanic-hosted Zn-Pb-Cu-Au-Ag massive sulphide deposit, Skellefte district, northern Sweden. Abstract at the 33rd International Geological Congress, Oslo.

Allen, R., Weihed, P. and Svenson, S.-Å. (1996). Setting of Zn-Cu-Au-Ag massive sulfide deposits in the evolution and facies architecture of a 1.9 Ga marine volcanic arc, Skellefte District, Sweden. Economic Geology 91: 1022-1053.

Almås, A. M. (2013). Geological setting and origin of a gold-mineralization zone at Myrefjellet, Mauken, Troms. Unpublished MSc thesis, University of Tromsø: 96.

Andresen, A. (1980). The age of the Precambrian basement in western Troms, Norway. Geol. F¨ren. Stockholm Förh. 101: 291-298.

Armitage, P. (2004). Structural geological reconnaissance in the Svanfjellet shear zone, Senja. Field Report, Department of Eart and Environmental Sciences, university of Greenwicj at Medway.

Armitage, P. B. and Bergh, S. G. (2005). Structural development of the Mjelde-Skorelvvatn Zone on Kvaløya, Troms: a metasupracrustal shear belt in the Precambrian West

Troms Basement Complex, North Norway. Norwegian Journal of Geology 85: 117-132.

Armitage, P. E. B. (2001). Structural geological reconnaissance on northwestern Ringvassøy. Field Report, Department of Eart and Environmental Sciences, university of Greenwicj at Medway.

Bargel, T. H., Bergstrøm, B., Boyd, R. and Karlsen, T. A. (1995). Geologisk kart, Narvik kommune M 1:100.000. Norges geologiske undersøkelse.

Bark, G. (2005). Genesis and tectonic setting of the hypozonal Fäboliden orogenic gold deposit, northern Sweden. Licentiate thesis, Luleå University of Technology, Luleå, Sweden, 2005. 64.

Bark, G., Broman, C. and Weihed, P. (2007). Fluid chemistry of the Palaeoproterozoic Fäboliden hypozonal orogenic gold deposit, northern Sweden: Evidence from fluid inclusions. GFF 129(3).

Bark, G. and Weihed, P. (2007). Orogenic gold in the Lycksele - Storuman ore province, northern Sweden; the Palaeoproterozoic Fäboliden deposits. Ore Geology Reviews 32: 431-451.

Bergh, S. G., Corfu, F., Myhre, P. I., Kullerud, K., Armitage, P. E. B., Zwaan, C. B., Ravna, E. J. K., Holdsworth, R. H. and Chattopadhya, A. (2012). Was the Precambrian basement of western Troms and Lofoten-Vesterålen in northern Norway linked to the Lewisian of Scotland? A comparison of crustal components, tectonic evolution and amalgamation history. Tectonics, In Tech 11: 283-330.

Bergh, S. G., K. Kullerud, K., Armitage, P. E. B., Zwaan, K. B., F. Corfu, F., Ravna, E. J. K. and Myhre, P. I. (2010). Neoarchaean to Svecofennian tectono-magmatic evolution of the West Troms Basement Complex, North Norway. Norwegian Journal of Geology 90: 21-48.

Bergh, S. G., Kullerud, K., Corfu, F., Armitage, P. E. B., Davidsen, B., Johansen, H. W., Pettersen, T. and Knudsen, S. (2007). Low-grade sedimentary rocks on Vanna, North Norway: a new occurrence of a Palaeoproterozoic (2.4-2.2 Ga) cover succession in northern Fennoscandia. Norsk Geologisk Tidsskrift 87.

Bergh, S. G., Kullerud, K., Myhre, P. I., Corfu, F., Armitage, P. E. B. and Zwaan, K. B. (2014). Archaean Elements of the Basement Outliers West of the Scandinavian Caledonides in Northern Norway: Architecture, Evolution and Possible Correlation with Fennoscandia. Springer 2014 7: 103 - 126.

Bergh, S. G. and Torske, T. (1988). Paleovolcanology and tectonic setting of a Proterozoic metatholeiitic sequence near the Baltic Shield margin, Northern Norway. Precambrian Research 39: 227-246.

Bergman-Weihed, J. (2001). Palaeoproterozoic deformation zones in the Skellefte and Arvisjaur areas, northern Sweden. In: Weihed (ed.) Economic geology research, Vol. 1, 1999-2000. Uppsala 2001. SGU C 833: 46-68.

Bergström, U. (2001). Geochemistry and tectonic setting of volcanic units in the northern Västerbotten county, northern Sweden. In Weihed, P. (ed.) Economic Geology Reasearch 1(SGU C 833): 69-92.

Berthelsen, A. and Maker, M. (1986). Tectonics of the Kola collision suture and adjacent Archean and Early Proterozoic terrains in the Northeastern region of the Baltic shield. Tectonophysics 126: 31–55.

Berthelsen, A. and Marker, M. (1986). 1.9-1.8 Ga Old strike-slip megashears in the Baltic shield, and therir plate tectonic implications. Tectonophysics 128: 163-181.

Beunk, F. F. and Page, L. M. (2001). Structural evolution of accretional continental margin of the Palaeoproterozoic Svercofennian orogen in southern Sweden. Tectonophysics 339: 67-92.

Billström, K., Frietsch, R. and Perdahl, J.-A. (1997). Regional variations in the Pb isotopic compositions of ore galena across the Archaean-Proterozoic border in northern Sweden Precambrian Research 81(1-2): 83-99.

Billström, K. and Weihed, P. (1996). Age and provenance of host rocks and ores in the Paleoproterozoic Skellefte District, northern Sweden. Economic Geology 91: 1054-1072.

Birkeland, T. (1976). Skjomen, berggrunnsgeologisk kart 1:100 000. Norges geologiske undersøkelse.

Bjørlykke, A., Nilsen, K., Anttonen, R. and Ekberg, M. (1993). Geological setting of the Bidjovagge deposit and related Gold-copper deposits in the northern part of the Baltic Shield. In: Maurice, Y.T. (ed.). Proceedings 8th Qadrenn IAGOD Symposium, Ottawa, Canada, 1990: 667-680.

Bjørlykke, A., Olerud, S. and Sandstad, J. S. (1985). Metallogeny of Finnmark, North Norway. NGU Bulletin 403: 183-196.

Bogdanova, S. V. and Bibikova, E. V. (1993). The 'Saamian' of the Belomorian mobile belt: new geochronological constraints. Precambrian Research 64: 131–152.

Braathen, A. and Davidsen, B. (2000). Structure and stratigraphy of the Palaeoproterozoic Karasjokk Greenstone Belt, north Norwa - regional implications. Norsk Geologisk Tidsskrift 80: 33-55.

Cagnard, F., Gapais, D. and Barbey, P. (2007). Collision tectonics involving juvenile crust: the example of the southern Finnish Svecofennides. Precambrian Research 154: 125–141.

Carey (1955). The Orocline Concept in Geotectonics. Papers and Proceedings of the Royal Society of Tasmania 89: 255–288.

Carlon, C. J. (1984). The BP-LKAB-Jokkmokk Mineral joint venture, Tjåmotis, Jokkmokk, Swedish lappland. LKAB Report No Bsg 84-372.

Cashman, P. H. (1990). Evidence for extensional deformation during a collisional orogeny, Rombak Window, north Norway. Techtonics 9(4): 859–886.

Claesson, S., Huhma, H., Kinny, P. D. and Williams, I. S. (1995). Svecofennian detrital zircon ages-implications for the Precambrian evolution of the Baltic Shield. Precambrian Research 64: 109–130.

Claesson, S. and Lundqvist, T. (1995). Origins and ages of Proterozoic granitoids in the Bothnian Basin, central Sweden; isotopic and geochemical constraints. Lithos 36: 115–140.

Coller, D. (2004). Varden Ridge Target Generation Report. Golden Chalice Resources Inc report GT 04-18D-01.

Corfu, F., Armitage, P., Kullerud, K. and Bergh, S. G. (2003). Preliminary U-Pb geochronology in the West Troms Basement Complex, North Norway: Archaean and Palaeoproterozoic events and younger overprints. NGU Bulletin 441: 61-72.

Daly, J. S., Balagansky, V. V., Timmerman, M. J. and Whitehouse, M. J. (2006). The Lapland-Kola orogen: Palaeoproterozoic collision and accretion of the northern Fennoscandian lithosphere. Geological Society, London, Memoirs 2006 32: 579-598.

Eilu, P. (2012). Mineral deposits and metallogeny of Fennoscandia. Geological Survey of Finland, Special Paper 53.

Eilu, P., Sorjonen-Ward, P., Nurmi, P. and Niiranen, T. (2003). A Review of Gold Mineralization Styles in Finland. Economic Geology 98(7): 1329-1353

Ekberg, M. and Sotka, P. (1991). Production mineralogy and selective mining at Bidjovagge mine, Northern Norway. International Conference on Applied Mineralogy, Pretoria, South Africa.

Eliasson, T., Greiling, R. O., Sträng, T. and Triumf, C. (2001). Bedrock map of map sheet Stensele NW, NE, SW, SE. Scale 1:50 000. SGU 126, 127, 128, 129.

Eliasson, T. and Sträng, T. (1998). Kartbladen 23 H Stensele. In:C.-H. Wahlgren (ed.): Regional Berggrundsgeologisk undersökning - Sammanfattning av pågående undersökningar 1997. SGU Rapporter och meddelanden 97: 55-59.

Ettner, D. C., Bjørlykke, A. and Andersen, T. (1993). Fluid evolution and Au-Cu genesis along a shear zone: a regional fluid inclusion study of shear zone-hosted alteration and gold and copper mineralization in the Kautokeino greenstone belt, Finnmark, Norway. Journal of geochemical Exploration 49: 233-267.

Ettner, D. C., Lindblom, S. and Karlsen, D. (1996). Identification and implications of fight hydrocarbon fluid inclusions from the Proterozoic Bidjovagge gold-copper deposit, Finnmark, Norway. Applied Geochemistry 11(6): 745–755.

Flood, B. (1984). The Rombak project area, North Norway. Summary of work done 1983 and work program proposal for 1984. Arco Norway Inc, Hard Mineral section 84-670-19.

Flood, B. (1985). The Rombaken Gold-basemetal project, Northern Norway. A participation offer. Arco Norway. Bergvesenet rapport BV 4185.

Gaál, G. and Gorbatschev, R. (1987). An outline of the Precambrian Evolution of the Baltic Shield. Precambrian Research 35: 15-52.

Gautier, A. M. (1975). Geology of the Alta-Kvænangen window. Bergvesenet rapport BV223.

Gautier, A. M., Bakke, I., Vik, E. and Zwaan, K. B. (1986). Berggrunnskart Flintfjellet 18344 1:50. NGU.

Gautier, A. M., Gulacar, F. and Delaloye, M. (1979). K-Ar age determinations of the Alta-Kvænangen window rocks, northern Norway. Norsk Geologisk Tidsskrift 59: 155-159.

Goldfarb, R. J., Groves, D. I. and Gardoll, S. (2001). Orogenic gold and geologic time: a global synthesis. Ore Geology Reviews 18: 1–75.

Gorbatschev, R. (2004). The Transscandinavian Igneous Belt – introduction and background. In: Högdahl, K., Andersson, U. B., and Eklund, O., 2004. Geological Survey of Finland, Special Paper 37.

Gorbatschev, R. and Bogdanova, S. (1993). Frontiers in the Baltic. Precambrian Research 64: 3-21.

Griffin, W. L., Taylor, P. N., Hakkinen, J. W., Heier, K. S., Iden, I. K., Krogh, E. J., Malm, O., Olsen, K. I., Ormaasen, D. E. and Tveten, E. (1978). Archaean and Proterozoic crustal evolution in Lofoten–Vesterålen, N Norway. Journal of the Geological Society 135: 629-647.

Groves, D. I., Goldfarb, R. J., Robert, F. and Hart, C. J. R. (2003). Gold deposits in metamorphic belts: Overview of current understanding, outstanding problems, future research, and exploration significance. Economic Geology 98: 1-29.

Gunner, J. D. (1981). A reconnaissance Rb-Sr study of Precambrian rocks from the Skjomen-Rombak Window and the pattern of initial 87Sr/86Sr ratios from northern Scandinavia. Norsk Geologisk Tidsskrift 61: 281-290.

Hallberg, A. (1994). The Enåsen gold deposit, central Sweden. 1. A Paleoproterozoic high sulphidation epithermal gold mineralization. Mineralium Deposita 29: 150–162.

Hallberg, A., Bergman, T., Gonzalez, J., Larsson, D., Morris, G. A., A., P. J., Ripa, M., Niiranen, T. and P., E. (2012). Metallogenic areas in Sweden. In Eilu, P. (ed.) Mineral deposits and metallogeny of Fennoscandia. Geologcal Survey of Finland, Special Paper 53: 401.

Hallberg, A., bergman, T., Gonzalez, J., Larsson, D., Morris, G. A., Perdahl, J. A., Ripa, M., Niiranen, T. and Eilu, P. (2012). Metallogenic areas in Sweden. In: Eilu, P. (ed.), Mineral deposits and metallogeny of Fennoscandia. Geological Survey of Finland Special paper 53: 139-206.

Hanski, E. (2001). History of stratigraphical research in northern Finland. In: Vaasjoki, M. (ed.) Radiometric Age Determinations from Finnish Lapland and Their Bearing on the Timing of Precambrian Volcano-Sedimentary Sequences. Geological Survey of Finland Special Paper 33: 15-43.

Hanski, E., Huhma, H. and Perttunen, V. (2005). SIMS U-Pb, sm-Nd isotope and geochemical study of arkosite-amfibolite suite, Peräpohja Schist Belt: evidence for ca. 1.98 Ga A-type felsic magmatism in northern Finland. Geological surveu of Finland Bulletin 77: 5-29.

Henderson, I. and Kendrick, M. (2003). Structural controls on graphite mineralization, Senja, Troms. NGU report 2003.011.

Henderson, I. and Viola, G. (2013). Structural analysis of the Kautokeino Greenstone Belt from geophysical and field studies: Towards a refined understanding of its gold mineralisation. NGF Abstract and Proceedings no.1.

Henkel, H. (1991). Magnetic crustal structures in Northern Fennoscandia. Tectonophysics 192.

Hermansson, T., Stephens, M. B., Corfu, F., Page, L. M. and Andersson, J. (2007). Migratory tectonic switching, western Svecofennian orogen, central Sweden – constraints from U/Pb zircon and titanite geochronology:. Precambrian Research.

Hietanen, A. (1975). Generation of potassium-poor magmas in the Northern Sierra nevada and the Svecofennian of Finland. Journal of Reasearch USGS 3(6): 631-645.

Holmqvist, A., Lundmark, C., Luppichini, E., Niva, B., Sjöstrand, T. and Westfal, T. (1982). Rapport över Wollastonitt-prospektering vid Latanjarka, Jokkmokks kommun. SGU brap 83008.

Hübert, J., Malehmir, A., Smirnow, M., Tryggvason, A. and Pedersen, L. B. (2009). MT measurements in the western part of the Paleoproterozoic Skellefte Ore District, Northern Sweden: A contribution to an integrated geophysical study. Tectonophysics 475(3-4): 493–502.

Härkönen, I., Kojonen, K. and Johanson, B. (1999). The Early Proterozoic Suurikuusikko refractory gold deposit, Kitilä, Western Finnish Lapland. In: Mineral Deposits: Processes to processing. Proceedings of the Fifth Biennial SGA Meeting, Bakema: 159-161.

Högdahl, K., Sjöström, H., Andersson, U. B. and Ahl, M. (2007). Continental margin magmatism and migmatisation in the west-central Fennoscandian Shield. Lithos.

Ihlen, P. M. and Furuhaug, L. (2000). Gold resources on Ringvassøy, Troms-III: Geochemistry of heavy-mineral consentrates from stream sediments and potential gold sources. NGU report 2000.059.

Jensen, P. A. (1996). The Altenes and Repparfjord tectonic windows, Finnmark, northern Norway: Remains of a Palaeoproterozoic Andean-type plate margin at the rim of the Baltic shield. Unpublished PhD thesis, University of Tromsø.

Johnston, S. T., Weil, A. B. and Gutiérrez-Alonso, G. (2013). Oroclines: Thick and thin. Geological Society of America Bulletin.

Juhlin, C., Elming, S.-Å., Mellquist, C., Öhlander, B., Weihed, P. and Wikström, A. (2002). Crustal reflectivity near the Archaean-Proterozoic boundary in northern Sweden and implications for the tectonic evolution of the area. Geophysical Journal International 150: 180–197.

Karig, D. E., Anderson, R. N. and Bibee, L. D. (1978). Characteristics of backarc spreading in the Mariana Trough. Journal of Geophysical Research 83: 1213–1226.

Kathol, B., Lundmark, C., Helström, F. and Rimsa, A. (2008). U-Pb zircon age of a feldspar-porphyrittic rhyodacite from the Trollforsen area, c. 20 km northwest of Moskosel, southern Norrbotten County, Sweden. In: F. Helström (ed): Results from radiometric datings and other isotope analyses 2. SGU report 2008 27: 33-35.

Kathol, B., Sadeghi, M., Aaro, S., Jönberger, J. and Larsson, D. (2011). In: S. Lundqvist (ed.) Berggrundsgeologisk undersøkning. Sammenfattning av pågående verksamhet 2010. SGU- rapport 2011 6: 37-69.

Kathol, B., Sadeghi, M., Triumf, C. and Larsson, D. (2012). Berggrundsgeologisk undersökning, Jäkkvik-Boden. SGU report 2012 5.

Koistinen, T., Stephens, M. B., Bogatchev, V., Nordgulen, Ø., Wennerström, M. and Korhonen, J. (2001). Geological map of the Fennoscandian Shield, scale 1:2 000 000. Espoo/Trondheim/Uppsala/Moscow/Geological Survey of Finland/Geological Survey of Norway/Geological Survey of Sweden/Ministry of Natural Resources of Russia.

Korja, A., Lahtinen, R. and Nironen, M. (2006). The Svecofennian orogen: a collage of microcontinents and island arcs. Geological Society, London, Memoirs 2006 32: 561-578.

Korneliussen, A., Larsen, T. and Bagas, L. (2013). On the Paleoproterozoic Andean type volcano-sedimentary setting of the Rombak basement window in Northern Norway, and the relevance for gold deposit. NGF abstract proceedings of the Geological Society of Norway Oslo, January 8-10, 2013.

Korneliussen, A. and Nilsson, L.-P. (2008). Gull i vulkansk-sedimentære bergarter, Skjomen-Rombaken. NGU report 2008.045.

Korneliussen, A. and Sawyer, E. W. (1989). The geochemistry of Lower Proterozoic mafic to felsic igneous rocks, Rombak Window, North Norway. NGU Bulletin 415: 7-21.

Korneliussen, A., Tollefsrud, J. I., Flood, B. and Sawyer, E. (1986). Precambrian volcano-sedimentary sequences and related ore deposits, with special reference to the Gautelisfjell carbonate-hosted gold deposit, Rombaken basement window, Northern Norway. NGU report 86(193): 44.

Korsman, K., Koistinen, T., Kohonen, J., Wennerström, M., Ekdahl, E., Honkamo, M., Idman, H. and Pekkala, Y. (1997). Bedrockmap of Finland 1:1000000:. Geol. Survey Finland, Espoo.

Krill, A. G., Bergh, S. G., Lindahl, I., Mearns, E. W., Often, M., Olerud, S., Olesen, O., Sandstad, J. S., Siedlecka, A. and Solli, A. (1985). Rb-Sr, U-Pb and Sm-Nd Isotopic Dates from Precambrian Rocks of Finnmark. NGU Bulletin 403: 37-54.

Kumpulainen, R. A. (2009). The Bothnian basin - Its rocks, its age, its origin. SGU Final report Dnr: 60-1931/2005.

Laajoki, K. (2005). Karelian supracrustal rocks. In: Lehtinen, M., Nurmi, P. A. and Rämö, O. T. (eds) Precambrian Geology of Finland - Key to the Evolution of the Fennoscandian Shield. Developments in Precambrian Geology, Elsevier, Amsterdam 14: 279-342.

Lahtinen, R., Garde, A. A. and Melezhik, V. A. (2008). Palaeoproterozoic evolution of Fennoscandia and Greenland. Episodes 31(1).

Lahtinen, R., Hallberg, A., Korsakova, M., Sandstad, J. S. and Eilu, P. (2012). Main Metallogenic events in Fennoscandia: Summary. In: Eilu, P. (ed.), Mineral deposits and metallogeny of Fennoscandia. Geological Survey of Finland Special Paper 53.

Lahtinen, R., Hölttä, P., Kontinen, A., Niiranen, T., Nironen, M., Saalmann, K. and Sorjonen-Ward, P. (2011). Tectonic and metallogenic evolution of the Fennoscandian shield: key questions with emphasis on Finland. Geological Survey of Finland, Special Paper 49: 23–33.

Lahtinen, R., Korja, A. and Nironen, M. (2005). Palaeoproterozoic tectonic evolution of the Fennoscandian Shield, in Lehtinen, M., Nurmi, P., and Rämö, T., eds, The Precambrian Bedrock of Finland – Key to the evolution of the Fennoscandian Shield. Elsevier Science B.V: 418–532.

Larsen, T., Bergh, S. G., Henderson, I., Korneliussen, A. and Kullerud, K. (2010). Svecofennian structural development and metallogenesis of Palaeoproterozoic volcano-sedimentary rocks of Rombak Tectonic widow. NGF abstract proceedings of the Geological Society of Norway 1, 2010, 29th Nordic Geological winter meeting, Oslo.

Larsen, T., Bergh, S. G. and Henderson, I. H. C. (2012). A model of tectonic transpression and strain partitioning for Paleoproterozoic ductile shear zones in the Rombak tectonic window, northern Norway. . 34th International Geological Congress (IGC), Brisbane, Australia, 5-10 August 2012.

Larsen, T., Sundblad, K., Henderson, I., Bergh, S. G., Bagas, L., Sandstad, J. S., Andersen, T. and Simonsen, S. (2013). Recognition of Svecofennian sulphide bearing crust in the Rombak region, northern Norway. NGF abstract proceedings of the Geological Society of Norway 1, 2013, 32nd Nordic Geological winter meeting, Oslo.

Larter, R. D., Vanneste, L. E., Morris, P. and Smythe, D. K. (2003). Structure and tectonic evolution of the South Sandwich arc. Geological Society, London, Special Publications 2003 219: 255-284.

Lehtonen, M., Airo, M.-L., Eilu, P., Hanski, E., Kortelainen, V., Lanne, E., Manninen, T., Rastas, P., J., R. and Virransalo, P. (1998). Kittilän vihreäkivialueen geologia. Lapin vulkaniittiprojektin raportti. Summary: The stratigraphy, petrology and geochemistry of the Kittilä, Finland. Special Paper 33 33: 15-43.

Lindahl, I. and Malm, O. A. (1979). Diamantboringer, geolosike og geo-kjemiske undersøkelser ved Ytre Sildviksskar Zn-Pb-forekomst, Narvik, Nordaland. NGU-rapport 1430(4B).

Lindh, A. (1987). Westward Growth of the Baltic Shield. Precambrian Research 35: 53-70.

Lundquist, T. (1987). Early Svekofennian stratigraphy of southern and central Norrland, Sweden, and the possible exixtence of an Archean basement west of the Svekokarelides. Precambrian Research 35: 343-352.

Lundqvist, T., Vaasjoki, M. and Persson, P.-O. (1998). U-Pb ages of plutonic and volcanic rocks in the Svecofennian Bothnian Basin, central Sweden, and their implications for the Palaeoproterozoic evolution of the Basin. GFF 120(4).

Lundström, I., Rodney L. Allen, Persson, P.-O. and Ripa, M. (1998). Stratigraphies and depositional ages of Svecofennian, Palaeoproterozoic metavolcanic rocks in E. Svealand and Bergslagen, south central Sweden. GFF 120(3).

Malemihr, A., Tryggvason, A., Lickorish, H. and Weihed, P. (2007). Regional structural profiles in the western part of the Palaeoproterozoic Skellefte Ore District, northern Sweden. Precambrian Research 159: 1-18.

Marker, M. (1985). Early Proterozoic (C.2000–1900 Ma) crustal structure of the northeastern Baltic Shield; tectonic division and tectogenesis. Norges Geol. Bull. 403: 55–74.

Marker, M. (1988). Early Proterozoic thrusting of the Lapland Granulite Belt and its geotectonic evolution, northern Baltic Shield. Geologiska Föreningen i Stockholm Förhandlingar 110(4): 405-410.

Martinsson, O. (1997). Paleoproterozoic greenstones at Kiruna in northern Sweden: a product of continental rifting and associated mafic-ultramafic volcanism. In O. Martinsson (ed.): Tectonic Setting and Metallogeny of the Kiruna Greenstones, Paper I, 49 p. Ph. D. Thesis, Lulea° University of Technology, Sweden.

Melezhik, V. A. and Sturt, B. A. (1994). General geology and evolutionary history of the early proterozoic Polmak-Pasvik-Pechenga-Imandra/Varzuga-Ust'Ponoy greenstone belt in the northeastern Baltic Shield. Earth-Science Reviews 36(3-4): 205–241.

Mellqvist, C., Öhlander, B., Skiöld, T. and Wikström, A. (1999). The Archaean–Proterozoic Palaeoboundary in the Luleå area, northern Sweden: field and isotope geochemical evidence for a sharp terrane boundary. Precambrian Research 96(3-4): 225–243.

Motuza, G. (1998). Description to the geological map of the eastern part of Kvaløya, Troms county, northern Norway. Geological Survey of Norway Report 111: 21.

Myhre, P. I., Corfu, F. and Bergh, S. G. (2011). Paleoproterozoic (2.0-1.95Ga) pre-orogenic supracrustal sequences in the West Troms Basement Complex, northern Norway. Precambrian Research 186: 89-100.

Mørk, K. (1970). En geologisk undersøkelse av området omkring Kåfjord Kobbergruve, Kåfjord i Alta, Finnmark. Thesis University of Oslo: 115.

Naruk, S. J. (1987). Kinematic significance of mylonittic foliation. PhD thesis, University of Arizona.

Nilsen, K. and Bjørlykke, A. (1991). Geological setting of the Bidjovagge gold-copper deposits, Finnmark, northern Norway. Geologiska Föreningen i Stockholm Förhandlingar 113: 60-61.

Nilsen, K. and Nilsson, L. P. (1996). VARGSUND berggrunnskart 1935 4, M 1: 50 000. Nor. geol. unders.

Nironen, M. (1997). The Svecofennian Orogen: a tectonic model. Precambrian Research 86: 21-44.

Nyheim, H., Bergh, S. G., Krogh, E. J. and Zwaan, K. B. (1994). Torsnes-skjærsonen i det vestlige (nord-norske) gneisterreng, Kvaløya, Troms: evidenser for kompleks skorpeforkortning og orogen-paralell oblik strike-slip. Nordic geological wintermeeting Luleå: 149.

Nylund, B. and Nisca, D. (1981). Regionale tyngdkraftsmätningar och flygmagnetisk tolkning över Jokkmokks kommun. SGU brap 81420.

Ofstad, F., Baranwal, V., Koziel, J., Lynum, R. and Rodionov, A. (2013). Helicopter-borne magnetic, electromagnetic and radiometric geophysical survey in Repparfjord area, Alta and Kvalsund, Finnmark NGU-rapport 2013.027: 25.

Often, M. (1985). The Early Proterozoic Karasjok Greenstonebelt, Norway: A preliminary description of lithology, stratigraphy and mineralization. NGU Bulletin 403: 75-88.

Olesen, O. and Sandstad, J. S. (1993). Interpretation of the Proterozoic Kautokeino Greenstone Belt, Finnmark, Norway from combined geophysical and geological data. NGU Bulletin 425: 43-64.

Olesen, O. and Solli, A. (1985). Geophysical and geological interpretation regional structures within the Precambrian Keutokeino Greenstone Belt, Finnmark, North Norway. NGU Bulletin 403: 119-133.

Olesen, O., Torsvik, T., Tveten, E., Swaan, K. B., Løseth, H. and Henningsen, T. (1997). Basement structure of the continental margin in the Lofoten-Lopphavet area, northern Norwaya: constrains from the potential field data, on-land structural mapping and paleomagnetic data. Norwegian Journal of Geology 77: 15-30.

Patison, N. J. (2007). Structural controlls on gold mineralization in the Central Lapland Greenstone Belt. Geological Survey of Finland Special paper 44: 105-122.

Pedersen, B. R. S. (1997). Strukturell analyse av en Prekambrisk, duktilt deformert meta-suprakrustal zone (Astridal-skjærzonen?) på NØ-Senja, Troms. Unpublished Cand. Scient thesis, University of Tromsø.

Perdahl, J. A. and Einarsson, Ö. (1994). The marine-continental transition of the Early Proterozoic Skellefte-Arvidsjaur volcanic arc in the Bure area, northern Sweden. GFF 116: 133-138.

Pharaoh, T. C. and Brewer, T. S. (1990). Spatial and temporal diversity of Early Proterozoic volcanic sequences-Comparisons between the Baltic and Laurentian Shields. Precambrian Research 47: 169-189.

Pharaoh, T. C. and Pearce, J. A. (1984). Geochemical evidence for the geotectonic setting of Early Proterozoic metavolcanic sequences in Lapland. Precambrian Research 25: 283-308.

Pharaoh, T. C., Ramsay, D. M. and Jansen, Ø. (1983). Stratigraphy and structure of the northern part of the Repparfjord-Komagfjord window, Finnmark, Northern Norway. Norges geol und. Bull 377: 1-45.

Pratt, A. O. (1989). Petrology of differnsiated gabbrosheets in the Altenes tectonic window, North Norway. NGU Bulletin 414: 21-35.

Priesemann, F. D. (1984a). Summary report - 1983, Rombak project, Foldal Verk A/S. Bergvesenet rapport 2953: 38 s.

Quezada, R. and Niva, B. (1981). Askelluokta. Sveriges Geologiska Undersõkning brap(81065).

Rodionov, A., Ofstad, F., Lynum, R. and Tassis, G. (2012). Helicopter-borne magnetic, electromagnetic and radiometric geophysical survey in the Alta - Kvænangen area, Troms and Finnmark. NGU report 2012.065.

Rodionov, A., Ofstad, F., Lynum, R. and Tassis, G. (2013). Helicopter-borne magnetic, electromagnetic and radiometric geophysical surv - 2013 - NGU report 2012.065.

Romer, R. L. (1987). The geology, geochemistry and metamorphism of the Sjangeli area, a tectonic basement window in the Caledonides of Northern Sweden. Research Report University of Technology, Luleå, Sweden.

Romer, R. L. (1987). The geology, geochemistry and metamorphism of the Sjangeli area, a tectonic window in the Caledonides of northern Sweden. Research report Luleå University Tulea 1987:16: 124.

Romer, R. L. (1988). Disturbance of Pb, Sr, and Nd isotope system related to medium and low grade metamorphism isustrated with data from the polymetamortphic early proterozoic (Rombak)-Sjangeli basement window of the Caledonian of Sweden. PhD thesis 1988, Technical Univerity of Luleå: 10.

Romer, R. L. (1989). Implications of isotope data on the metamorphism of basic volcanites from the Sjangeli Window, northern Sweden. NGU Bulletin 415: 39–56.

Romer, R. L. (1989). Interpretation of the lead isotopic composition from sulfide mineralizations in the Proterozoic Sjangeli area, northern Sweden. NGU Bulletin 415: 57-69.

Romer, R. L. and Boundy, T. M. (1988). Interpretation of lead isotope data from the uraniferous Cu-Fe-sulphide mineralizations in the Proterozoic greenstone belt at Kopparåsen, northern Sweden. Mineral Deposita 23: 256-261.

Romer, R. L. and Boundy, T. M. (1988). Lithologic and tectonic profile across the Muohtaguobla area, Rombak basement window, northern Norway. NGU report 88.116.

Romer, R. L., Kjøsnes, B., Korneliussen, A., Lindahl, I., Stendal, H. and Sundvoll, B. (1992). The Archaean-Proterozoic boundary beneath the Caledonides of northern Norway and Sweden: U-Pb, Rb-Sr and eNd isotope data from the Rombak-Tysfjord area. Norges geologiske undersøkelse rapport 91.225: 67.

Rutland, R. W. R., Kero, L., Nilsson, G. and Stølen, L. K. (2001). Nature of a major tectonic discontinuity in the Svecofennian province of northern Sweden. Precambrian Research 112: 211–237.

Räsänen, J., Hanski, E., Juopperi, H., Kortelainen, V., Lanne, E., Lehtonen, M. I., Manninen, T., Rastas, P. and Väänänen, J. (1995). New stratigraphical map of central Finnish Lapland. The 22nd Nordic Geological Winter Meeting, 8-11 January, 1996, Turku, Finland, Abstracts: 182.

Saalmann, K., Mänttäri, I., Ruffet, G. and Whitehouse, M. J. (2009). Age and tectonic framework of structurally controlled Palaeoproterozoic gold mineralization in the Hämebelt of southern Finland. Precambrian Research 174: 53-77.

Samskog, P. (2011). Geochemical and kinematic study of shear zones within the "gold line", Lycksele-Storuman province, northern Sweden. Master thesis from Luleå University of Technology, Department of Chemical Engeneering and Geosciences.

Sandstad, J. S., Bjerkgård, T., Boyd, R., Ihlen, P., Korneliussen, A., Nilsson, L. P., Often, M., Eilu, P. and Hallberg, A. (2012). Metallogenic areas in Norway. In: Eilu, P. (ed.), 2012. Minera deposits and metallogeny of Fennoscandia. Geological Survey of Finland Special Paper 53: 35-138.

Sandstad, J. S. and Nilsson, L. P. (1998). Gullundersøkelser på Ringvassøy, sammenstilling av tidligere prospektering og feltbefaring 1997. NGU report 98.072.

Sandstad, J. S. e. (1985). Proterozoic copper mineralisations in northern Norway. Sveriges Geologiska Underõkning Ser Ca. 64, Excursion guide no. 6: 22.

Sawyer, E. W. and Korneliussen, A. (1989). The geochemistry of Lower Siliciclastic turbidites from the Rombak Window: implications for palaeogeography and tectonic settings. NGU Bulletin 415: 23-38.

Siedlecka, A., Iversen, E., Krill, A. G., Lieungh, B., Often, M., Sandstad, J. S. and Solli, A. (1985). Lithostratigraphy and correlation of the Archean and Early Proterozoic rocks of Finnmarksvidda and the Sørvaranger district. NGU Bulletin 403: 7-36.

Siedlecka, A. and Roberts, D. (1996). Finnmark fylke. Berggrunnsgeologi M 1:500000. Norges geologiske undersøkelse.

Skiöld, T. and Rutland, R. W. R. (2006). Successive ~1.94 Ga plutonism and ~1.92 Ga deformation and metamorphism south of the Skellefte district, northern Sweden: Substantiation of the marginal basin accretion hypothesis of Svecofennian evolution. Precambrian Research 148(3-4).

Skiöld, T., Öhlander, B., Markkula, H., Widenfalk, L. and Claeson, L.-Å. (1993). Chronology of Proterozoic orogenic processes at the Archean continental margin in northern Sweden. Precambrian Research 64: 225-238.

Skonseng, E. E. (1985). Berggrunnsgeologisk kartlegging i Gautelis området, Skjomen, Nordland. Feltrapport. NGU-rapport 85.214: 16.

Skyttä, P., Väisänen, M. and Mänttäri, I. (2006). Preservation of Palaeoproterozoic early Svecofennian structures in the Orijärvi area, SW Finland—Evidence for polyphase strain partitioning. Precambrian Research 150: 153–172.

Strachan, R. A. and Holdsworth, E. E. (2000). Proterozoic sedimentation, orogenesis and magmatism on the Laurentian Craton (2500-750 Ma). In: Woodcock, N and Strachan, R. A. (eds.) Geological history of Britain and Ireland. Blackwell Science Ltd.: 52-72.

Sundblad, K. (1991). Evidence for pre-Svecofennian influence in the Proterozoic Cu-Zn-Pb sulphide deposit at Tjåmotis, northern Sweden. GFF, Meeting proceedings 113.

Sundblad, K. and Ihlen, P. M. (1995). Gold mineralization in Fennoscandia: An overview. In: Ihlen, P., Pedersen and Stendal, H., (eds.). Gold mineralization in the Nordic countries and Greenland. GEUS Open file series, extended abstracts and field trip guide 95/10.

Sundblad, K. and Røsholt, B. (1986). A lead isotopic study of galena and amazonite in the Kiuri-Rassåive sulphide deposit - Consequences for the timing of ore forming processes in the Proterozoic of northernmost Sweden. Abstract for??

Theolin, T. and Wikström, S. (1979). Preliminär geologisk rapport; Ultevis. SGU brap 79048.

Torgersen, E., Viola, G., Sandstad, J. S. and Smeplass, H. (2013). Structurally controlled copper mineralizations in the Paleoproterozoic Repparfjord Tectonic Window, Northern Norway. EGU General Assembly 2013, held 7-12 April, 2013 in Vienna, Austria, id. EGU2013-4566.

Torske, T. and Bergh, S. G. (2004). The Caravarri Formation of the Kautokeino Greenstone Belt, Finnmark, North Norway; a Palaeoproterozoic foreland basin succession. NGU Bulletin 442: 5-22.

Vik, E. (1985). En geologisk undersøkelse av kobbermineraliseringene i Alta-Kvænangenvinduet, Troms og Finnmark. Dr. ing. avhandling, Universitetet i Trondheim, NTH: 295.

Viola, G., Sandstad, J. S., Nilsson, L. P. and Heincke, B. (2008). Structural and ore geological studies in the Northwest part of the Repparfjord window, Kvalsund, Finnmark, Norway. NGU report 2008.029.

Vivallo, W. and Claesson, L. Å. (1987). Intra-rifting and massive sulphide mineralization in an Early Proterozoic volcanic arc, Skellefte district, northern Sweden. In Pharaoh, T. C., Beckinsale, R. D. and Rikard, D. (eds.) Geochemistry and mineralization of Proterozoic volcanic suites. Soc. Spec. Publ. 33: 69-79.

Vognsen, M. (2010). The Mauken gold project, Northern Norway; Newly discovered gold deposit, situated in a Paleoproterozoic greenstone belt. Report from Scandinavian Highlands.

Weihed, P. (1996). Au metallogeny in the Palaeoproterozoic Skellefte district, northern Sweden: A uniformitarian plate tectonic view. GFF 118(S4): 48-49.

Weihed, P. (2003). A discussion on papers “Nature of a major tectonic discontinuity in the Svecofennian province of northern Sweden” by Rutland et al. (PR 112, 211–237, 2001) and “Age of deformation episodes in the Palaeoproterozoic domain of northern Sweden, and evidence for a pre-1.9 Ga crustal layer” by Rutland et al. (PR 112, 239–259, 2001). Precambrian Research 121: 141–147.

Weihed, P., Arndt, N., Billström, K., Duchesne, J.-C., Eilu, P., Martinsson, O., Papunen, H. and Lahtinen, R. (2005). 8: Precambrian geodynamics and ore formation: The Fennoscandian Shield. Ore Geology Reviews 27: 273-322.

Weihed, P., Bergman, J. and Bergström, U. (1992). Metallogeny and tectonic evolution of the Early Proterozoic Skellefte District, northern Sweden. Precambrian Research 58: 143–167.

Weihed, P., Billström, K., Persson, P.-O. and Bergman Weihed, J. (2002). Relationship between 1.90–1.85 Ga accretionary processes and 1.82–1.80 Ga oblique subduction at the Karelian craton margin, Fennoscandian Shield. GFF 124: 163-180.

Weihed, P., Billström, K., Persson, P.-O. and Bergman Weihed, J. (2002). Relationship between 1. 90–1.85 Ga accretionary processes and 1. 82–1.80 Ga oblique subduction at the Karelian craton margin, Fennoscandian Shield. GFF 124: 163–180.

Weihed, P. and Schönberg, H. (1991). Age of the porphyry-type deposits in the Skellefte District, Northern Sweden. Geologiska Föreningens i Stockholm Förhandlingar 113: 289-294.

Welin, E. (1987). The depositional evolution of the supracrustal sequence in Finland and Sweden. Precambrian Research 35: 95-113.

Wilson, M. R., Claesson, L.-Å., Sehlstedt, S., Aftalion, J. A. T., Hamilton, P. J. and Fallick, A. E. (1987). Jörn: An early Proterozoic intrusive complex in an vulcanic arc environment. Precambrian Research 36: 201-225.

Zhao, G., Cawood, P. A., Wilde, S. A. and Sun, M. (2002). Review of global 2.1–1.8 Ga orogens: implications for a pre-Rodinia supercontinent. Earth-Science Reviews 59: 125–162

Zwaan, C. B. (1992). Database for alle geologiske opplysninger om om den prekambriske geologien på Kvaløya, Troms. Norges geologiske undersøkelse rapport 92.104.

Zwaan, K. B. (1989). Berggrunnsgeologisk kartlegging av det prekambriske grønnsteinsbelte på Ringvassøy, Troms. Norges geologiske undersøkelse Report 89.101.

Zwaan, K. B. (1995). Geology of the Precambrian West Troms Basement Complex, northern Norway, with special emphasis on the Senja Shear Belt: a preliminary account. NGU Bulletin 427: 33-36.

Zwaan, K. B. (1995). Geology of the Precambrian West Troms Basement Complex, northern Norway, with special emphasis on the Senja Shear Belt: a preliminary account. . Norges geologiske undersøkelse Bulletin 427: 33-36.

Zwaan, K. B. and Gautier, A. M. (1980). Beskrivelse til de berggrunnsgeologiske kart 1834 I og 1934 IV, M 1:50000. Norges geologiske undersøkelse 357: 1-47.

Ödman, O. H. (1957). Beskrivning til berggrundskarta över urberget i Norrbottens län. SGU CA. 41.

Åhäll, K.-I. and Larson, S. Å. (2000). Growth-related 1.85-1.55 Ga magmatism in the Baltic shield; a review addressing the tectonic characteristics of Svecofennian, TiB 1-related, and Gothian events. GFF 122: 193-206.

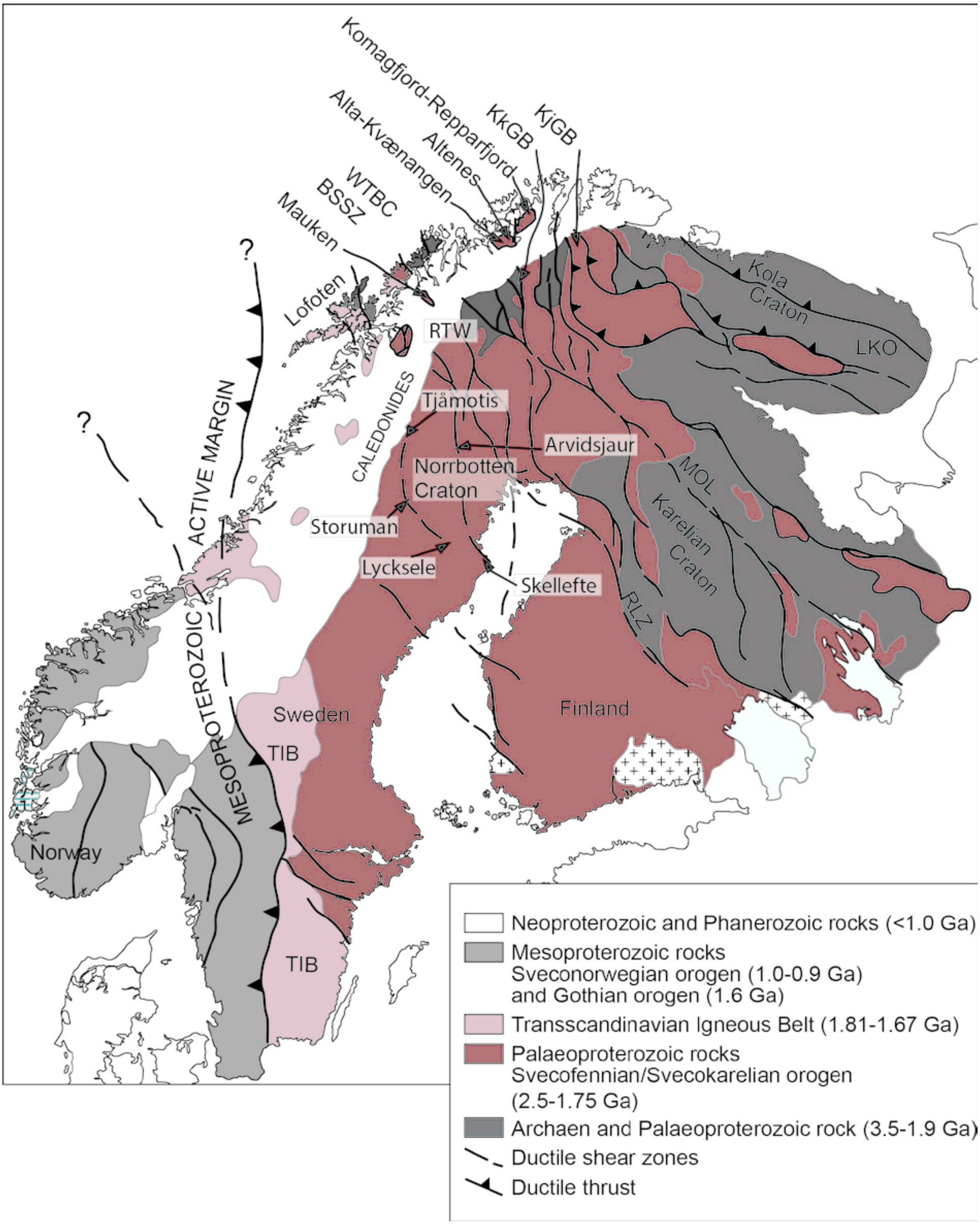

Fig. 1. An overview over the Fennoscandian shield with the main depositional and structural domains with the locations discussed in this article. (modified from Koistinen et al., 2001; Bergh et al., 2014).

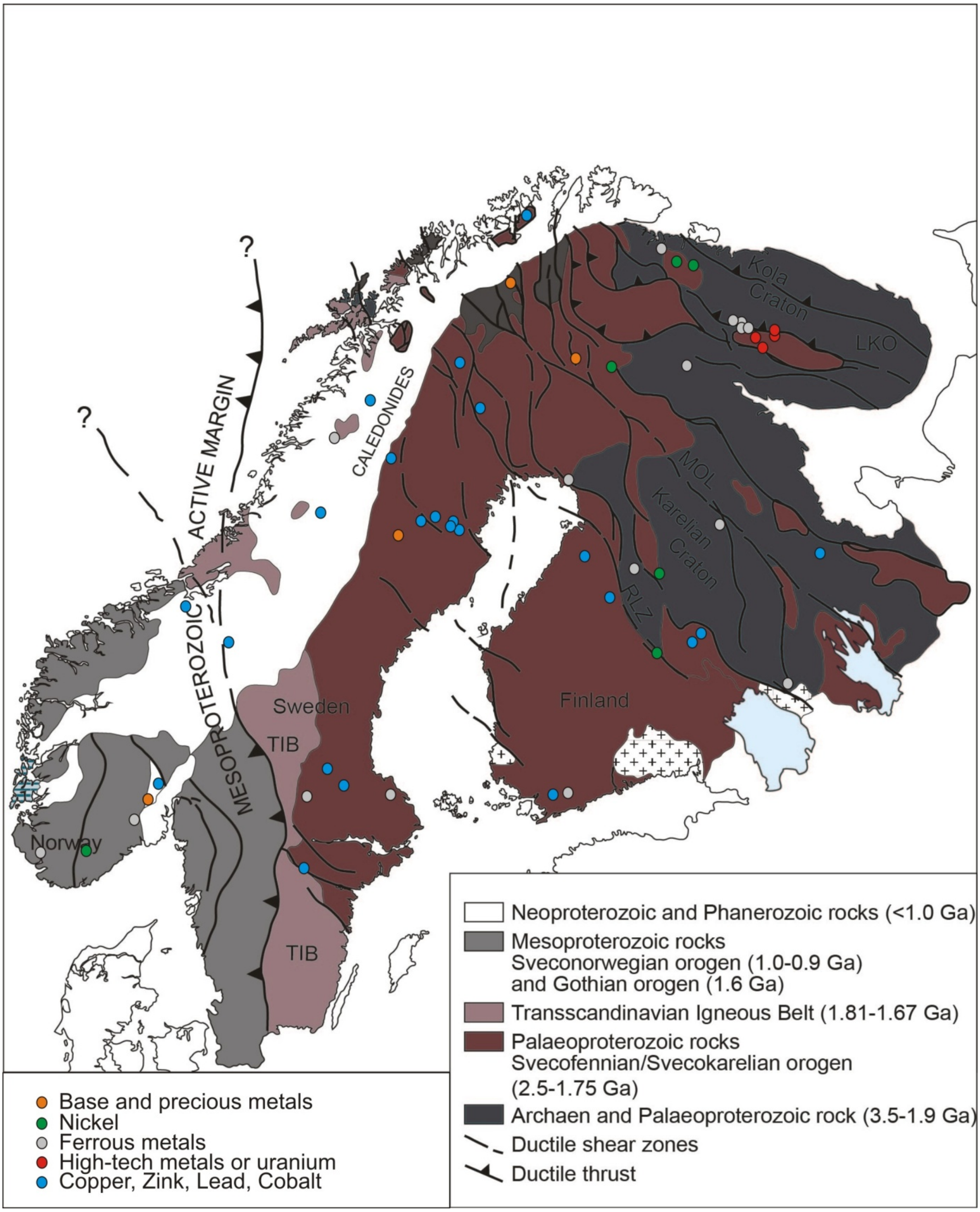

Fig. 2. The Fennoscandian shield with the locations of the most significant mines and mining camps of their time. (Modified from Koistinen et al., 2001; Eilu, 2012 and Bergh et al., 2014).

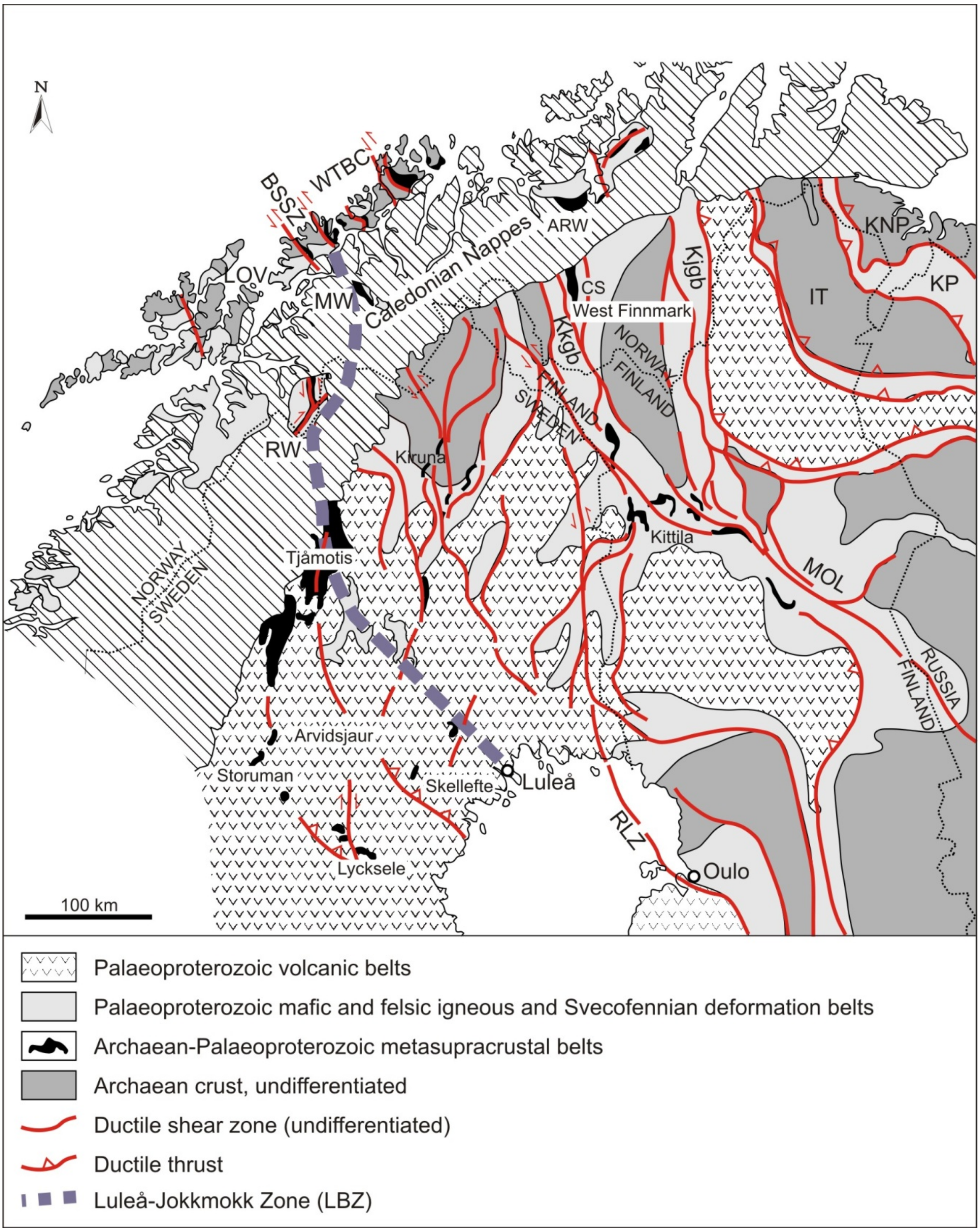

Fig. 3. An overview of the Northern part of the Fennoscandian shield with focus on the metasedimentary belts and the structural pattern from the Svecofennian orogeny. Note the Archaean-Paleoproterozoic boundary, the Luleå-Jokkmokk zone, is extended into Norway. (Modified from Bergh et al., 2012).

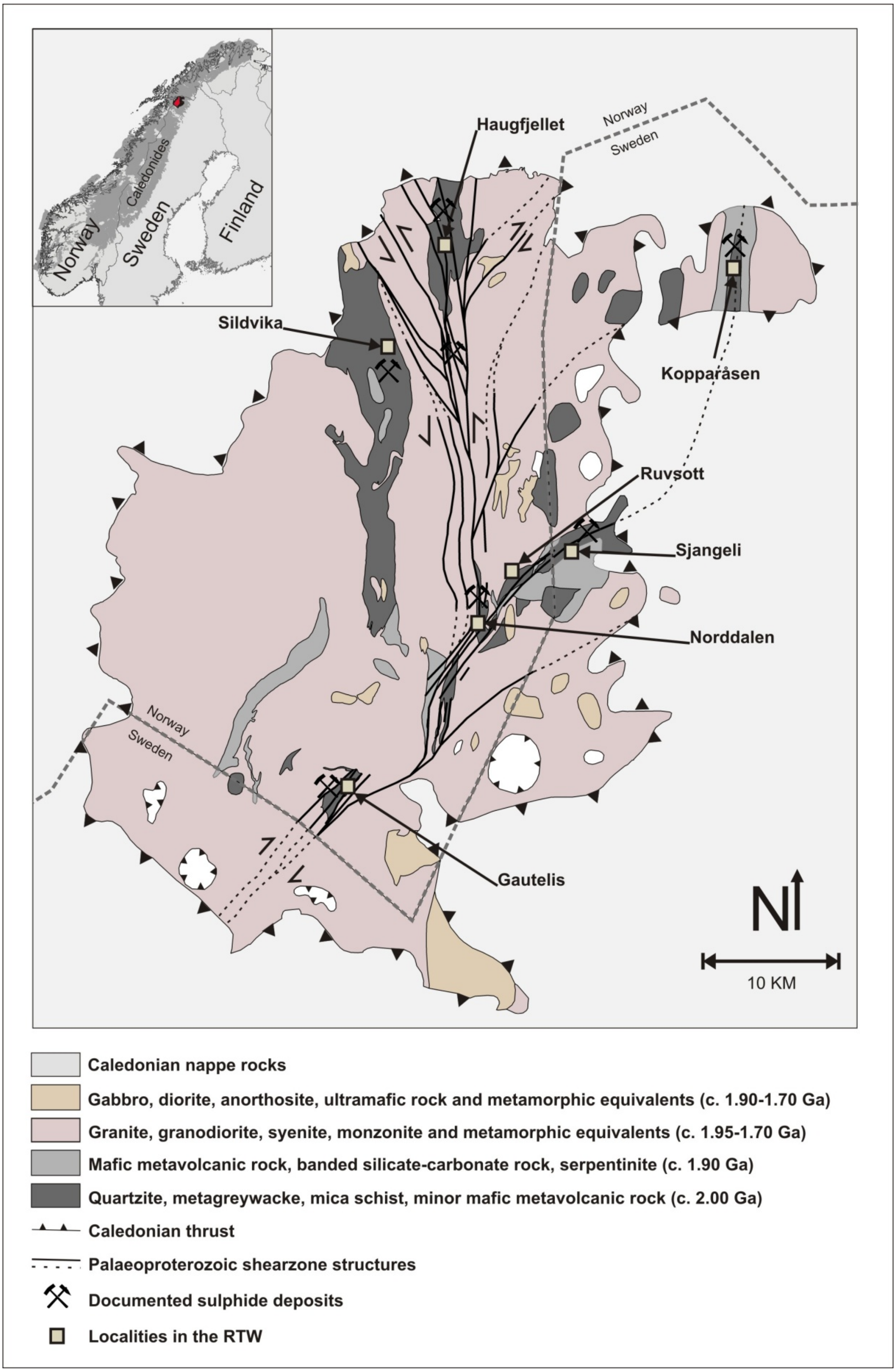

Fig. 4. An geological map over Rombak Tectonic Window (RTW) with the Kuokkel window on the top right side. Note that the Rombaken-Skjomen Shear Zone (RSSZ) can be traced into Sweden (modified from Larsen et al., 2013).

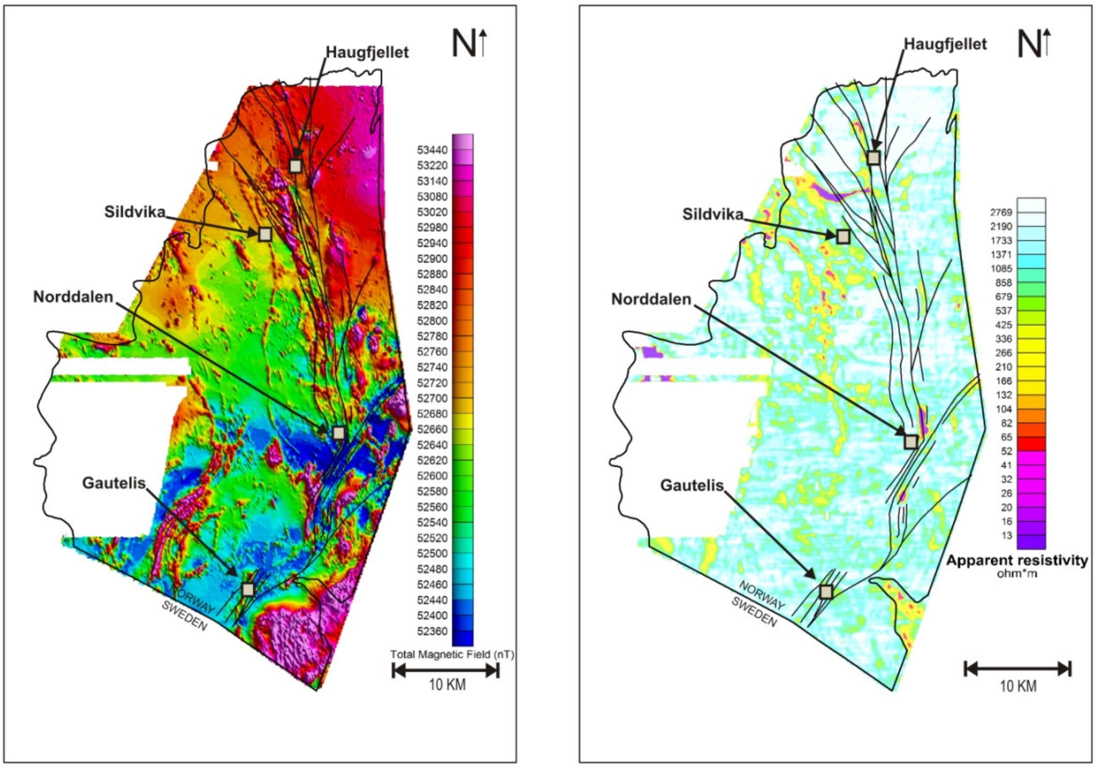

Fig. 5. Radiometric and electromagnetic maps over the RTW. The Radiometric map shows many of the N-S lines of the RSSZ. The shear zone can be traced across the border into Sweden. On the electromagnetic map a 5km displacement of the late dextral shear zone can be seen by the displacement of the anomaly from graphitic schist in Norddalen (Modified from Rodinov et al., 2012).

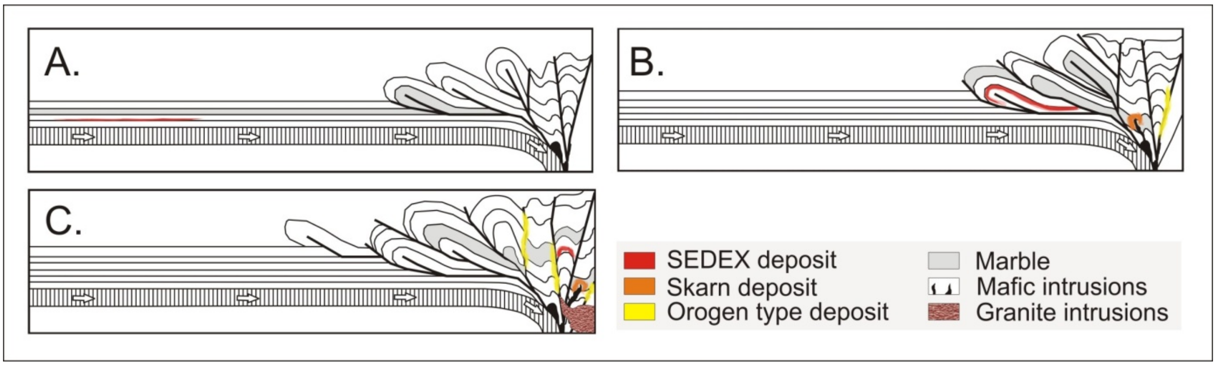

Fig. 6. The metallogenic evolution of the RTW in relation to the development of an active margin until accretion an orogeny. The SEDEX deposit are formed syn-sedimentary but close to an active margin. The metasomatic skarn deposit are formed syn-orogen in relation to shear zone parallel mafic intrusions cutting marble. The orogenic gold are deposited from fluids circulating along regional shear zone extending on kilometer scale syn depositional to the granite intrusions. (Modified from Larsen et al., 2012).

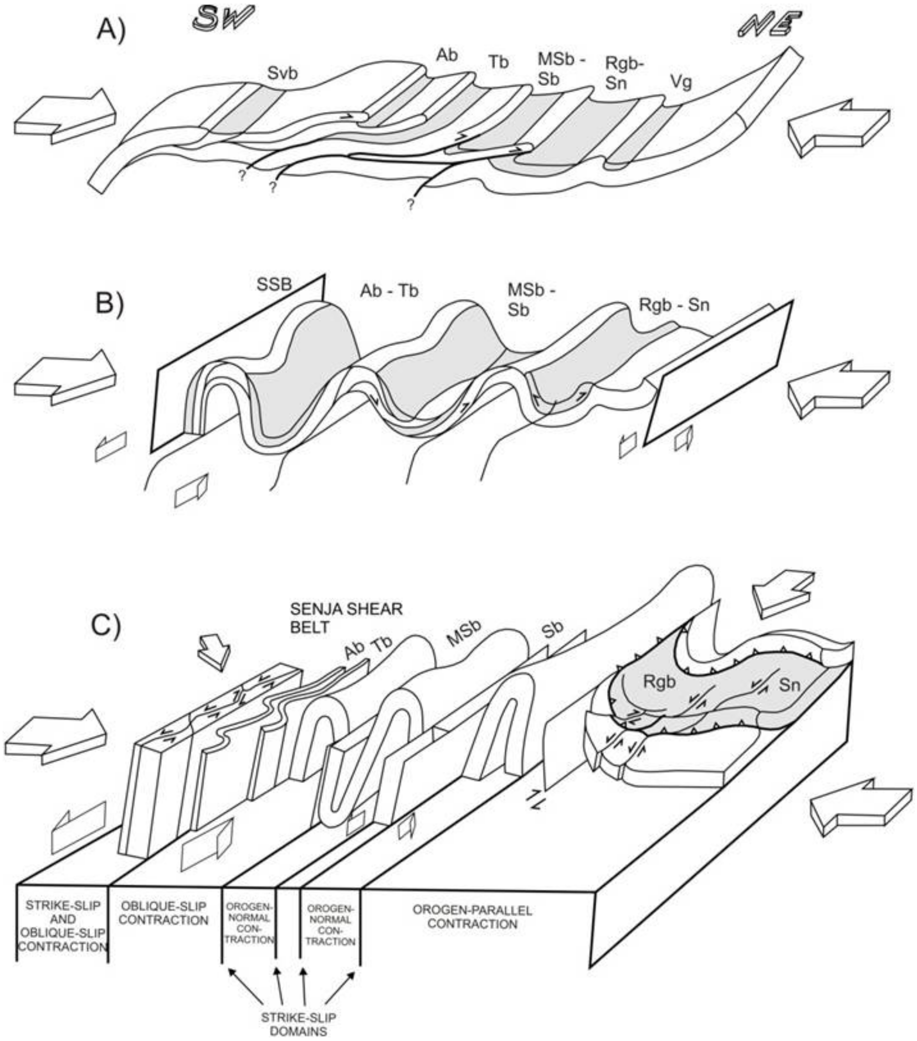

Fig. 7. The structural model of the West Troms Basement Complex (WTBC). The model shows the stages of early thrusting and folding being cut by later steep strike-slip structures limb parallel to the folds. Modified from Bergh et al. 2010.

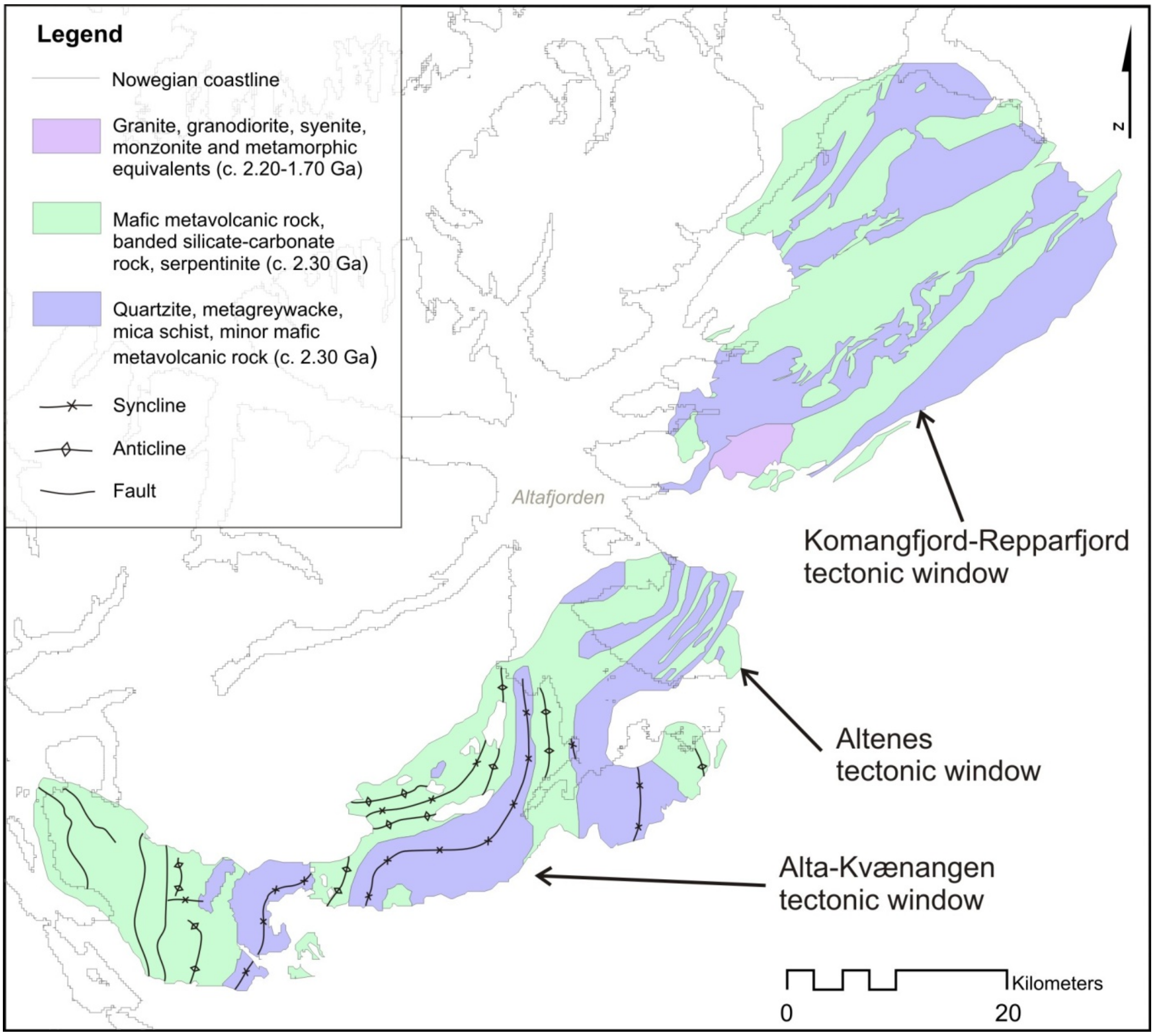

Fig. 8. Geological map over Alta-Kvænangen, Altaneset and Repparfjord Tectonic Window that shows how the bedrock are changing from a N-S direction in Alta-Kvænangen to more NE-SW in Repparfjord. Structures are only documented from the southern windows and drawn on to the map. Modified from Gautier, 1975 and, Koistinen et al., 2001)

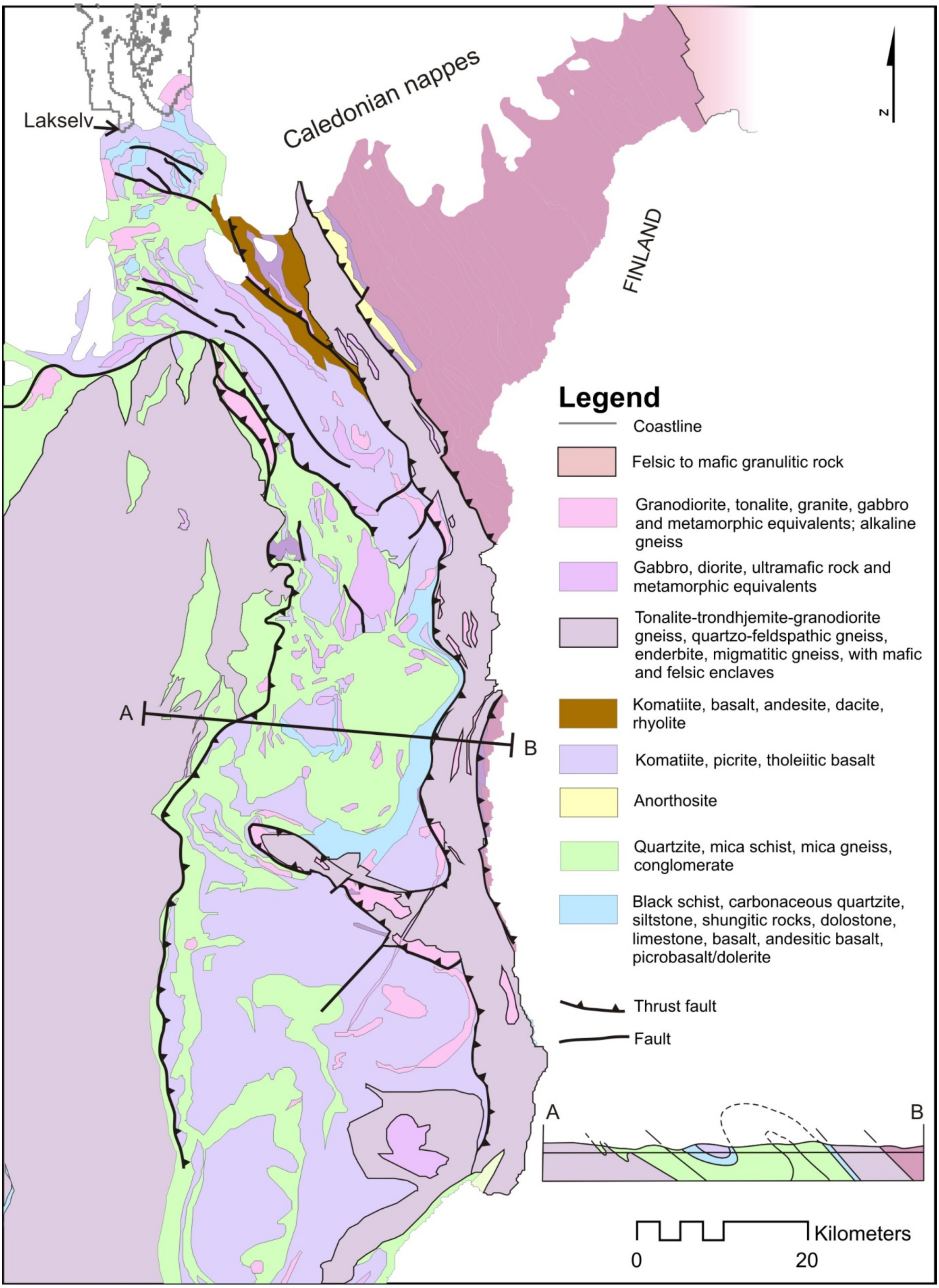

Fig. 9. A geological and structural map of the Karasjok area that shows the N-S striking fold-thrust belt parallel to the greenstone belt. Modified from Braathen and Davidsen (2000).

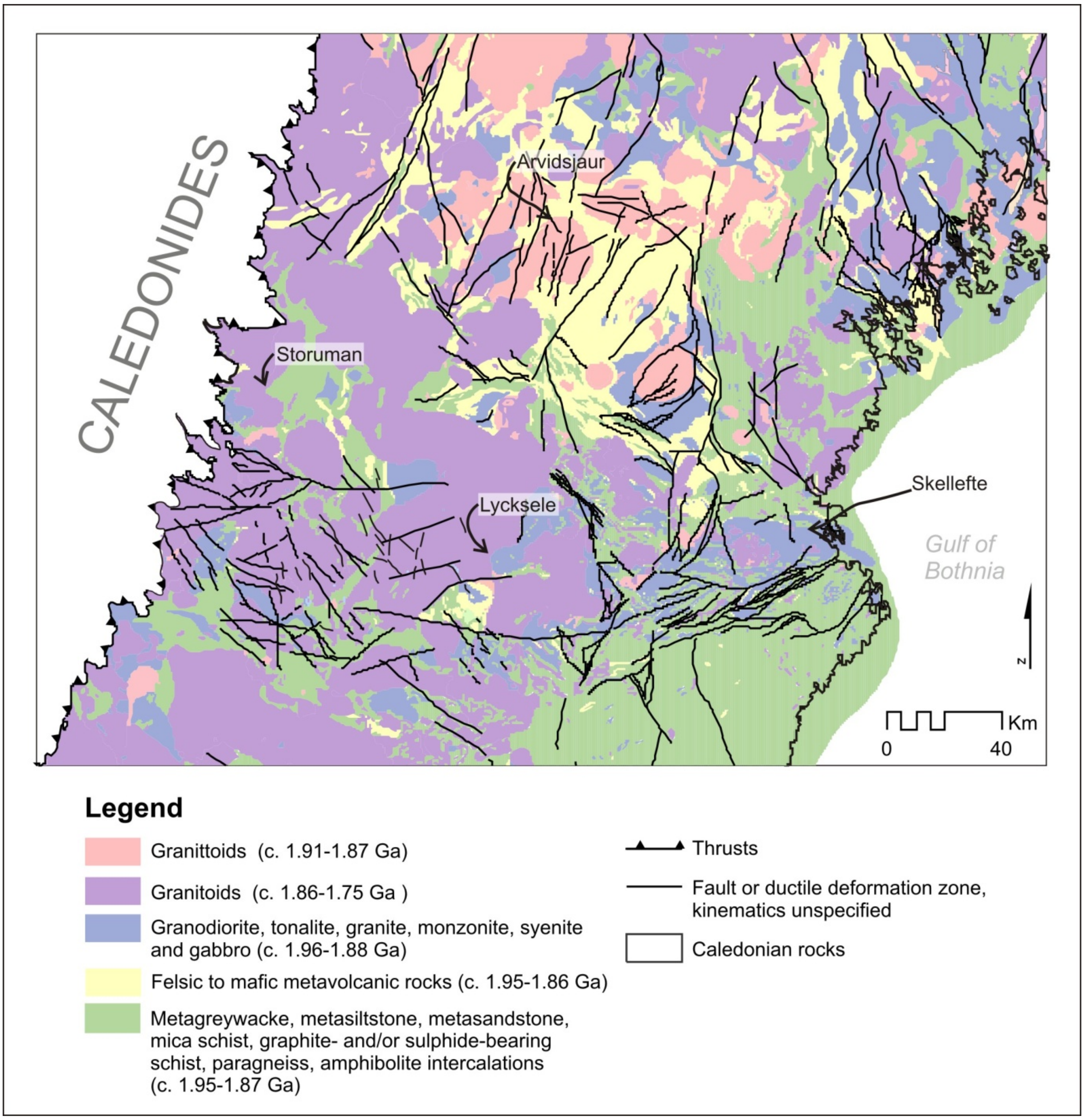

Fig. 10. A geological and structural map over the Skellefte district that shows the E-W striking thrusts (or faults) and the NE-SW striking shear zones (or faults). Modified from Koistinen et al., 2001 and Bark, 2005).

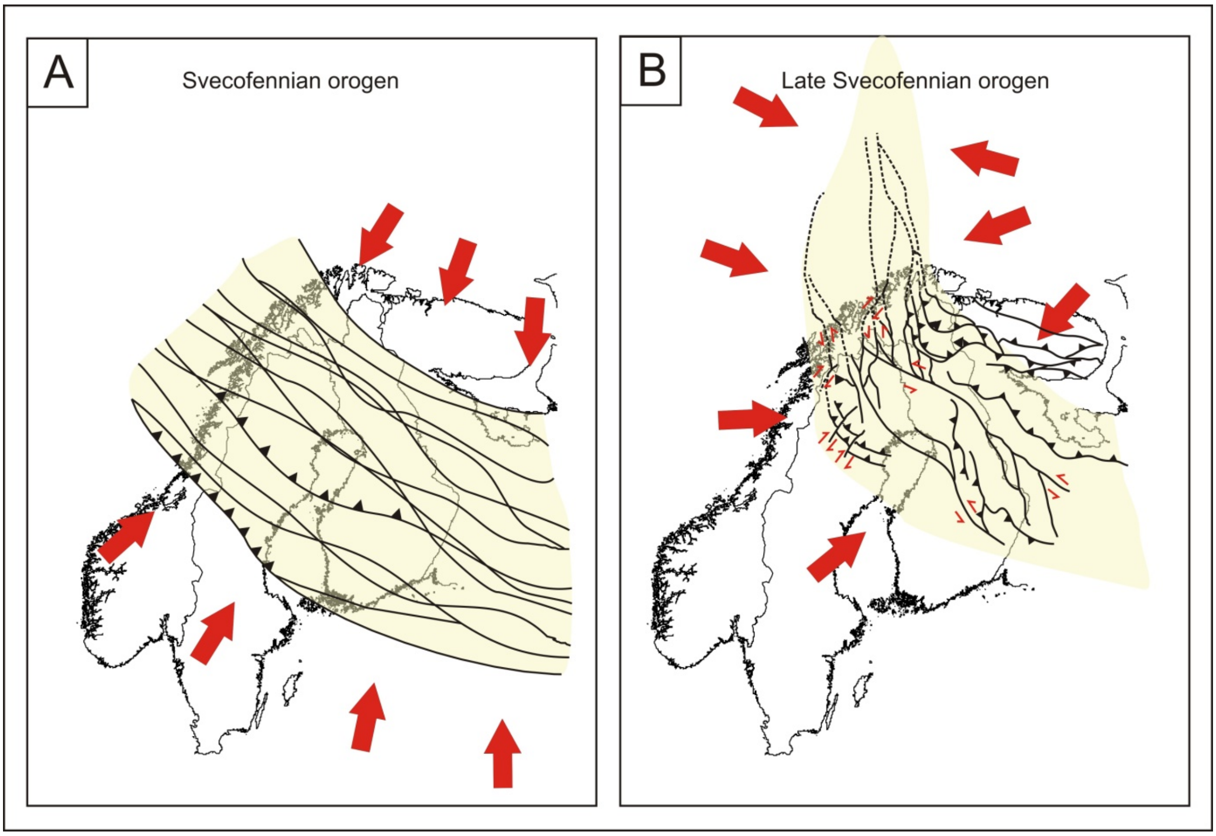

Fig. 11: A tectonic model over the Fennoscandian shield where the early stages of the orogen was dominated by N-S movement and the late stage of orogeny was dominated by a shift of movement to NE-SW collision which caused the western part to med northwards and developed a secondary orocline model.

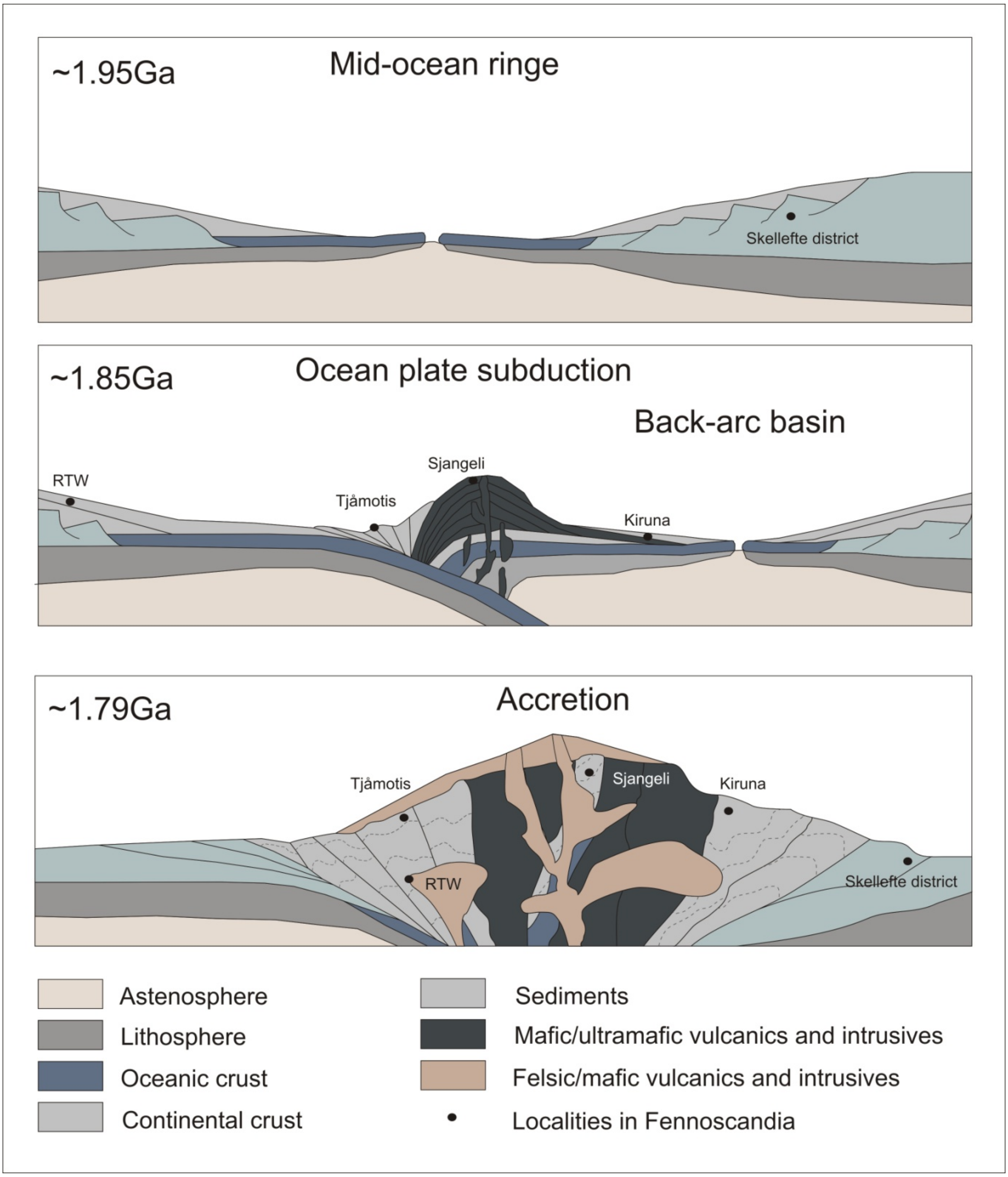

Fig. 12. A schematic regional tectono-metallogenetic model over the RTW as an case showing how the different rocks with adjacent sulphide deposits have developed during time and through the progress of the accretion and orogeny. The model is believed to be on a line at the margin and across the Svecofennian orogeny The model also include well known deposits surrounding the RTW. Modified from Larsen et al., 2013.

Table 1. Gives an overview for comparison of the different areas mentioned in the paper.

	Rocks	Structures	Metamorphism	Metallogeny
Rombaken Tectonic Window	Greywacke, graphitic schist, quartzite, quartzittic conglomerate and tuff on top of a Tonalittic basement. Intruded by granite plutons and mafic dykes.	**D1)** E-W folding **D2)** E-W top-to-the-east folding and thrusting **D3)** N-S striking sinistral strike-slip shearing **D4)** NE-SW striking dextral strike-slip shearing	Amphibolite facies with greenschist retrogradation along the regional shear zones	SEDEX (Zn-Pb), Metasomatic (As, Cu, Fe, Au), Orogenic gold
Sjangeli and Kopparåsen	Greywacke, meta-tuff, biotite- and graphitic schist, breccia, quartzite and conglomerate, basic and ultrabasic rocks. Deposited on Archaean basement. Intruded by Svecofennian granites	N-S and NE-SW striking and steep dipping mylonite zones. I Sjangeli also post granite but pre-Caledonian mylonitic shear zones in with a ENE-WSW strike.	Upper greenschist facies to lower amphibolite facies	Syn orogenic uranitite Syn genetic bornite, chalcopyrite and chalcocite with some magnetite, pyrite, pyrrhotite, galena, sphalerite, gersdoffite, arsenopyrite and molybdenite in veins and along beds.
West Troms Basement Complex *	Neoarchaean TTG-gneisses of tonalite, trondhjemite and granitic compositions with some intercalations of metasedimentary units intruded of a major mafic dyke swarm. The rocks are overlain by Paleoproterozoic volcanic and sedimentary rocks, intruded by large felsic/granitic and locally, mafic plutons.	**D1)** Main mylonitic foliation in meta-sedimentary rocks, initially flat-lying. tight to isoclinal intrafolial folds with NW-SE trend and moderately plunging folds, NE-directed ductile shear zones (thrusts) with a dip-slip stretching lineation. **D2)** Regional NW-SE trending open to tight upright folding of the mylonitic foliation; flat hinges and steep limbs. **D3)** Regional and meso-scale steeply N-plunging sinistral folds and conjugate NNW-SSE and NW-SE striking, steep ductile shear zones (strike-slip) in the Senja Shear Belt, Mjelde-Skorelvvatn belt and Ringvassøya greenstone belt. **D4)** NE-SW trending upright folds of the Vanna group and SE-directed thrust (in Skipsfjord nappe), steep NE-SW and ESE-WNW striking semi-ductile strike-slip shear zones.	Amphibolite facies with greenschist retrogradation along the regional shear zones and metasedimentary units in the NE.	Sulphides and gold deposits seem to have been remobilized and enriched along the youngest Svecofennian-aged, low-angle thrusts and steep strike-slip shear zones of the area.
Mauken Tectonic Window	Basalts, amphibolites, schist and meta-sandstone. Intruded by granodiorites	NW-striking ductile steep strike-slip shear zone	Greenschist to lower amphibolite facies	Shear zone related gold

Komagfjord-Repparfjord, Alta-Kvænangen and Altneset tectonic windows*	**Raipas Group:** low-grade tholeiitic volcanics, carbonates/dolomites and clastic sedimentary rocks. The lower Raipas group consist of Kvenvik and Storviknes Formations. **Brattholmen Group**: volcano-sedimentary rocks with calk-alkaline composition. **Sagelv Group:** clastic conglomerates, shales and carbonates **Holmvatn- Saltvatn, Nussir and Porsa Group:** metavolcanic and metasedimentary rocks. Consisting of Ulveryggen, Djupelv and Stangvatn Formations	**D1)** regional E/ENE-W/WSW trending upright and open to tight folds. **D2)** SW-NE trending, upright to inclined, tight to isoclinal folds with a moderate plunge and axial plane dipping to the NW. **D3)** Open folds trending SSW-NNE and plunge moderately to NE. Large NE-SW striking strike-slip shear zones with a dextral shear sense. **D4)** Caledonian structures	Lower greenschist facies during the Caledonian Orogeny	Volcanic and sediment hosted copper Cu-Au deposits with epigenetic and syngenetic origin
Karasjok greenstone belt	Meta-basalts, meta-sedimentary rocks, komatites and gneisses with intrusion of meta-gabbros. The Gneiss complex is thought to be the basement of the Greenstone belt.	East dipping tectonic wedge of several fold and thrust events. **D1)** East dipping thrusts caused by E-W contraction **D2)** NNE dipping thrusting and folding plunging to the east. NNE-SSW shortening **D3)** N-S striking folding. E-W shortening **D4)** NE-SW dextral post-orogenic brittle faulting related to a shield strike-slip event	Amphibolite facies. Granulite facies in Archean metasedimentary basement rocks.	Placer gold, komatite associated BIF in the volcano-sedimentary rocks and Ni-Cu-PGE deposits in ultramafic and mafic intrusions.
The Kautokeino greenstone belt*	**Caravarri Formation, Bickkacåkka Formation and Caskejas Formations:** Metavulcanic tholeiitic to komatiitic rocks and metasedimentary rocks intruded by quartz mononitic to granitic intrusives and Svecofennian granitoids in Finland. **Raisadno Gneiss Complex:** Archaean basement gneiss	**D1)** top-to-east and -to-the-west orthogonal thrusting and folding **D2)** ductile sinistral NNW trending strike-slip shearing	Upper greenschist to lower amphibolite facies	Orogenic gold with atypical metal associations

Tjåmotis district*	**Snavva-Sjöfalls Group**: meta-arkoses, quartzite, siltstone, mudstone, micaschist and greywacke Intruded by granite plutons (1.8 Ga Lina granite) **Arvidsjaur Group**: basaltic to rhyolitic volcanoclastic rocks and sandstones. equivalent to the Vargfors Group found in the Skellefte district	**D1)** Isoclinal parasitic folds, with flat lying fold axes and steep east dipping axial plane. These are interpreted to be related to large overturned syn- and anti forms dominating the area. **D2)** Folding around steep NE-SW trending axes and an event of **D3)** Open folding or doming related to the granite intrusions **D4)** Steep NNE striking faults or shear zones.	Amphibolitefacies	Skarn (Mo-W), skarn (As-Zn)
Skellefte district	**Vargfors group:** 1.875Ga, shallow-water meta-sedimentary, greywacke and volcanic rocks with a MORB tholeiitic composition Intruded by several generations of granite plutons; the 1.89-1.88 Ga Jörn granite, 1.88 Ga Sikträsk granite and the 1.81-1.77Ga Revsund Granite **Skellefte group:** subaqueous volcanic rocks.	**D1)** Foliation sub parallel to bedding **D2)** NE to NW striking upright tight to isoclinal folds and WNW-ESE striking thrust faults dipping to the north, with associated hanging wall anticline structures **D3)** N-NE striking open folds and N-S strike-slip shear zones	Greenschist to lower amphibolite facies	Gold rich VMS, Porphyry copper, Orogenic gold
Bothnian Basin (northern most part**)***	Greywacke, graphitic schist and mudstone Intruded by I-type granite (1.95-1.85Ga), S-type granite (1.82-1.80Ga) and alkali-calcic granite (1.81-1.77)	**D1)** NNE-SSW striking main foliation and steep dipping axial plane to subhorisonal isoclinal folds. **D2)** E-W striking ductile, top to the S thrusts are similar to the structures on the boundary to Skellefte district **D3)** Steep NW to NE striking ductile shear zones with a transpressive oblique reverse and dextral shear sense.	Amphibolite facies to locally granulite facies	Orogenic gold

*These deformation stages have not been categorized into D1, D2…..etc. from the original literature, but have in this table been interpreted into such categories.